INAUGURAL – DISSERTATION

zur
Erlangung der Doktorwürde
der
Naturwissenschaftlich-Mathematischen Gesamtfakultät
der
Ruprecht – Karls – Universität
Heidelberg

vorgelegt von
Dipl. math. Thomas-Peter Stiehl
aus *Wiesbaden*

Tag der mündlichen Prüfung:

Mathematical Modeling of Stem Cell Dynamics in Acute Leukemias

Gutachter:

Prof. Dr. Anna Marciniak-Czochra (Universität Heidelberg)
Prof. Dr. (Universität)

ABSTRACT

This thesis is devoted to mathematical modeling of acute leukemias, which form a heterogeneous group of severe blood cancers. New models of dynamic behavior of blood forming (hematopoietic) and leukemic cells are developed and studied analytically. Bone marrow aspiration data contributed from the University Hospital of Heidelberg (Prof. Dr. A. D. Ho) and clonal tracking experiments from literature serve as a test scenario for the proposed models. To reflect the compartmental architecture of the hematopoietic and leukemic cell line, the models are represented by systems of nonlinear ordinary differential equations. Different possible modes of interaction between healthy and leukemic cells are proposed such as competition for environmental signals or autonomous leukemic cell growth and competition for marrow space. Extensive analytical studies of system dynamics and the derived criteria for coexistence and out-competition of the different cell types result in biologically meaningful characterizations of the cancer stem cell state by dynamic cell properties. Numerical studies allow to investigate the impact of different cell parameters on the clinical course and patient prognosis. A model-based prognostic marker for survival of relapsing acute myeloid leukemia patients is developed and tested based on clinical data. The obtained results underline the strong impact of leukemia stem cell behavior on the clinical dynamics. Extensions of the models including multiple leukemic clones allow to link experimental observations of clonal evolution to yet not measurable but clinically meaningful cell parameters at different stages of the disease. The models derived in this thesis depend on a quasi-steady state approximation describing the dependence of cytokine concentrations on mature cell density. In the last part of this work it is rigorously shown that solutions depending on the quasi-steady state approximation are close to solutions of a singular perturbation problem including dynamics of the signal molecules as a separate ordinary differential equation that is scaled with a small parameter. L^∞ bounds for the difference of solutions based on the quasi steady state approximation and solutions of the singular perturbation problem are established for the infinite time interval.

ZUSAMMENFASSUNG

Akute Leukämien bilden eine heterogene Gruppe schwerwiegender neoplastischer Erkrankungen des blutbildenden Systems. Die in der vorliegenden Arbeit entwickelten und analysierten mathematischen Modelle beschreiben die Dynamik von blutbildenden und aberranten Zellen bei akuten Leukämien. Knochenmark-Aspirations-Daten aus dem medizinischen Universiätsklinikum Heidelberg (Prof. Dr. A. D. Ho) sowie Daten aus der Literatur über die klonale Zusammensetzung von Leukämien dienen als Referenz-Szenario zum Test der entwickelten Modelle. Entsprechend der kompartimentellen Architektur von blutbildenden und leukämischen Zellpopulationen bestehen die betrachteten Modelle aus Systemen nichtlinearer gewöhnlicher Differentialgleichungen. Es werden verschiedene mögliche Interaktionen zwischen benignen und malignen Zellen betrachtet. Diese sind Konkurrenz um Signalfaktoren einerseits, sowie autonomes Wachstum von malignen Zellen und Konkurrenz um Knochenmarksraum andererseits. Die aus dem ausführlichen analytischen Studium der Modelle hervorgehenden Kriterien für Koexistenz und Verdrängung der verschiedenen Zelltypen liefern eine biologisch bedeutungsvolle auf dynamischem Zellverhalten beruhende Charakterisierung von Leukämiestammzellen. Die numerische Untersuchung der Modelle erlaubt die Bestimmung des Einflusses verschiedener Zellparameter auf klinischen Verlauf und Prognose. Ein modellbasierter prognostischer Marker für Patienten mit rezidivierender akuter myeloischer Leukämie wird entwickelt und an klinischen Daten getestet. Die erhaltenen Ergebnisse unterstreichen die herausragende Bedeutung der Eigenschaften von Leukämiestammzellen für den klinischen Verlauf. Eine Erweiterung der Modelle auf die Betrachtung mehrerer leukämischer Klone erlaubt es, experimentelle Daten zur klonalen Evolution mit wichtigen, derzeit nicht messbaren, Zelleigenschaften zu verschiedenen Zeitpunkten der Erkrankung in Verbindung zu bringen. Die in der vorliegenden Arbeit hergeleiteten Modelle beruhen auf einer Quasi-Gleichgewichts-Annahme, die es ermöglicht, die Konzentration von Signalfaktoren als Funktion der Dichte terminal differenzierter Zellen darzustellen. Im letzten Teil dieser Arbeit wird bewiesen, dass die Lösungen des auf der Quasi-Gleichgewichts-Annahme beruhenden Systems in der Nachbarschaft der Lösungen eines singulären Störungsproblems verlaufen, bei dem die Dynamik der Signalfaktoren durch eine mit einem kleinen Parameter skalierte, zusätzliche gewöhliche Differentialgleichung beschrieben wird. Es wird die Existenz von L^∞-Schranken für die Differenz der Lösungen dieser beiden Systeme auf unbeschränkten Zeitintervallen gezeigt.

ACKNOWLEDGMENTS

I express my sincere thanks to Prof. Dr. Anna Marciniak-Czochra for supervision of the research leading to this thesis, submitted at the Faculty of Mathematics and Computer Science at the University of Heidelberg. I am deeply grateful for continuous support, valuable discussions and expert advice. I like to express my gratitude for the opportunity to meet international experts and to contribute to various conferences. I am very thankful to the Collaborative Research Center SFB 873, "Maintenance and Differentiation of Stem Cells in Development and Disease", for funding the work leading to this thesis and for providing opportunities to discuss with scientists from various fields of stem cell biology.

I sincerely thank Prof. Dr. Anthony Ho and Natalia Baran for contribution of clinical data and discussions about the work presented in Chapters 6 and 7. I like to express deep gratitude to Prof. Dr. Marek Kimmel for important discussions and helpful advice during preparation of Chapters 6 and 7 and various manuscripts. I am deeply grateful to Prof. Dr. Andro Mikelic for his valuable guidance resulting in the work presented in Chapter 9.

Finally, I want to express deep appreciation to Prof. Dr. Dr. h.c. mult Willi Jäger for his outstanding lecture series drawing my attention to the field of applied analysis and for encouraging my interdisciplinary studies.

Contents

RELATED PUBLICATIONS

STIEHL, T., BARAN, N., HO, AD., AND MARCINIAK - CZOCHRA, A. Clonal selection and therapy resistance in acute leukaemias: mathematical modelling explains different proliferation patterns at diagnosis and relapse. *J. R. Soc. Interface* 11, 2014, 20140079.

STIEHL, T., HO, A., AND MARCINIAK - CZOCHRA, A. The impact of CD34+ cell dose on engraftment after SCTs: personalized estimates based on mathematical modeling. *Bone Marrow Transplant* 49, 2014, 30–7.

WALENDA*, T., STIEHL*, T., BRAUN, H., FROBEL, J., HO, A.,SCHRODER, T., GOECKE, T., RATH , B., GERMING, U., MARCINIAK - CZOCHRA, A., AND WAGNER, W. Feedback signals in myelodysplastic syndromes: increased self-renewal of the malignant clone suppresses normal hematopoiesis. *PLoS Comput Biol* 10, 2014, e1003599. $*$: equal contribution

STIEHL, T., HO, AD., MARCINIAK - CZOCHRA, A., Assessing Hematopoietic (Stem-) Cell Behavior during Regenerative Pressure. In: "Systems Biology of Blood" Corey, S., Kimmel, M., Leonard, J., Springer, New York, to appear.

STIEHL, T., AND MARCINIAK - CZOCHRA, A. Mathematical modelling of leukemogenesis and cancer stem cell dynamics. *Math. Mod. Natural Phenomena*. 7, 2012, 166–202.

MARCINIAK - CZOCHRA, A., AND STIEHL, T. Mathematical models of hematopoietic reconstitution after stem cell transplantation. In Model Based Parameter Estimation: Theory and Applications., H. Bock, T. Carraro, W. Jaeger, and S. Koerkel, Eds. Heidelberg, Springer, 2011, 191-206.

STIEHL, T., AND MARCINIAK - CZOCHRA, A. Characterization of stem cells using mathematical models of multistage cell lineages. *Mathematical and Computer Modelling* 53(7-8), 2011, 1505–1517.

STIEHL, T., BARAN, N., HO, AD., AND MARCINIAK-CZOCHRA, A. Pattern of divisions of leukemia stem cells is a major determinant of the clinical course of acute myeloid leukemias: Mathematical models predict patient survival, *submitted*.

MARCINIAK-CZOCHRA, A., MIKELIC, A., AND STIEHL, T. A rigorous renormalization group second order approximation for singularly perturbed nonlinear ODEs, *submitted*.

NOTATIONS

$\mathbb{R}^+ := \{x \in \mathbb{R} \mid x > 0\}$	positive real numbers
$\mathbb{R}_0^+ := \{x \in \mathbb{R} \mid x \geq 0\}$	non-negative real numbers
$[a, b] := \{x \in \mathbb{R} \mid a \leq x \leq b\}$	closed interval of real numbers
$(a, b) := \{x \in \mathbb{R} \mid a < x < b\}$	open interval of real numbers
$(a, b] := \{x \in \mathbb{R} \mid a < x \leq b\}$	semi-open interval of real numbers
$[a, b) := \{x \in \mathbb{R} \mid a \leq x < b\}$	semi-open interval of real numbers
$\mathbb{R}^{n,n}$	Space of $n \times n$-matrices with real entries
$\langle ., . \rangle$	standard scalar product on $\mathbb{R}^n$
$\lvert \cdot \rvert = \lvert\lvert \cdot \rvert\rvert_2$	Euclidean norm
$\mathrm{dist}(x, A) := \inf_{y \in A} d(x, y)$	Distance of a point x from the set A w.r.t. metric d.
$\log(\cdot)$	natural logarithm
$(x_1, \cdots, x_n), [x_1, \cdots, x_n]$	row vector
$\mathbf{x}^T$	Transposition of vector $\mathbf{x}$
A^T	Transposition of matrix A
$\mathbf{x} \otimes \mathbf{y} = \mathbf{x}^T \mathbf{y}$	dyadic product of vectors from $\mathbf{x}, \mathbf{y} \in \mathbb{R}^n$
$D_x \mathbf{f}(\mathbf{x}, y)$	Jacobi matrix of a vector valued function $\mathbf{f} : \mathbb{R}^n \times \mathbb{R} \to \mathbb{R}^m$ w.r.t its first n-dimensional argument
$\partial_y \mathbf{f}(\mathbf{x}, y)$	derivative of a vector valued function $\mathbf{f} : \mathbb{R}^n \times \mathbb{R} \to \mathbb{R}^m$ w.r.t its second one-dimensional argument (component-wise derivative)
$\nabla_x g(\mathbf{x}, y)$	gradient of real valued function $g : \mathbb{R}^n \times \mathbb{R} \to \mathbb{R}$ w.r.t its first n-dimensional argument

$D_u\mathbf{f}(\mathbf{u},\varphi(\mathbf{u})) =$ $D_x\mathbf{f}(\mathbf{x},y)\vert_{\mathbf{x}=\mathbf{u},\ y=\varphi(u)}$ $+ (\partial_y\mathbf{f}(\mathbf{x},y) \otimes \nabla_x\varphi(\mathbf{x})\vert_{\mathbf{x}=\mathbf{u},\ y=\varphi(u))}$	Jacobi matrix w.r.t. vector $\mathbf{u}$ of the function $\mathbb{R}^n \to \mathbb{R}^m$: $\mathbf{u} \mapsto \mathbf{f}(\mathbf{u},\varphi(\mathbf{u}))$ for $\mathbf{f} : \mathbb{R}^n \times \mathbb{R} \to \mathbb{R}^m$, $\varphi : \mathbb{R}^n \to \mathbb{R}$
$c_i > 0, i = 1, \cdots, n$	$c_i > 0$ for all $i \in \{1, \cdots, n\} \subset \mathbb{N}$
$Int\ A$	Interior of the set A

CHAPTER 1

INTRODUCTION

1.1 Approach and results

This thesis is devoted to mathematical modeling of acute leukemias. Leukemias are malignant diseases of the blood forming (hematopoietic) system, leading to excessive production of aberrant cells and impairment of healthy blood cell production, [64, 174]. Clinical heterogeneity is a hallmark of acute leukemias, [64].

The goal of this work is to develop a rigorous mathematical framework to study the dynamics of healthy and malignant cells in acute leukemias.

1.1.1 Hypotheses and methodology

We use the methodology of nonlinear dynamical systems and singular perturbation theory to derive and analyze mathematical models.

The models are based on the cancer stem cell hypothesis according to which the heterogeneous leukemic cell bulk is maintained by a small population of so called leukemia stem cells (LSCs), [31, 44, 47, 100, 181]. LSCs are hypothesized to survive therapies and trigger relapse, [35, 41, 47, 210]. Similarly, all types of blood cells are derived from the hematopoietic stem cell (HSC) population during a multi-step process called hematopoiesis, [111, 116, 209]. In the models time evolution of each cell sub-population is described based on biological properties such as rate of proliferation, rate of death and fraction of self-renewal. The latter describes the probability that a cell arising from division is of the identical type as its parent cell (self-renewal). In the opposite scenario (differentiation), the parent cell gives rise to more specialized cells, [99, 111, 181]. All considered cell properties are regulated by nonlinear feedback mechanisms.

The interaction (competition) of leukemic and hematopoietic cells is not well characterized and may differ between individuals, [8,54,55,93,137,146,192,206,229]. Therefore, we model different mechanisms of interaction and compare their impact on system dynamics. We focus on two main mechanisms, which are biologically justified:

(1) Leukemic and hematopoietic cells compete for the same signal factors, which they need to maintain their populations, [126, 206]. In the following, this mechanism is denoted as "signal dependent leukemia".

(2) Leukemic cells expand independently of environmental signals, [98], high cell concentrations in the marrow space cause enhanced cell death in healthy and leukemic cells, [34,67,107,128,243]. In the following, this mechanism is denoted as "signal independent leukemia".

Bone marrow aspiration data contributed from the University Hospital of Heidelberg (Prof. Dr. A. D. Ho) and clonal tracking experiments from literature serve as a test scenario for the proposed models.

Due to the different timescales of cell division and environmental signal dynamics, singular perturbation problems naturally arise in the models. In applications the canonical quasi-steady state approximation is often used to reduce the model systems. In this thesis, singular perturbation methods are applied to show rigorously the validity of the quasi-steady state approximation. It is proved that the resulting reduced models describe the essential dynamics. The performed stability analysis involves linearized stability and center manifold theory. Global dynamics of the models is investigated using numerical simulations.

1.1.2 Results

This thesis contributes to both, understanding of blood cancer dynamics and mathematical methodology for model reduction. The main results are:

(1) Comparison of system dynamics for different nonlinear feedback mechanisms: The proposed models possess unique and uniformely bounded solutions. The mode of interaction between healthy and leukemic cells has an impact on existence, structure and stability of relevant equilibrium states. Model analysis provides necessary and sufficient criteria for destabilization of the healthy steady state by leukemic stem cells and criteria for stability of coexistence or out-competition of the different cell populations. Based on analytical criteria from linearized stability analysis and central manifold theory, properties of leukemic stem cells are characterized and compared to properties of hematopoietic stem cells. This is relevant for selective eradication of LSC during treatment, [35, 41, 47, 210], but has not been done so far, due to experimental shortcomings. Limitations of stem cell markers

and change of cell properties under culture conditions do not allow to directly observe human HSCs and LSCs, [68, 104, 147, 202]. Main biological implications of the obtained results are:

- Properties of LSC depend on the mode of interaction between leukemic and healthy cells: In case of signal dependent leukemias, self-renewal of leukemic stem cells under maximal stimulation has to be larger than self-renewal of hematopoietic stem cells under maximal stimulation. This condition is sufficient for out-competition of healthy cells. In case of signal independent leukemias, the self-renewal probability of leukemic stem cells has to be larger than one half and can be smaller than HSC self-renewal under maximal stimulation. In this case, it depends on the proliferation rate of LSCs, if HSCs are out-competed or if coexistence is established.
- Increased self-renewal of LSCs compared to HSCs is a key mechanism of leukemogenesis always leading to leukemic cell growth. Increased proliferation of LSCs alone is not always sufficient. This challenges a key paradigm of cancer biology stating that cancer cells divide more frequently than their benign counterparts, [94, 204], accumulate mutations, [84, 115, 204] and out-compete healthy cells.
- The interplay of nonlinear feedbacks and increased death rates of hematopoietic cells can result in steady states with high numbers of immature cells and low numbers of mature cells. This finding provides a mechanism for the yet unexplained observation that certain diseases are linked to increased counts of non-mutated healthy immature marrow cells but reduced numbers of mature cells, [53, 119, 176, 191, 232, 233].
- Variability of interaction mechanisms but also variability in cell behavior contribute to the clinically observed heterogeneity of the disease.

(2) Characterization of parameters that are essential for kinetics of the total cell population: The impact of leukemic stem and progenitor cell properties in terms of proliferation and self-renewal on the clinical course and patient prognosis is yet unclear, [56, 208]. We provide numerical studies showing that parameters describing leukemic stem cell behavior have more impact on clinical dynamics than parameters describing behavior of leukemic non-stem cells. Based on this observation a model-based prognostic marker for survival of relapsing acute myeloid leukemia patients is developed and tested based on clinical data. Model-based assessment of stem cell behavior might be a complementary and more direct approach to risk-stratification, compared to scores based on mutation analysis. The impact of mutations clinically used for risk-assessment and their interplay often remains unknown, [17, 64, 78, 179]. New biological implications of the obtained results are:

- Leukemic stem cell properties differ significantly among individuals and have impact on patient prognosis. Properties of leukemic non-stem cells have only negligible impact on the clinical course.
- Clinical bone marrow aspiration data allow to compare LSC properties in different individual patients.

(3) Characterization of short and long term dynamics of the competition and selection process between different cell types: Analytical results suggest that feedback mechanisms have a strong influence on the competition among different leukemic clones. In case of signal dependent leukemias only clones with maximal self-renewal probability show long-term survival. Their proliferation rate has no impact on long-term persistence. Nevertheless, high proliferation rates combined with non-maximal self-renewal can lead to transient expansion of a cell clone. In case of signal-independent leukemias, high proliferation rates increase fitness of a clone also on long time scales. This is relevant, since high proliferation is often linked to high drug-sensitivity, [26]. Acute leukemias frequently relapse and relapsed disease has a poor prognosis, [46,64,70,74,142,177,189]. Up to now it is under discussion, which mechanisms may lead to relapse (mutations, selection) and why relapsed disease is more resistant to chemotherapies. Simulation of our models with chemotherapy suggests that the combination of high self-renewal and slow proliferation is a main mechanism of the observed treatment-resistant relapses. New biological implications are the following:

- Leukemic cell properties differ at different time-points of the disease. This difference can be explained by selection processes alone and does not require occurrence of new mutations.
- The observed and so far poorly understood varying in time contribution of individual leukemic clones, [9, 56], can be explained by competition of clones with different self-renewal probabilities.
- The models predict that cells at primary diagnosis have high proliferation rates and high self-renewal probabilities, while cells at relapse have small proliferation rates and high self-renewal probabilities. This result allows to link observed mutations to qualitative cell properties.
- High self-renewal and slow proliferation may be responsible for treatment failure at relapse. This is clinically relevant, since classical treatments only eliminates fast proliferating cells, [26].
- The models predict that clonal competition limits the number of large leukemic clones. More sensitive methods may reveal a high number of small leukemic clones. This might cause difficulties in treatment and also in follow-up examination relying on genetic signatures.

(4) Development of a rigorous approach for quasi-stationary model reduction: A mathematical novelty of this work is to show that solutions of the reduced model system (quasi-steady state approximation) stay close to solutions of the singular perturbation problem with respect to the L^∞ norm on the *infinite* time interval. This result is proven for a general Cauchy problem and then applied to the stem cell models. Assumptions needed for this result are fulfilled for parameter regimes compatible with the biological behavior of the model, such as existence of a positive equilibrium of blood cell counts.

1.2 Outline of the thesis

The point of departure of this thesis is a mathematical model of stem cell dynamics in healthy blood formation (hematopoiesis), [157, 215]. The model includes nonlinear feedback signaling, which links the concentration of mature blood cells, such as white blood cells, red blood cells or platelets to dynamic properties of stem and immature cells. The model has been calibrated and applied to clinical scenarios, [214].

In Section 1.3, we provide an overview of classical and recent literature from the field of mathematical modeling of the blood system and its diseases.

In the **first part (Chapters 2-5)** of the thesis new mathematical models of leukemias are developed and analyzed.

In **Chapter 2**, two new models of acute leukemias are developed. The models proposed are given as systems of nonlinear ordinary differential equations. They include one lineage of healthy cells and at least one lineage of leukemic cells. The new features of the developed models are threefold:

(i) The models explicitly include the possibility that non-stem cells may self-renew. In one of the models self-renewal of healthy and leukemic stem and non-stem cells is regulated by cytokine concentrations. In the other model, self-renewal of leukemic cells is constant, but also non-stem cells can have self-renewal probabilities larger than one half.

(ii) The models incorporate different possible modes of interactions between healthy and leukemic cells such as competition for cytokine molecules or increased death rates, due to overcrowding of the marrow space. The possibility of signal independent leukemic cell growth is also considered. The impact of the different modes of interaction on population dynamics is systematically investigated.

(iii) The models can be straightforwardly extended to study the competition between multiple leukemic cell lines. This is done in Chapter 7. The multiclonal versions of the models are important for a better understanding of the recently described heterogeneity of leukemic cells.

In Model 1, it is assumed that leukemic cells respond to the same signals as hematopoietic cells and that healthy and malignant cells compete for these signals. Model 2 is based on the the assumption that leukemic cells expand independently from hematopoietic growth factors. In this model, leukemic and hematopoietic cells compete for bone marrow (niche) space, where overcrowding leads to cell death. The two models can be interpreted as two extreme cases of a continuum: In Model 1, leukemic cells are fully dependent on hematopoietic signals, while in Model 2 they are fully independent of hematopoietic signals. Model assumptions are motivated by experimental data stating that response of leukemic cells to growth factors shows high variability. Therefore, the two models may provide complementary insights into leukemia dynamics.

In **Chapter 3**, Model 1, where leukemic cells depend on hematopoietic growth factors, is analyzed. A systematic classification of necessary and sufficient scenarios for malignant cell expansion is developed and treatment strategies are discussed. The results stress the importance of high self-renewal of leukemic stem cells. Some of the conditions lead to new and biologically unexpected insights into leukemic stem cell properties. Non-negative steady states of the model are characterized and linked to cancerous diseases of the hematopoietic system. For a minimal version of the model linear stability and behavior in the neighborhood of a center manifold are studied and related to the clinical picture of different hematological diseases. The results suggest that enhanced self-renewal of leukemic cells leads to faster leukemia cell expansion and poorer prognosis than enhanced proliferation. There may even exist cases, where leukemic cells proliferate slower than hematopoietic cells. This is a biologically new result that has not been concluded from experimental data so far. The results of this Chapter have been published in [216].

In **Chapter 4**, Model 2, where leukemic cells are independent of hematopoietic growth factors, is analyzed. We establish necessary and sufficient conditions for expansion of a leukemic cell population and discuss corresponding treatment strategies. Characterization of steady states of the system reveals a broad parameter range for coexistence of leukemic and hematopoietic cells. It is discussed that these equilibria may allow long term survival in presence of leukemic cells, as observed in chronic leukemias. Detailed linear stability analysis including behavior near a center manifold of a minimal version of the model is performed. This shows that whenever coexistence of leukemic and hematopoietic cells is possible, this coexistence is stable and all other equilibria, especially extinction of healthy cells, are unstable. This view leads to new candidate treatment strategies.

The model has led to new biological hypotheses: If the hematopoietic lineage comprises more than two maturation stages, this model exhibits multiple isolated steady states that are maintained by the same stem cell population. The model leads to the new hypothesis that hematopoietic steady states with high cell density might allow out-competition of leukemic cells. The model also suggests that, based on the properties of the leukemic cell line, different sub-populations of the hematopoietic lineage may act a stem cell population. The model developed in this Chapter has been published in [213].

In **Chapter 5**, we compare the proposed models with respect to (i) properties allowing leukemic stem cells to expand, (ii) steady states, especially coexistence of hematopoietic and leukemic cells, (iii) competition and selection processes. Based on the different possible modes of competition between hematopoietic and leukemic cells, different system dynamics and stable states emerge. The comparison of the models reveals that stemness is linked to certain cell properties, which depend on the type of interaction between the hematopoietic and the leukemic cell line. In Model 1, either all stages of a lineage (hematopoietic or leukemic) survive or all become extinct, whereas in Model 2 properties of the leukemic stem cell compartment determine, which hematopoietic cell compartment acts as stem cell population. This finding is new and important, since it demonstrates that stemness is not a fixed property but can depend on the environment and on the properties of competitors. Based on this finding, different types of selection are defined and discussed in a clinical context.

The **second part (Chapters 6-7)** of the thesis is devoted to numerical studies of the proposed models. These Chapters provide a calibration of the models to clinical data contributed by Prof. Dr. Anthony Ho and Natalia Baran (University Hospital of Heidelberg) and their application to open clinical questions.

In **Chapter 6**, we consider a version of the model of signal-dependent leukemia consisting of three hematopoietic and three leukemic cell stages. We systematically investigate the impact of different cell types, namely stem and progenitor cells of both lineages on the dynamics of the system. Simulations show that for a clinically relevant range of parameters dynamics of the system depends on self-renewal and proliferation of leukemic stem cells, while the impact of leukemic progenitor cells is negligible. This finding is new and unexpected, since it implies that the observed clinical picture is mainly determined by leukemic stem cell properties. Based on this finding, surrogate parameters for leukemia stem cell proliferation and self renewal are estimated based on routine clinical data and linked to inter-individual heterogeneity of the disease. Patient data analysis shows that the derived surrogate parameters allow to divide patients in different prognostic groups. This finding is new, since it leads to a complementary approach to risk stratification. Up to now risk stratification has been based on statistical

parameters (patient age, sex etc.) and molecular markers. The impact of all such parameters and their combinations on dynamic stem cell properties is, nevertheless, not straightforward. The view proposed here leads to a new and more direct way of risk stratification based on estimation of surrogate parameters of leukemic stem cell behavior.

In **Chapter 7**, the models are extended to take into account selection processes between different leukemic clones. To investigate clonal selection processes under treatment conditions, a simple model of classical cytotoxic therapy is proposed. The framework developed in this Chapter allows to investigate, which cell properties are selected before diagnosis of the disease and at relapse. The models reveal that at different stages of the disease cells with different properties dominate the malignant cell mass. This finding may help to link detected aberrations to functional cell properties. The model proposes that presentation of different genetic markers at diagnosis and relapse may originate from selection processes and does not necessarily require occurrence of new mutations. Leukemic cell self-renewal is identified as the driving force behind clonal selection and relapse. Based on the mathematical models, we propose that enhanced self-renewal can explain resistance to a broad spectrum of cytotoxic agents and fast expansion of cells at relapse. Based on the model, we formulate different testable hypotheses concerning the number of detectable leukemic clones, the impact of detected aberrations and the origin of therapy resistance. Finally, we perform a mathematical analysis of simplified versions of the models to investigate, which cell properties lead to long term-survival of a leukemic clone and which lead to out-competition. Main results of this Chapter have been published in [213].

The **third part (Chapters 8-9)** of the thesis is devoted to study properties of the quasi-steady state approximation applied to model concentrations of hematopoietic signal factors. In the models developed in Chapter 2 cytokine dynamics are described using a Hill-function dependent on mature cell density. This quasi-steady state approximation is motivated by the different time scales of cell division and cytokine kinetics, [30]. Alternatively cytokine dynamics can be described using an additional ODE. Then, we obtain a singular perturbation problem. We study the approximation of solutions of the quasi-steady state approximation by solutions of the singular perturbation problem on finite and infinite time intervals.

Singular perturbation problems naturally arise in mathematical modeling, due to the inherently different timescales of the considered processes. Different approaches to perturbation problems have been developed, [169,207], such as the geometric singular perturbation theory, [69, 114], the Tikhonov-Theorem, [19, 221, 236], and the renormalization group approach, [42, 43]. The classical Tikhonov-Theorem, [221,236], is valid on finite time intervals. It was extended in [101,103] and error estimates for finite times have been developed in [228].

In **Chapter 8**, we apply the Tikhonov Theorem to the model of healthy hematopoiesis from Chapter 2. The model is based on a quasi-steady state approximation taking into account that dynamics of hematopoietic signal factors is fast compared to cell proliferation and differentiation (cell division and differentiation take place at the time scale of days or weeks, [203], while cellular signaling takes place at the time scale of minutes, [30, 160]). We use Tikhonov theorem to show that on finite time intervals solutions of the model including the quasi-steady state approximation are close to solutions of the full model without the quasi-steady state approximation.

In **Chapter 9**, we study properties of the quasi-steady state approximation for infinite time intervals. For this purpose we consider the Cauchy problem

$$\frac{d\mathbf{u}_\varepsilon}{dt} = \mathbf{f}(\mathbf{u}_\varepsilon, v_\varepsilon),\ t > 0, \quad \mathbf{u}_\varepsilon(0) = \mathbf{u}^0; \tag{1.1}$$

$$\varepsilon\frac{dv_\varepsilon}{dt} = -\alpha v_\varepsilon + \Phi(\mathbf{u}_\varepsilon, v_\varepsilon),\ t > 0, \quad v_\varepsilon(0) = v^0. \tag{1.2}$$

We show rigorously that under appropriate assumptions the solutions of the reduced system, consisting of the ODE for $\mathbf{u}_\varepsilon$ and the quasi-steady state approximation for v_ε, approximate solutions of the original Cauchy problem (1.1)-(1.2) for $\varepsilon \to 0$. The proof first shows approximation of the fast species v_ε and, based on this, the approximation of the slow species $\mathbf{u}_\varepsilon$ is shown. It is obtained that the difference of the quasi-steady state approximation and the exact solution is of order $\mathcal{O}(\varepsilon)$. The work, [102], states existence of similar error estimates without proof. We then check the assumptions of the proof for the model of hematopoiesis from Chapter 2.

In **Chapter 10**, we conclude with a discussion of main challenges and restrictions of the considered models and their mathematical analysis. We summarize main results and relate them to recent biological findings. Possible application of the obtained insights to open clinical and biological questions are discussed.

The Appendices contain technical proofs and biological details used for model calibration.

Appendix A summarizes analytical results for the models in absence of leukemic cells. **Appendix B** contains technical proofs of Chapters 3 and 4. **Appendix C** provides a calibration of the hematopoietic branch of the model for three hematopoietic compartments, which is used in Chapter 6. **Appendix D** contains details about simulations of fast relapsing patients in Chapter 6. In this Appendix, reasons for early relapse after treatment are discussed and corresponding modification of the models are proposed. **Appendix E** provides a calibration of the hematopoietic branch of the model for two hematopoietic compartments. This calibration is used

in Chapter 7. **Appendix F** presents proofs of propositions in Chapter 7. **Appendix G** contain supplementary Figures for Chapters 6 and 7. **Appendix H** formulates technical details of proofs in Chapter 9.

1.3 State of the art

Due to the relative facility of blood and bone marrow sampling, the hematopoietic system and its diseases have been studied extensively, [241]. For this purpose different types of models have been developed. In the following, we give an overview over classical and more recent models of the hematopoietic system, their applications and underlying assumptions.

1.3.1 Compartmental versus structured population models

One established method to describe time evolution of the different hematopoietic cell types are compartmental models. In this type of models, each maturation stage (cell type) is identified with one compartment. Due to the enormous amount of hematopoietic cells, [111, 133], each compartment can be treated as a "well-mixed tank" and its dynamics is described by one ordinary differential equation (ODE). The use of finite systems of ordinary differential equations is motivated by the classical understanding of the hematopoietic system, where it is assumed that the hematopoietic system consists of an ordered sequence of discrete maturation states, which are sequentially traversed, [111]. Compartmental models have been applied to investigate different aspects of the hematopoietic system and its disorders.

If maturation is considered as a continuous process, structured population models are obtained, [61]. In many cases structured population models are used to take into account cell cycle duration or maturation time. They can be formulated in terms of delay differential equations (DDEs) or transport-type partial differential equations (PDEs).

1.3.2 Compartmental models of blood cell production

In [149] a two compartment model (quiescent and mitotic stem cells) with constant delay has been proposed to understand stem cell dynamics in aplastic anemia (shortage of all blood cell types) and periodic hematopoiesis (periodic oscillations of blood cell counts). In this model, the regulation of proliferation rate (flux to the mitotic compartment) is described using a Hill-function that increases if the number of quiescent stem cells decreases. The model has been used to show that both diseases, aplastic anemia and periodic hematopoiesis, could be explained by an increased death of cycling stem cells. Depending on the flux from the stem cell compartment to differentiation and depending on the rate of stem cell loss either

anemia or periodically oscillating blood cell counts are observed. This model and a slightly more complex version have been studied analytically in [175] and [5]. In [5] it is assumed that transition to the mature cell compartment decreases, if the number of quiescent stem cells decreases. Furthermore, stem cell proliferation increases, if concentration of a cytokine (signal molecule) increases. Dynamics of the cytokine concentration is modeled by an ODE including increasing production in absence of mature cells and constant degradation, [5]. The focus of the mathematical analysis in [175] and [5] is the existence of Hopf bifurcations. A similar type of model, [72], has been used to study treatment of cyclical neutropenia (periodic shortage of the major type of white blood cells). In this model, differentiation of stem cells increases, if there is a shortage of mature cells. In [49] the model from [149] has been extended to account for dynamics of stem cells, erythrocytes, platelets and leukocytes. Fluxes from the stem cell compartment to the different lineages are regulated using Hill-functions increasing, if the concentration of mature cells of the respective type decreases. The extended model has been used to investigate for which parameter ranges oscillations occur as they are observed in periodic chronic myeloid leukemia.

A detailed ODE model of human granulopoiesis (formation of granulocytes, the major type of white blood cells) under chemotherapy has been proposed in [199] and applied to clinical data, [63]. The model includes two cytokines acting on different maturation stages. If there is a shortage of mature cells or stem cells, self-renewal of the stem cell population and proliferation rate of all cell types increase. Cytokine dynamics is described using kinetic ODE models. Production of each cytokine depends on the concentrations of cells responding to it, furthermore, cell dependent and independent elimination are taken into account. It is assumed that increased cytokine concentrations lead to increased amplification rates, i.e., the number of cell divisions performed before a cell leaves a given compartment increases. Additionally, in case of low granulocyte concentrations in blood stream the release of granulocytes from bone marrow increases. Chemotherapy is modeled as a constant or dose/toxicity-dependent increase of death rates. The model is used to optimize chemotherapies and to compare the toxicity of different regimens.

In [153] a multi-compartment ODE model of hematopoiesis in mice is proposed and fitted to data. The model is applied to obtain insights into system dynamics in steady state and under perturbations. The model includes all major cell types of the different hematopoietic lineages. Proliferation and differentiation are regulated by negative feedback mechanisms depending on mature and immature cell counts. Using piece-wise linear functions the respective quantities are modified between a maximum and a minimum value. Regulatory mechanisms are only active, if cell counts decrease below a defined threshold and saturation is obtained in case of extreme perturbations. If there is a moderate shortage of one cell type,

proliferation rate of the respective cell type is increased. If there is a severe shortage of one cell type, also differentiation of the upstream cell type increases. The model is used to study system dynamics in presence and absence of these feedbacks. It is concluded that regulatory mechanisms without thresholds or absence of regulation lead to unphysiological behavior of the system.

In [156, 157] an ODE model for hematopoietic reconstitution after bone marrow transplantation is proposed. The model includes one cytokine and takes into account cytokine-dependent self-renewal of all maturation stages. Cytokine dynamics is modeled using a Hill-function decreasing, if the concentration of mature cells increases. This function has been obtained using a quasi-steady state approximation. The model is used to show that in case of shortage of mature cells up-regulation of self-renewal is a more efficient mechanism to obtain fast recovery of cell counts than up-regulation of proliferation. A generalized version of the model has been analyzed in [215]. Using this model a classification of the stem cell population based on the response to survival factors has been obtained and the impact of self-renewal probability, proliferation and apoptosis rates on loss and gain of the stemness property of the different cell types has been investigated. For this purpose the so called 'fraction of self-renewal' has been introduced. The fraction of self-renewal of a given cell type describes the fraction of progeny cells originating from divisions that are of the same type as the parent cells. In absence of immature cell death the stem cell population is characterized by a fraction of self-renewal that is higher than that of less immature celltypes. An extended version of the model with multiple signaling factors has been calibrated to clinical data and applied to show that there may exist patient populations that could benefit from enlargement of stem cell transplants, [214]. Dynamic behavior of this type of model and construction of a Lyapunov function for a two-compartment-version has been considered in [7, 85]. A version of the model studying replicative senescence is given in [158]. An application of this type of models to myelodysplastic syndrome has been described in [231]. In [182] a two compartment model similar to that in [157] is investigated. It is shown that only if stem cell self-renewal under maximal stimulation is close to 0.5 cell counts monotonically approach steady states after perturbations. Negative feedback of mature cell counts on proliferation rates reduces or eliminates damped oscillations around steady state cell counts occurring after perturbations.

Similar as in [215], in [124] linear stability analysis is used to study regulation of cell properties on the level of populations. In this work, possible feedbacks on self-renewal and proliferation leading to linear stability of a two compartment system are analyzed and compared to biological literature. Minimal controls are discussed and some results are generalized to the case of more than two compartments. It is shown that in a two compartment system there must exist at least two control loops to obtain linear stability of the positive equilibrium.

A classical work on the impact of stem cell regulation on system stability is [11]. Also in this work, the hematopoietic system serves as an example. The work considers a three compartment model in the framework of nonlinear delay differential equations. The stability of the system in presence of different monotonous regulatory feedbacks is analyzed using different methods such as Lyapunov functions. From that analysis it is concluded that different scenarios lead to biologically reasonable results. These are (a) increasing stem cell differentiation in case of large stem cell numbers and recruitment of stem cells to cell cycle in case of a lack of mature cells, (b) decreasing stem cell differentiation in case of high mature cell counts and reduced proliferation in case of large numbers of stem cells.

1.3.3 Compartmental models of stem cell self-renewal in non-hematopoietic tissues

Application of compartment models to diverse tissues stresses the importance of feedback mechanisms and especially of regulated stem cell self-renewal for efficient expansion of cell populations. The effect of stem cell regulation and self-renewal on population dynamics and robustness to perturbations has been investigated e.g., in neurogenesis in the olfactory bulb, [131, 141], or in development of intestinal crypts, [108]. The work [131] contains a general systematic numerical study of negative feedback regulation of self-renewal and proliferation by Hill-functions. The considered regulatory modes include different signals for proliferation and self-renewal of different cell stages. Scenarios with simultaneous regulation of multiple stages and cell properties are compared to scenarios with single regulatory loops. As in [157], an important conclusion of this work is that up-regulation of self-renewal is more efficient that up-regulation of proliferation, if mature cells are needed. In [141] stability properties of an ODE system describing neurogenesis of the olfactory bulb is investigated. It is concluded that auto-regulation of the progenitor cell compartment and small death rates of mature cells lead to a wide parameter range, where the equilibria are stable. In [108] the optimal temporal control of symmetric versus asymmetric cell divisions during the development of intestinal crypts is sought. Analytic results in the framework of control theory prescribe that in the considered system, optimality is only achieved, if there exists a sharp transition between purely symmetric and purely asymmetric cell divisions (so called bang-bang-control).

1.3.4 Compartmental models of (stem) cell dynamics in leukemias and other cancers

Furthermore, compartment models have been used as a tool to study the dynamics of cancer (stem) cell populations. In [162] an ODE model is proposed describing dynamics of chronic myeloid leukemia (CML) under imatinib (a tyrosine kinase

inhibitor) treatment. The model consists of 12 compartments, 4 compartments describe the different maturation stages of hematopoietic cells, 4 compartment describe different maturation stages of leukemic cells sensitive to treatment and 4 compartments describe the different maturation stages of resistant leukemic cells. It is assumed that hematopoietic stem cells regulate their own expansion to obtain convergence to a healthy equilibrium. Further regulations or interactions between leukemic and healthy cells are not included and, consequently, leukemic cells grow exponentially in absence of treatment. Mutations leading to resistance are assumed to occur at constant rates. Furthermore, it is assumed that in leukemic cells proliferation and differentiation are increased compared to healthy hematopoietic cells. Treatment is supposed to reduce the production of leukemic progenitor cells out of leukemic stem cells and of leukemic differentiated cells out of progenitors. The model is fitted to patient data showing a biphasic decrease of leukemic cell load under treatment. Since leukemic progenitors and leukemic differentiated cells have different lifespans, it is concluded that in a first phase differentiated leukemic cells decline and later in a second phase leukemic progenitors decline. The model is further applied to estimate the time until detection of resistance. In [135] an extension of the model from [162] is proposed that includes dedifferentiation of progenitor cells into stem cells. In this model, stem cell proliferation and dedifferentiation are regulated using logistic terms. In [118] the model of [162] is linked to a delay differential equation describing T-cell dynamics to study the impact of immune response on CML treatment. The interaction of leukemic cells with the immune system is also investigated in [18]. In [150] a Bayesian approach is applied to ODE models of leukemia and hematopoietic cell dynamics to characterize parameter regimens that with high probabilities lead to out-competition of hematopoiesis by leukemic cells. Another application of ODE models of leukemia is described in [242]. In this work, a two-compartment linear ODE model is used to estimate kinetic parameters describing the redistribution of chronic lymphatic leukemia (CLL) cells between blood stream and lymph nodes under therapy and to compare the effect of treatment in the two tissues.

A more general approach to model cancer cell dynamics has been described in [83], and similarly in [13]. Here, ODEs are used to model serial acquisition of mutations during carcinogenesis. It is assumed that cancer stem cells require 3 mutations, one leading to reduced apoptosis, one leading to genetic instability, i.e., increased mutation rates, and one leading to increased expansion either due to increasing proliferation or due to increasing symmetric self-renewal. The model considers the stem cell compartment and the compartment of post-mitotic cells. Taking into account that each of these two cell types can carry 0 to 3 mutations, an 8 compartment model is obtained. The model considers the following stem cell processes: death, asymmetric division, symmetric self-renewal, symmetric differentiation. It is assumed that the probability of symmetric stem cell self-renewal depends on signals secreted by stem cells with less than 3 mutations and on the

total concentration of cells with 0 to 3 mutations. Regulation is modeled using a product of a Hill-function and a logistic term: Symmetric self-renewal decreases, if stem cell counts increase and the probability of symmetric differentiation increases, if counts of mature cells with less than 3 mutations decrease or if the concentration of stem cells with 0 to 3 mutations increases. The model is used to study the impact of the order of the considered mutations on time needed for generation of one stem cell carrying all 3 hits. It is concluded that if the mutations increasing proliferation/self-renewal and genetic instability do not simultaneously increase death rates, cancer is formed fastest, if the mutation leading to genetic instability occurs first. If the mutations acting on proliferation/self-renewal and genetic instability simultaneously increase apoptosis unless the mutation, which decreases apoptosis, has occurred, cancer appears fastest, if the mutation reducing apoptosis occurs first. It has been shown that if mutations increase symmetric self-renewal, onset of cancer is much faster than in case, where they increase proliferation rate. This holds for any order of mutations. This is in line with the results from [157] on the importance of self-renewal for efficient expansion of cell populations. In [82] a maturity structured counterpart to the model from [83] is proposed and leads to similar conclusions. An ODE model describing dynamics of an arbitrary number of mutations in hierarchical cell systems can be found in [239]. Other ODE models describing effects of mutations and genetic instability on cancer dynamics can be found in [125].

1.3.5 PDE models of blood cell production

The use of ODE models requires the assumption that differentiation is a discrete process, i.e., that there exists a finite number of discrete maturation stages. To model differentiation as a continuous process partial differential equations (PDEs) of the transport type have been used. In [24] an age structured model of erythropoiesis (red blood cell formation) is proposed. The model consists of two transport equations, one for mitotic precursors and one for post-mitotic cells. Both equations are coupled by the boundary conditions. It is assumed that the outflux from the stem cell compartment and the division rate of precursors increase, if EPO (the main cytokine of erythropoiesis) concentration is high. EPO dynamics is modeled using an ODE accounting for constant degradation and EPO-production, which is described by a Hill-function decreasing with increasing mature cell counts. Reducability of the model to a system of delay differential equations and stability of the reduced system is investigated. The model is fitted to data from healthy human subjects and to experimental data from rabbits suffering autoimmune hemolytic anemia with oscillating red blood cell counts. Oscillation of blood cell counts in hemolytic anemia is explained by occurrence of a Hopf bifurcation in case of increased degradation of mature cells.

A similar approach is chosen for the analytical work in [3]. Here, the model consists of two transport equations, one describing quiescent and one describing cy-

cling stem cells. It is assumed that the rate of cells recruited to cell cycle increases, if the number of quiescent cells decreases, furthermore, apoptosis of cycling cells decreases with increasing EPO levels. EPO production is assumed to be delayed and dependent on the number of quiescent cells using a Hill-function, degradation is assumed to be constant. The model is reduced to two ODEs with constant and distributed delays. Global stability and existence of Hopf-Bifurcations of the reduced system is investigated. A similar model is analyzed in [4] and the existence of Hopf bifurcations is interpreted as occurrence of periodic hematological diseases.

A more detailed model of erythropoiesis has been proposed in [77]. The model consists of five transport equations corresponding to the different cell types of erythropoiesis. Depending on the cell type proliferation rate, apoptosis rate and maturation velocity change non-linearly in dependence of EPO and iron levels. Concerning EPO dynamics it is assumed that EPO production by kidney can be directly computed from erythrocyte concentrations and that EPO is degraded at a constant rate. Kinetics of administered EPO are also described by an ODE. The model is carefully fitted to patient data and applied to different medical scenarios, e.g., erythrocyte regeneration after blood donation and optimization of therapeutic EPO administration in dialysis patients.

In [170] a transport equation coupled with two ODEs is used to model recovery of granulocytes after bone marrow transplantation. The transport equation describes maturation of cells, dynamics of mature cells and dynamics of the cytokine are described by one ODE respectively. Cytokine (G-CSF, the major cytokine of granulocytopoiesis) dynamics are governed by production, which decreases for increasing granulocyte counts, by cell dependent and cell independent degradation. It is assumed that proliferation rates increase with increasing cytokine concentrations, simultaneously maturation speed decreases for the more immature marrow cells and increases for the more mature ones. Mobilization of cells into bloodstream increases with maturity and with cytokine stimulation. Furthermore, it is assumed that cells from bloodstream have higher clearance, if blood cell counts are low. The latter is motivated by increased cell migration to tissue, if the number of cells in the tissue compartment is low. The model is fitted to data from patients after bone marrow transplantation. Main conclusions are that the time to engraftment (recovery to $5 \cdot 10^8$ granulocytes per liter of blood after transplantation) mainly depends on the number of CFU-GM (one differentiation stage of granulocytes) in the transplant and on the sensitivity of the regulated quantities to changes in cytokine concentration. Especially, reduced maturation speed of mitotic immature stages shortens engraftment time. Furthermore, cytokine dependence of maturation speed and proliferation rates seem necessary to reproduce clinical observations. These findings are in line with the results reported in [157], where it has been shown that up-regulation of self-renewal accelerates engraftment.

More theoretical works on the application of PDE models in hematopoiesis have been proposed in [61] and [91]. In [61] continuous maturation of progenitor cells is described using a transport equation and dynamics of stem and mature cells are modeled using ODEs. This model is a continuous counterpart of the model in [157]. A Hill function dependent on mature cell concentration is used to model that stem cell differentiation and maturation speed decrease in case of a shortage of mature cells. It has been shown that absence of a regulation of progenitor cell self-renewal may lead to persistent oscillations. Comparison of this model to its discrete counterpart shows important differences between the discrete (ODE) and the continuous (PDE) approach: In contrast to the continuous model the discrete model has semi-trivial steady states. Furthermore, the continuous model cannot be obtained as a limit of discrete models, since in the discrete model it is assumed that differentiation can only occur after a division.

In [91] a trait structured 2 compartment model is considered to investigate selection processes e.g., in leukemia. It is shown that if all cells have the same proliferation rate, only cells with maximal self-renewal are able to expand and converge to a positive steady state, while all other cells go to extinction.

1.3.6 Stochastic and individual based models of hematopoiesis and its disorders

Both, ODE and PDE models are based on the assumption of large homogeneous cell populations. In case of small cell populations stochastic effects have to be taken into account. In opposite to population models, individual based models describe phenomena on the level of individual cells. Therefore, they are also valid in case of small cell numbers. One major issue of this approach is its computational inefficiency in case of large numbers of individuals.

A prominent example for individual based models of the hematopoietic system is described in [184]. This model treats differentiation as a process that is reversible up to a certain threshold. It is assumed that cell behavior emerges from switching of cells between two 'environments'. In one 'environment' cells do not divide, the longer cells reside there, the higher becomes their affinity to it. In the second environment cells divide and loose their affinity to the resting environment. The probability that an individual cell switches from one 'environment' to the other depends on its affinity to the resting 'environment' and on the cell number in the 'environment' to which it switches. Affinity to the resting 'environment' is interpreted as a measure for stemness. In [183] this type of model is applied to describe treatment of CML. In this framework, leukemic cells possess different transition characteristics, i.e., higher probability to switch between environments in comparison to healthy hematopoietic cells. Continuous approximations for this

model have been developed in the framework of age-structured populations, [60].

Also the Gillespie Algorithm can be used simulate population dynamics on the basis of single cells. In [182] an individual based two compartment model with stem cell regulations similar as in [157] is considered. As an additional feature the model includes space and considers contact inhibition of stem cells. Simulations of this model suggest that in comparison to the model without space, damped oscillations occurring due to perturbations of steady states, are diminished in amplitude or even absent.

Another approach to model stochastic effects is the framework of branching processes. In [222] a combination of ODEs and branching processes is used to estimate the number of drug-resistant cancer cells at the time of tumor detection. Fitting of the model to CML data suggests that the rate of self-renewal is enhanced in LSC compared to HSC. Using a similar methodology estimates for the number of somatic (non tumor specific) mutations taking place before tumor initiation have been derived, [223].

The Moran process is often used to take into account stochastic effects. A review of application of the Moran process to hematopoietic diseases is given in [57]. The study of mutation acquisition and the expansion of mutant clones is one application of the Moran process. In [201] a two compartment (stem and transit amplifying cells) Moran process model is used to investigate the impact of symmetric versus asymmetric stem cell divisions on the occurrence of cells carrying two different mutations. It is assumed that with a fixed probability one of the daughter cells arising from division of a wild type (non-mutated) cell, carries a mutation. Similarly, one of the daughter cells arising from division of a cell carrying one mutations will carry two mutations, with a fixed probability. Numerical and analytic results show that independent of the mutant fitness higher rates of symmetric cell divisions lead to reduced production of double hit mutants. This observation might explain why stem cells preferentially divide symmetrically in many systems.

In [240] a Moran process model is proposed to investigate response of leukemia cell cultures to imatinib. It is assumed that the fitness of imatinib resistant cells is reduced compared to that of imatinib sensitive cells in absence of drugs and that fitness of sensitive cells decreases with increasing imatinib concentrations. The impact of phenotypic switching, i.e., change of cell properties in absence of mutations on imatinib resistance in cell cultures is discussed.

In [225] a Moran process model is used to describe the dynamics of neutral mutations, i.e., mutations that do not affect fitness of an individual. The model is used to explain outbreak of diseases caused by mutations without fitness advantage.

Applications to chronic myeloid leukemia and paroxysmal nocturnal hematuria are discussed. In [138] a model of the hematopoietic system is proposed that combines ODEs for compartments with high cell counts and Moran type models for compartments with low cell counts. This approach has been applied to study wash-out of CML cells under imatinib-treatment.

Other examples for stem cell models can be found e.g., in [59, 172], where the impact of noise on stem cell dynamics is studied or in [130], where the impact of senescence on cancer cell dynamics and cancer treatment is studied. In [154] a combination of stochastic and deterministic methods is used to investigate under which conditions stem cells showing altered behavior successfully invade a stem cell niche.

In summary, different mathematical approaches to model leukemia cell dynamics have been developed. Depending on the question that is investigated, the mathematical approach and the level of detail vary considerably. In the simplest case periodic solutions of deterministic models of the blood system are interpreted as leukemias, since very rarely leukemias with oscillating blood cell levels have been observed, [3, 49, 175] (for a medical example and a list of more case reports see [151]). Also unstable parameter regimens for models of hematopoiesis have been interpreted as occurrence of leukemia, [60]. On a more detailed level, different cancer cell types are explicitly incorporated, either on the level of cell populations or on the level of individual cells, e.g., [150, 162, 183]. In [150] a Bayesian approach is applied to ODE models to characterize parameter regimens that with high probabilities lead to out-competition of hematopoiesis by leukemic cells.

Part I

Development and analysis of mathematical models of acute leukemias

CHAPTER 2

MODELS OF LEUKEMIA

2.1 Outline of the chapter

In this Chapter, we develop two mathematical models of leukemia. The models considered here focus on the interaction between hematopoietic and leukemic cells. Since main symptoms of leukemias originate from the impairment of healthy blood cell formation, [139], it is crucial to understand how presence of leukemic cells affects hematopoiesis. Up to now, the interaction between healthy and malignant cells has not been well understood and different hypotheses concerning possible regulatory modes have been proposed; see [163] and references below. The models developed in this Chapter will be applied to analyze the impact of different interaction modes on clinical course and dynamic properties of the system. In Section 2.2, we present the derivation of a model of healthy blood cell production, which is, then, extended to describe dynamics of leukemias in Sections 2.3 and 2.4.

2.2 Model of hematopoiesis

2.2.1 Compartmental structure and model parameters

For simplicity, we only consider one hematopoietic lineage consisting of an ordered sequence of n maturation steps (compartments), which are sequentially traversed. This discrete view of the hematopoietic system is in line with the clinical literature, [111, 209]. The first compartment describes the population of hematopoietic stem cells (HSC) and the nth compartment stands for the population of post-mitotic mature cells, e.g., mature white blood cells. We denote by $c_i(t)$ $(i = 1, \ldots, n)$ the cell counts in the compartment i of the healthy hematopoiesis at time t. A scheme of the model is presented in Figure 2.1.

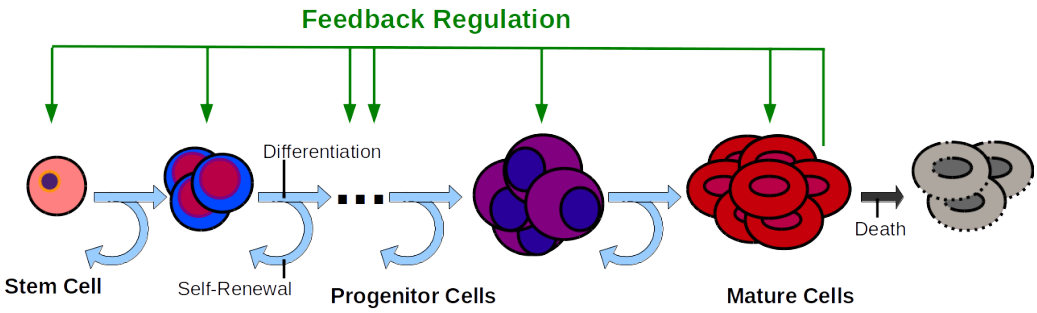

Figure 2.1: Scheme of the model of hematopoiesis.

Healthy cells in compartment i are characterized by the following properties.

- **Proliferation rate** $p_i^c(t)$ in compartment i at time t, describing how often a cell divides per unit of time. We assume that cells of the most mature compartment are post-mitotic, i.e., $p_n^c(t) \equiv 0$.

- **Fraction of self-renewal** $a_i^c(t)$ in compartment i at time t, i.e., the fraction of progeny cells returning to the compartment occupied by the parent cells that gave rise to them (process referred to as self-renewal). The fraction $1–a_i^c(t)$ of progeny cells moves on to the compartment $i+1$ (process referred to as differentiation). Based on our earlier work, [157], we assume that the fraction of self-renewal is regulated by feedback-signaling. Figure 2.2 illustrates the fraction of self-renewal.

- **Death rate** d_i^c in compartment i, describing which fraction of cells dies per unit of time. For simplicity, death rates are assumed to be zero or constant in time. In accordance with biology, we further assume $d_n^c > 0$.

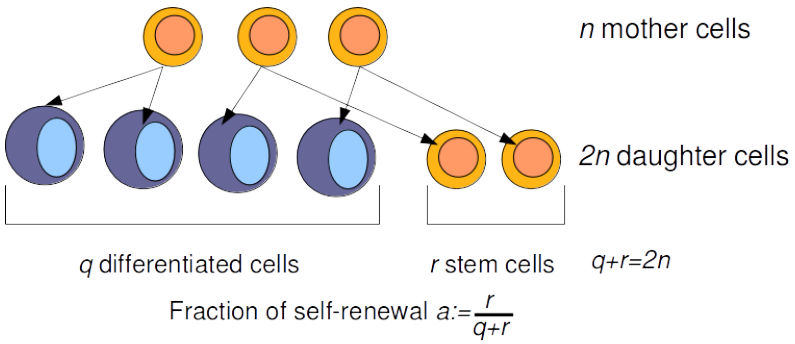

Figure 2.2: Illustration of the fraction of self-renewal. The fraction of self-renewal is defined as the fraction of progeny cells adopting the same fate as the parent cells that gave rise to them.

Based on the notation specified above, the flux to mitosis in compartment $i < n$ at time t equals $p_i^c(t)c_i(t)$. During mitosis a parent cell disappears and gives rise to two progeny cells. The outflux from mitosis at time t equals $2p_i^c(t)c_i(t)$, of which the fraction $2a_i^c(t)p_i^c(t)c_i(t)$ stays in compartment i. The fraction $2\big(1 - a_i^c(t)\big)p_i^c(t)c_i(t)$ moves to compartment $i+1$. Since stem cells are the most primitive cells, there exists no influx to the stem cell compartment due to differentiation. These processes are illustrated in Figure 2.3. With the additional assumption that the most mature cells are post-mitotic, time evolution of the healthy hematopoietic compartments is described by the system of equations (2.1).

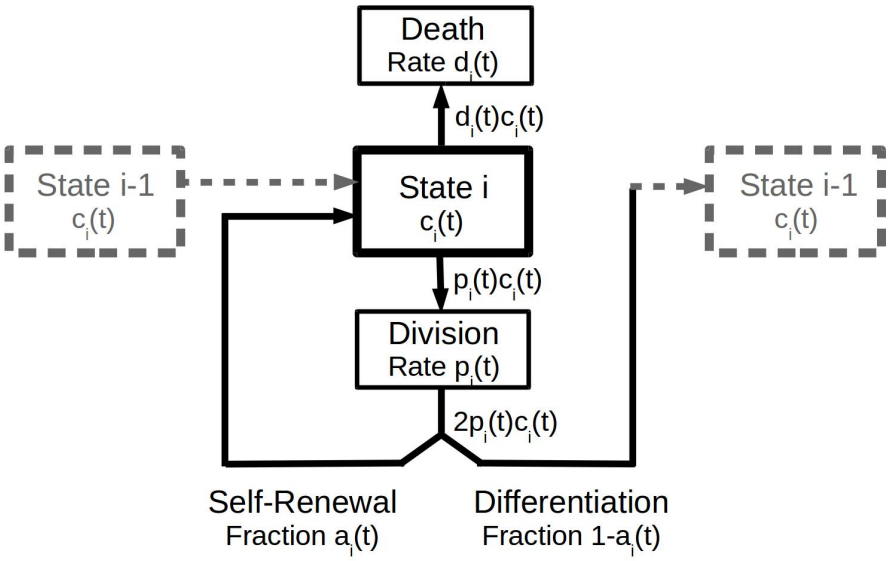

Figure 2.3: Cell fluxes in compartment i. Cell fluxes resulting from proliferation, self-renewal and cell death in cell compartment i.

$$
\begin{aligned}
\frac{d}{dt}c_1(t) &= \big(2a_1^c(t) - 1\big)p_1^c(t)c_1(t) - d_1^c c_1(t), \\
&\vdots \quad \vdots \quad \vdots \\
\frac{d}{dt}c_i(t) &= 2\big(1 - a_{i-1}^c(t)\big)p_{i-1}^c(t)c_{i-1}(t) + \big(2a_i^c(t) - 1\big)p_i^c(t)c_i(t) - d_i^c c_i(t), \quad 1 < i < n, \\
&\vdots \quad \vdots \quad \vdots \\
\frac{d}{dt}c_n(t) &= 2\big(1 - a_{n-1}^c(t)\big)p_{n-1}^c(t)c_{n-1}(t) - d_n^c c_n(t).
\end{aligned}
\tag{2.1}
$$

with initial data given by $c_1(0) > 0, c_2(0) \geq 0, \cdots, c_n(0) \geq 0$.

2.2.2 Regulatory feedback

Formation of healthy blood cells is regulated by a negative feedback. If there is a need for more blood cells of a certain type, the concentration of signaling molecules (cytokines) increases and stimulates formation of mature cells, [76, 134, 160]. Important examples of hematopoietic cytokines are erythropoietin (EPO) for erythropoiesis (red blood cell formation) and granulocyte colony stimulating factor (G-CSF) for granulopoiesis (formation of granulocytes, the major type of white blood cells), [160].

White blood cells (leukocytes) are important for immune function. Most leukemias are diseases of white blood cells. Therefore, we model the dynamics of white blood cells and leukemic cells. For simplicity, we consider only one cytokine and focus on G-CSF, which is the major signaling factor regulating granulocyte formation, [160]. G-CSF concentrations influence properties of stem cells, [155], and more mature cells, [145]. Based on knowledge of G-CSF, [134, 160, 206], we assume that cytokine molecules are produced at a constant rate α, degraded at a constant rate β (e.g., by liver or kidney, [244]) and eliminated proportionally to the density of mature cells at a constant positive rate μ. The latter is motivated by the mechanism of cell dependent G-CSF degradation: G-CSF is eliminated by receptor-mediated endocytosis, [244]. The density of receptors on mature cells is much higher that on immature cells. For this reason we neglect signal degradation by immature cells, [206]. We obtain the following model for dynamics of cytokine concentration, denoted by $S(t)$,

$$\frac{d}{dt}S(t) = \alpha - \beta S(t) - \mu S c_n(t). \tag{2.2}$$

Assuming that the process is fast in comparison to cell cycle duration as proposed by biological data, [30, 164], we apply a quasi-steady state approximation. Substitution of $s(t) := \frac{\mu}{\alpha}S(t)$ and $k := \frac{\beta}{\mu}$ leads to

$$s(t) = \frac{1}{1 + k c_n(t)} \in (0, 1].$$

Numerical solutions of the proposed model, validated based on the clinical observations of hematopoiesis after bone marrow transplantation, [156, 157, 214], as well as analytic stability results in [85, 157, 167] indicate that the regulation of self-renewal is a more efficient mechanism than the regulation of proliferation rates. Similar conclusions were drawn using the models of multistage cell lineages applied to regeneration and maintenance of the mouse olfactory epithelium, [131, 141].

In the remainder of this thesis, we assume that the regulatory mechanism is based on the feedback inhibition of self-renewal depending on the level of mature cells. Since the exact relationship of cell properties and signal concentration is not

known, we parsimoniously assume it to be linear, i.e., $a_i^c(t) := a_{i,max}^c s(t)$, where $a_{i,max}^c \in (0,1)$.

2.2.3 Model equations

The above assumptions result in the following model of healthy hematopoiesis.

$$
\begin{aligned}
\frac{d}{dt}c_1(t) &= \big(2a_{1,max}^c s(t) - 1\big)p_1^c c_1(t) - d_1^c c_1(t), \\
&\vdots \quad \vdots \quad \vdots \\
\frac{d}{dt}c_i(t) &= 2\big(1 - a_{i-1,max}^c s(t)\big)p_{i-1}^c c_{i-1}(t) + \big(2a_{i,max}^c s(t) - 1\big)p_i^c(t)c_i(t) \\
&\quad -d_i^c c_i(t), \quad 1 < i < n, \\
&\vdots \quad \vdots \quad \vdots \\
\frac{d}{dt}c_n(t) &= 2\big(1 - a_{n-1,max}^c s(t)\big)p_{n-1}^c c_{n-1}(t) - d_n^c c_n(t), \\
s(t) &= \frac{1}{1 + kc_n(t)}.
\end{aligned}
\tag{2.3}
$$

with initial data given by $c_1(0) > 0, c_2(0) \geq 0, \cdots, c_n(0) \geq 0$.

Remark 2.1
This model is based on the quasi-steady state assumption. As proven in Chapter 9, Model (2.3) *is an* $\mathcal{O}(\varepsilon)$ *approximation of the following system* (2.4)*, where cytokine dynamics is described by a rescaled and slightly modified version of equation* (2.2)*.*

$$
\begin{aligned}
\frac{d}{dt}c_1(t) &= \big(2a_{1,max}^c s(t) - 1\big)p_1^c c_1(t) - d_1^c c_1(t), \\
&\vdots \quad \vdots \quad \vdots \\
\frac{d}{dt}c_i(t) &= 2\big(1 - a_{i-1,max}^c s(t)\big)p_{i-1}^c c_{i-1}(t) + \big(2a_{i,max}^c s(t) - 1\big)p_i^c(t)c_i(t) \\
&\quad -d_i^c c_i(t), \quad 1 < i < n, \\
&\vdots \quad \vdots \quad \vdots
\end{aligned}
$$

$$\begin{aligned} &\vdots \quad \vdots \quad \vdots \\ \frac{d}{dt}c_n(t) &= 2\big(1 - a^c_{n-1,max}s(t)\big)p^c_{n-1}c_{n-1}(t) - d^c_n c_n(t), \\ \varepsilon\frac{d}{dt}s(t) &= 1 - kc_n(t)s(t) - s(t), \end{aligned} \tag{2.4}$$

with initial data given by $c_1(0) > 0, c_2(0) \geq 0, \cdots, c_n(0) \geq 0, s(0) \geq 0$.
We make the following assumptions on parameters in models (2.3) *and* (2.4).

Assumptions 2.2

(i) $a^c_{i,max} \in (0,1)$ *for* $1 \leq i \leq n-1$,

(ii) $p^c_i > 0$ *for* $1 \leq i \leq n-1$,

(iii) $d^c_i \geq 0$ *for* $1 \leq i \leq n-1$, $d^c_n > 0$,

(iv) $k > 0$.

Model (2.3) has been developed in [157, 212] and analyzed in [85, 123, 167, 212, 215].

2.3 Model of a signal-dependent leukemia (Model 1)

2.3.1 Compartmental structure

We now extend the model (2.3) of the hematopoietic system and include one leukemic cell line. There is evidence that in case of acute myeloid leukemia (AML) the leukemic cell population consists of an ordered sequence of cell states, similar to the healthy hematopoietic cell line, [31, 100]. The cell type at the top of the hierarchy is referred to as leukemic stem cell (leukemia stem cell, leukemia initiating cell, LIC) and gives rise to all leukemic cell types.

For simplicity, we model the interaction of one hematopoietic lineage consisting of n compartments and one leukemic lineage consisting of m compartments. Cells of each compartment are characterized by proliferation rate, fraction of self-renewal and death rate, as defined in Section 2.2.1. Proliferation rate at time t of cells in leukemic compartment i is denoted as $p^l_i(t)$. In analogy fraction of self-renewal and death rate of leukemic cell type i at time t are denoted as $a^l_i(t)$ and $d^l_i(t)$. We denote by $l_i(t), (i = 1, \cdots, m)$ the density of leukemic cells of type i at time t. A scheme of the model is presented in Figure 2.4.

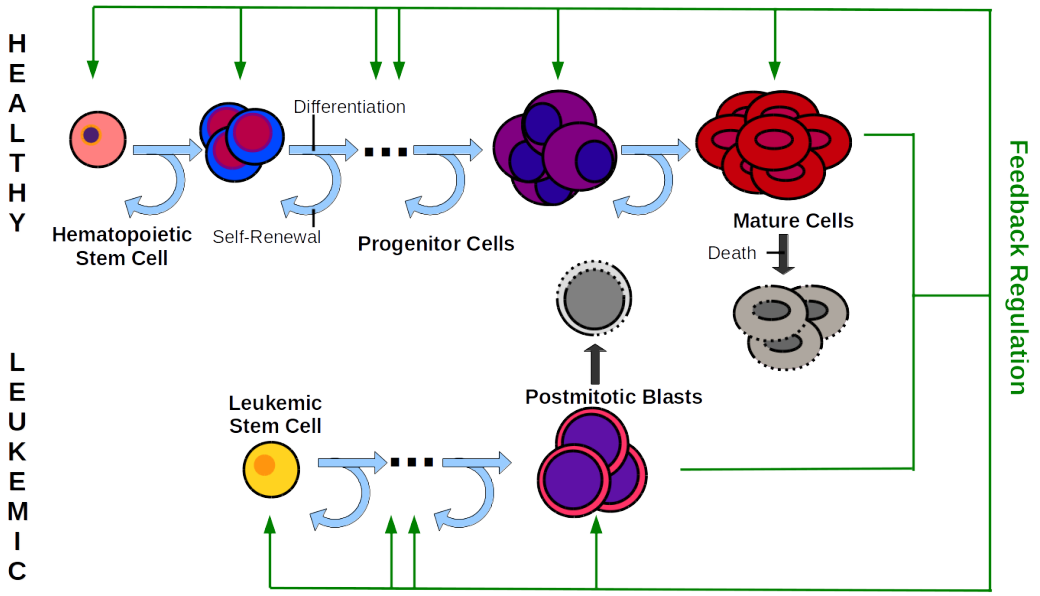

Figure 2.4: Model of signal-dependent leukemia. Both cell lines, hematopoietic and leukemic, depend on the same feedback signal.

2.3.2 Regulatory feedback

In Model 1, we assume that leukemic cells depend on the same cytokines as healthy hematopoietic cells. This assumption is justified by the following biological findings:

- Leukemic cells express the same cytokine receptors as hematopoietic cells, [126, 206].
- Leukemic cells of some patients expand in the presence of cytokines, [230].
- Leukemic stem cell proliferation and maintenance of stemness properties require bone marrow niche factors known to maintain hematopoietic stem cells, [217].

We assume that dynamics of the hematopoietic system are described by the model (2.3) in Section 2.2. As for hematopoietic cells, we assume that self-renewal of leukemic cells depends on the cytokine level s. Since hematopoietic and leukemic cells can absorb cytokine molecules, [126, 206], the two cell lineages interact through competition for the cytokine. To model this competition we assume degradation of the signal s by the most mature leukemic cells and by mature blood cells. Based on the steady state assumption described in Section 2.2 we obtain:

$$s(t) := \frac{1}{1 + k^c c_n(t) + k^l l_m(t)}$$

or

$$s(t) := \frac{1}{1 + k^c c_n(t) + \sum_{i=1}^{m} k_i^l l_i(t)},$$

if we take into account signal degradation by all leukemic cell types. Here k^c, k^l and k_i^l are non-negative constants.

2.3.3 Model equations

We obtain the following system of model equations.

$$\begin{aligned}
\frac{d}{dt}c_1(t) &= \big(2a_{1,max}^c s(t) - 1\big)p_1^c c_1(t) - d_1^c c_1(t),\\
\frac{d}{dt}c_i(t) &= 2\big(1 - a_{i-1,max}^c s(t)\big)p_{i-1}^c c_{i-1}(t) + \big(2a_{i,max}^c s(t) - 1\big)p_i^c(t)c_i(t)\\
&\quad -d_i^c c_i(t), \quad 1 < i < n,\\
\frac{d}{dt}c_n(t) &= 2\big(1 - a_{n-1,max}^c s(t)\big)p_{n-1}^c c_{n-1}(t) - d_n^c c_n(t),\\
\frac{d}{dt}l_1(t) &= \big(2a_{1,max}^l s(t) - 1\big)p_1^l l_1(t) - d_1^l l_1(t),\\
\frac{d}{dt}l_i(t) &= 2\big(1 - a_{i-1,max}^l s(t)\big)p_{i-1}^l l_{i-1}(t) + \big(2a_{i,max}^l s(t) - 1\big)p_i^l(t)l_i(t)\\
&\quad -d_i^l l_i(t), \quad 1 < i < m,\\
\frac{d}{dt}l_m(t) &= 2\big(1 - a_{m-1,max}^l s(t)\big)p_{m-1}^l l_{m-1}(t) - d_m^l l_m(t),\\
s(t) &= \frac{1}{1 + k^c c_n(t) + k^l l_m(t)},
\end{aligned} \tag{2.5}$$

with given initial data $c_1(0), \cdots, c_n(0), l_1(0), \cdots, l_m(0)$.

Following biological interpretation, we make the following assumptions on parameters.

Assumptions 2.3

(i) $p_i^c > 0$ *for* $1 \le i \le n-1$, $p_i^l > 0$ *for* $1 \le i \le m-1$,

(ii) $a_i^c \in (0,1)$ *for* $1 \le i \le n-1$, $a_i^l \in (0,1)$ *for* $1 \le i \le m-1$,

(iii) $d_i^c \ge 0$ *for* $1 \le i \le n-1$, $d_i^l \ge 0$ *for* $1 \le i \le m-1$,

(iv) $d_n^c > 0$, $d_m^l > 0$,

(v) $k^c > 0$, $k^l > 0$,

(vi) $c_1(0) > 0$, $c_i(0) \geq 0$ *for* $2 \leq i \leq n$, $l_1(0) > 0$, $l_i(0) \geq 0$ *for* $2 \leq i \leq m$.

This model has been published as *Stiehl and Marciniak-Czochra, Mathematical modeling of leukemogenesis and cancer stem cell dynamics, 2012*, [216].

2.4 Model of a signal-independent leukemia (Model 2)

2.4.1 Compartmental structure

We consider again the interaction of one leukemic cell line consisting of m compartments and one hematopoietic cell line consisting of n compartments. We use the same notation as in Section 2.3. The model is illustrated in Figure 2.5.

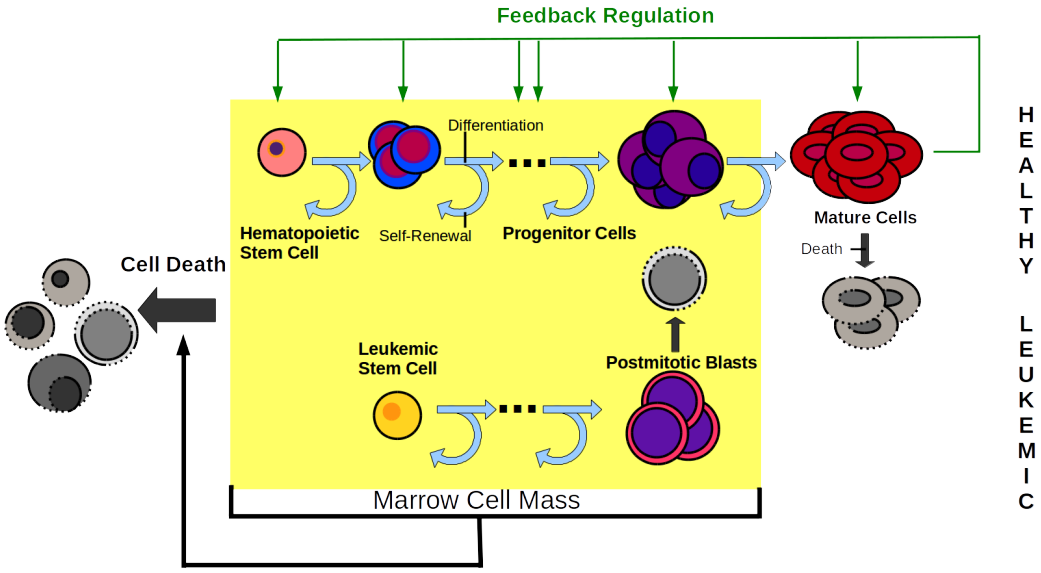

Figure 2.5: Model of signal-independent leukemia. The leukemic cell line is independent of hematopoietic cytokines. Crowding in marrow space results in increased apoptosis.

2.4.2 Regulatory feedback

There is evidence that in some patients malignant cells show constitutive activation of certain signaling cascades and, thus, may become independent of external signals, [98, 173, 178]. Hence, in contrast to the previous Section, we assume that leukemic cells are independent of hematopoietic cytokines, whereas the

hematopoietic cell types depend on the nonlinear feedback described in Section 2.2. Interaction between the healthy and cancerous cell lines is modeled through a competition for space resulting in an increased cellular degradation, for example, due to overcrowded bone marrow space. These assumptions are justified by the following evidence.

- In the presence of certain mutations, leukemic cells expand independently of basic environmental signaling cues, [98].

- Markers for cell death such as LDH, [34, 67, 128, 243], are increased in bloodstream of leukemic patients and enhanced cell death is observed in marrow samples, [107].

- Several mechanisms for spatial competition have been described. These are (i) physical stress owing to overcrowding leads to extinction of cells (e.g. [86]; recently challenged by [163]), (ii) competition for a limited niche surface expressing certain receptors (contact molecules) necessary for survival of healthy and leukemic cells, [37, 246], and apoptosis (cell death) occurs, if no contacts to these molecules can be established, [80].

We model the space competition by introducing a death (apoptosis) rate that increases with the number of cells in bone marrow and acts on all cell types residing in bone marrow, i.e., leukemic cells as well as mitotic hematopoietic cells. This rate is described by a function $d_c : \mathbb{R}_0^+ \to \mathbb{R}_0^+$, where $\mathbb{R}_0^+ := \{x \in \mathbb{R} \mid x \geq 0\}$. We assume that d_c is a non-negative increasing, locally Lipschitz continuous function with $\lim_{x\to\infty} d_c(x) = \infty$. We further assume that under healthy conditions there exists no cell death due to space competition. This assumption is in line with bone marrow histology, [143]. Therefore, we assume that $d_c(x) = 0$, if the total cell count is below a certain threshold and that it is strictly monotonically increasing otherwise.

For simplicity, we assume that all leukemic cells, except those of the last stage, stay in bone marrow. Cells of the last stage can either leave marrow space or not. The number of leukemic cells exiting bone marrow is highly variable among individuals and only partially dependent on the leukemia subtype, [27, 58, 218].

2.4.3 Model equations

We obtain the following system of ODEs:

$$
\begin{aligned}
\frac{d}{dt}c_1(t) &= (2a_1^c s(t) - 1)p_1 c_1(t) - d_1^c c_1(t) - d_c(t)c_1(t)\\
\frac{d}{dt}c_2(t) &= 2(1 - a_1^c s(t))p_1^c c_1(t) + (2a_2^c s(t) - 1)p_2 c_2(t) - d_2^c c_2(t) - d_c(t)c_2(t)\\
&\vdots\\
\frac{d}{dt}c_i(t) &= 2(1 - a_{i-1}^c s(t))p_{i-1}^c c_{i-1}(t) + (2a_i^c s(t) - 1)p_i c_i(t) - d_i^c c_i(t) - d_c(t)c_i(t)\\
&\vdots\\
\frac{d}{dt}c_{n-1}(t) &= 2(1 - a_{n-2}^c s(t))p_{n-2}^c c_{n-2}(t) + (2a_{n-1}^c s(t) - 1)p_{n-1} c_{n-1}(t) - d_{n-1}^c c_{n-1}(t)\\
&\quad - d_c(t)c_{n-1}(t)\\
\frac{d}{dt}c_n(t) &= 2(1 - a_{n-1}^c s(t))p_{n-1}^c c_{n-1}(t) - d_n c_n(t)
\end{aligned}
\tag{2.6}
$$

$$
\begin{aligned}
\frac{d}{dt}l_1(t) &= (2a_1^l - 1)p_1^l l_1(t) - d_1^l l_1(t) - d_c(t)l_1(t)\\
\frac{d}{dt}l_2(t) &= 2(1 - a_1^l)p_1^l l_1(t) + (2a_2^l - 1)p_2^l l_2(t) - d_2^l l_2(t) - d_c(t)l_2(t)\\
&\vdots\\
\frac{d}{dt}l_i(t) &= 2(1 - a_{i-1}^l)p_{i-1}^l l_{i-1}(t) + (2a_i^l - 1)p_i^l l_i(t) - d_i^l l_i(t) - d_c(t)l_i(t)\\
&\vdots\\
\frac{d}{dt}l_{m-1}(t) &= 2(1 - a_{m-2}^l)p_{m-2}^l l_{m-2}(t) + (2a_{m-1}^l - 1)p_{m-1}^l l_{m-1}(t) - d_{m-1}^l l_{m-1}(t)\\
&\quad - d_c(t)l_{m-1}(t)\\
\frac{d}{dt}l_m(t) &= 2(1 - a_{m-1}^l)p_{m-1}^l l_{m-1}(t) - d_m^l l_m(t) - d_c(t)l_m(t)\chi
\end{aligned}
\tag{2.7}
$$

$$
\begin{aligned}
s(t) &= \frac{1}{1 + kc_n(t)}\\
d_c(t) &\equiv \hat{d}_c \left(\sum_{i=1}^{n-1} c_i(t) + \sum_{i=1}^{m-1} l_i(t) + \chi l_m(t) \right)
\end{aligned}
\tag{2.8}
$$

and $\chi \in [0, 1]$ and given non-negative initial conditions.

Remark 2.4
The choice $\chi = 0$ corresponds to the scenario that all leukemic cells of the last stage leave bone marrow, the choice $\chi = 1$ corresponds to the opposite scenario that all leukemic cells stay in bone marrow.

Motivated by their biological meaning, we make the following assumptions on model parameters.

Assumptions 2.5

(i) $a_i^l \in (0,1) \subset \mathbb{R}$,

(ii) $p_i^l > 0$, *for* $1 \leq i \leq m-1$,

(iii) $d_i^l \geq 0$, *for* $1 \leq i \leq m-1$, $d_m^l > 0$,

(iv) $\hat{d}_c : \mathbb{R} \to \mathbb{R},\ x \mapsto \begin{cases} 0,\ x < \hat{x} \\ g(x),\ x \geq \hat{x} \end{cases}$,
where $g : \mathbb{R}_0^+ \to \mathbb{R}_0^+$ is a locally Lipschitz continuous, strictly monotonically increasing function with $g(\hat{x}) = 0$, $\lim_{x\to\infty} g(x) = \infty$ and $\hat{x} > \sum_{i=1}^n \bar{c}_i^+$. Here, $\bar{c}_i^+$ denote the unique positive steady state values of c_i of the model system (2.3) *describing healthy hematopoiesis.*

(v) The initial conditions fulfill $c_1(0) > 0, c_2(0) \geq 0, \cdots, c_n(0) \geq 0$, $l_1(0) > 0, l_2(0) \geq 0, \cdots, l_m(0) \geq 0$.

The model described here has been introduced in *Stiehl, Baran, Ho, Marciniak-Czochra, Clonal selection and therapy resistance in acute leukaemias: mathematical modelling explains different proliferation patterns at diagnosis and relapse, 2014*, [213].

2.5 Summary

In this Chapter, we develop two different models describing the interaction of leukemic and hematopoietic cells. The models can be interpreted as two extremes of a continuum: In the first model, we assume that leukemic cells are fully dependent on growth signals, whereas in the second model, we assume that they are fully independent of hematopoietic growth factors. The following Table 2.1 summarizes the basic assumptions of the two models.

	Signal-dependent Leukemia (Model 1)	**Signal-independent Leukemia (Model 2)**
Leukemic cells	need hematopoietic cytokines for expansion	expand independently of hematopoietic cytokines
Healthy cells	regulated by cytokine feedback	regulated by cytokine feedback
Interaction	competition for cytokine molecules, decreased self-renewal in case of low cytokine concentrations	competition for bone marrow space, death in case of overcrowded marrow space

Table 2.1: Comparison of the proposed leukemia models.

CHAPTER 3

ANALYSIS OF THE MODEL OF A SIGNAL-DEPENDENT LEUKEMIA (MODEL 1)

3.1 Outline of the chapter

In this Chapter, we present mathematical analysis of the model of signal-dependent leukemias (Model 1) introduced in Chapter 2, Section 2.3 (pp. 28).

Main achievements of this Chapter are

- Characterization of the non-negative steady states (Proposition 3.16 and Remark 3.18): We show that the model allows two types of non-negative steady states. The first type requires that either all hematopoietic or all leukemic cells become extinct. The second type of steady states consists of a one dimensional manifold. The different types of steady states are linked to cancerous diseases of the hematopoietic system such as preleukemic states, myelodysplasias, gammopathies (Example 3.19) or acute myeloid leukemias (Example 3.20).

- Establishment of necessary and sufficient conditions for destabilization of the steady state corresponding to healthy homeostasis (Proposition 3.21): We show that enhanced self-renewal of leukemic stem cells is a crucial feature for development of leukemias and even more important than increased cell proliferation (Remark 3.27). We provide a systematic classification of parameter relations (proliferation rate, death rate, fraction of self-renewal) allowing for expansion of leukemic cells (Corollary 3.23). We state hematological malignancies adopting the predicted strategies (Biological Remarks 3.24-3.26) and discuss possible treatment approaches (Remark 3.28).

- Full linear stability analysis of a minimal version of the system (4 equations): We show that the steady state, where hematopoietic cells become extinct, is linearly stable under the assumptions that leukemic cell properties allow expansion of leukemic cells (Proposition 3.30). We show that if there exists a manifold of steady states, this manifold is a center manifold (Proposition 3.36) and we characterize the behavior of the system in the vicinity of this center manifold (Proposition 3.42). We demonstrate that for wide parameter ranges the system converges to this center manifold and we characterize parameter ranges for which the center manifold is not stable (Proposition 3.42). We link the results to clinical observations and discuss possible treatment approaches (Biological Remarks 3.45 and 3.46).

The analysis provided in this Chapter has been published as *Stiehl and Marciniak-Czochra, Mathematical modeling of leukemogenesis and cancer stem cell dynamics, 2012*, [216].

3.2 Existence, uniqueness, boundedness

Proposition 3.1 (Existence, uniqueness and boundedness)
Let Assumptions 2.3 hold. Then, the system (2.5) *has unique global solutions. The solutions are non-negative and uniformly bounded.*

PROOF
It holds $\frac{d}{dt}c_i|_{c_i=0} \geq 0$ for all $1 \leq i \leq n$ and $\frac{d}{dt}l_i|_{l_i=0} \geq 0$ for all $1 \leq i \leq m$. This implies non-negativity of solutions for non-negative initial values. The non-negativity implies that $0 < s \leq 1$. For showing boundedness, we can assume that $c_i(0) > 0$ for all i. Otherwise there exists $t_0 > 0$ such that $c_i(t_0) > 0$ for all i, since $c_1(0) > 0$. We consider $q_{1/2} := \frac{c_1}{c_2}$ fulfilling the initial value problem

$$\begin{aligned}\frac{d}{dt}q_{1/2} &= \frac{\left(\frac{d}{dt}c_1\right)c_2 - \left(\frac{d}{dt}c_2\right)c_1}{c_2^2} \\ &= [(2a_1s-1)p_1 - d_1]q_{1/2} - \frac{(2(1-a_1s)p_1c_1 + (2a_2s-1)p_2c_2 - d_2c_2)c_1}{c_2^2} \\ &= [(2a_1s-1)p_1 - d_1]q_{1/2} - 2(1-a_1s)p_1q_{1/2}^2 - (2a_2s-1)p_2q_{1/2} + d_2q_{1/2} \\ &< [(2a_1-1)p_1 - d_1]q_{1/2} - 2(1-a_1)p_1q_{1/2}^2 + p_2q_{1/2} + d_2q_{1/2}, \qquad (3.1)\end{aligned}$$

due to non-negativity of $q_{1/2}$. Equation (3.1) implies

$$\frac{d}{dt}q_{1/2} < 0 \text{ for } q_{1/2} > \frac{[(2a_1-1)p_1 - d_1] + d_2 + p_2}{2(1-a_1)p_1} =: Q_{1/2} \qquad (3.2)$$

Therefore, we obtain $q_{1/2}(t) \leq \max\{q_{1/2}(0), Q\} =: K_{1/2}$ for all $t > 0$. Consequently, we obtain

$$c_1 \leq K_{1/2} c_2. \tag{3.3}$$

If $n > 3$, we iteratively denote $q_{k/k+1} = \frac{c_k}{c_{k+1}}$ for $k = 2, \cdots, n-2$ and calculate

$$\begin{aligned}
\frac{d}{dt} q_{k/k+1} =& \frac{\left(\frac{d}{dt} c_k\right) c_{k+1} - \left(\frac{d}{dt} c_{k+1}\right) c_k}{c_{k+1}^2} \\
=& \frac{[(2a_k s - 1)p_k - d_k]c_k + 2(1 - a_{k-1}s)p_{k-1}c_{k-1}}{c_{k+1}} \\
& - \frac{(2(1 - a_k s)p_k c_k + (2a_{k+1}s - 1)p_{k+1}c_{k+1} - d_{k+1}c_{k+1})c_k}{c_{k+1}^2} \\
<& [(2a_k - 1)p_k - d_k]q_{k/k+1} + \frac{2p_{k-1}c_{k-1}}{c_{k+1}} - 2(1 - a_k)p_k q_{k/k+1}^2 \\
& + p_{k+1}q_{k/k+1} + d_{k+1}q_{k/k+1} \\
<& [(2a_k - 1)p_k - d_k]q_{k/k+1} + 2p_{k-1}K_{k-1/k}q_{k/k+1} - 2(1 - a_k)p_k q_{k/k+1}^2 \\
& + p_{k+1}q_{k/k+1} + d_{k+1}q_{k/k+1}
\end{aligned} \tag{3.4}$$

Consequently, it holds

$$q_{k/k+1} > \frac{[(2a_k - 1)p_k - d_k] + 2p_{k-1}K_{k-1/k} + p_{k+1} + d_{k+1}}{2(1 - a_k)p_k},$$

which implies

$$\frac{d}{dt} q_{k/k+1} < 0,$$

and hence

$$\begin{aligned}
q_{k/k+1} \leq \max\left\{ \frac{[(2a_k - 1)p_k - d_k] + 2p_{k-1}K_{k-1/k} + p_{k+1} + d_{k+1}}{2(1 - a_k)p_k}, q_{k/k+1}(0) \right\} \\
=: K_{k/k+1},
\end{aligned}$$

which yields

$$c_k \leq K_{k/k+1} c_{k+1} \text{ for } k = 2, \cdots, n-2. \tag{3.5}$$

Finally, we set $q_{n-1/n} = \frac{c_{n-1}}{c_n}$ and calculate

$$\begin{aligned}
\frac{d}{dt}q_{n-1/n} =& \frac{\left(\frac{d}{dt}c_{n-1}\right)c_n - \left(\frac{d}{dt}c_n\right)c_{n-1}}{c_n^2} \\
=& \frac{[(2a_{n-1}s-1)p_{n-1} - d_{n-1}]c_{n-1} + 2(1-a_{n-2}s)p_{n-2}c_{n-2}}{c_n} \\
& - \frac{(2(1-a_{n-1}s)p_{n-1}c_{n-1} - d_n c_n)c_{n-1}}{c_n^2} \\
<& [(2a_{n-1}-1)p_{n-1} - d_{n-1}]q_{n-1/n} \\
& + \frac{2p_{n-2}c_{n-2}}{c_n} - 2(1-a_{n-1})p_{n-1}q_{n-1/n}^2 + d_n q_{n-1/n} \\
<& [(2a_{n-1}-1)p_{n-1} - d_{n-1}]q_{n-1/n} + \frac{2p_{n-2}K_{n-2/n-1}c_{n-1}}{c_n} \\
& - 2(1-a_{n-1})p_{n-1}q_{n-1/n}^2 + d_n q_{n-1/n}.
\end{aligned} \tag{3.6}$$

Consequently, it holds

$$q_{n-1/n} > \frac{[(2a_{n-1}-1)p_{n-1} - d_{n-1}] + 2p_{n-2}K_{n-2/n-1} + d_n}{2(1-a_{n-1})p_{n-1}},$$

which implies

$$\frac{d}{dt}q_{n-1/n} < 0.$$

We obtain the estimate

$$\begin{aligned}
q_{n-1/n} \leq \max\left\{\frac{[(2a_{n-1}-1)p_{n-1} - d_{n-1}] + 2p_{n-2}K_{n-2/n-1} + d_n}{2(1-a_{n-1})p_{n-1}}, q_{n-1/n}(0)\right\} \\
=: K_{n-1/n},
\end{aligned}$$

from which follows by definition of $q_{n-1/n}$

$$c_{n-1} \leq K_{n-1/n}c_n. \tag{3.7}$$

Inductively, we obtain $c_1 \leq K_{1/2} \cdot \ldots \cdot K_{n-1/n}c_n$. Analogously we obtain

$$c_i \leq K_i c_n \text{ for } 1 \leq i < n, \tag{3.8}$$

for appropriate positive K_i. We note that $k^l l_m \geq 0$ and, therefore,

$$\begin{aligned}
\frac{d}{dt}c_1 &= \left(\frac{2a_1p_1}{1 + k^c c_n + k^l l_m} - p_1 - d_1\right)c_1 \\
&\leq \left(\frac{2a_1p_1}{1 + k^c c_n} - p_1 - d_1\right)c_1 \\
&\leq \left(\frac{2a_1p_1}{1 + kc_1/K_1} - p_1 - d_1\right)c_1.
\end{aligned}$$

We thus obtain

$$c_1 > \frac{[(2a_1 - 1)p_1 - d_1]K_1}{k(p_1 + d_1)} \Rightarrow \frac{d}{dt}c_1 < 0. \tag{3.9}$$

This implies that

$$c_1(t) \leq \max\left\{c_1(0), \frac{[(2a_1 - 1)p_1 - d_1]K_1}{k(p_1 + d_1)}\right\} := L_1. \tag{3.10}$$

Consequently, c_1 is globally bounded in time. For $k = 2, \cdots, n-1$, we obtain iteratively (using estimate 3.8)

$$\begin{aligned}
\frac{d}{dt}c_k =& 2\left(1 - \frac{a_{k-1}}{1 + k^c c_n + k^l l_m}\right) p_{k-1}c_{k-1} + \left(\frac{2a_k}{1 + k^c c_n + k^l l_m} - 1\right) p_k c_k - d_k c_k \\
<& 2p_{k-1}c_{k-1} + \left(\frac{2a_k}{1 + k^c c_n} - 1\right) p_k c_k - d_k c_k \\
<& 2p_{k-1}L_{k-1} + \left(\frac{2a_k}{1 + kc_k/K_k} - 1\right) p_k c_k - d_k c_k =: \mathcal{P}_k(c_k).
\end{aligned}$$

We see that $\mathcal{P}_k(c_k) \to -\infty$ for $c_k \to \infty$. Therefore, there exists $\tilde{c}_k > 0$ such that $\mathcal{P}_k(x) < 0$ for $x > \tilde{c}_k$, consequently, it holds $c_k < \max\{\tilde{c}_k, c_k(0)\} =: L_k$ uniformly in time.

In analogy, it holds

$$\begin{aligned}
\frac{d}{dt}c_n =& 2\left(1 - \frac{a_{n-1}}{1 + k^c c_n + k^l l_m}\right) p_{n-1}c_{n-1} - d_n c_n \\
<& 2p_{n-1}c_{n-1} - d_n c_n \\
<& 2p_{n-1}L_{n-1} - d_n c_n.
\end{aligned}$$

This is negative, if $c_n > \frac{2p_{n-1}L_{n-1}}{d_n} =: \hat{L}_n$. Consequently, we obtain $c_n \leq \max\{\hat{L}_n, c_n(0)\} =: L_n$ uniformly in time. We obtain that all c_i, $i = 1, \cdots, n$ are globally bounded with respect to time. For l_i we proceed analogously.

Differentiability of the right hand-side and bounds in time imply uniqueness and global existence of solutions, due to Picard-Lindelöf's theorem, [21, 97, 106].

■

In the following, we analyze, which properties of the leukemic cells present at $t = 0$, are necessary and sufficient to destabilize the equilibrium of healthy cells.

3.2.1 Steady states

We define healthy hematopoiesis as absence of leukemic cells and existence of a positive steady state of the non-leukemic cell line. Steady state values of c_i and l_i are denoted as $\bar{c}_i$ and $\bar{l}_i$, respectively. We consider three types of steady states:

Definition 3.2 (Purely hematopoietic steady state)
A steady state satisfying $\bar{c}_i > 0$ *for an* $i \in \{1, \cdots, n\}$ *and* $\bar{l}_k = 0$, *for* $k = 1, \ldots, m$ *is referred to as a purely hematopoietic steady state. A purely hematopoietic steady state, where all* $\bar{c}_i > 0$ *for* $1 \leq i \leq n$ *is referred to as a healthy steady state.*

Remark 3.3
The purely hematopoietic steady state is characterized by the absence of leukemic cells ($\bar{l}_k = 0,\ k = 1, \ldots, m$*). This is an abstract idealization, since in each organism mutations accumulate over lifetime, due to replication errors (*1 *per* 10^9 *base pairs per division after repair, or environmental damage:* 1 *AP site per* 10^5 *base pairs in steady state of formation and repair), [132]. Mutated cells that may exist in healthy organisms, [112,200], but that do not lead to formation of relevant neoplastic cell populations are not considered in the above definition.*

Definition 3.4 (Purely leukemic steady state)
A steady state satisfying $\bar{c}_i = 0$, *for* $i = 1, \ldots, n$ *and* $\bar{l}_k > 0$, *for a* $k \in \{1, \cdots, m\}$ *is referred to as a purely leukemic steady state.*

Remark 3.5
A purely leukemic steady state is an abstract reference that cannot be observed in reality, since the organism dies in absence of healthy blood cells.

Definition 3.6 (Mixed (Composite) steady state)
Steady states, where $\bar{c}_i > 0$ *for at least one* $i \in \{1, \cdots, n\}$ *and* $\bar{l}_j > 0$ *for at least one* $j \in \{1, \cdots, m\}$*, are referred to as mixed (composite) steady states.*

Remark 3.7
If $l_1(0) = \cdots = l_m(0) = 0$*, then* $l_1(t) = \cdots = l_m(t) = 0$*, for all* $t > 0$ *and the model* (2.3) *for healthy hematopoiesis is obtained.*

We now calculate steady states of the system and find parameter conditions for existence of different types of steady states. Our analysis indicates that the system

can have composite steady states or steady states consisting of only healthy or only leukemic cell types. Composite steady states are not unique and they occupy a one-dimensional manifold. This result is summarized in the following Proposition.

Proposition 3.8 (Types of Steady States)
Let Assumptions 2.3 hold. We consider steady states of Model (2.5).

(i) *Assume that there exist* $i \in \{1,\dots,m\}$ *and that there exist* $j \in \{1,\dots,n\}$ *such that*

$$\frac{\frac{d_i^l}{p_i^l}+1}{2a_i^l} = \frac{\frac{d_j^c}{p_j^c}+1}{2a_j^c} := \bar{s} < 1,$$

where $\bar{s}$ *denotes the steady state value of* s*. Then, for each* $\bar{s}$ *with* $i,\ j$ *chosen maximal, there exists a one-dimensional manifold of steady states:*

$$\bar{l}_m \in \mathbb{R},\ \bar{c}_n = \frac{\frac{1}{\bar{s}}-1-k^l\bar{l}_m}{k^c},$$
$$\bar{l}_1 = \cdots = \bar{l}_{i-1} = 0,\ \bar{c}_1 = \cdots = \bar{c}_{j-1} = 0.$$
For $i \le k \le m : \bar{l}_k = \bar{l}_m \Pi_{i=k+1}^m \Theta_i^l$*, for* $j \le k \le n : \bar{c}_k = \bar{c}_n \Pi_{i=k+1}^n \Theta_i^c$*, where*
$\Theta_i^l := \frac{d_i^l + p_i^l - 2a_i^l p_i^l \bar{s}}{2(1-a_{i-1}^l \bar{s}) p_{i-1}^l},\ \Theta_i^c := \frac{d_i^c + p_i^c - 2a_i^c p_i^c \bar{s}}{2(1-a_{i-1}^c \bar{s}) p_{i-1}^c},\ \Theta_m^l := \frac{d_m^l}{2(1-a_{m-1}^l \bar{s}) p_{m-1}^l},$
$\Theta_n^c := \frac{d_n^c}{2(1-a_{n-1}^c \bar{s}) p_{n-1}^c}.$

There exist also steady states with either $\bar{l}_i = 0$ *for all* $i = 1,\dots,m$*, or* $\bar{c}_j = 0$ *for all* $j = 1,\dots,n$.

(ii) *Assume that for all pairs* $i,\ j,\ (i = 1,\dots,m;\ j = 1,\dots,n)$

$$\frac{\frac{d_i^l}{p_i^l}+1}{2a_i^l} \neq \frac{\frac{d_j^c}{p_j^c}+1}{2a_j^c}.$$

Then either $\bar{l}_i = 0$ *for all* $i = 1,\dots,m$*, or* $\bar{c}_j = 0$ *for all* $j = 1,\dots,n$ *in a steady state.*

PROOF
(i) The steady state conditions of the equations for l_i and c_j require that $\bar{s} = \frac{d_i^l + p_i^l}{2a_i^l p_i^l} = \frac{d_j^c + p_j^c}{2a_j^c p_j^c}$, which implies $k^c\bar{c}_n + k^l\bar{l}_m = \left(\frac{1}{s} - 1\right)$. The remainder follows from the steady state conditions for $c_n \dots c_{j+1}$ and those for $l_m \dots l_{i+1}$.

(ii) Assume that there exists $1 \le i \le n$ with $\bar{c}_i \neq 0$, note that it is not possible that $\bar{c}_n \neq 0$ and $\bar{c}_{n-1} = 0$. Choose i minimal. Then either $i = 1$ or $\bar{c}_{i-1} = 0$.

Then it holds $\bar{s} = \frac{p_i^c + d_i^c}{2a_i^c p_i^c}$. Due to the assumptions, we have $\bar{s} = \frac{p_i^c + d_i^c}{2a_i^c p_i^c} \neq \frac{p_1^l + d_1^l}{2a_1^l p_1^l}$, which implies $(2a_1^l s - 1)p_1^l - d_1^l \neq 0$. Therefore, $\bar{l}_1 = 0$. We then repeat the same argument for $\bar{l}_2$ and obtain iteratively $\bar{l}_i = 0$ for all $1 \leq i \leq m$. The other case works analogously by exchanging l and c. ■

Remark 3.9
These steady states are not necessarily non-negative.

In the following Lemma, we are interested only in non-negative steady states.

Lemma 3.10
Let $(\bar{c}_1, \cdots, \bar{c}_n, \bar{l}_1, \cdots, \bar{l}_m)$ *be a non-negative steady state of system* (2.5). *Define*

$$i_0 := \max\left\{ i \,\middle|\, \frac{d_i^c + p_i^c}{2a_i^c p_i^c} \leq \frac{d_k^c + p_k^c}{2a_k^c p_k^c} \text{ for all } k = 1, \cdots, n \right\}$$

and

$$j_0 := \max\left\{ j \,\middle|\, \frac{d_j^l + p_j^l}{2a_j^l p_j^l} \leq \frac{d_k^l + p_k^l}{2a_k^l p_k^l} \text{ for all } k = 1, \cdots, m \right\}.$$

Then $\bar{c}_i = 0$ *for* $i < i_0$ *and* $\bar{l}_j = 0$ *for* $j < j_0$.

PROOF
We denote the steady state value of s by $\bar{s}$. We note that $0 < \bar{s} \leq 1$. Therefore, $2(1 - a_i^c \bar{s}) > 0$ for all $0 < i < n$ and $2(1 - a_j^l \bar{s}) > 0$ for all $0 < j < m$. If we have $\bar{c}_i > 0$ in a non-negative steady state, then also $\bar{c}_{i+1} > 0$, since otherwise the steady state condition for c_{i+1} reduces to $2(1 - a_i^c \bar{s})\bar{c}_i = 0$, which cannot be satisfied. The analogous reasoning holds for l_j.

Assume that $\bar{c}_k > 0$ for a $0 < k < i_0$. Let k be chosen minimal, i.e., either $k = 1$ or $\bar{c}_{k-1} = 0$. Then, due to the above reasoning, it holds $\bar{c}_{i_0 - 1} > 0$. The steady state condition for c_k implies that $\bar{s} = \frac{d_k^c + p_k^c}{2a_k^c p_k^c}$. Due to the definition of i_0, it holds $\frac{d_k^c + p_k^c}{2a_k^c p_k^c} \geq \frac{d_{i_0}^c + p_{i_0}^c}{2a_{i_0}^c p_{i_0}^c}$. This is equivalent to $(2a_{i_0}^c \bar{s} - 1)p_{i_0}^c - d_{i_0}^c \geq 0$. Due to positivity of $\bar{c}_{i_0 - 1}$, the steady state condition for c_{i_0}, i.e., $0 = 2(1 - a_{i_0 - 1}^c \bar{s} - 1)p_{i_0 - 1}^c \bar{c}_{i_0 - 1} + (2a_{i_0}^c \bar{s} - 1)p_{i_0}^c \bar{c}_{i_0} - d_{i_0} \bar{c}_{i_0}^c$ cannot be satisfied for non-negative $\bar{c}_{i_0}$. Therefore, we obtain a contradiction. The reasoning for l_i is analogous.

■

Corollary 3.11
If $\bar{c}_i > 0$ *and* $\bar{c}_{i-1} = 0$ *in a non-negative steady state, then it holds* $\frac{p_i^c + d_i^c}{2a_i^c p_i^c} < \frac{p_j^c + d_j^c}{2a_j^c p_j^c}$ *for all* $j > i$ *and* $\bar{c}_1 = \cdots = \bar{c}_{i-1} = 0$. *The analogous condition holds for* l_i.

Remark 3.12 (Stemness property)
The above Corollary compares properties of the stem cell population (i.e., the compartment with lowest index that is non-zero in an equilibrium) to properties of the downstream populations. In this sense, it characterizes the stem cell populations based on its properties.

Remark 3.13
If it holds $(2a_1^c - 1)p_1^c - d_1^c < 0$*, then* $c_1 = 0$ *in all non-negative steady states of system* (2.5)*. If it holds* $(2a_1^c - 1)p_1^c - d_1^c = 0$*, then also* $c_1 = 0$ *in all non-negative steady states of system* (2.5)*, since positivity of* $\bar{c}_1$ *requires that* $\bar{s} = 1$*, which implies* $\bar{c}_n = 0$ *and* $\bar{l}_m = 0$*, which in turn leads to* $\bar{c}_1 = 0$ *and* $\bar{l}_1 = 0$*. Therefore, we assume in the following* $(2a_1^c - 1)p_1^c - d_1^c > 0$*. The analogous reasoning holds for* l_1*.*

We know from the analysis of the model (2.3) of the hematopoietic system in Chapter 2 and [215] the following Lemma.

Lemma 3.14 (Existence and uniqueness of the healthy steady state)
Let Assumptions 2.3 hold. The healthy steady state of system (2.5) *exists, if and only if the following conditions are satisfied:*

(i) $(2a_1^c - 1)p_1^c > d_1^c$,

(ii) $\frac{a_1^c p_1^c}{d_1^c + p_1^c} > \frac{a_i^c p_i^c}{d_i^c + p_i^c}$ *for* $i = 2, \cdots, n-1$,

(iii) $d_n > 0$.

If (i)-(iii) are satisfied, there exists only one healthy steady state.

Corollary 3.15
Necessary and sufficient conditions for existence of a purely leukemic steady state are obtained by replacing $p_i^c,\ a_i^c,\ d_i^c$ *by* $p_i^l,\ a_i^l,\ d_i^l$*.*

We are now interested in non-negative steady states, where either $\bar{c}_1 > 0$ or $\bar{l}_1 > 0$. The following Proposition characterizes these steady states.

Proposition 3.16 (Nonnegative steady states with $\bar{c}_1 > 0$ or $\bar{l}_1 > 0$)
Let Assumptions 2.3 hold. Assume

(i) $(2a_1^c - 1)p_1^c > d_1^c$, $(2a_1^l - 1)p_1^l > d_1^l$,

(ii) $\frac{a_1^c p_1^c}{d_1^c + p_1^c} > \frac{a_i^c p_i^c}{d_i^c + p_i^c}$, $1 < i < n$, $\frac{a_1^l p_1^l}{d_1^l + p_1^l} > \frac{a_i^l p_i^l}{d_i^l + p_i^l}$, $1 < i < m$,

(iii) $d_n^c > 0$, $d_m^l > 0$.

Then, it holds

(a) If $\frac{d_1^c + p_1^c}{2a_1^c p_1^c} = \frac{d_1^l + p_1^l}{2a_1^l p_1^l}$, *then there exists a one dimensional manifold of nonnegative steady states. The manifold includes composite steady states with* $\bar{l}_1 > 0$ *and* $\bar{c}_1 > 0$ *and the unique purely leukemic and the purely hematopoietic steady state with* $\bar{l}_1 > 0$ *or* $\bar{c}_1 > 0$. *The manifold is given by*

$$\bar{l}_m \in \left[0, \tfrac{\frac{1}{\bar{s}} - 1}{k^l}\right], \ \bar{c}_n = \tfrac{\frac{1}{\bar{s}} - 1 - k^l \bar{l}_m}{k^c},$$

$$\bar{l}_1 = \cdots = \bar{l}_{i-1} = 0, \ \bar{c}_1 = \cdots = \bar{c}_{j-1} = 0.$$

For $i \le k \le m : \bar{l}_k = \bar{l}_m \Pi_{i=k+1}^m \Theta_i^l$, *for* $j \le k \le n : \bar{c}_k = \bar{c}_n \Pi_{i=k+1}^n \Theta_i^c$, *where*

$$\Theta_i^l := \tfrac{d_i^l + p_i^l - 2a_i^l p_i^l \bar{s}}{2(1 - a_{i-1}^l \bar{s}) p_{i-1}^l}, \ \Theta_i^c := \tfrac{d_i^c + p_i^c - 2a_i^c p_i^c \bar{s}}{2(1 - a_{i-1}^c \bar{s}) p_{i-1}^c}, \ \Theta_m^l := \tfrac{d_m^l}{2(1 - a_{m-1}^l \bar{s}) p_{m-1}^l},$$

$$\Theta_n^c := \tfrac{d_n^c}{2(1 - a_{n-1}^c \bar{s}) p_{n-1}^c}, \ \bar{s} = \tfrac{d_1^c + p_1^c}{2a_1^c p_1^c}.$$

(b) If $\frac{d_1^c + p_1^c}{2a_1^c p_1^c} \neq \frac{d_1^l + p_1^l}{2a_1^l p_1^l}$, *then there exists no composite steady state with* $\bar{l}_1 > 0$ *and* $\bar{c}_1 > 0$. *There exists a unique purely hematopoietic steady state with* $\bar{c}_1 > 0$ *and a purely leukemic steady state with* $\bar{l}_1 > 0$. *These are given by*

$$\bar{c}_1 = \cdots = \bar{c}_n = 0,$$

$$\bar{s} = \tfrac{d_1^l + p_1^l}{2a_1^l p_1^l}, \ \bar{l}_m = \tfrac{\frac{1}{\bar{s}} - 1}{k^l}.$$

For $i \le k \le m : \bar{l}_k = \bar{l}_m \Pi_{i=k+1}^m \Theta_i^l$, *where*

$$\Theta_i^l := \tfrac{d_i^l + p_i^l - 2a_i^l p_i^l \bar{s}}{2(1 - a_{i-1}^l \bar{s}) p_{i-1}^l}, \ \Theta_m^l := \tfrac{d_m^l}{2(1 - a_{m-1}^l \bar{s}) p_{m-1}^l}.$$

or

$$\bar{l}_1 = \cdots = \bar{l}_m = 0,$$

$$\bar{s} = \tfrac{d_1^c + p_1^c}{2a_1^c p_1^c}, \ \bar{c}_n = \tfrac{\frac{1}{\bar{s}} - 1}{k^c}.$$

For $i \le k \le m : \bar{l}_k = \bar{l}_m \Pi_{i=k+1}^m \Theta_i^l$, *where*

$$\Theta_i^c := \tfrac{d_i^c + p_i^c - 2a_i^c p_i^c \bar{s}}{2(1 - a_{i-1}^c \bar{s}) p_{i-1}^c}, \ \Theta_n^c := \tfrac{d_n^c}{2(1 - a_{n-1}^c \bar{s}) p_{n-1}^c}.$$

PROOF
a) Existence of the composite steady states follows from Proposition 3.8 (i). We note that the non-negativity of $\bar{c}_n$ and $\bar{l}_m$ is equivalent to $\bar{l}_m \in \left[0, \frac{\frac{1}{\bar{s}}-1}{k^l}\right]$, $\bar{c}_n = \frac{\frac{1}{\bar{s}}-1-k^l\bar{l}_m}{k^c}$. Due to the assumptions, all species are non-negative. The purely hematopoietic and the purely leukemic steady state are part of the manifold from Proposition 3.8 (i). Uniqueness of the pure steady states follows from Lemma 3.14 and Corollary 3.15.

(b) Positivity of $\bar{c}_1$ implies for the steady state value $\bar{s}$ of s that $\bar{s} = \frac{d_1^c+p_1^c}{2a_1^cp_1^c}$. Positivity of $\bar{l}_1$ implies $\bar{s} = \frac{d_1^l+p_1^l}{2a_1^lp_1^l}$. Since $\frac{d_1^c+p_1^c}{2a_1^cp_1^c} \neq \frac{d_1^l+p_1^l}{2a_1^lp_1^l}$, it holds either $\bar{l}_1 = 0$ or $\bar{c}_1 = 0$. Existence and uniqueness of the pure steady states follow from Lemma 3.14 and Corollary 3.15. The expressions for $\bar{c}_i$ are obtained as in 3.8 (i) by setting all $\bar{l}_i = 0$, $\bar{s} = \frac{d_1^c+p_1^c}{2a_1^cp_1^c}$ and $\bar{c}_n = \left(\frac{1}{\bar{s}} - 1\right)\frac{1}{k_c}$. The case for $\bar{l}_i > 0$ works analogously. Positivity follows from the assumptions.

■

Remark 3.17
Assumption (i) is motivated by Remark 3.13. Assumption (ii) is motivated by Lemmas 3.10 and 3.14.

Remark 3.18
If we are interested in steady states with $\bar{c}_1 = 0$, we erase the equation for c_1 from system (2.5) *and set $c_1 = 0$ in the remaining equations. We then apply Proposition 3.16 to the system with $n + m - 1$ equations. We can do the analogous procedure for l_1. We can repeat this procedure to obtain steady states with $\bar{c}_2 = \bar{l}_2 = 0$ etc.*

Example 3.19 (Case (a) of Proposition 3.16)
Figure 3.1 depicts the coexistence of healthy and leukemic cell populations in equilibrium. Numerical solutions show a moderate and slow change of healthy cell counts to a new equilibrium. This scenario is comparable to preleukemic states, myelodysplasias, monoclonal gammopathy of unknown significance or the so-called smoldering myelomas, [23, 127], that can persist for years without major impairment of blood function. Transformation to leukemia is possible, if parameters change in favor of the leukemic population, e.g., by mutation and selection. Re-establishment of the healthy equilibrium is possible, if parameters change in favor of the healthy population. Since case (a) of Proposition 3.16 requires a sharp condition on the parameters, it can be considered a rare case.
Figure 3.2 shows coexistence of leukemic and healthy cells in equilibrium without a measurable change of healthy cell counts. This scenario may describe the existence of sub-clinical mutated cell-lines that can be found in the marrow of healthy individuals, [112, 200].

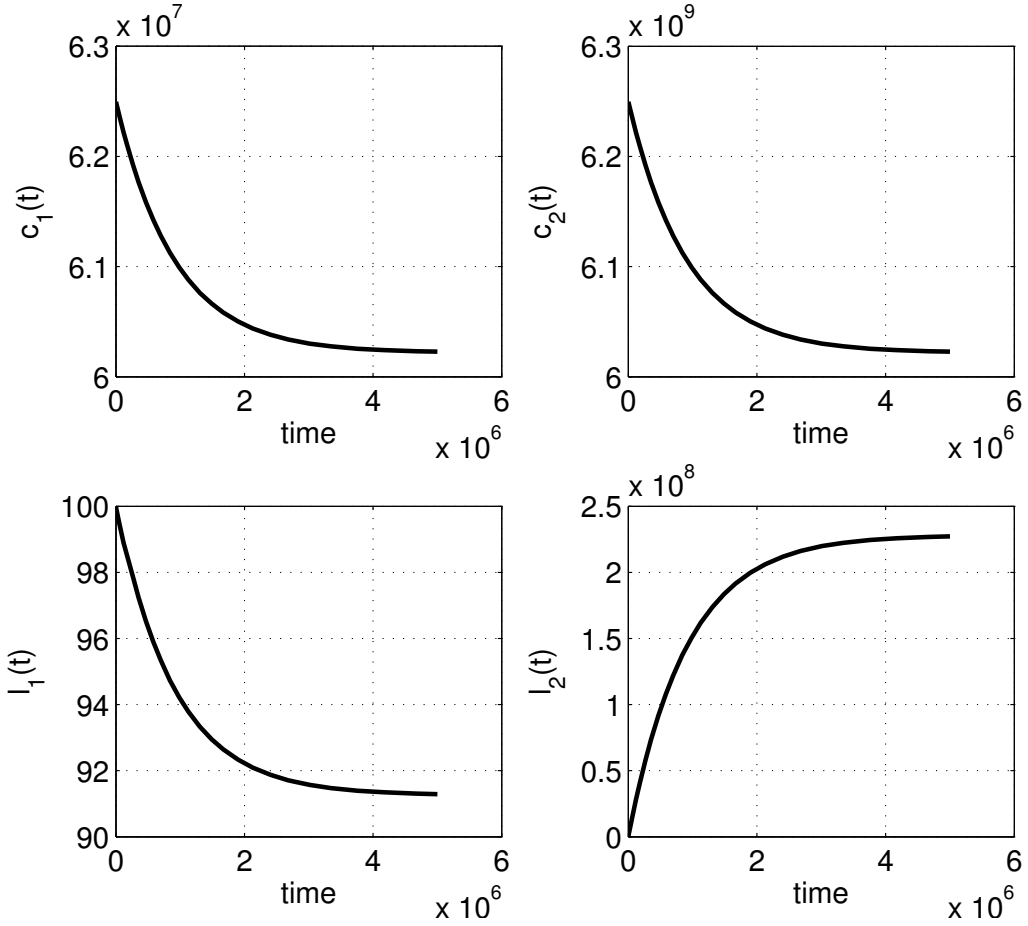

Figure 3.1: Equilibrium with coexistence of healthy and leukemic cells. The leukemic cell count is in order of magnitude of the count of healthy mature cells. Parameters: $a_1^c = 0.55,\ p_1^c = 1,\ d_1^c = 0,\ d_2^c = 0.01;\ a_1^l = a_1^c,\ p_1^l = 2.5,\ d_1^l = 0,\ d_2^l = 10 \cdot 10^{-6},\ k = 1.6 \cdot 10^{-11}$. Initial conditions: Healthy cell levels are values of healthy equilibrium, $l_1(0) = 100$, $l_2(0) = 0$.

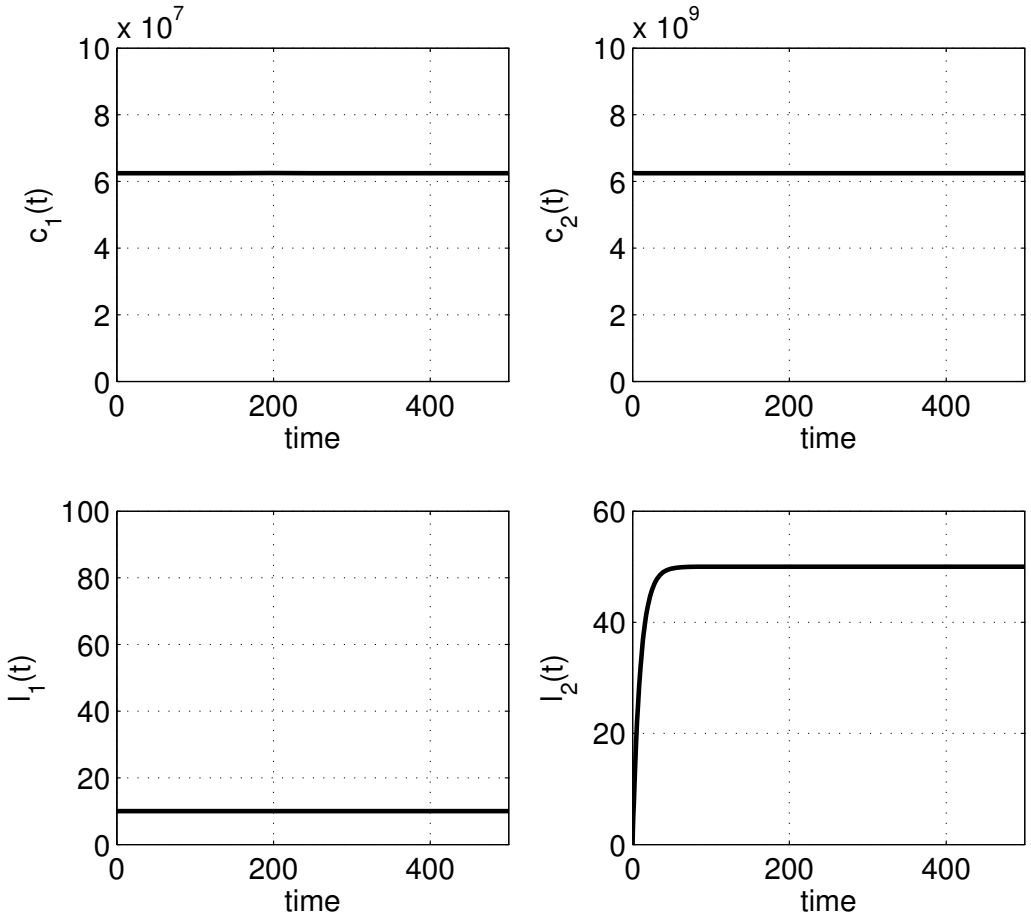

Figure 3.2: Equilibrium with coexistence of healthy and leukemic cells. The leukemic cell count is small and the change of healthy cell counts is invisible on a clinically relevant scale. Parameters: $a_1^c = 0.55,\ p_1^c = 1,\ d_1^c = 0,\ d_2^c = 0.01;\ a_1^l = a_1^c,\ p_1^l = 0.5,\ d_1^l = 0,\ d_2^l = 0.1,\ k = 1.6 \cdot 10^{-11}$. Initial conditions: Healthy cell levels are values of healthy equilibrium, $l_1(0) = 10$, $l_2(0) = 0$.

Example 3.20 (Case (b) of Proposition 3.16)
An example is given in Figure 3.3. This scenario with increasing leukemic cell counts and decreasing blood cell counts is typical for acute leukemias, [139].

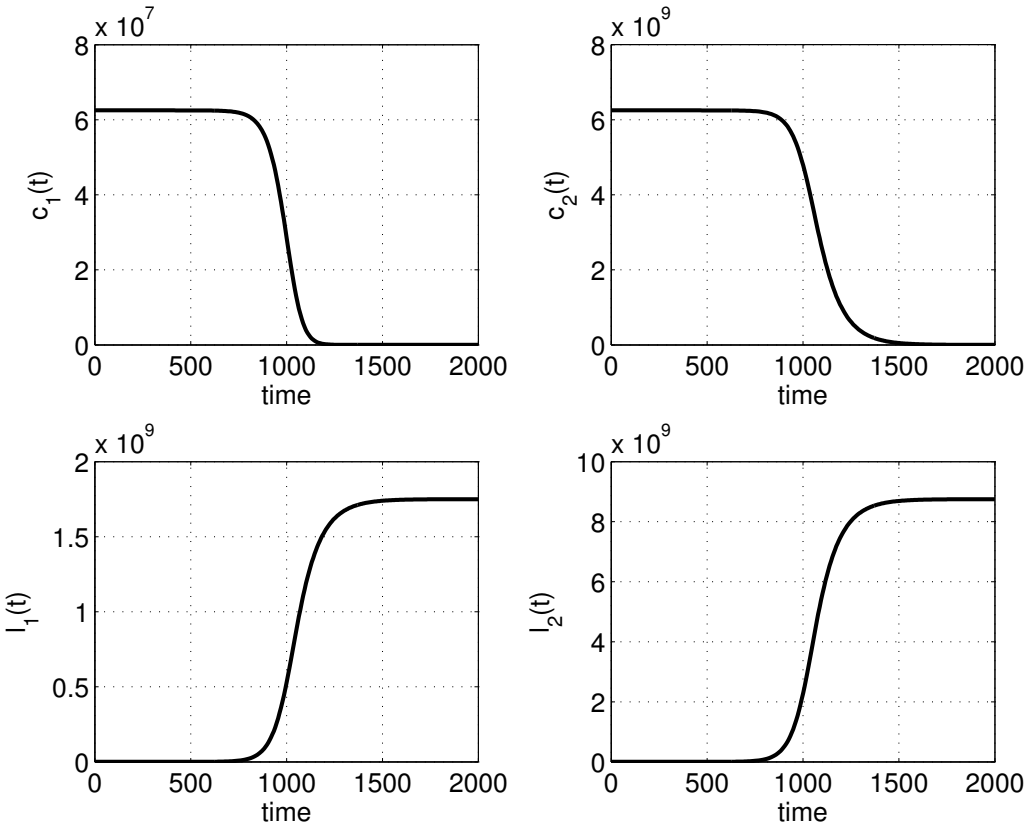

Figure 3.3: Establishment of a leukemic steady state and extinction of healthy cells. Leukemia establishes, although proliferation of leukemic cells is smaller than proliferation of healthy cells. Parameters: $a_1^c = 0.55,\ p_1^c = 1,\ d_1^c = 0,\ d_2^c = 0.01;\ a_1^l = 0.57,\ p_1^l = 0.5,\ d_1^l = 0,\ d_2^l = 0.1,\ k = 1.6 \cdot 10^{-11}$. Initial conditions: Healthy cell levels are values of healthy equilibrium, $l_1(0) = 10$, $l_2(0) = 0$.

3.3 Establishment of a leukemic stem cell population

In this paragraph, we ask, what properties of LSCs are necessary for establishment of a leukemic stem cell population. Mathematically speaking, we search for the conditions of instability of l_1 at the healthy steady state. We will call this "instability in the direction of l_1". Biologically, this means that a sufficiently small population of LSCs introduced into the healthy steady state will expand.

Proposition 3.21 (Destabilization of the healthy steady state)
The healthy steady state is unstable in the direction of l_1, if and only if

$$\frac{a_1^l p_1^l}{d_1^l + p_1^l} > \frac{a_1^c p_1^c}{d_1^c + p_1^c}$$

PROOF
We resort the equations of system (2.5) in the order $\frac{d}{dt}l_1, \ \cdots, \ \frac{d}{dt}l_m$, $\frac{d}{dt}c_1, \ \cdots, \ \frac{d}{dt}c_n$. We linearize the system around the healthy steady state. The first row of the linearization matrix contains a non-zero entry in the first column, namely, $(2a_1^l \bar{s} - 1)p_1^l - d_1^l$, and zeros otherwise. Hence, we immediately see that $(2a_1^l \bar{s} - 1)p_1^l - d_1^l$ is an eigenvalue, where $\bar{s}$ is the steady state value of s. Instability in the direction of l_1 depends on the sign of the eigenvalue $(2a_1^l \bar{s} - 1)p_1^l - d_1^l$ with $\bar{s} := \frac{d_1^c + p_1^c}{2a_1^c p_1^c}$. This eigenvalue is positive, if and only if $\frac{a_1^l p_1^l}{d_1^l + p_1^l} > \frac{a_1^c p_1^c}{d_1^c + p_1^c}$. ■

Corollary 3.22
The healthy steady state is unstable in the direction of l_1, if and only if the purely leukemic steady state is stable in the direction of c_1.

PROOF
We have $(2a_1^l \bar{s}^c - 1)p_1^l - d_1^l > 0$, if and only if $(2a_1^c \bar{s}^l - 1)p_1^c - d_1^c < 0$, where $\bar{s}^c := \frac{d_1^c + p_1^c}{2a_1^c p_1^c}$ and $\bar{s}^l := \frac{d_1^l + p_1^l}{2a_1^l p_1^l}$ denote signal intensity in the healthy steady state and the purely leukemic steady state respectively:

$$\begin{aligned} \left(2a_1^l \frac{d_1^c + p_1^c}{2a_1^c p_1^c} - 1\right) p_1^l - d_1^l > 0 \quad &\Leftrightarrow \\ 2a_1^l p_1^l (d_1^c + p_1^c) > 2a_1^c p_1^c (d_1^l + p_1^l) \quad &\Leftrightarrow \\ \left(2a_1^c \frac{d_1^l + p_1^l}{2a_1^l p_1^l} - 1\right) p_1^c - d_1^c < 0 \end{aligned}$$

■

Corollary 3.23

(i) *The following parameter relations are sufficient for instability of the healthy equilibrium in the direction of l_1 :*

(a) $a_1^l > a_1^c$, $p_1^l > p_1^c$, $d_1^l \leq d_1^c$
(b) $a_1^l = a_1^c$, $p_1^l > p_1^c$, $d_1^l < d_1^c$
(c) $a_1^l = a_1^c$, $p_1^l > p_1^c$, $d_1^l = d_1^c > 0$
(d) $a_1^l \geq a_1^c$, $p_1^l \geq p_1^c$, $d_1^l < d_1^c$
(e) $a_1^l > a_1^c$, $p_1^l = p_1^c$, $d_1^l = d_1^c$

(ii) *The parameter relations obtained exchanging superscripts l and c lead to linear stability of the healthy equilibrium in the direction of l_1.*

In the following, we consider different parameter relations leading to growth of a leukemic cell population and link them to biological evidence from literature. The cell properties have been experimentally observed for cells in the leukemic lineages. Nevertheless, leukemic stem cells have not yet been observed for all of the provided examples. In the following, the most immature cell type of the leukemic cell line is referred to as the leukemic stem cell. This reasoning does not imply that leukemic stem cells have to derive from hematopoietic stem cells. In many of the presented cases the leukemogenic modification occurs on the level of committed precursors.

Biological Remark 3.24
Parameter relation: $a_1^l > a_1^c$, $p_1^l = p_1^c$, $d_1^l = d_1^c$

Interpretation: Self-renewal in the leukemic cell line is enhanced in comparison to healthy cells, due to mutation or impairment of differentiation. The latter is therapeutically exploited in acute promyelocytic leukemia, [2].

Biological Remark 3.25
Parameter relation: $a_1^l = a_1^c$, $p_1^l = p_1^c$, $d_1^l < d_1^c$
Interpretation:

- *Scenario 1: Reduced apoptosis in leukemia cells, due to mutations (as observed in B-CLL, [165])*
- *Scenario 2: Induction of apoptosis in healthy cells by malignant cells (as observed in myelodysplastic syndromes, [224])*

Biological Remark 3.26
Parameter relation: $a_1^l = a_1^c$, $p_1^l > p_1^c$, $d_1^l = d_1^c \neq 0$
Interpretation: Proliferation in malignant cells is enhanced in comparison to healthy cells (as observed in Burkitt-Lymphoma, [25])

Remark 3.27 (Importance of self-renewal for evolution of leukemia)
The case $a_1^l = a_1^c$, $p_1^l > p_1^c$, $d_1^l = d_1^c = 0$ *necessarily leads to existence of multiple composite steady states, as discussed in Proposition 3.8 (i). However, the case* $a_1^l > a_1^c$, $p_1^l = p_1^c$, $d_1^l = d_1^c \geq 0$ *does not. Since composite steady states may cause less severe symptoms, this result demonstrates that changes in differentiation may have more severe consequences than changes in proliferation. This result is biologically new, since, traditionally, cancerous diseases have been understood in the context of increased cell proliferation. This result underlines that for expansion of a malignant cell line at the expense of healthy cells enhanced proliferation alone is not sufficient.*

Remark 3.28 (Candidate treatment strategies)
Corollary 3.23 (ii) describes qualitative strategies leading to the extinction of small populations of leukemic stem cells. Such strategies are, e.g., reduction of self-renewal of leukemic stem cells, enhancement of self-renewal of healthy stem cells, enhanced death of leukemic stem cells, reduced death of healthy stem cells, enhanced proliferation of healthy stem cells, reduced proliferation of leukemic stem cells. It depends on the coefficients of the model of leukemic and healthy stem cells, if one of these approaches is sufficient or if a combination is required to accomplish that $l_i \to 0$, as $t \to \infty$, $i = 1, ..., m$. Parameter relations that lead to the extinction of leukemic cells are necessary to obtain the complete remission. An important issue in the applications is the rate of leukemic cell elimination, which depends on the values of model parameters. In some cases it might be slow and, therefore, not relevant for the time span corresponding to a realistic lifetime.

Proposition 3.29 (Non-maximal steady states)
Let $(0, \cdots, 0, \bar{c}_k, \cdots, \bar{c}_n, 0, \cdots, 0, \bar{l}_j, \cdots, \bar{c}_m)$ *be a steady state of system* (2.5)*, where either* $\bar{c}_k > 0$ *or* $\bar{l}_j > 0$*. Assume that this steady state does not have the maximal possible number of nonzero components, i.e., if* $\bar{c}_k > 0$ *there exists* $k' < k$ *such that* $\frac{d^c_{k'}+p^c_{k'}}{2a^c_{k'}p^c_{k'}} < \frac{d^c_k+p^c_k}{2a^c_k p^c_k}$ *or if* $\bar{l}_j > 0$ *there exists* $j' < j$ *such that* $\frac{d^l_{j'}+p^l_{j'}}{2a^l_{j'}p^l_{j'}} < \frac{d^l_j+p^l_j}{2a^l_j p^l_j}$*. Then this steady state is unstable.*

PROOF
We consider the case that $\frac{d^l_{j'}+p^l_{j'}}{2a^l_{j'}p^l_{j'}} < \frac{d^l_j+p^l_j}{2a^l_j p^l_j}$ and $\bar{l}_j > 0$. The other case works analogously. We resort the equations of system (2.5) in the order $\frac{d}{dt}l_1, \cdots, \frac{d}{dt}l_m, \frac{d}{dt}c_1, \cdots, \frac{d}{dt}c_n$. We linearize the system around $(0, \cdots, 0, \bar{c}_k, \cdots, \bar{c}_n, 0, \cdots, 0, \bar{l}_j, \cdots, \bar{c}_m)$. We immediately see that $(2a^l_{j'}\bar{s} - 1)p^l_{j'} - d^l_{j'}$ is an eigenvalue, where $\bar{s}$ is the steady state value of s with $\bar{s} := \frac{d^l_j+p^l_j}{2a^l_j p^l_j}$. This eigenvalue is positive, since $(2a^l_{j'}\bar{s} - 1)p^l_{j'} - d^l_{j'} > 0 \Leftrightarrow \frac{d^l_{j'}+p^l_{j'}}{2a^l_{j'}p^l_{j'}} < \frac{d^l_j+p^l_j}{2a^l_j p^l_j}$. ■

3.4 System with 4 equations

The results about destabilization of the healthy steady state holds for arbitrary compartment numbers. To obtain insight into dynamics of the considered system, we focus on the case $n = 2$, $m = 2$ in the remainder of this Chapter. This is the minimal set of equations describing the healthy and leukemic hematopoiesis. Numerical simulations suggest that a reduced model consisting only of two differentiation steps for each cell lineage shows dynamics qualitatively similar to the models consisting of more equations for a range of parameters.

3.4.1 Linearized stability analysis of purely hematopoietic and purely leukemic steady states

Proposition 3.30 (Linearized stability of purely leukemic steady state) *Assume*

(i) $\frac{d_1^c+p_1^c}{a_1^c p_1^c} > \frac{d_1^l+p_1^l}{a_1^l p_1^l}$

(ii) $(2a_1^c-1)p_1^c > d_1^c$

(iii) $d_2^c > 0,\ d_2^l > 0.$

Then, there exists a unique healthy and a unique purely leukemic steady state. The purely leukemic steady state is locally stable and the healthy steady state is unstable in the direction of l_1.

PROOF
The existence of a unique healthy steady state follows from Proposition 3.14. Assumption (ii) is equivalent to $\frac{2a_1^c p_1^c}{d_1^c+p_1^c} > 1$. Assumption (i) implies $1 > \frac{d_1^c+p_1^c}{2a_1^c p_1^c} > \frac{d_1^l+p_1^l}{2a_1^l p_1^l}$ and, thus, $\frac{2a_1^l p_1^l}{d_1^l+p_1^l} > 1$. Therefore, $(2a_1^l-1)p_1^l > d_1^l$. Due to the symmetry of the considered ODE system with respect to interchange of c_i and l_i, these relations and application of Proposition 3.14 lead to existence and uniqueness of the purely leukemic steady state.

Since $\bar{c}_1 = \bar{c}_2 = 0$ and, due to the steady state condition, $(2a_1^l\bar{s}-1)p_1^l - d_1^l = 0$, with $\bar{s} := \frac{d_1^l+p_1^l}{2a_1^l p_1^l}$, the characteristic polynomial of the linearization around the purely leukemic steady state calculates as:

$$\begin{aligned}
\chi(\lambda) &= \begin{vmatrix} \lambda & 2a_1^l p_1^l k^l \bar{s}^2 \bar{l}_1 \\ -2(1-a_1^l\bar{s})p_1^l & \lambda - (2a_1^l p_1^l k^l \bar{s}^2 \bar{l}_1 - d_2^l) \end{vmatrix} \\
&\qquad \cdot(\lambda + d_2^c)(\lambda - [(2a_1^c\bar{s}-1)p_1^c - d_1^c]) \\
&= \left[\lambda^2 - \left(\frac{d_2^l}{p_1^l - d_1^l}\frac{d_1^l+p_1^l}{(2a_1^l p_1^l)}\big((2a_1^l-1)p_1^l - d_1^l\big) - d_2^l\right)\lambda \right. \\
&\qquad \left. +4a_1^l(p_1^l)^2 k^l \bar{s}^2(1-a_1^l\bar{s})\bar{l}_1\right](\lambda + d_2^c)(\lambda - [(2a_1^c\bar{s}-1)p_1^c - d_1^c]).
\end{aligned}$$

We recognize from this expression that $-d_2$ and $[(2a_1^c\bar{s}-1)p_1^c - d_1^c]$ are eigenvalues. We now check, if the eigenvalues have negative real parts. To obtain the signs of the real parts of the remaining eigenvalues, we will apply Vieta's Theorem. It holds $\bar{s} := \frac{d_1^l+p_1^l}{2a_1^l p_1^l} < 1$, due to conditions (i) and (ii), and $\bar{l}_1 = \frac{d_2^l(1/\bar{s}-1)}{2(1-a_1^l\bar{s})p_1^l k^l}$.

Therefore, $4a_1^l(p_1^l)^2k^l\bar{s}^2(1-a_1^l\bar{s})\bar{l}_1 > 0$. It holds that

$$2a_1^l p_1^l - d_1^l - p_1^l < 2p_1^l - d_1^l - p_1^l = p_1^l - d_1^l,$$

since $a_1^l < 1$. This implies

$$\begin{aligned}\frac{d_2^l}{p_1^l - d_1^l}\frac{d_1^l + p_1^l}{(2a_1^l p_1^l)}\big((2a_1^l - 1)p_1^l - d_1^l\big) - d_2^l &< \frac{d_2^l}{p_1^l - d_1^l}\frac{d_1^l + p_1^l}{(2a_1^l p_1^l)}\big(p_1^l - d_1^l\big) - d_2^l \\ &= d_2^l(\bar{s} - 1) \\ &< 0.\end{aligned}$$

Therefore,

$$-\left(\frac{d_2^l}{p_1^l - d_1^l}\frac{d_1^l + p_1^l}{(2a_1^l p_1^l)}\big((2a_1^l - 1)p_1 - d_1^l\big) - d_2^l\right) > 0.$$

Vieta's theorem implies that all eigenvalues of the quadratic polynomial have negative real parts. Since $(2a_1^c\bar{s} - 1)p_1^c - d_1^c < 0$, due to (i), all eigenvalues of the linearization have negative real part. ■

Remark 3.31
Assumption (i) is necessary and sufficient for establishment of a leukemic cell line, see Proposition 3.21. Assumptions (ii) and (iii) are necessary and sufficient for existence of a healthy steady state, see Proposition 3.14.

Example 3.32
The time evolution shown in Figure 3.3 is an example for a case, where leukemic stem cells have enhanced self-renewal potential and decreased proliferative activity, compared to healthy stem cells. Numerical solutions show a clinically insignificant phase with normal healthy and low leukemic cell counts followed by a sudden rise of leukemic and a sudden reduction of healthy cell counts. This behavior is comparable to this seen in acute leukemias, such as AML.

Example 3.33
Figure 3.4 gives an example of the extinction of a mutated cell clone. In comparison to the healthy stem cells, the mutated cells show reduced self-renewal and enhanced proliferation. Since $d_1^l = d_1^c = 0$, assumption (i) of Proposition 3.30 is not fulfilled. In this example, enhanced proliferation is not sufficient to compensate for reduced self-renewal potential. This example demonstrates the complex interplay of different cell properties that is necessary for persistence of the mutant clone. The numerical solution shows decrease of the mutant cell clone in a relatively short time scale. This scenario describes a benign mutation. The changes of healthy cell counts are negligible on the clinically relevant scale.

Corollary 3.34 (Linear stability of healthy steady state)
Renaming variables ($p_i^c \leftrightarrow p_i^l$, $a_i^c \leftrightarrow a_i^l$, $c_i \leftrightarrow l_i^l$) in Proposition 3.30 leads to the existence of a unique healthy and a unique purely leukemic steady state and linear stability of the healthy steady state.

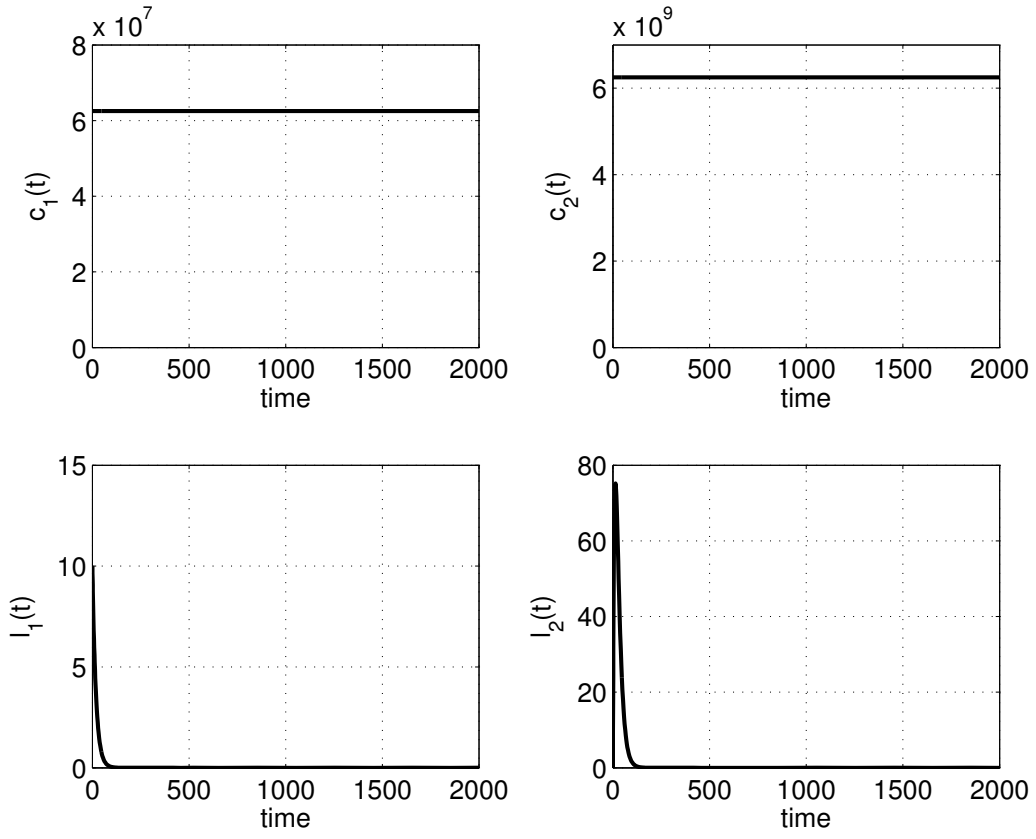

Figure 3.4: Extinction of the leukemic cell population and reestablishment of healthy equilibrium. Stability of healthy steady state. Parameters: $a_1^c = 0.55,\ p_1^c = 1,\ d_1^c = 0,\ d_2^c = 0.01;\ a_1^l = 0.53,\ p_1^l = 1.5,\ d_1^l = 0,\ d_2^l = 0.1,\ k = 1.6 \cdot 10^{-11}$. Initial conditions: Healthy cell levels are values of healthy equilibrium, $l_1(0) = 10, l_2(0) = 0$.

3.4.2 Linearized stability analysis of composite steady states

In this Section, we study stability of composite steady states. For simplicity of calculations, we set $k^l = k^c =: k$. Let the assumptions of Proposition 3.16 (a) hold. We linearize around the composite steady state discussed in Proposition 3.8 (i). The linearization M calculates

$$M := \begin{vmatrix} 0 & -\alpha^c & 0 & -\alpha^c \\ \nu^c & \rho^c & 0 & \alpha^c \\ 0 & -\alpha^l & 0 & -\alpha^l \\ 0 & \alpha^l & \nu^l & \rho^l \end{vmatrix},$$

where

$$\begin{aligned} \alpha^c &:= 2a_1^c k p_1^c \bar{c}_1 \bar{s}^2 > 0, \\ \nu^c &:= 2(1 - a_1^c \bar{s}) p_1^c > 0, \\ \rho^c &:= \alpha^c - d_2^c, \\ \alpha^l &:= 2a_1^l k p_1^l \bar{l}_1 \bar{s}^2 > 0, \\ \nu^l &:= 2(1 - a_1^l \bar{s}) p_1^l > 0, \\ \rho^l &:= \alpha^l - d_2^l. \end{aligned}$$

Then the characteristic polynomial of the linearization around the composite steady state is of the form:

$$\begin{aligned} \chi_M(\lambda) :=& \big(\lambda^3 + \left(-\rho^l - \rho^c\right)\lambda^2 + \left(-\alpha^l\alpha^c + \nu^l\alpha^l + \rho^l\rho^c + \nu^c\alpha^c\right)\lambda \\ &+ \nu^c\alpha^c(\alpha^l - \rho^l) + \nu^l\alpha^l(\alpha^c - \rho^c)\big)\lambda. \end{aligned} \tag{3.11}$$

Remark 3.35
We observe that χ_M has one zero eigenvalue.

Proposition 3.36 (Center Manifold)
If there exists only one eigenvalue with zero real part, then the manifold of the steady states is a center manifold.

PROOF
We have exactly one zero eigenvalue. We search for a one dimensional center manifold.

- The linearization L around the composite steady $(\bar{c}_1, \bar{c}_2, \bar{l}_1, \bar{l}_2)$ state with

$\bar{s} = \frac{1}{2a_1}$ is given by

$$L := \begin{pmatrix} 0 & -\frac{kp_1^c}{2a_1^c}\bar{c}_1 & 0 & -\frac{kp_1^c}{2a_1^c}\bar{c}_1 \\ p_1^c & \frac{kp_1^c}{2a_1^c}\bar{c}_1 - d_2^c & 0 & \frac{kp_1^c}{2a_1^c}\bar{c}_1 \\ 0 & -\frac{kp_1^l}{2a_1^l}\bar{l}_1 & 0 & -\frac{kp_1^l}{2a_1^l}\bar{l}_1 \\ 0 & \frac{kp_1^l}{2a_1^l}\bar{l}_1 & p_1^l & \frac{kp_1^l}{2a_1^l}\bar{l}_1 - d_2^l \end{pmatrix}.$$

This follows using $\bar{s} = \frac{1}{2a_1^l} = \frac{1}{2a_1^c}$, $\frac{\partial}{\partial c_2}s = \frac{\partial}{\partial l_2}s = -ks^2$.

- Let $v := (-\frac{d_2^c}{p_1^c}, -1, \frac{d_2^l}{p_1^l}, 1)^T$, then

$$L \cdot v = 0.$$

- The center manifold of the equilibrium point $(\bar{c}_1, \bar{c}_2, \bar{l}_1, \bar{l}_2)$ is invariant under the flow of the system and is tangent to the center eigenvector in the equilibrium point, c.f. Section 3.2 of ref. [87].
  Due to Proposition 3.8, the manifold of steady states is given as:

$$\begin{pmatrix} c_1 \\ c_2 \\ l_1 \\ l_2 \end{pmatrix} = \begin{pmatrix} \frac{d_2^c}{p_1^c}(\frac{2a_1^c-1}{k} - l_2) \\ \frac{2a_1^c-1}{k} - l_2 \\ \frac{d_2^l}{p_1^l}l_2 \\ l_2 \end{pmatrix} = \begin{pmatrix} \frac{d_2^c}{p_1^c}\frac{2a_1^c-1}{k} \\ \frac{2a_1^c-1}{k} \\ 0 \\ 0 \end{pmatrix} + l_2 \begin{pmatrix} -\frac{d_2^c}{p_1^c} \\ -1 \\ \frac{d_2^l}{p_1^l} \\ 1 \end{pmatrix}.$$

  Therefore, v is parallel to the manifold of steady states. Since $(\bar{c}_1, \bar{c}_2, \bar{l}_1, \bar{l}_2)$ lies on the manifold of steady states, it is tangent to v in $(\bar{c}_1, \bar{c}_2, \bar{l}_1, \bar{l}_2)$. Since on each point on the manifold of steady states the system is in an equilibrium, the manifold is invariant under the flow of the system. Therefore, the manifold of steady states is a center manifold in the case, where only one eigenvalue has zero real part.

■

We continue to analyze the eigenvalues of

$$\begin{aligned}\tilde{\chi}_M(\lambda) :=& \lambda^3 + \left(-\rho^l - \rho^c\right)\lambda^2 + \left(-\alpha^l\alpha^c + \nu^l\alpha^l + \rho^l\rho^c + \nu^c\alpha^c\right)\lambda \\ &+ \nu^c\alpha^c(\alpha^l - \rho^l) + \nu^l\alpha^l(\alpha^c - \rho^c).\end{aligned}$$

We intend to use the Routh-Hurwitz-Criterion, [79], and, therefore, calculate Hurwitz determinants of $\tilde{\chi}_M(\lambda)$.

Lemma 3.37
We define $\tilde{\chi}_M(\lambda) := \lambda^3 + \left(-\rho^l - \rho^c\right)\lambda^2 + \left(-\alpha^l\alpha^c + \nu^l\alpha^l + \rho^l\rho^c + \nu^c\alpha^c\right)\lambda + \nu^c\alpha^c(\alpha^l - \rho^l) + \nu^l\alpha^l(\alpha^c - \rho^c) := \lambda^3 + a_2\lambda^2 + a_1\lambda + a_0$.
It holds:

(i) *The absolute term* a_0 *of* $\tilde{\chi}_M(\lambda)$ *is positive.*

(ii) *The quadratic term* a_2 *of* $\tilde{\chi}_M(\lambda)$ *is positive.*

(iii) *Assume* $k := k^l = k^c$ *and* $d_1^c = d_1^l = 0$*, then the second determinant of Hurwitz* $H_2 := a_2a_1 - a_3a_0$ *can be written as*

$$H_2(X) = \tilde{\alpha}X^2 + \tilde{\beta}X + \tilde{\gamma},$$

where

$$X := k\bar{l}_2,$$
$$\tilde{\alpha} := \hat{\alpha}\bar{s}^2, \text{ with } \hat{\alpha} := (p_1^l d_2^l - p_1^c d_2^c)(d_2^c - d_2^l),$$
$$\tilde{\beta} := -\bar{s}(1-\bar{s})\hat{\alpha} + \bar{s}^2[p_1^l(d_2^l)^2 - p_1^c(d_2^c)^2 + d_2^c d_2^l(d_2^c - d_2^l)],$$
$$\tilde{\gamma} := d_2^c(d_2^l)^2\bar{s} + (d_2^c)^2 d_2^l\bar{s}^2 + (d_2^c)^2 p_1^c(2a_1^c - 1)\bar{s}^2 > 0.$$

The proof is presented in the Appendix B on page 233. For the remainder of this Section we assume $d_1^l = d_1^c = 0$, for simplicity.

We now ask, which range of parameters is biologically relevant. Since $\bar{s} = \frac{1}{2a_1^c} = \frac{1}{1+k\bar{l}_2+k\bar{c}_2}$ with $\bar{c}_2 \geq 0$, $\bar{l}_2 \geq 0$, it is necessary that for $k\bar{l}_2$ it holds $0 \leq k\bar{l}_2 \leq (2a_1^c - 1)$. Since we assume $1/2 < a_1^c < 1$, it follows $\frac{1}{2} < \bar{s} = \frac{1}{2a_1^c} = \frac{1}{1+k\bar{l}_2+k\bar{c}_2} < 1$. This motivates the following Definition.

Definition 3.38 (Biologically relevant range of parameters)
Let a_i^c, p_i^c, d_i^c, k^l, k^c, a_i^l, p_i^l, d_i^l *fulfill the Assumptions 2.3, then the following range of parameters is referred to as biologically relevant range of parameters:*

- $\frac{1}{2} < \bar{s} < 1$,
- $0 \leq k\bar{l}_2 \leq (2a_1^c - 1),\ 0 \leq k\bar{c}_2 \leq (2a_1^c - 1)$.

In the following, we investigate the sign of $H_2(X)$ within the ranges of this Definition.

Lemma 3.39

(i) If $\hat{\alpha} < 0$, it holds $H_2(X) > 0$ in the biologically relevant range of parameters.

(ii) If $\hat{\alpha} = 0$, it holds $H_2(X) > 0$ in the biologically relevant range of parameters.

The proof is presented in the Appendix B.2.

Remark 3.40 (Interpretation of case (i))
It holds $\hat{\alpha} < 0$, if and only if either ($p_1^l d_2^l > p_1^c d_2^c$ and $d_2^c < d_2^l$) or ($p_1^l d_2^l < p_1^c d_2^c$ and $d_2^c > d_2^l$). If $d_2^c < d_2^l$ and p_1^c is small enough or p_1^l is large enough, the system asymptotically approaches the center manifold for initial conditions in its neighborhood. The same is true, if $d_2^c > d_2^l$ and p_1^l is small enough or p_1^c is large enough.

Remark 3.41 (Interpretation of case (ii))
It holds $\hat{\alpha} = 0$, if and only if either $p_1^l d_2^l = p_1^c d_2^c$ or $d_2^c = d_2^l$. In these cases, the system asymptotically approaches the center manifold for initial conditions in the neighborhood of it.

Summarizing these results, we obtain statement (i) of the following Proposition. Statements (ii)-(iii) treat the remaining parameter constellations.

Proposition 3.42 (Stability in the neighborhood of the center manifold)

(i) *If $\hat{\alpha} \leq 0$, then the system asymptotically approaches the center manifold for initial conditions in the vicinity of it.*

(ii) *If $\hat{\alpha} > 0$ and $k\bar{l}_2$ small enough, then the system asymptotically approaches the center manifold, if it starts in the neighborhood of it.*

(iii) *There exist parameters such that the system becomes unstable for $\hat{\alpha} > 0$. These are characterized as follows. Set $P_{max} := \frac{p_1^l d_2^l (d_2^c - d_2^l)(1-\bar{s}) + d_2^c d_2^l (d_2^c - d_2^l)\bar{s} + p_1^l (d_2^l)^2 \bar{s}}{d_2^c (d_2^c - d_2^l)(1-\bar{s}) + (d_2^c)^2 \bar{s}}$,*
$P_{min} := \frac{d_2^l (p_1^l d_2^c \bar{s} + (d_2^c)^2 \bar{s} - d_2^c d_2^l \bar{s} - p_1^l d_2^c + p_1^l d_2^l)}{d_2^c (2 d_2^c \bar{s} - d_2^l \bar{s} - d_2^c + d_2^l)}$. Then, instability occurs, if and only if one of the following conditions (a)-(b) is fulfilled

(a)
- *$P_{max} \geq p_1^c > P_{min}$ and*
- *$p_1^l > d_2^c$, $d_2^c > d_2^l$, $p_1^l d_2^l > p_1^c d_2^c$ and*
- *$\frac{-\tilde{\beta}^2}{4\hat{\alpha}\bar{s}^2 + \tilde{\gamma}} < 0$ and*
- *$k\bar{l}_2 \in \left\{ \left[0,\ \frac{1}{\bar{s}} - 1\right] \cap \left(\frac{-\tilde{\beta}}{2\hat{\alpha}\bar{s}^2} - \sqrt{\frac{\tilde{\beta}^2 - 4\hat{\alpha}\bar{s}^2\tilde{\gamma}}{(2\hat{\alpha}\bar{s}^2)^2}},\ \frac{-\tilde{\beta}}{2\hat{\alpha}\bar{s}^2} + \sqrt{\frac{\tilde{\beta}^2 - 4\hat{\alpha}\bar{s}^2\tilde{\gamma}}{(2\hat{\alpha}\bar{s}^2)^2}} \right) \right\}$*

(b) The conditions obtained from (a) by renaming $p_i^c \leftrightarrow p_i^l$, $a_i^c \leftrightarrow a_i^l$, $d_2^l \leftrightarrow d_2^c$

The proof and a characterization of the corresponding parameter ranges are presented in the Appendix B.3.

Example 3.43 (Case (iii) of Proposition 3.42)
The case (iii) of Proposition 3.42 is fulfilled for $a_1^c = a_1^l = 0.98039$, $p_1^c = 22$, $p_1^l = 4000$, $d_1^c = d_1^l = 0$, $d_2^c = 0.5$, $d_2^l = 0.2$, $k^l = k^c = 12.8 \cdot 10^{-10}$, $\bar{l}_2 = 0.15/k^l$, *which leads to* $H_2 \approx -0.061$.

Example 3.44
Figures 3.5 and 3.6 compare the behavior of the system for initial conditions being a perturbation of the composite steady state. Numerical solutions with parameters from Example 3.43 are shown in Figure 3.6 for different time scales. For comparison, a numerical solution with parameters of linear stable coexistence and perturbations of the same relative order of magnitude is shown in Figure 3.5. Depending on parameters and initial conditions small perturbations of initial conditions lead to convergence to nearby steady-states (see Figure 3.5), or to convergence to relatively distant states (see Figure 3.6). The latter case occurs for specific parameter conditions only and, therefore, might not be observed in healthy organisms.

Biological Remark 3.45
For a long time there exists a hypothesis that instability and chaos (in the mathematical sense) may play a role in cancer formation, [10, 22, 48]. Mathematical studies and experimental evidence suggest that the hematopoietic system may exhibit chaos and instability, [4, 73, 190]. The above finding of instability is, therefore, in line with results from literature.

Biological Remark 3.46 (Biological Interpretation)

(i) *The fact that there exists no instability for* $k\bar{l}_2$ *small enough might explain, why some syndromes with small amounts of malignant cells, such as myelodysplastic syndromes or MGUS, are stable over years, [23, 127].*

(ii) *The necessary condition* $\hat{\alpha} > 0$ *is equivalent to* $d_2^c > d_2^l$ *and* $p_1^l d_2^l > p_1^c d_2^c$. *This implies* $p_1^l > p_1^c$. *These conditions are synergistic in the sense that the cell line that dies slower shows stronger proliferation of stem cells. Such synergism is necessary for the emergence of instability. The necessary condition obtained after renaming of variables leads to the same result.*

(iii) *The proposition shows that instability of coexistence emerges only for some parameter ranges. If the proliferation rate of stem cells,* p_1^c, *is large enough, coexistence is linearly stable. That might lead to the conclusion that stimulation of healthy stem cells stabilizes preleukemic states.*

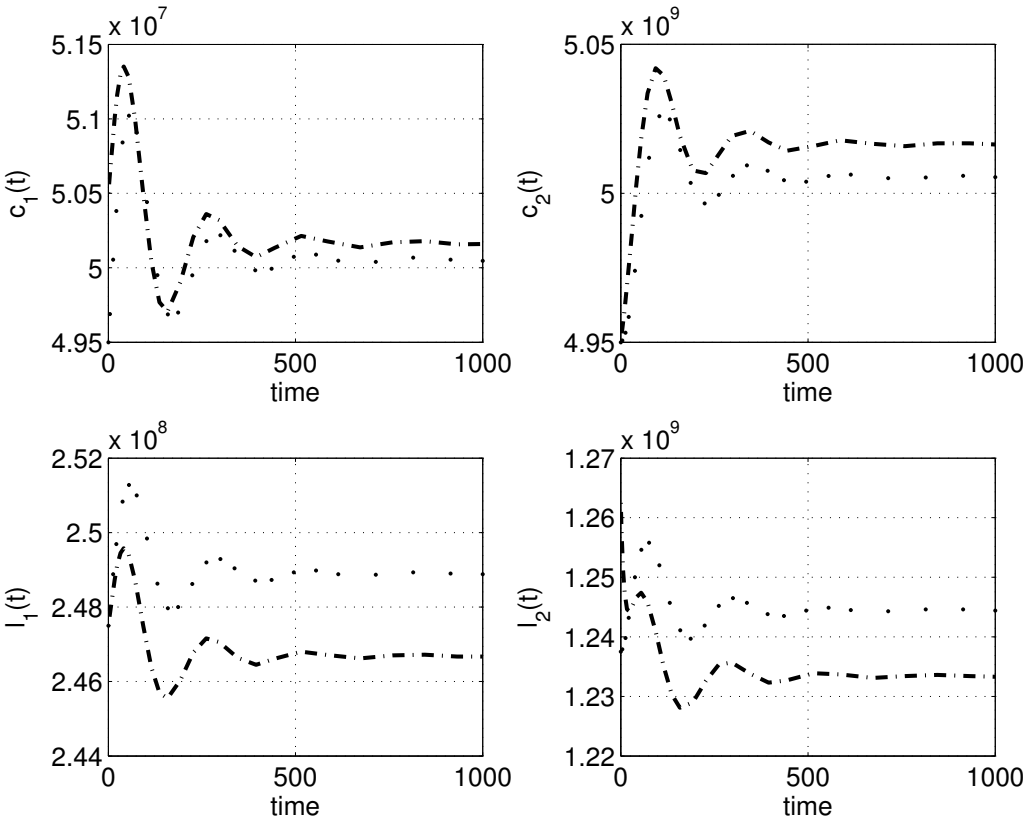

Figure 3.5: Perturbation of equilibrium with coexistence of healthy and leukemic cells. Small perturbations of points on the manifold of steady states lead to similar time dynamics and steady states. The perturbation is about 1% of the point $(c_1^m, c_2^m, l_1^m, l_2^m)$ on the manifold of steady states characterized by $c_2^m = 0.8\bar{c}_2^h$, where $\bar{c}_2^h$ is the count of mature cells in the healthy equilibrium. Different line types visualize dynamics for different inital conditions. Parameters: $a_1^c = 0.55,\ p_1^c = 1,\ d_1^c = 0,\ d_2^c = 0.01;\ a_1^l = a_1^c,\ p_1^l = 0.5,\ d_1^l = 0,\ d_2^l = 0.1,\ k = 1.6 \cdot 10^{-11}$. Initial conditions: $c_1(0) = 1.01 \cdot c_1^m$, $c_2(0) = 0.99 \cdot c_2^m$, $l_1(0) = 0.99 \cdot l_1^m$, $l_2(0) = 1.01 \cdot l_2^m$ or $c_1(0) = 0.99 \cdot c_1^m$, $c_2(0) = 0.99 \cdot c_2^m$, $l_1(0) = 0.99 \cdot l_1^m$, $l_2(0) = 0.99 \cdot l_2^m$ resp.

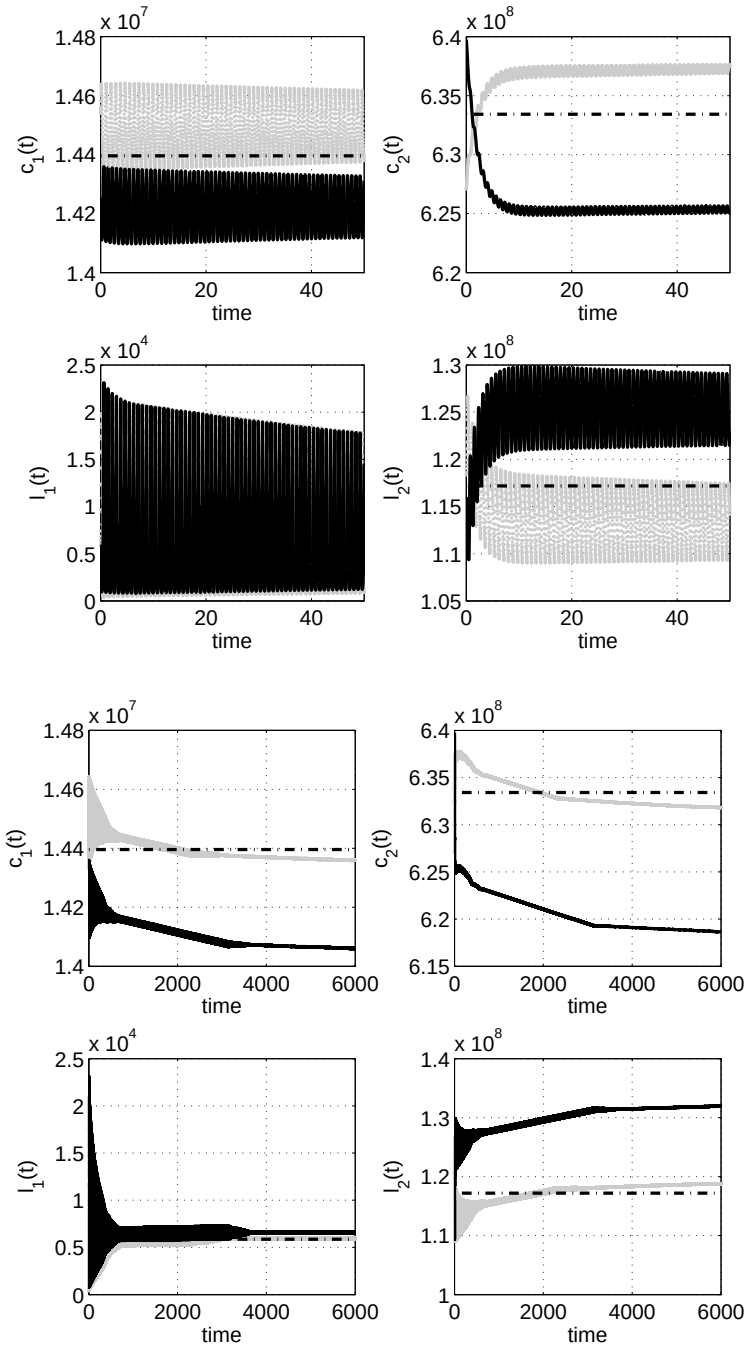

Figure 3.6: Perturbation of equilibrium with coexistence of healthy and leukemic cells. Small perturbations lead to oscillations. The perturbation is about 1% of the point $(c_1^m, c_2^m, l_1^m, l_2^m)$ on the manifold of steady states characterized by $l_2^m = 0.15/k$. Parameters: $a_1^c = 0.98039$, $p_1^c = 22$, $d_1^c = 0$, $d_2^c = 0.5$, $a_1^l = a_1^c$, $p_1^l = 4000$, $d_1^l = 0$, $d_2^l = 0.2$, $k = 12.8 \cdot 10^{-10}$. The discontinuous line visualizes the steady state $(c_1^m, c_2^m, l_1^m, l_2^m)$. Different colors correspond to different initial conditions. Initial conditions: $c_1(0) = 0.99 \cdot c_1^m$, $c_2(0) = 1.01 \cdot c_2^m$, $l_1(0) = 1.01 \cdot l_1^m$, $l_2(0) = 0.99 \cdot l_2^m$ or $c_1(0) = 1.01 \cdot c_1^m$, $c_2(0) = 0.99 \cdot c_2^m$, $l_1(0) = 0.99 \cdot l_1^m$, $l_2(0) = 1.01 \cdot l_2^m$ resp. Above: short time scale, below: long time scale.

3.5 Summary

In this Chapter, we analyze a mathematical model of signal-dependent leukemias. It is assumed that leukemic cells depend on the same growth signals as hematopoietic cells. This model shows two types of non-negative steady states: Either there exists a one dimensional manifold of steady states, where hematopoietic and leukemic cells coexist, or there exist isolated steady states of only hematopoietic or only leukemic cells (Proposition 3.16). The case of coexistence can be related to diseases with a good prognosis or preleukemic states (Example 3.19), while steady states with absence of hematopoietic cells correspond to the (idealized) end stage of acute leukemias (Example 3.20). The model allows to systematically analyze conditions sufficient and necessary for expansion of a leukemic stem cell population. These are of medical importance, since they constitute treatment approaches (Corollary 3.23, Remark 3.28). The results underline that changes in self-renewal behavior lead to more efficient expansion of leukemic cells than changes in proliferation rates (Remark 3.27). This result is biologically new and unexpected. In a minimal version of the model the isolated leukemic steady state is linearly stable, if and only if the isolated hematopoietic steady state is unstable (Proposition 3.30). In the minimal model the one dimensional manifold of steady states of coexisting leukemic and hematopoietic cells is a center manifold that can be, depending on parameters, either attractive or repulsive (Propositions 3.36 and 3.42).

CHAPTER 4

ANALYSIS OF THE MODEL OF A SIGNAL-INDEPENDENT LEUKEMIA (MODEL 2)

4.1 Outline of the chapter

In this Chapter, we provide mathematical analysis of the model of signal-independent leukemias (Model 2) introduced in Chapter 2, Section 2.4 (pp. 31).

Main results of this Chapter are:

- Characterization of the non-negative steady states (Proposition 4.19): We show that depending on leukemic and hematopoietic stem cell properties, there exist isolated nontrivial equilibria describing a coexistence of hematopoietic and leukemic cells. Only if expansion rates of leukemic stem cells exceed a certain threshold, which depends on properties of hematopoietic stem cells, the hematopoietic stem cells become extinct. We provide a biological explanation for this behavior (Remark 4.22). The different steady states are linked to diseases of the hematopoietic system (Biological Remark 4.24) and treatment approaches are discussed (Biological Remark 4.23). We show that if parameters and compartment number (number of equations) are chosen appropriately, there exist multiple purely hematopoietic steady states that are maintained by the same stem cell population (Remark 4.25, Example 4.27, Biological Remarks 4.26 and 4.29).

- Establishment of necessary and sufficient conditions for destabilization of the steady state corresponding to healthy homeostasis (Proposition 4.34): We show that also in this model enhanced self-renewal is crucial for es-

tablishment of leukemias and that high proliferation rates are not always sufficient (Remark 4.32).

- Linearized stability analysis of a minimal version of the system (4 equations): We show instability of all semi-trivial steady states in the parameter regime, in which a strictly positive steady state exists. In such parameter regime, the strictly positive steady state is linearly stable (Proposition 4.40). Only if there exists no steady state, where both lines coexist, the steady state, where the hematopoietic cell line becomes extinct, is linearly stable, provided that leukemic stem cells have high enough self-renewal (Propositions 4.38, 4.42). We show that under certain parameter conditions there exist center manifolds that are attractive (Proposition 4.42).

- Characterization of stemness properties in case of coexistence: We show that in this model leukemic cell properties determine, which hematopoietic cell population can act as stem cell population (Corollary 4.6, Biological Remark 4.7, Example 4.46) in a steady state, where both cell lines coexist.

A comparison of the properties of the two proposed models is presented in Chapter 5.

4.2 Existence, uniqueness and boundedness

Proposition 4.1 (Existence, Uniqueness and Nonnegativity)
Let Assumptions 2.5 hold. Then, the system (2.6) - (2.8) *has unique solutions existing for all times. The solutions stay non-negative and are uniformly bounded.*

PROOF
Local existence and uniqueness of solutions follow from the Theorem of Picard-Lindelöf, [21,97], since the right hand-side is a locally Lipschitz continuous function. It holds $\frac{d}{dt}c_i|_{c_i=0} \geq 0$ for all $1 \leq i \leq n$ and $\frac{d}{dt}l_i|_{l_i=0} \geq 0$ for all $1 \leq i \leq m$. This implies non-negativity of solutions for non-negative initial values.

Next, we show uniform boundedness of the solutions, which implies existence of solutions for all times, [97,106]. It holds $\frac{d}{dt}c_1 \leq ((2a_1^c-1)p_1^c - d_1^c - d_c(c_1))c_1$, due to non-negativity. Due to assumptions on d_c, there exists x_1^c such that $d_c(x) > (2a_1^c - 1)p_1^c - d_1^c$ for $x > x_1^c$. Therefore, $\frac{d}{dt}c_1 < 0$ for $c_1 > x_1^c$. This implies that $c_1 \leq \max\{x_1^c, c_1(0)\} =: c_1^{max}$.

Similarly, we obtain $\frac{d}{dt}c_i \leq 2p_{i-1}^c c_{i-1}^{max} + ((2a_i^c-1)p_i^c - d_i^c - d_c(c_i))c_i$ for $1 < i < n$. Therefore, $(-(2a_i^c-1)p_i^c + d_i^c + d_c(c_i))c_i > 2p_{i-1}^c c_{i-1}^{max}$ implies that $\frac{d}{dt}c_i < 0$. Since

$d_c(x) \to \infty$ for $x \to \infty$, there exists x_i^c such that

$$(-(2a_i^c - 1)p_i^c + d_i^c + d_c(c_i))c_i > 2p_{i-1}^c c_{i-1}^{max} \text{ for } c_i > x_i^c.$$

Therefore, $c_i \leq \max\{x_i^c, c_i(0)\} =: c_i^{max}$.

Finally, for $i = n$ we obtain $\frac{d}{dt}c_n \leq 2p_{n-1}c_{n-1}^{max} - d_n c_n$. Therefore, if $c_n > \frac{2p_{n-1}c_{n-1}^{max}}{d_n}$, it holds $\frac{d}{dt}c_n < 0$. This implies that $c_n \leq \max\{\frac{2p_{n-1}c_{n-1}^{max}}{d_n}, c_n(0)\}$. We obtain uniform boundedness for all c_i. Using the analogous estimates (replacing c by l), we obtain uniform boundedness for all l_j with $1 \leq j \leq m$.

■

4.3 Steady states

Remark 4.2 (Healthy steady state)
For all steady states $(\bar{c}_1, \cdots, \bar{c}_n)$ *of model* (2.3)*,* $(\bar{c}_1, \cdots, \bar{c}_n, 0, \cdots, 0)$ *is a steady state of the system* (2.6) - (2.8)*.*

Biological Remark 4.3
If $(\bar{c}_1, \cdots, \bar{c}_n)$ *is the unique positive equilibrium of model* (2.3)*, then* $(\bar{c}_1, \cdots, \bar{c}_n, 0, \cdots, 0)$ *corresponds to the healthy equilibrium of system* (2.6) - (2.8) *in the sense of Definition 3.2, see Assumption 2.5 (iv).*

4.3.1 Steady states of the hematopoietic subsystem

To classify steady states of system (2.6) - (2.8), we first analyze the impact of increased death rates of marrow cells (stages 1 to $n-1$) on the non-negative steady states of model (2.3). For this purpose we subtract dc_i from equation i of system (2.3) for all $i = 1, \cdots, n-1$, where d is a non-negative real constant. We obtain the following system (4.1).

$$\begin{aligned}
\frac{d}{dt}c_1^d(t) &= (2a_1^c s(t) - 1)p_1 c_1^d(t) - d_1^c c_1^d(t) - dc_1^d(t) \\
\frac{d}{dt}c_2^d(t) &= 2(1 - a_1^c s(t))p_1^c c_1^d(t) + (2a_2^c s(t) - 1)p_2 c_2^d(t) - d_2^c c_2^d(t) - dc_2^d(t) \\
&\vdots \quad \vdots \quad \vdots \\
\frac{d}{dt}c_i^d(t) &= 2(1 - a_{i-1}^c s(t))p_{i-1}^c c_{i-1}^d(t) + (2a_i^c s(t) - 1)p_i c_i^d(t) - d_i^c c_i^d(t) - dc_i^d(t) \\
&\vdots \quad \vdots \quad \vdots
\end{aligned}$$

$$
\begin{aligned}
&\vdots \qquad \vdots \qquad \vdots \\
\frac{d}{dt}c^d_{n-1}(t) &= 2(1-a^c_{n-2}s(t))p^c_{n-2}c^d_{n-2}(t) + (2a^c_{n-1}s(t)-1)p_{n-1}c^d_{n-1}(t) - d^c_{n-1}c^d_{n-1}(t) \\
&\quad - dc^d_{n-1}(t) \\
\frac{d}{dt}c^d_n(t) &= 2(1-a^c_{n-1}s(t))p^c_{n-1}c^d_{n-1}(t) - d_n c^d_n(t) \\
\\
s(t) &= \frac{1}{1+kc^d_n(t)},
\end{aligned}
\tag{4.1}
$$

where $c^d_1(0) = c^0_1 > 0$, $c^d_2(0) = c^0_2 \geq 0, \ldots, c^d_n(0) = c^0_n \geq 0$, $d \geq 0$.

Lemma 4.4
Let Assumptions 2.2 be fulfilled. Set $s_i := \frac{d^c_i + d + p^c_i}{2a^c_i p^c_i}$. *Assume*

(i) there exists $i \in \{1, \ldots, n-1\}$ *such that* $0 < s_i < 1$,

(ii) $d^c_n > 0$.

Set $i_0 := \max\big\{i \mid s_i = \min\{s_k, k = 1, \ldots, n-1\}\big\}$.
Then, it holds for system (4.1)*:*

(a) In each non-negative steady state $\bar{c}^d_k = 0$ *for all* $k < i_0$.

(b) There exists a unique non-negative steady state with $\bar{c}^d_{i_0} > 0$.

PROOF
(a) We denote the steady state value of s by $\bar{s}$. Let $k \in \{1, \ldots, i_0 - 1\}$ be the smallest index satisfying $\bar{c}^d_k > 0$. Then, $\frac{d}{dt}c^d_k = 0$ implies that $\bar{s} = s_k$. Then, condition $\frac{d}{dt}c^d_{i_0} = 0$ implies that

$$(2a^c_{i_0}s_k - 1)p^c_{i_0}\bar{c}^d_{i_0} + 2(1 - a^c_{i_0-1}s_k)\bar{c}_{i_0-1} - d^c_{i_0}\bar{c}^d_{i_0} - d\bar{c}^d_{i_0} = 0.$$

Due to the definition of i_0, it holds

$$s_k \geq s_{i_0} \Leftrightarrow s_k \geq \frac{d^c_{i_0} + d + p^c_{i_0}}{2a^c_{i_0}p^c_{i_0}} \Leftrightarrow (2a^c_{i_0}s_k - 1)p^c_{i_0} - d^c_{i_0} - d \geq 0.$$

Since $\bar{s} = s_k = \frac{1}{1+kc_n} \leq 1$, it holds $2(1 - a^c_{i_0-1}s_k) > 0$. This implies that $\bar{c}_{i_0-1} = 0$. If $k < i_0 - 1$, the condition $\frac{d}{dt}c^d_{i_0-1} = 0$ and the requirement $\bar{c}^d_{i_0-1} = 0$ lead to $\bar{c}^d_{i_0-2} = 0$, since $2(1 - a^c_{i_0-2}s_k) > 0$. Inductively, it follows $\bar{c}^d_k = 0$, which is a contradiction.

(b) The condition $\frac{d}{dt}c^d_{i_0} = 0$ implies that $\bar{s} = s_{i_0}$. Since $0 < s_{i_0} < 1$, the condition $\bar{s} = \frac{1}{1+k\bar{c}^d_n}$ leads to a unique positive $\bar{c}^d_n$. The condition $\frac{d}{dt}c^d_{n-1} = 0$ implies that $\bar{c}^d_{n-1} = \frac{d^c_n}{2(1-a^c_{n-1}s_{i_0})p^c_{n-1}}\bar{c}^d_n$. This leads to a unique positive $\bar{c}^d_{n-1}$.

The definition of i_0 implies that $s_k > s_{i_0}$ for all $k \in \{i_0+1, \ldots, n-1\}$. It holds $s_k > s_{i_0} \Leftrightarrow s_{i_0} < \frac{d^c_k+d+p^c_k}{2a^c_k p^c_k} \Leftrightarrow (2a^c_k s_{i_0} - 1)p^c_k - d^c_k - d < 0$. Due to assumption (i), it holds $0 < s_{i_0} < 1$. Therefore, $2(1 - a^c_k s_{i_0}) > 0$ for all $k \in \{i_0+1, \ldots, n-1\}$.

The condition $\frac{d}{dt}c^d_k = 0$ implies that $\bar{c}^d_{k-1} = -\frac{(2a^c_k s_{i_0}-1)p^c_k - d^c_k - d}{2(1-a^c_{k-1}s_{i_0})p^c_{k-1}}\bar{c}^d_k$,
where $-\frac{(2a^c_k s_{i_0}-1)p^c_k - d^c_k - d}{2(1-a^c_{k-1}s_{i_0})p^c_{k-1}} > 0$. This equation defines a unique positive $\bar{c}^d_{k-1}$, if $\bar{c}^d_k > 0$ is known. Iteratively, we obtain positive unique $\bar{c}^d_i$ for $i \geq i_0$. And due to (a), it holds $\bar{c}_i = 0$ for $i < i_0$.

■

Corollary 4.5
Let Assumptions 2.2 be fulfilled. Let $(0, \cdots, 0, \bar{c}^d_{i_0}, \cdots, \bar{c}^d_n)$ *be a non-negative steady state of system* (2.6) - (2.8) *with* i_0 *defined in Lemma 4.4. Then, there exists no non-negative steady state with more nonzero components. It holds* $\bar{s} = s_{i_0} < s_k$ *for all* $k > i_0$ *and* $\bar{s} = \min\{s_i \mid i = 1, \cdots, n-1\}$.

Corollary 4.6
Let Assumptions 2.2 be fulfilled. Set $s_i := \frac{d^c_i+d+p^c_i}{2a^c_i p^c_i}$ *and* $r_i := \frac{d^c_i+p^c_i}{2a^c_i p^c_i}$. *Set* $i^d_0 := \max\left\{i \mid r_i = \min\{r_k, k = 1, \ldots, n-1\}\right\}$ *and, analogously, define* $i^0_0 := \max\left\{i \mid s_i = \min\{s_k, k = 1, \ldots, n-1\}\right\}$. *Assume that* $s_{i^0_0} < 1$ *and* $r_{i^d_0} < 1$. *Then, the steady state with the most nonzero components for* $d = 0$ *has the form* $(0, \ldots, 0, \bar{c}^0_{i^0_0} > 0, \ldots \bar{c}^0_n > 0)$ *and the steady state with the most nonzero components for given* $d > 0$ *has the form* $(0, \ldots, 0, \bar{c}^d_{i^d_0} > 0, \ldots \bar{c}^d_n > 0)$. *The maximal number of positive components is the same, if and only if* $i^d_0 = i^0_0$.

Biological Remark 4.7 (Impact of external death rates on stemness)
The stem cell population c_α *of a given non-negative nontrivial steady state is defined by* $\alpha := \min\{k \mid \bar{c}_k > 0\}$. *The above Corollary implies that, if* $i^d_0 \neq i^0_0$ *for different values of* d, *different populations may act as a stem cell population. This means that imposing additional death rates* d, *e.g., due to presence of a leukemic population, might influence the stemness property of a cell population. In this sense, stemness is a property depending on environmental conditions. An example for this observation is given in Figures 4.8 and 4.9.*

To understand how increased death rates affect hematopoietic equilibria, we need the following Lemma.

Lemma 4.8
Let Assumptions 2.2 be fulfilled. Let $d > 0$. *Set* $s_i := \frac{d^c_i+d+p^c_i}{2a^c_i p^c_i}$. *Assume*

(i) $d_n^c > 0$,

(ii) $d_1^c < (2a_1^c - 1)p_1^c$,

(iii) $a_1^c p_1^c (d_i^c + p_i^c) > a_i^c p_i^c (d_1^c + p_1^c)$ *for* $i = 2, \ldots, n-1$,

(iv) there exists $i \in \{1, \ldots, n-1\}$ *such that* $0 < s_i < 1$.

Let $(\bar{c}_1^d, \ldots \bar{c}_n^d)$ *be a steady state with* $\bar{c}_{i_0} > 0$ *for*

$$i_0 := \max\left\{i \mid s_i = \min\{s_k, k = 1, \ldots, n-1\}\right\}.$$

(a) It holds $\bar{c}_n^d < \bar{c}_n^0$ *and* $\bar{c}_{n-1}^d < \bar{c}_{n-1}^0$ *for each* $0 < d < (2a_{i_0}^c - 1)p_{i_0}^c - d_i^c$. *For the corresponding steady state values* $\bar{s}^0$ *and* $\bar{s}^d$ *of* s *it holds* $\bar{s}^d > \bar{s}^0$.

(b) There exist $n \in \mathbb{N}$ *and parameters* a_i^c, p_i^c $(1 \leq i < n)$ *such that* $\bar{c}_i^d < \bar{c}_i^0$ *for* $i \geq i_0$.

(c) There exist $n \in \mathbb{N}$ *and parameters* a_i^c, p_i^c $(1 \leq i < n)$ *such that for a* k *fulfilling* $n - 1 > k \geq i_0$ *it holds* $\bar{c}_k^d > \bar{c}_k^0$ *and, furthermore,* $\sum_{i=1}^n \bar{c}_i^0 < \sum_{i=1}^n \bar{c}_i^d$.

The proof is presented in the Appendix B on page 243.

Remark 4.9
Lemma 4.8 (a) states that in the case $n = 2$ *increased death rates lead to decreased steady state cell counts. Depending on parameters this can be also true for* $n > 2$, *see Lemma 4.8 (b). Nevertheless, there exist* $n \in \mathbb{N}$ *and parameter values such that increased death rates lead to increased marrow cell counts, see Lemma 4.8 (c). This happens due to nonlinear feedback mechanisms that increase stem cell self-renewal, if there is a lack of mature cells.*

Example 4.10 (Examples to Lemma 4.8)
An example for Lemma 4.8 (b) is shown in Figure 4.1 (a), an example for Lemma 4.8 (c) is shown in Figure 4.1 (b).

Biological Remark 4.11 (Environmentally-induced myeloproliferation)
The additional death rate d *in system* (4.1) *can be interpreted as the influence of environmental constraints or processes on stem cell dynamics. Lemma 4.8 (c) states that these additional death rates can lead to system states with increased total cell numbers but reduced mature blood cell counts, see Figure 4.1 (b). This constellation is often observed in myelodysplasia, [53]. The combination of high immature cell counts in presence of high death rates and the decreased mature cell concentrations in presence of increased marrow cell load have often been considered as a paradox, [53]. Lemma 4.8 (c) demonstrates that feedbacks of*

(a) Parameter set 1

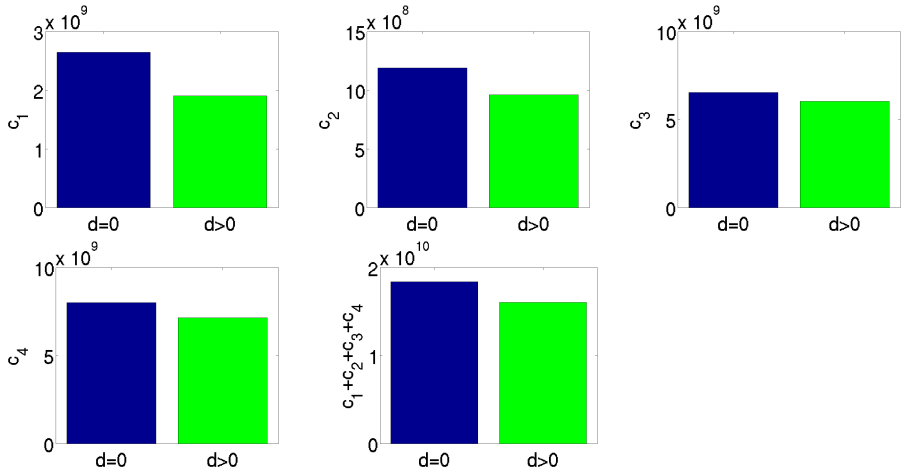

(b) Parameter set 2

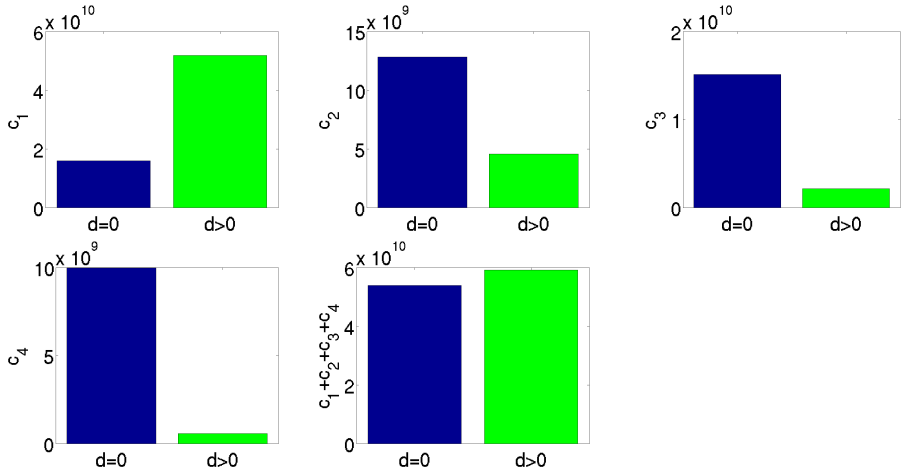

Figure 4.1: Impact of d on steady state values. The Figure illustrates cases (b) and (c) of Lemma 4.8. Depending on parameter values, increased death rates d can either lead to decreased total cell mass (Panel a) or to increased total cell mass (Panel b). Panel a: The parameters are $k = 10^{-10}$, $a_1^c = 0.9$, $a_2^c = a_3^c = 0.7$, $p_1^c = 0.1$, $p_2^c = p_3^c = 1$, $d_1^c = d_2^c = d_3^c = 0$, $d_4^c = 1$, $d \in \{0, 0.005\}$. Panel b: The parameters are $k = 10^{-10}$, $a_1^c = 0.999$, $a_2^c = a_3^c = 0.8$, $p_1^c = 0.45$, $p_2^c = p_3^c = 0.55$, $d_1^c = 0$, $d_2^c = d_3^c = 0.45$, $d_4^c = 1$, $d \in \{0, 0.4\}$.

healthy hematopoiesis together with an increased apoptosis rate are sufficient to explain the observed constellations of cell counts. This is in line with recent data reporting that aberrations of the micro-environment can be sufficient to induce myelodysplasia with a variety of patterns of deviating cell counts, [119, 176, 191, 232, 233].

For the next section we need the following definition and lemma:

Definition 4.12
Due to Lemma 4.4, the steady state of system (4.1) *with the maximal possible numbers of nonzero components is unique. We denote this steady state for given* d *as* $(\hat{c}_1^d, \ldots, \hat{c}_n^d)$*. We define the function* $\Phi : \mathbb{R}_0^+ \to \mathbb{R}_0^+$, $d \mapsto \sum_{i=1}^{n-1} \hat{c}_i^d$.

Remark 4.13
Lemma 4.8 states that Φ *given in Definition 4.12 is in general not monotonically decreasing.*

Lemma 4.14
The function Φ *from Definition 4.12 is continuous.*

PROOF
We define $s_i^d := \frac{d+p_i^c+d_i^c}{2a_i^c p_i^c}$ for $i = 1, \ldots, n-1$. We further set $i_0 := \max\{i \mid s_i = \min\{s_k, k = 1, \ldots, n-1\}\}$. Lemma 4.4 implies that in a non-negative steady state all c_i have to be equal to zero for $i < i_0$. If there exists a nontrivial non-negative steady state, the nonzero component with lowest index is, therefore, c_{i_0}. This implies that $\bar{s} = s_{i_0}^d$ for the steady value $\bar{s}$ of s. If $0 < s_{i_0}^d < 1$, we can calculate unique steady state values for all c_i with $i_0 \leq i \leq n$.

We define $\bar{s}(d) := \min\{s_i^d \mid 1 \leq i < n\}$. Since s_i^d depend continuously on d, $\bar{s}(d)$ depends continuously on d. We always have $\bar{s}(d) > 0$. We define $\hat{c}_n^d := \max\{0, (\frac{1}{\bar{s}(d)} - 1)\frac{1}{k}\}$. This depends continuously on d and is positive, if and only if $\bar{s}(d) < 1$. We set $\alpha_n(d) := \frac{d_n^c}{2(1-a_{n-1}^c \bar{s}(d))p_{n-1}^c}$. For $n > i > 1$ we set $\alpha_i(d) := \max\{0, -\frac{(2a_i^c \bar{s}(d)-1)p_i^c - d_i^c - d}{2(1-a_{i-1}\bar{s}(d))}\}$. The α_i depend continuously on d. We set $\hat{c}_i^d = \hat{c}_n^d \Pi_{k=i+1}^n \alpha_k(s)$ for $1 \leq i < n$. Then $\hat{c}_i$ depend continuously on d. Therefore, Φ depends continuously on d.

It remains to show that the $\hat{c}_i^d$ are the steady state with the maximal number of nonzero components. We note that $\bar{s}(d) \geq s_{i_0}^d$ implies $\alpha_i(d) = 0$ and, therefore, $\hat{c}_{i-1}^d = \cdots = \hat{c}_1^d = 0$. Furthermore,

$$\hat{c}_j^d > 0 \Rightarrow \bar{s}(d) < s_k^d \text{ for all } k > i. \tag{4.2}$$

We note that if $\bar{s}(d) > 1$, then $\hat{c}_n^d = 0$ and, therefore, all $\hat{c}_i^d = 0$. In this case, there exists no nontrivial non-negative steady state. If all $\hat{c}_i^d > 0$, then (4.2) implies that $\bar{s}(d) < s_i^d$ for all $i > 1$. This implies that $i_0 = 1$. In this case, we have a unique fully positive steady state, due to Lemma 4.4. We easily check that $\hat{c}_i^d$ fulfill the steady state conditions.

In all other cases there exists $1 < k < n$ such that $\hat{c}_k^d > 0$ and $\hat{c}_{k-1}^d = 0$. This implies that $\alpha_k^d = 0$ and, therefore, $\bar{s}(d) \geq s_k^d$. On the other hand, since $\bar{s}(d) := \min\{s_i^d \mid 1 \leq i < n\}$, it follows $\bar{s}(d) \leq s_k^d$. Therefore, $\bar{s}(d) = s_k^d$ and $s_k^d = \min\{s_i^d \mid 1 \leq i < n\}$. Using $\hat{c}_k^d > 0$ and (4.2) we obtain $\bar{s}(d) < s_j^d$ for all $j > k$. This implies that $i_0 = k$. Therefore, $\hat{c}_i^d$ is the required steady state with the maximal number of nonzero components.

■

4.4 Steady states of the full system

We define purely leukemic, purely hematopoietic and mixed steady states for system (2.6)-(2.8) in analogy to Definitions 3.2, 3.4 and 3.6.

For simplicity, we focus on steady states with $l_i > 0$ for all $i = 1, \ldots m$. The case $l_1 = \cdots = l_k = 0$ for a $k < m$ works analogously to the case presented below.

Lemma 4.15
Let Assumptions 2.2 be fulfilled. Consider a non-negative steady state $(\bar{c}_1, \ldots, \bar{c}_n, \bar{l}_1, \ldots, \bar{l}_m)$ *of system* (2.6)-(2.8). *Define*

$$j := \max\{i | (2a_i^l - 1)p_i^l - d_i^l \geq (2a_k^l - 1)p_k^l - d_k^l \text{ for all } k\}.$$

Then, $\bar{l}_i = 0$ *for all* $1 \leq i < j$.

PROOF
Let $j > 1$. Let d_c be defined as in Assumption 2.5. We denote the steady state value of d_c by $\bar{d}_c$. Let $k < j$ be the minimal index satisfying $\bar{l}_k > 0$. This implies that $\bar{d}_c = (2a_k^l - 1)p_k^l - d_k^l \geq 0$. Due to the definition of j, it then follows $(2a_j^l - 1)p_j^l - d_j^l - \bar{d}_c \geq 0$. Furthermore, $2(1 - a_{k-1})p_{k-1}^l > 0$. The steady state condition for l_j then implies that $\bar{l}_{j-1} = 0$. If $j > 2$ the steady state condition for l_{j-1} implies that $\bar{l}_{j-2} = 0$, due to $2(1 - a_{j-2})p_{j-2}^l > 0$. Iteratively, we obtain $\bar{l}_k = 0$ for $k < j$, which is a contradiction.

■

Remark 4.16
Consider steady states of system (2.6) - (2.8). *To obtain steady states with* $l_1 > 0$,

we assume in the following that $\left((2a_1^l - 1)p_1^l - d_1^l\right) - (2a_i^l - 1)p_i^l + d_i^l > 0$ *for all* $i > 1$.

Remark 4.17
Consider steady states of system (2.6) - (2.8). *If* $(2a_1^l - 1)p_1^l - d_1^l < 0$, *then* l_1 *decays exponentially and it follows* $l_1 = 0$ *in a steady state. Therefore, we assume in the following that* $(2a_1^l - 1)p_1^l - d_1^l > 0$.

Remark 4.18
Consider steady states $(\bar{c}_1, \cdots, \bar{c}_n, \bar{l}_1, \cdots, \bar{l}_m)$ *of system* (2.6) - (2.8). *Let* $(2a_1^l - 1)p_1^l - d_1^l = 0$.

(i) If there exists j *with* $(2a_j^l - 1)p_j^l - d_j^l > 0$, *then, due to Lemma 4.15, it follows* $\bar{l}_1 = 0$.

(iia) If $(2a_j^l - 1)p_j^l - d_j^l < 0$ *for all* $1 < j < m$, *then there exists a one dimensional manifold of* $\bar{l}_i$ *satisfying* $\frac{d}{dt}l_1 = \cdots = \frac{d}{dt}l_m = 0$. *Denote by* $(\bar{c}_1^0, \ldots, \bar{c}_n^0)$ *a non-negative steady state of system* (4.1) *with* $d = 0$. *As long as* $\bar{d}_c := d_c(\sum_{i=1}^{m-1} \bar{l}_i + \bar{l}_m\chi + \sum_{i=1}^{n-1} \bar{c}_i^0) = 0$, $(\bar{c}_1^0, \ldots, \bar{c}_n^0, \bar{l}_1, \ldots \bar{l}_m)$ *is a steady state of the full system* (2.6)-(2.8). *In this case, steady state values of* $\bar{c}_i^0$ *are independent of steady state values of* $\bar{l}_i$.

(iib) If $(2a_j^l - 1)p_j^l - d_j^l < 0$ *for all* $1 < j < m$ *and if* $\bar{d}_c > 0$ *in a steady state, then* $(2a_j^l - 1)p_j^l - d_j^l - \bar{d}_c < 0$ *for all* $1 \leq j < m$ *and there exists no steady state with positive* $\bar{l}_i$.

Remarks 4.16-4.18 motivate the assumptions of the following Proposition 4.19.

Proposition 4.19 (Classifications of steady states)
Let Assumptions 2.2 be fulfilled. Let d_c be defined as in Assumption 2.5. Assume

(i) $d_n^c > 0$, $d_m^l > 0$,

(ii) $d_1^c < (2a_1^c - 1)p_1^c$,

(iii) $a_1^c p_1^c (d_i^c + p_i^c) > a_i^c p_i^c (d_1^c + p_1^c)$ *for* $i = 2, \ldots, n-1$,

(iv) $\big((2a_1^l - 1)p_1^l - d_1^l\big) - (2a_i^l - 1)p_i^l + d_i^l > 0$ *for* $i = 2, \ldots, m-1$,

(v) $\bar{d} := (2a_1^l - 1)p_1^l - d_1^l > 0$.

Then, there exists a unique purely leukemic steady state $(0, \cdots, 0, \bar{l}_1, \cdots, \bar{l}_n)$ *with* $\bar{l}_1 > 0$ *and a unique purely hematopoietic steady state* $(\bar{c}_1, \cdots, \bar{c}_n, 0, \cdots, 0)$ *of system* (2.6) - (2.8) *with* $\bar{c}_1 > 0$ *and* $d_c(\sum_{i=1}^{n-1} \bar{c}_i) = 0$. *Furthermore, it holds:*

(a) If there exists no $i \in \{1, \ldots, n\}$ *such that* $(2a_i^c - 1)p_i^c - d_i^c - \bar{d} > 0$, *then there exists no mixed steady state* $(\bar{c}_1, \cdots, \bar{c}_n, \bar{l}_1, \cdots, \bar{l}_m)$ *of system* (2.6) - (2.8) *with* $\bar{l}_1 > 0$ *and* $\bar{c}_i > 0$ *for an* $i \in \{1, \cdots, n\}$.

(b) Assume, there exists $i \in \{1, \ldots, n\}$ *such that* $(2a_i^c - 1)p_i^c - d_i^c - \bar{d} > 0$. *Define* $i_0 := \max\{i | \frac{p_i^c + d_i^c + \bar{d}}{2a_i^c p_i^c} \leq \frac{p_j^c + d_j^c + \bar{d}}{2a_j^c p_j^c}$ *for all* $j = 1, \ldots n\}$. *Then, there exists a unique non-negative steady state* $(\bar{c}_1^{\bar{d}}, \ldots, \bar{c}_n^{\bar{d}})$ *with* $\bar{c}_{i_0}^{\bar{d}} > 0$ *of system* (4.1) *with* $d = \bar{d} = (2a_1^l - 1)p_1^l - d_1^l$.

(b1) Let $\bar{x}$ *be uniquely defined by* $d_c(\bar{x}) = (2a_1^l - 1)p_1^l - d_1^l$. *If* $\sum_{i=1}^{n-1} \bar{c}_i^{\bar{d}} < \bar{x}$, *then there exists a unique mixed steady state* $(\bar{c}_1, \cdots, \bar{c}_n, \bar{l}_1, \cdots, \bar{l}_m)$ *of system* (2.6) - (2.8) *with* $\bar{c}_i > 0$ *for* $i \geq i_0$ *and* $\bar{l}_i > 0$ *for* $1 \leq i \leq m$. *In all mixed steady states it holds* $\bar{c}_i = 0$ *for* $i < i_0$.

(b2) If $\sum_{i=1}^{n-1} \bar{c}_i^{\bar{d}} \geq \bar{x}$, *then there exists no mixed steady state with* $\bar{c}_{i_0} > 0$ *and* $\bar{l}_1 > 0$. *If* $\sum_{i=1}^{n-1} \bar{c}_i^d > \bar{x}$, *there exist a purely hematopoietic steady state* $(\bar{c}_1, \cdots, \bar{c}_n, 0, \cdots, 0)$ *of system* (2.6) - (2.8) *with* $d_c(\sum_{i=1}^{n-1} \bar{c}_i) > 0$.

PROOF
We search for steady states $(\bar{c}_1, \cdots, , \bar{c}_n, \bar{l}_1, \cdots, \bar{l}_m)$ of system (2.6) - (2.8). We denote the steady state value of $d_c(t)$ as $\bar{d}_c$ and that of $s(t)$ as $\bar{s}$. Assumptions (i)-(iii) imply that, if $\bar{l}_1 = \cdots = \bar{l}_m = 0$, there exists a unique steady state $(\bar{c}_1, \cdots, , \bar{c}_n, 0, \cdots, 0)$ with $\bar{c}_i > 0$ for all $i \in \{1, \cdots, n\}$ and $d_c(\sum_{i=1}^{n-1} \bar{c}_i) = 0$ (Proposition A.1).

We now consider the case $\bar{l}_1 > 0$ and $\bar{c}_1 = ... = \bar{c}_n = 0$. It holds

$$\begin{aligned}\frac{d}{dt}l_1(t) = 0 &\Leftrightarrow (2a_1^l - 1)p_1^l - d_1^l - \bar{d}_c = 0\\ &\Leftrightarrow \bar{d}_c = (2a_1^l - 1)p_1^l - d_1^l.\end{aligned}$$

We note that $\bar{d}_c = (2a_1^l - 1)p_1^l - d_1^l$. Insertion into the ODE for l_i $(i = 2, \ldots, m-1)$ leads to

$$\begin{aligned}&\frac{d}{dt}l_i(t) = 0\\ &\Leftrightarrow 2(1 - a_{i-1}^l)p_{i-1}^l\bar{l}_{i-1} + (2a_i^l - 1)p_i^l\bar{l}_i - d_i^l\bar{l}_i - \bar{d}_c\bar{l}_i = 0\\ &\Leftrightarrow 2(1 - a_{i-1}^l)p_{i-1}^l\bar{l}_{i-1} + (2a_i^l - 1)p_i^l\bar{l}_i - d_i^l\bar{l}_i - \big((2a_1^l - 1)p_1^l - d_1^l\big)\bar{l}_i = 0\\ &\Leftrightarrow \bar{l}_{i-1} = -\frac{(2a_i^l - 1)p_i^l - d_i^l - \big((2a_1^l - 1)p_1^l - d_1^l\big)}{2(1 - a_{i-1}^l)p_{i-1}^l}\bar{l}_i =: \alpha_i\bar{l}_i. \qquad (4.3)\end{aligned}$$

Since $2(1 - a_{i-1}^l)p_{i-1}^l > 0$, existence of a steady state of the form $(0, \cdots, 0, \bar{l}_1, \cdots, \bar{l}_n)$ with $\bar{l}_i > 0$ for all $i \in \{1, \cdots, m\}$ requires that

$$(2a_i^l - 1)p_i^l - d_i^l - \big((2a_1^l - 1)p_1^l - d_1^l\big) < 0.$$

This is fulfilled, due to Assumption (iv).

The ODE for l_m leads to

$$\begin{aligned}\frac{d}{dt}l_m(t) = 0 &\Leftrightarrow 2(1 - a_{m-1}^l)p_{m-1}^l\bar{l}_{m-1} - d_m^l\bar{l}_m - \bar{d}_c\bar{l}_m\chi = 0\\ &\Leftrightarrow 2(1 - a_{m-1}^l)p_{m-1}^l\bar{l}_{m-1} - d_m^l\bar{l}_m - \big((2a_1^l - 1)p_1^l - d_1^l\big)\bar{l}_m\chi = 0\\ &\Leftrightarrow \bar{l}_{m-1} = \frac{d_m^l + \chi\big((2a_1^l - 1)p_1^l - d_1^l\big)}{2(1 - a_{m-1}^l)p_{m-1}^l}\bar{l}_m =: \alpha_m\bar{l}_m. \qquad (4.4)\end{aligned}$$

Since $2(1 - a_{m-1}^l)p_{m-1}^l > 0$, it is necessary that $d_m^l + \chi\big((2a_1^l - 1)p_1^l - d_1^l\big) > 0$. This holds, due to Assumption (v).

We obtain inductively for $i = 1, \ldots, m$:

$$\bar{l}_i = \big(\Pi_{k=i}^{m-1}\alpha_{k+1}\big)\,\bar{l}_m.$$

Consequently,

$$\sum_{i=1}^{m-1}\bar{l}_i + \chi\bar{l}_m = \left[\sum_{i=1}^{m-1}\big(\Pi_{k=i}^{m-1}\alpha_{k+1}\big) + \chi\right]\bar{l}_m. \qquad (4.5)$$

Due to the definition of the function d_c, there exists exactly one value $\bar{x}$ such that $d_c(\bar{x}) = \bar{d} > 0$. If we set $\bar{c}_1 = \cdots = \bar{c}_n = 0$ and choose $\bar{l}_m$ such that $\bar{x} = \left[\sum_{i=1}^{m-1} \left(\Pi_{k=i}^{m-1}\alpha_{k+1}\right) + \chi\right] \bar{l}_m$, then we obtain a purely leukemic steady state with $\bar{l}_i > 0$ for all $i \in \{1, \cdots, m\}$.

We now consider the cases (a) and (b).

(a) If $\bar{l}_1 > 0$, the steady state condition for l_1 implies that $\bar{d}_c = \bar{d}$. The assumption $(2a_i^c - 1)p_i^c - d_i^c - \bar{d} \leq 0$ for all $i \in \{1, \cdots, , n-1\}$ implies that $(2a_i^c\bar{s} - 1)p_i^c - d_i^c - \bar{d}_c \leq 0$ for all $i \in \{1, \ldots, n-1\}$, since $0 \leq \bar{s} \leq 1$. If there exists i such that $(2a_i^c - 1)p_i^c - d_i^c - \bar{d}_c = 0$, it holds $\bar{s} = 1$, which implies that $\bar{c}_n = 0$. Then, $\frac{d}{dt}c_n = 0$ implies that $\bar{c}_{n-1} = 0$, since $(2a_i\bar{s} - 1)p_i > 0$ for all $i \in \{1, \ldots, n-1\}$. For the same reason, $\bar{c}_{n-1} = 0$ implies that $\bar{c}_{n-2} = 0$. Inductively, we obtain $\bar{c}_i = 0$ for all $i \in \{1, \ldots, n\}$.

If $(2a_i^c - 1)p_i^c - d_i^c - \bar{d}_c < 0$ for all $i \in \{1, \ldots, n-1\}$, it follows $(2a_i^c\bar{s} - 1)p_i^c - d_i^c - \bar{d}_c < 0$ for all $0 \leq \bar{s} \leq 1$. Therefore, $\frac{d}{dt}c_1 = 0$ implies that $\bar{c}_1 = 0$. This and $\frac{d}{dt}c_2 = 0$ implies that $\bar{c}_2 = 0$. Inductively, we obtain $\bar{c}_i = 0$ for all $i \in \{1, \ldots, n\}$.

Therefore, $\bar{c}_i = 0$ for all $i \in \{1, \ldots, n\}$.

(b) For a given $d \geq 0$, we denote the unique non-negative steady state of system (4.1) with the maximal number of positive components as $(\bar{c}_1^d, \cdots, \bar{c}_n^d)$. For $d = \bar{d}$ Lemma 4.4 implies that $\bar{c}_i^{\bar{d}} = 0$ for $i < i_0$ and $\bar{c}_i^{\bar{d}} > 0$ otherwise.

(b1) The condition $\bar{l}_1 > 0$ requires that $\bar{d}_c = (2a_1^l - 1)p_1^l - d_1^l > 0$. This implies existence of a unique $\bar{x}$ such that $d_c(\bar{x}) = \bar{d}_c$. Existence of a mixed steady state requires that $\bar{x} = \sum_{i=1}^{m-1} \bar{l}_i + \bar{l}_m\chi + \sum_{i=1}^{n-1} \bar{c}_i$. For given $\bar{d}_c > 0$ the steady state conditions for the c_i are equivalent to the steady state conditions of system (4.1) with $d = \bar{d}_c$. As argued above, due to Lemma 4.4, there exists a steady state of system (4.1) with $\bar{c}_i^{\bar{d}} = 0$ for $i < i_0$ and $\bar{c}_i^{\bar{d}} > 0$ otherwise. We set $\bar{c}_i = \bar{c}_i^{\bar{d}}$.

Due to the assumptions, it holds $\bar{x} - \sum_{i=1}^{n-1} \bar{c}_i = \bar{x} - \sum_{i=1}^{n-1} \bar{c}_i^d =: \bar{y} > 0$. Existence of a mixed steady state then requires $\bar{y} = \sum_{i=1}^{m-1} \bar{l}_i + \bar{l}_m\chi$. Using equation (4.5) yields a unique $\bar{l}_m$. Using equations (4.4) and (4.3), we obtain unique positive $\bar{l}_i$ for $0 < i < m - 1$.

(b2) The condition $\bar{l}_1 > 0$ requires $\bar{d}_c = (2a_1^l - 1)p_1^l - d_1^l > 0$. The shape of d_c implies existence of a unique $\bar{x}$ satisfying $d_c(\bar{x}) = \bar{d}_c$. It has to hold $\bar{x} = \sum_{i=1}^{m-1} \bar{l}_i + \bar{l}_m\chi + \sum_{i=1}^{n-1} \bar{c}_i$. For given $\bar{d}_c > 0$ the steady state conditions for the c_i are equivalent to the steady state conditions of system (4.1) with $d = \bar{d}_c$. Due to Lemma 4.4, the constraint $\bar{c}_{i_0} > 0$ leads to $\bar{c}_1 = \cdots = \bar{c}_{i_0-1} = 0$ and $\bar{c}_i = \bar{c}_i^{\bar{d}} > 0$ for $i_0 \leq i \leq n$. As above, we denote by $(\bar{c}_1^{\bar{d}}, \cdots, \bar{c}_n^{\bar{d}})$ the unique

equilibrium of system (4.1) for $d = \bar{d}_c$ and $\bar{c}_{i_0}^{\bar{d}} > 0$. Since, due to the assumptions, $\bar{x} < \sum_{i=1}^{n-1} \bar{c}_i$, there exist no positive $\bar{l}_i$ satisfying $\bar{x} = \sum_{i=1}^{m-1} \bar{l}_i + \bar{l}_m \chi + \sum_{i=1}^{n-1} \bar{c}_i$. For this reason there exists no mixed steady state with $\bar{c}_{i_0} > 0$ and $\bar{l}_1 > 0$.

The assumption $\bar{x} < \sum_{i=1}^{n-1} \bar{c}_i^{\bar{d}}$ implies that $d_c(\Phi(\bar{d}_c)) = d_c(\sum_{i=1}^{n-1} \bar{c}_i^{\bar{d}}) > d_c(\bar{x}) = \bar{d}_c$, where Φ is specified in Definition 4.12. For d large enough it holds $\Phi(d) = 0$, i.e., $d_c(\Phi(d)) = 0 < \bar{d}_c$. Denote by $\mathrm{id}(\cdot)$ the identity mapping $x \mapsto x$. Since d_c and Φ are continuous, see Lemma 4.14, $d_c \circ \Phi$ is continuous. It holds $d_c \circ \Phi(\bar{d}_c) > \mathrm{id}(\bar{d}_c)$. We know that the functions id and $d_c \circ \Phi$ intersect for a $d^* > \bar{d}_c$, since $\lim_{d\to\infty} d_c \circ \Phi(d) = 0$ and id is an increasing function. Therefore, there exists $d^* > 0$ such that $d_c(\Phi(d^*)) = d^*$, see Figure 4.2. Then, $(\bar{c}_1^{d^*}, \cdots, \bar{c}_n^{d^*}, 0, \cdots, 0)$ is a purely hematopoietic steady state of system (2.6)-(2.8) with $\bar{d}_c = d^* > 0$. By $(\bar{c}_1^{d^*}, \cdots, \bar{c}_n^{d^*})$ we denote the steady state of system (4.1) with $d = d^*$ and the maximal number of positive components.

■

Remark 4.20
Assumptions (i)-(iii) are necessary and sufficient for existence of unique positive $\bar{c}_i$ $(i = 1, \ldots, n)$ *such that* $(\bar{c}_1, \ldots \bar{c}_n, 0, \ldots 0)$ *is a steady state of system* (2.6) - (2.8)*. This steady state corresponds to the healthy hematopoietic equilibrium.*

Remark 4.21
Assumptions (iv) and (v) are motivated by Lemma 4.15 and Remarks 4.16-4.18.

Remark 4.22 (Interpretation of Proposition 4.19 (a))
As the relative expansion rate of a compartment, we understand the number of cells entering the compartment per unit of time divided by the total number of cells in the respective compartment at the respective time-point. The relative expansion rate of the stem cell compartment at time t *is given by* $(2a_1^c s(t) - 1)p_1^c - d_1^c$*. Under maximal stimulation (*$s = 1$*) this is equal to* $(2a_1^c - 1)p_1^c - d_1^c$*. The relative growth rate of the leukemic stem cell compartment at time* t *is given by* $(2a_1^l - 1)p_1^l - d_1^l$*. Proposition 4.19 states that there exists no mixed steady state, if the relative growth rate of LSC is greater than or equal to the maximal growth rate of HSC. In the opposite case, feedback stimulation of HSC allows to compensate increased apoptosis rates caused by leukemic cell expansion and coexistence of both lineages is possible.*

Biological Remark 4.23 (Candidate treatment strategy)
A major problem of acute leukemias is the decline of healthy blood cells. One aim of treatment is to maintain healthy blood cell production. For survival of a patient, it may be sufficient, if a treatment drives the system to a state, where HSCs and LSCs can coexist. This could be achieved by increasing HSC proliferation and / or self-renewal such that $(2a_1^c - 1)p_1^c - d_1^c > (2a_1^l - 1)p_1^l - d_1^l$.

Biological Remark 4.24
As argued in Example 3.19, steady states with coexistence of both lineages can be observed in preleukemic states, chronic leukemias, myelodysplasias, monoclonal gammopathy of unknown significance or the so-called smoldering myelomas, [23,127]. They can persist for years without major impairment of blood function. Another example is (smoldering) macroglobulinemia Waldenström, where patients can survive over years and main symptoms do not come from impairment of bone marrow function but from immunoglobulines produced by the malignant clone, [129, 226]. These diseases can be interpreted as a stable coexistence of hematopoietic and neoplastic cells.

Remark 4.25 (Purely hematopoietic steady states with $d_c > 0$)
Denote the unique positive steady state of system (4.1) *for* $d = 0$ *as* $(\bar{c}_1^0, \cdots, \bar{c}_n^0)$. *Lemma 4.8 (c) implies that, for appropriate number of compartments and appropriate parameter values, there exists* $d > 0$ *and a corresponding unique steady state* $(\bar{c}_1^d, \cdots, \bar{c}_n^d)$ *of system* (4.1) *with the maximal number of positive components such that* $\sum_{i=1}^{n-1} c_i^0 < \sum_{i=1}^{n-1} c_i^d$. *We define a function* $q_n : \mathcal{A} \to \mathbb{R}_0^+$, $d \mapsto \sum_{i=1}^{n-1} \bar{c}_i^d$. *Here,* $\mathcal{A} := \{d > 0 \mid \bar{c}_i^d > 0,\ i = 1, \ldots, n;\ \sum_{i=1}^{n-1} c_i^0 < \sum_{i=1}^{n-1} c_i^d\}$. *Let* d_c *be defined as in equation* (2.8) *and Assumption 2.5 (iv). If there exists a* $\tilde{d} \in \mathcal{A}$ *satisfying* $d_c(q_n(\tilde{d})) = \tilde{d}$, *then there exists a steady state* $(\bar{c}_1^{\tilde{d}}, \cdots, \bar{c}_n^{\tilde{d}}, 0, \cdots, 0)$ *of system* (2.6)-(2.8) *with* $d_c(\sum_{i=1}^{n-1} \bar{c}_i^{\tilde{d}}) > 0$. *An example for this case is given in Figures 4.2 and 4.3. Due to non-linearity of the considered system, a systematic analysis of steady states of this type will be omitted.*

Biological Remark 4.26 (Hyper-crowded hematopoietic steady states)
The steady states in Remark 4.25 correspond to purely hematopoietic steady states, where hematopoietic cell density and, consequently, the apoptosis rate of hematopoietic cells are increased. Since in this type of steady states, cell density is higher compared to purely hematopoietic steady states with $d_c = 0$ *(healthy steady states), we denote this type of steady states as hyper-crowded steady state (hyper= increased, greek). Increased densities of immature cells causing high apoptosis rates have been observed in myelodysplastic syndromes, [53]. Due to Lemma 4.8 (a), this type of steady states does not exists for* $n = 2$.

Example 4.27
Figure 4.2 illustrates cases (b1) and (b2) described in Proposition 4.19, Figure 4.3 gives a numerical example for case (b2).

Biological Remark 4.28
Experiments in mice suggest that aberrant niche cells can lead to system states characterized by reduced numbers of mature leukocytes, higher number of primitive cells and increased cell turnover. Nevertheless, the hematopoietic stem cells preserve normal functionality, if transplanted into physiological micro-environments and no mutations can be detected, [176]. The properties of hyper-crowded

steady states of the model system coincide with these experimental observations. The death rate function d can be interpreted as an environmental impact on cell dynamics. In this sense, the hyper-crowded steady states describe diseases originating from interaction of healthy cells with their (pathological) micro-environment. Recent experiments suggest that environment-induced diseases exist in vivo, [119, 176, 191, 232, 233].

Biological Remark 4.29
Figure 4.3 shows that the healthy equilibrium is destabilized by a leukemic cell population. Nevertheless, the leukemic cell population eventually declines and a new purely hematopoietic steady state with high hematopoietic marrow cell concentrations is established. In this sense, the existence of purely hematopoietic steady states with $\bar{d}_c > 0$ might act as a protection against expansion of cancer cells. The enhanced apoptosis $\bar{d}_c > 0$, due to marrow crowding of hematopoietic cells, can out-compete leukemic clones. Nevertheless, in a real organisms the high cell turn-over in the newly established steady state is prone to occurrence of mutations and can, therefore, be seen as a precancerous state. The model suggest that transient appearance of aberrant clones can drive the system from the healthy steady state to a hyper-crowded steady state with criteria similar to some forms of MDS, i.e., reduced numbers of mature cells, high marrow cellularity, high cell turnover, [53]. In summary, the model suggests the following hypothetical mechanism leading to MDS phenotype in absence of detectable mutations in the cell bulk:

(i) Aberrant cells destabilize the healthy equilibrium and expand at the expense of healthy marrow cells.

(ii) Shortage of mature cells increases the concentration of the feedback signal and in turn expansion rates of healthy immature cells. The system converges to a state with high counts of immature healthy cells.

(iii) Expansion rates of stimulated healthy cells are larger than that of aberrant cells. High cell counts lead to increased apoptosis rates and, thus, to decline of the aberrant cell population.

(iv) Density of healthy immature cells and apoptosis rates remain high. Due to increased apoptosis rate, the number of mature cells is smaller than in the healthy steady state. Therefore, cytokine feedback stimulates immature cells. The cytokine stimulation allows immature cells to establish a new equilibrium, although apoptosis rates are increased.

It might be an interesting question, if such a mechanism plays a role in the development of MDS.

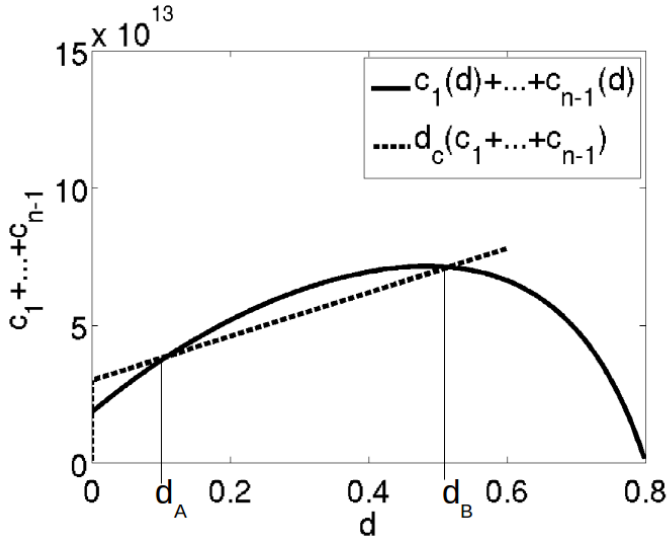

Figure 4.2: Illustration of Proposition 4.19 (b1)-(b2). The Figure shows how $\sum_{i=1}^{n-1} \bar{c}_i$ depends on the constant apoptosis rates d (continuous line). The dashed line shows the dependence of d_c from $\sum_{i=1}^{n-1} \bar{c}_i$. Intersection points correspond to purely hematopoietic steady states with $\bar{d}_c > 0$ (see Remark 4.25). As long as $(2a_1^l - 1)p_1^l - d_1^l \in (d_A, d_B)$, there exists no mixed steady state with $\bar{l}_1 > 0$. For $(2a_1^l - 1)p_1^l - d_1^l \in (0, d_A)$ and $(2a_1^l - 1)p_1^l - d_1^l \in (d_B, (2a_1^c - 1)p_1^c - d_1^c)$ there exist mixed steady states with $\bar{c}_1 > 0$ and $\bar{l}_1 > 0$. Parameters for the hematopoietic part of the system are as in Figure 4.1 and $d_c(x) = \max(0, (x - 3 \cdot 10^{13})/8)10^{-13}$.

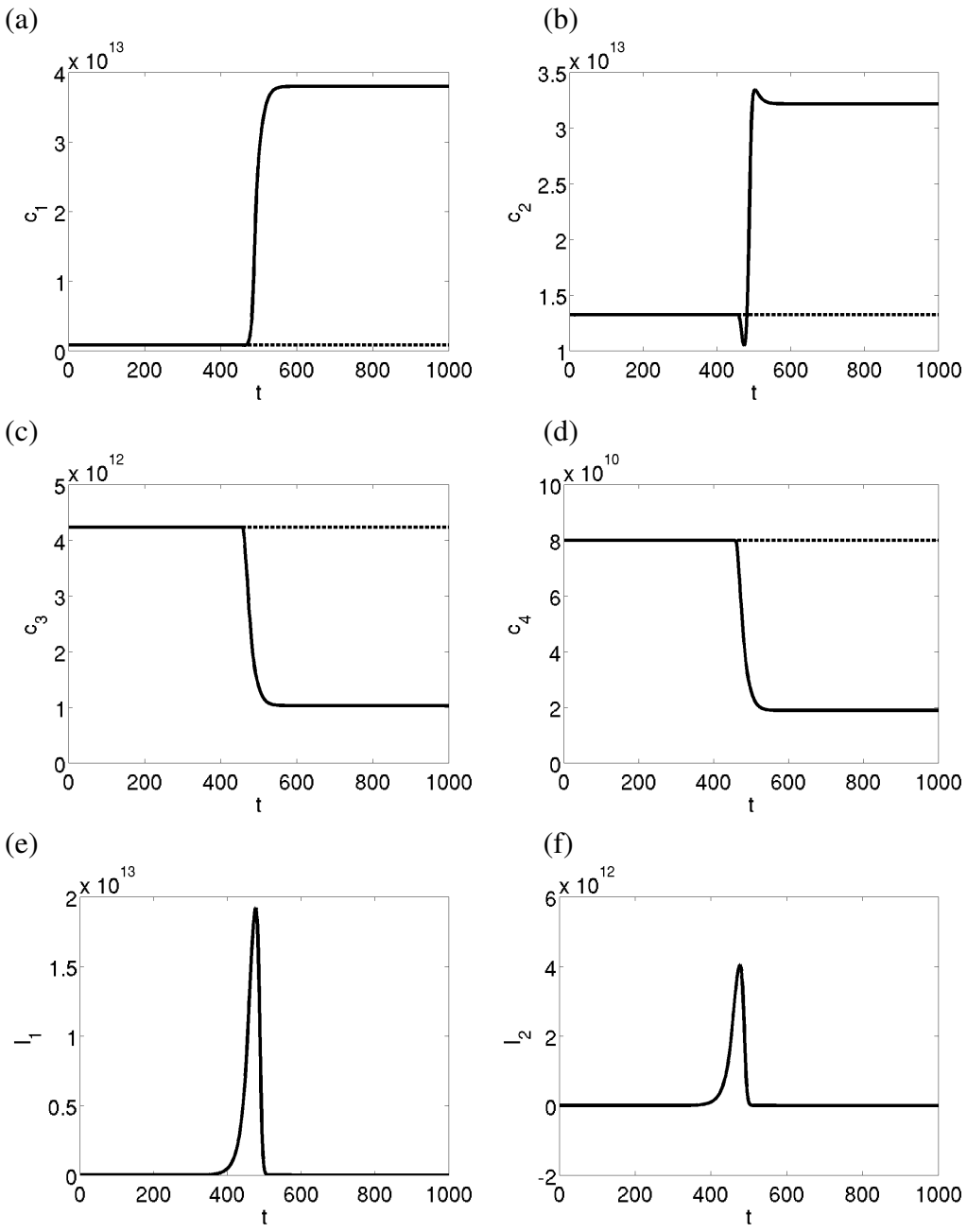

Figure 4.3: Example for Proposition 4.19 (b2). Panels (a)-(f) show time evolution of all cell types for initial conditions of c_i at the purely hematopoietic steady state with $\bar{d}_c = 0$. This steady state corresponds to the dashed lines (and is positive). Furthermore, $l_1(0) = 100$, $l_2(0) = 0$. In this case, the system converges to a purely hematopoietic steady state with $\bar{d}_c > 0$. Here, we have $n = 4$, $m = 2$. Parameters for the hematopoietic part of the system are as in Figure 4.1. Parameters for the leukemic lineage are $p_1^l = 0.27$, $a_1^l = 0.6$, $d_1^l = 0$, $d_2^l = 1$ and $d_c(x) = \max(0, (x - 3 \cdot 10^{13})/8) \cdot 10^{-13}$.

Remark 4.30
Proposition 4.19 considers steady states with either $\bar{l}_1 > 0$ or $\bar{c}_{i_0} > 0$. If we are interested in steady states with $\bar{l}_1 = 0$, we erase the ODE for l_1 in system (2.6)-(2.8) *and set $l_1 = 0$ in the remaining equations. We, then, apply Proposition 4.19 to the modified system. If we are interested in steady states with $\bar{c}_{i_0} = 0$, we set $c_1 = c_2 = \cdots = c_{i_0} = 0$ and erase the ODEs for c_1, c_2, $\ldots$, c_{i_0} in the system and apply Proposition 4.19 to the modified system.*

4.5 Linearized stability of steady states

Lemma 4.31
Let Assumptions 2.2 be fulfilled. Consider a non-negative steady state $(\bar{c}_1, \cdots, \bar{c}_n, \bar{l}_1, \cdots, \bar{l}_m)$ of system (2.6) - (2.8)*. Denote by $\bar{d}_c$ the steady state value of of d_c . Define*

$$j := \max\{i \mid (2a_i^l - 1)p_i^l - d_i^l - \bar{d}_c \geq (2a_j^l - 1)p_j^l - d_j^l - \bar{d}_c \text{ for all } j\}.$$

If $(2a_j^l - 1)p_j^l - d_j^l - \bar{d}_c > 0$ and $\bar{l}_j = 0$, this steady state is unstable.

PROOF
We know from Lemma 4.15 that, for all $k < j$, it holds $\bar{l}_k = 0$. We reorder the system and consider equations in the order $\frac{d}{dt}l_1, \cdots, \frac{d}{dt}l_m, \frac{d}{dt}c_1, \cdots, \frac{d}{dt}c_n$. It holds:
$\frac{d}{dt}l_1 = (2a_1^l - 1)p_1^l l_1 - d_1^l l_1 - d_c(\sum_{i=1}^{m-1} l_i + \chi l_m + \sum_{i=1}^{n-1} c_i)l_1 =: f_1(l_1, \cdots, c_n)$, where we use the notation$\bar{d}' := \frac{d}{dx}d_c(x)|_{x=\sum_{i=1}^{m-1}\bar{l}_i+\chi\bar{l}_m+\sum_{i=1}^{n-1}\bar{c}_i}$. We linearize this equation around the considered steady state, which fulfills $\bar{l}_1 = 0$ and obtain:

$$\begin{aligned}
\partial_{l_1} f_1|_{l_1=0,c_i=\bar{c}_i} &= (2a_1^l - 1)p_1^l - d_1^l - \bar{d}_c - \bar{d}'l_1 = (2a_1^l - 1)p_1^l - d_1^l - \bar{d}_c \\
\partial_{l_2} f_1|_{l_1=0,c_i=\bar{c}_i} &= -\bar{d}'l_1 = 0 \\
&\vdots \qquad \vdots \\
\partial_{l_{m-1}} f_1|_{l_1=0,c_i=\bar{c}_i} &= -\bar{d}'l_1 = 0 \\
\partial_{l_m} f_1|_{l_1=0,c_i=\bar{c}_i} &= 0 \\
\partial_{c_1} f_1|_{l_1=0,c_i=\bar{c}_i} &= -\bar{d}'l_1 = 0 \\
\partial_{c_2} f_1|_{l_1=0,c_i=\bar{c}_i} &= -\bar{d}'l_1 = 0 \\
&\vdots \qquad \vdots \\
\partial_{c_{m-1}} f_1|_{l_1=0,c_i=\bar{c}_i} &= -\bar{d}'l_1 = 0 \\
\partial_{c_m} f_1|_{l_1=0,c_i=\bar{c}_i} &= 0.
\end{aligned}$$

Furthermore, for each k with $1 < k \leq j$, it holds $\frac{d}{dt}l_k = 2(1-a_{k-1}^l)p_{k-1}^l l_{k-1} + (2a_k^l - 1)p_k^l l_k - d_k^l l_k - d_c(\sum_{i=1}^{m-1} l_i + l_m\chi + \sum_{i=1}^{n-1} c_i)l_k =: f_k(l_1, \cdots, c_n)$. Therefore,

$$\partial_{l_k} f_k|_{l_1=\cdots=l_j=0, c_i=\bar{c}_i} = (2a_k^l - 1)p_k^l - d_k^l - \bar{d}_c - \bar{d}' l_k = (2a_k^l - 1)p_k^l - d_k^l - \bar{d}_c$$

We derive f_k in direction of l_q with $m \geq q > k$ and obtain :

$$\partial_{l_q} f_k|_{l_1=\cdots=l_j=0, c_i=\bar{c}_i} = -\bar{d}' l_k = 0.$$

For $1 \leq i \leq n$ it holds

$$\partial_{c_i} f_k|_{l_1=\cdots=l_j=0, c_i=\bar{c}_i} = -\bar{d}' l_k = 0.$$

Therefore, $(2a_k^l - 1)p_k^l - d_k^l - \bar{d}_c$ is an eigenvalue for all $1 \leq k \leq j$. Since $(2a_j^l - 1)p_j^l - d_j^l - \bar{d}_c > 0$, the equilibrium is unstable. ■

Remark 4.32 (Leukemic stem cell properties)
Denote by $\bar{c}_i$ the healthy equilibrium of the hematopoietic system (2.3)*. Let $\bar{l}_i = 0$ and $j = 1$ in Lemma 4.31. In the healthy equilibrium it holds $\bar{d}_c = 0$, due to Assumption 2.5 (iv). Then, the necessary and sufficient condition for expansion of the leukemic stem cells l_1 is $2(a_1^l - 1)p_1^l - d_1^l > 0$. In the case $d_1^l = 0$ this leads to $2(a_1^l - 1)p_1^l > 0$. This implies that leukemic stem cells expand, if and only if $a_1^l > 0.5$ for all possible positive values of p_1^l. If $a_1^l < 0.5$, leukemic cells become extinct for all values of p_1^l. Expansion or extinction of leukemic stem cells depends only on a_1^l. In this sense, high self-renewal is more important than high proliferation for establishment of a leukemic cell line.*

Lemma 4.33
Let Assumptions 2.2 be fulfilled. Assume there exists a non-negative steady state $(\bar{c}_1, \cdots, \bar{c}_n, \bar{l}_1, \cdots, \bar{l}_m)$ of system (2.6) - (2.8)*, where $\bar{l}_k > 0$ for a $k \in \{1, \cdots, n\}$. Let $\hat{k} := \min\{i \mid \bar{l}_i > 0\}$. Let $\bar{d}_c$ be the steady state value of d_c. Assume there exists j such that $\frac{p_j^c + d_j^c + \bar{d}_c}{2a_j^c p_j^c} < 1$. Define $i_0 := \max\left\{i | \frac{p_i^c + d_i^c + \bar{d}_c}{2a_i^c p_i^c} \leq \frac{p_j^c + d_j^c + \bar{d}_c}{2a_j^c p_j^c} \text{ for all } j = 1, \ldots n-1\right\}$. Then, all steady states with $\bar{c}_{i_0} = 0$, $\bar{l}_{\hat{k}} > 0$, $\bar{l}_i = 0$ for all $i < \hat{k}$ are unstable.*

PROOF
It holds $\bar{d}_c = (2a_{\hat{k}}^l - 1)p_{\hat{k}}^l$. The condition $\bar{c}_{i_0} = 0$ implies that $\bar{s} > \frac{d_{i_0}^c + p_{i_0}^c + \bar{d}_c}{2a_{i_0}^c + p_{i_0}^c}$, due to definition of i_0.

We set $f_1 := (2\frac{a_1^c}{1+kc_n} - 1)p_1^c c_1 - d_1^c c_1 - d_c(\sum_{i=1}^{n-1} c_i + \sum_{i=1}^{m-1} l_i + \chi l_m)c_1$. For $i_0 \geq i > 1$ we set $f_i := 2(1 - \frac{a_{i-1}^c}{1+kc_n})c_{i-1} + (2\frac{a_i^c}{1+kc_n} - 1)p_i^c c_i - d_i^c c_i - d_c(\sum_{i=1}^{n-1} c_i + \sum_{i=1}^{m-1} l_i + \chi l_m)c_i$. We notice that $\frac{\partial}{\partial c_j} f_i|_{c_i=0} = 0$ for all $1 \leq i \leq i_0$, $n \geq j > i$ and that $\frac{\partial}{\partial l_i} f_i|_{c_i=0} = 0$ for all $1 \leq i \leq m$.

Therefore, $(2a_{i_0}^c \bar{s} - 1)p_{i_0}^c - d_{i_0}^c - d_c(\sum_{i=1}^{n-1} \bar{c}_i + \sum_{i=1}^{m-1} \bar{l}_i + \chi \bar{l}_m)$ is an eigenvalue. We note that for $\bar{s} > \frac{d_{i_0}^c + p_{i_0}^c + \bar{d}_c}{2a_{i_0}^c + p_{i_0}^c}$ this eigenvalue is positive. This implies instability.

■

Proposition 4.34
Let Assumptions 2.2 be fulfilled. Assume there exists a steady state $(0, \ldots, 0, \bar{c}_k, \ldots \bar{c}_n, 0, \ldots, 0, \bar{l}_j, \ldots, \bar{l}_m)$ *of system* (2.6) - (2.8) *with* $\bar{c}_k > 0$ *and* $\bar{l}_j > 0$ *then*

(i) each steady state with $\bar{c}_k = 0$ *and* $\bar{l}_{j-1} = 0$ *and* $\bar{l}_j > 0$ *is unstable,*

(ii) each steady state with $\bar{l}_j = 0$ *is unstable.*

If $k = 1$ *we consider the condition* $\bar{c}_{k-1} = 0$ *as fulfilled, if* $j = 1$ *we consider the condition* $\bar{c}_{j-1} = 0$ *as fulfilled.*

PROOF
(i) We apply the above Lemmas to the ODE system consisting of the equations for $c_k, \ldots, c_n, l_j, \ldots, l_m$. The steady state condition for l_j requires $\bar{d}_c := (2a_j^l - 1)p_j^l - d_j^l > 0$, where $\bar{d}_c$ is the steady state value of d_c. We now apply Lemma 4.4 with $d = \bar{d}_c$. The existence of the steady state with $\bar{c}_k > 0$ implies that $k = \max\{i \mid s_i = \min\{s_i, i = k, \ldots, n-1\}\}$ (i.e., $s_i > s_k$ for $i > k$) and $s_k < 1$. Then, Lemma 4.33 implies instability.

(ii) It holds $\bar{d}_c = (2a_j^l - 1)p_j^l - d_j^l > 0$. We apply the above Lemmas to the ODE system consisting of the equations for $c_k, \ldots, c_n, l_j, \ldots, l_m$: Lemma 4.15 and existence of a steady state with $\bar{l}_j > 0$ implies that

$$(2a_j^l - 1)p_j^l - d_j^l > (2a_k^l - 1)p_k^l - d_k^l \text{ for all } k > j. \tag{4.6}$$

If l_k with $k > j$ is the positive population with lowest index, then $\bar{d}_c = (2a_k^l - 1)p_k^l - d_k^l > 0$. Due to condition (4.6), it holds $(2a_j^l - 1)p_j^l - d_j^l - \bar{d}_c > (2a_k^l - 1)p_k^l - d_k^l - \bar{d}_c$ for all $k > j$ and $(2a_j^l - 1)p_j^l - d_j^l - \bar{d}_c > 0$. Then, Lemma 4.31 implies instability.

■

Biological Remark 4.35
Proposition 4.34 states that for a given leukemic stem cell population all mixed steady states, which do not have the maximal number of positive components, are unstable. Furthermore, all steady states, which do not have the maximal number of positive leukemic populations, are unstable.

4.6 Linearized stability analysis for $n = m = 2$

We now consider the case $n = m = 2$. For simplicity of calculations, we assume $d_1^c = d_1^l = \chi = 0$. In analogy to Lemma 4.19, we make the following assumptions for the remainder of this Section.

Assumptions 4.36
(i) $d_2^l > 0$, $d_2^c > 0$, $d_1^l = d_1^c = \chi = 0$,

(ii) $0 < (2a_1^c - 1)p_1^c$,

(iii) $0 < (2a_1^l - 1)p_1^l$.

We consider the following system

$$\begin{aligned} \frac{d}{dt}c_1 &= (2a_1^c s - 1)p_1^c c_1 - d(c_1 + l_1)c_1 \\ \frac{d}{dt}c_2 &= 2(1 - a_1^c s)p_1^c c_1 - d_2^c c_2 \\ s &= \frac{1}{1 + kc_2} \end{aligned} \tag{4.7}$$

$$\begin{aligned} \frac{d}{dt}l_1 &= (2a_1^l - 1)p_1^l l_1 - d(c_1 + l_1)l_1 \\ \frac{d}{dt}l_2 &= 2(1 - a_1^l)p_1^l l_1 - d_2^l l_2 \end{aligned} \tag{4.8}$$

with

$$c_1(0) = c_1^0 > 0,\ c_2(0) = c_2^0 \geq 0,\ l_1(0) = l_1^0 > 0,\ l_2(0) = l_2^0 \geq 0. \tag{4.9}$$

Remark 4.37
We know from Remark 4.17 that in case $(2a_1^l - 1)p_1^l - d_1^l < 0$ *we have exponential decay of* l_1. *In the case* $m = 2$ *it follows that then in all steady states* $l_1 = l_2 = 0$. *If Assumption 4.36 (ii) is fulfilled, then there exists a positive purely hematopoietic steady state. We immediately see from linearization that this steady state is linearly stable. An example is shown in Figure 4.4*

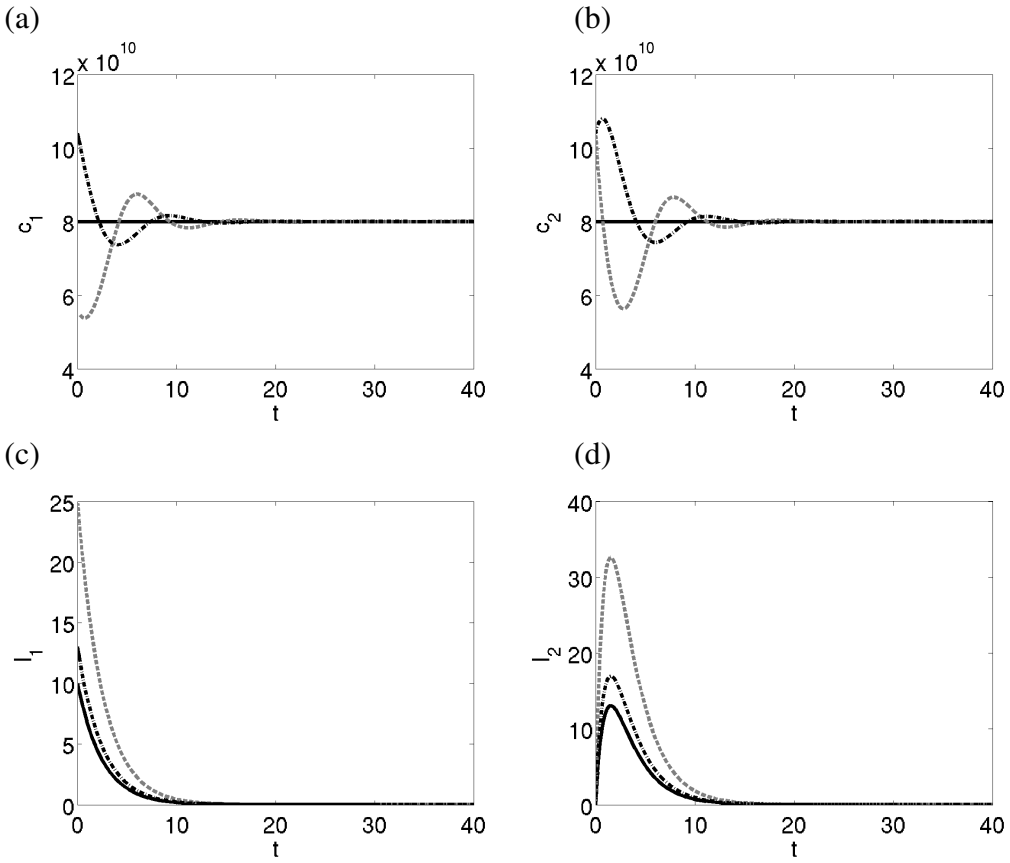

Figure 4.4: Case $(2a_1^l - 1)p_1^l - d_1^l < 0$**.** The Figure shows behavior in a vicinity of the purely hematopoietic steady state. Different line types denote different initial condition. The system converges to the purely hematopoietic state and the leukemic lineage disappears. The parameters are $n = m = 2$, $\chi = 0$, $k = 10^{-11}$, $a_1^c = 0.9$, $a_1^l = 0.4$, $p_1^c = 1$, $p_1^l = 2$, $d_1^c = d_1^l = 0$, $d_2^c = d_2^l = 1$ and $d_c(x) = \max(0, (x - 3 \cdot 10^{13})/8)10^{-13}$. Panels (a)-(d) depict time evolution of different cell types.

Proposition 4.38 (Case $[2a_1^c - 1]p_1^c < [2a_1^l - 1]p_1^l$)
Consider system (4.7)-(4.9)*, i.e.,* $n = 2$*,* $m = 2$*. Let Assumptions 4.36 hold. Let* $(2a_1^c - 1)p_1^c < (2a_1^l - 1)p_1^l$.

(i) Then, there exist only the purely hematopoietic and the purely leukemic steady state. The purely hematopoietic steady state is unique.

(ii) Then, the purely leukemic steady state is linearly asymptotically stable. The purely hematopoietic steady state is unstable.

Example 4.39
A numeric example for Proposition 4.38 is given in Figure 4.5.

PROOF of Proposition 4.38

(i) We denote the steady state value of d_c as $\bar{d}_c$. Assume $\bar{l}_1 > 0$. Then, it has to hold $\bar{d}_c = (2a_1^l - 1)p_1^l$. Consequently, $(2a_1^c - 1)p_1^c - \bar{d}_c < 0$. Then, the steady state condition for c_1 implies that $\bar{c}_1 = 0$, which yields $\bar{c}_2 = 0$. For $\bar{l}_i = 0$ we obtain the purely hematopoietic steady state. The hematopoietic steady state with $d_c(\sum_{i=1}^{n-1} \bar{c}_i) = 0$ is unique, we denote it as $(\bar{c}_1^0, \bar{c}_2^0)$. If there exits another purely hematopoietic steady state $(\bar{c}_1^*, \bar{c}_2^*)$, it has to hold $d_c(\bar{c}_1^*) > 0$. Due to the properties of d_c, this is only possible for $\bar{c}_1^* > \bar{c}_1$. Due to Lemma 4.8 (a), this is not possible for $n = 2$, since $d_c > 0$ in steady state implies that $\bar{c}^* < \bar{c}_1$.

(ii) We denote the steady state value of d_c as $\bar{d}_c$. We obtain the following linearization

$$\mathcal{L} = \begin{pmatrix} (2a_1^c - 1)p_1^c - (2a_1^l - 1)p_1^l & 0 & 0 & 0 \\ 2(1 - a_1^c)p_1^c & -d_2^c & 0 & 0 \\ -\bar{d}_c' \bar{l}_1 & 0 & -\bar{d}_c' \bar{l}_1 & 0 \\ 0 & 0 & 2(1 - a_1^l)p_1^l & -d_2^l \end{pmatrix}$$

We notice that the steady state condition of l_1 requires that $\bar{d}_c > 0$. We use the notation $\bar{d}_c' := \frac{d}{dx} d_c(x)|_{x=\sum_{i=1}^{m-1} \bar{l}_i + \chi \bar{l}_m + \sum_{i=1}^{n-1} \bar{c}_i}$. Due to the assumptions on d_c, it holds $\bar{d}_c' > 0$. Therefore, all eigenvalues are negative.

The instability of the purely hematopoietic steady state follows from Lemma 4.31.

■

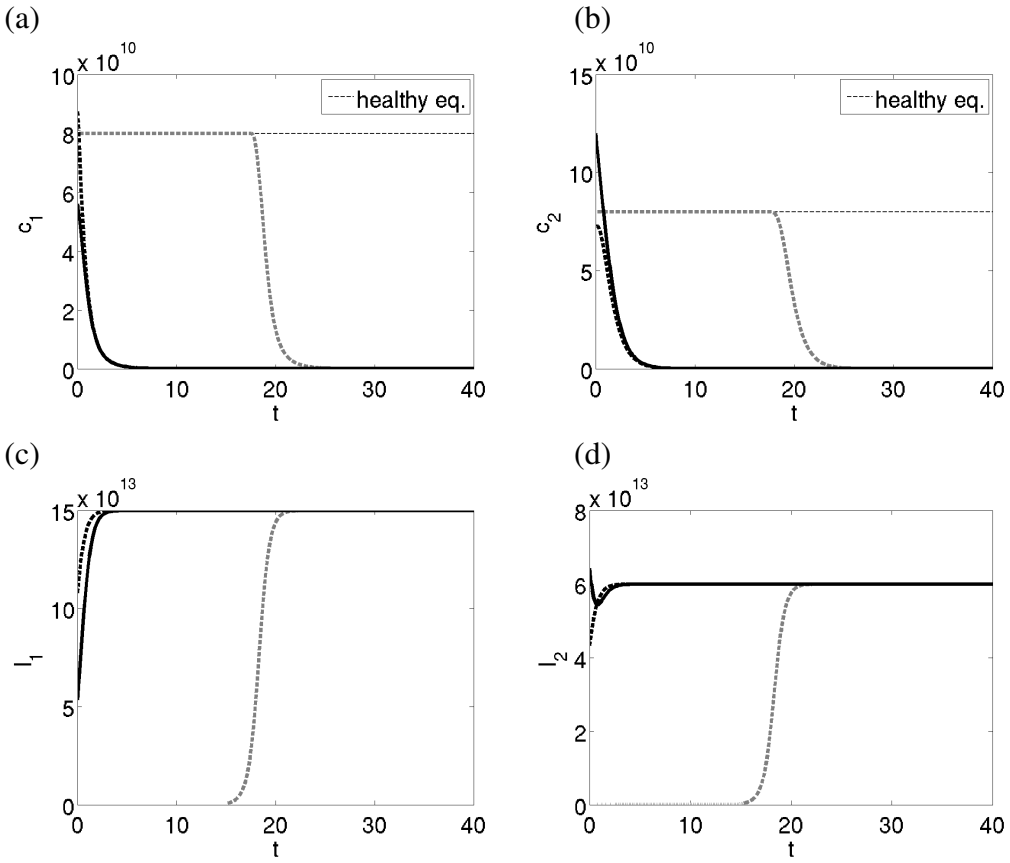

Figure 4.5: Case $(2a_1^l - 1)p_1^l - d_1^l > (2a_1^c - 1)p_1^c - d_1^c$**.** The Figure depicts the behavior in a vicinity of the purely hematopoietic and the purely leukemic steady state. Different line types denote different initial condition. The system converges to the purely leukemic state and the hematopoietic lineage disappears. The purely hematopoietic equilibrium is unstable. The parameters are $n = m = 2$, $\chi = 0$, $k = 10^{-11}$, $a_1^c = 0.9$, $a_1^l = 0.8$, $p_1^c = 1$, $p_1^l = 2.5$, $d_1^c = d_1^l = 0$, $d_2^c = d_2^l = 1$ and $d_c(x) = \max(0, (x - 3 \cdot 10^{13})/8)10^{-13}$. Panels (a)-(d) depict time evolution of different cell types. The thin dashed lines in Panels (a) and (b) show the purely hematopoietic ('healthy') steady state. By "healthy eq.", we denote the healthy equilibrium.

Proposition 4.40 (Case $[2a_1^c - 1]p_1^c > [2a_1^l - 1]p_1^l$)
Let $(2a_1^c - 1)p_1^c > (2a_1^l - 1)p_1^l$. Under the Assumptions 4.36 there exists a steady state $(\bar{c}_1, \bar{c}_2, \bar{l}_1, \bar{l}_2)$ of system (4.7)-(4.9) such that all species are positive. This steady state is locally asymptotically stable. The full leukemic steady state $\bar{c}_1 = \bar{c}_2 = 0, \bar{l}_1 > 0, \bar{l}_2 > 0$ is unstable. The purely hematopoietic steady state is unstable.

Example 4.41
A numeric example for Proposition 4.40 is given in Figure 4.6.

PROOF of Proposition 4.40

Since we are interested in $\bar{l}_1 > 0$, the condition $\frac{d}{dt}l_1 = 0$ is equivalent to $(2a_1^l - 1)p_1^l = d_c(c_1 + l_1)$. Due to monotony of d_c, there exists a unique $\bar{C}$ such that $(2a_1^l - 1)p_1^l = d_c(\bar{C})$. We then obtain form the condition $\frac{d}{dt}c_1 = 0$ that

$$\begin{aligned}
(2a_1^c\bar{s} - 1)p_1^c &= (2a_1^l - 1)p_1^l \Leftrightarrow \\
2a_1^c\bar{s} &= (2a_1^l - 1)\frac{p_1^l}{p_1^c} + 1 \Leftrightarrow \\
\frac{1}{1 + k\bar{c}_2} = \bar{s} &= \frac{1}{2a_1^c}\left((2a_1^l - 1)\frac{p_1^l}{p_1^c} + 1\right) = \frac{(2a_1^l - 1)p_1^l + p_1^c}{2a_1^c p_1^c} \Leftrightarrow \\
k\bar{c}_2 &= \frac{2a_1^c p_1^c}{(2a_1^l - 1)p_1^l + p_1^c} - 1 \Leftrightarrow \\
\bar{c}_2 &= \frac{1}{k}\frac{(2a_1^c - 1)p_1^c - (2a_1^l - 1)p_1^l}{(2a_1^l - 1)p_1^l + p_1^c}.
\end{aligned}$$

We introduce the notations $\xi_c := (2a_1^c - 1)p_1^c$ and $\xi_l := (2a_1^l - 1)p_1^l$.
Then, we obtain

$$\begin{aligned}
\bar{c}_2 &= \frac{1}{k}\frac{\xi_c - \xi_l}{\xi_l + p_1^c}, \\
\bar{s} &= \frac{\xi_l + p_1^c}{2a_1^c p_1^c}.
\end{aligned}$$

The condition $\frac{d}{dt}c_2 = 0$ implies that $\bar{c}_1 = \frac{d_2^c\bar{c}_2}{2(1-a_1^c\bar{s})p_1^c}$. It holds $2(1 - a_1^c\bar{s})p_1^c = 2p_1^c - 2a_1^c p_1^c\bar{s} = 2p_1^c - \xi_l - p_1^c = p_1^c - \xi_l$.

Consequently, we obtain $\bar{c}_1 = \frac{d_2^c}{p_1^c - \xi_l}\frac{1}{k}\frac{\xi_c - \xi_l}{\xi_l + p_1^c}$. Due to the assumptions, it holds $\xi_l < \xi_c$, furthermore, since $0.5 < a_1^c < 1$, we have $p_1 > (2a_1^c - 1)p_1$, which

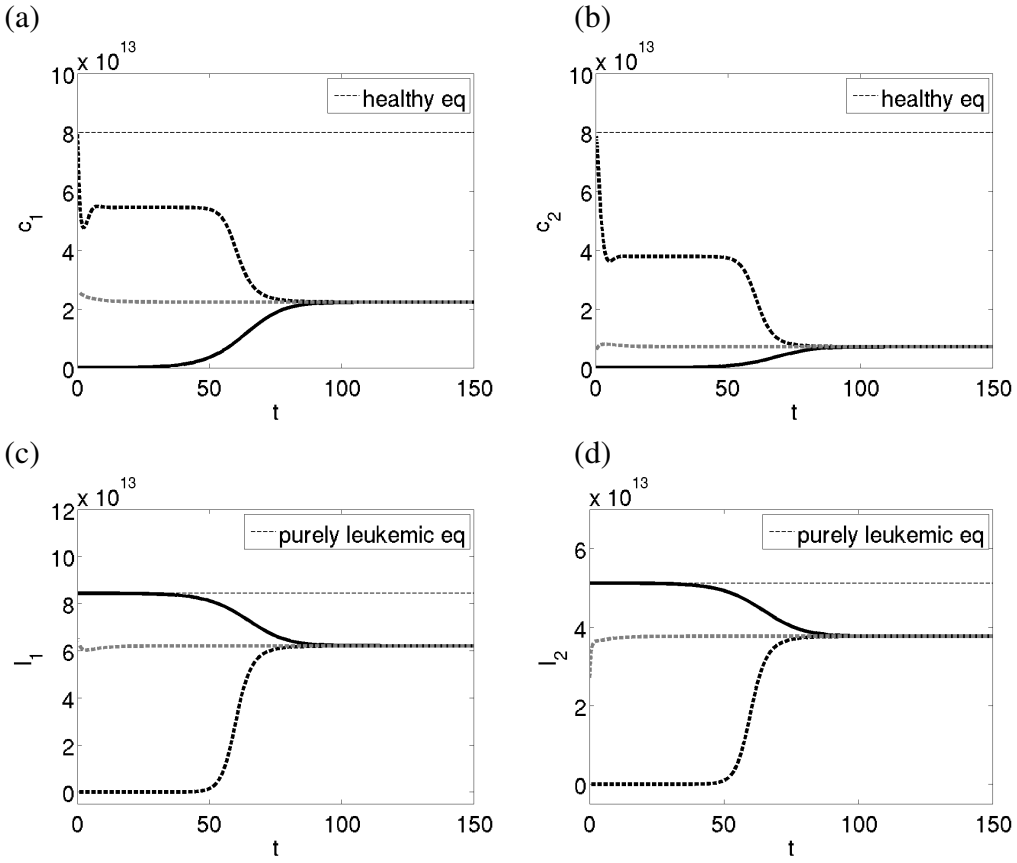

Figure 4.6: Case $(2a_1^l - 1)p_1^l - d_1^l < (2a_1^c - 1)p_1^c - d_1^c$**.** The Figure depicts the behavior in a vicinity of the mixed, the purely hematopoietic and the purely leukemic steady state. Different line types denote different initial condition. The system converges to the mixed state, the purely leukemic and the purely hematopoietic steady state are unstable. The parameters are $n = m = 2$, $\chi = 0$, $k = 10^{-14}$, $a_1^c = 0.9$, $a_1^l = 0.7$, $p_1^c = 1$, $p_1^l = 1.7$, $d_1^c = d_1^l = 0$, $d_2^c = d_2^l = 1$ and $d_c(x) = \max(0, (x - 3 \cdot 10^{13})/8)10^{-13}$. Panels (a)-(d) depict time evolution of different cell types. The thin dashed lines in panels (a) and (b) show the purely hematopoietic ('healthy') steady state, the thin dashed line in panels (c) and (d) show the purely leukemic steady state. By "healthy eq." ("purely leukemic eq."), we denote the healthy (purely leukemic) equilibrium.

implies that $p_1^c - \xi_l > \xi_c - \xi_l > 0$. Therefore, $\bar{c}_1 > 0$, $\bar{c}_2 > 0$.

We linearize around this positive steady state. We note that

$$\begin{aligned}
&\frac{d}{dc_1}[(2a_1^c s - 1)p_1^c c_1 - d_c(c_1 + l_1)c_1]|_{c_1=\bar{c}_1, l_1=\bar{l}_1, s=\bar{s}} \\
&= (2a_1^c \bar{s} - 1)p_1^c - d_c(\bar{c}_1 + \bar{l}_1) - \frac{d}{dx}d_c(x)|_{x=\bar{c}_1+\bar{l}_1}\bar{c}_1 \\
&= -\frac{d}{dx}d_c(x)|_{x=\bar{c}_1+\bar{l}_1}\bar{c}_1,
\end{aligned}$$

since the steady state conditions imply that $(2a_1^c \bar{s} - 1)p_1^c - d_c(\bar{c}_1 + \bar{l}_1) = 0$. Analogously, we obtain

$$\frac{d}{dl_1}[(2a_1^l - 1)p_1^l l_1 - d_c(c_1 + l_1)l_1]|_{c_1=\bar{c}_1, l_1=\bar{l}_1, s=\bar{s}} = -\frac{d}{dx}d_c(x)|_{x=\bar{c}_1+\bar{l}_1}\bar{l}_1.$$

We use the notation $\bar{d}' := \frac{d}{dx}d_c(x)|_{x=\bar{c}_1+\bar{l}_1}$. Furthermore, we notice $\frac{d}{dc_2}\frac{1}{1+kc_2} = \frac{-k}{(1+kc_2)^2} = -ks^2$. We obtain the following linearization:

$$\mathcal{L} = \begin{pmatrix} -\bar{d}'\bar{c}_1 & -2a_1^c p_1^c k\bar{s}^2\bar{c}_1 & -\bar{d}'\bar{c}_1 & 0 \\ 2(1-a_1^c\bar{s})p_1^c & 2a_1^c p_1^c k\bar{s}^2\bar{c}_1 - d_2^c & 0 & 0 \\ -\bar{d}'\bar{l}_1 & 0 & -\bar{d}'\bar{l}_1 & 0 \\ 0 & 0 & 2(1-a_1^l)p_1^l & -d_2^l \end{pmatrix}.$$

We immediately see that one eigenvalue is $-d_2^l$. For the remaining 3×3 matrix we simplify notation. We set:

$$\tilde{\mathcal{L}} := \begin{vmatrix} a & b & a \\ c & -b-e & 0 \\ d & 0 & d \end{vmatrix}.$$

We calculate the characteristic polynomial.

$$\begin{aligned}
\chi_{\tilde{\mathcal{L}}}(X) &= \begin{vmatrix} X-a & -b & -a \\ -c & X+b+e & 0 \\ -d & 0 & X-d \end{vmatrix} \\
&= -ad(X+b+e) + (X-d)[(X-a)(X+b+e) - bc] \\
&= -adX - adb - ade + (X-d)[X^2 + bX + eX - aX - ab - ae - bc] \\
&= -adX - adb - ade + X^3 + bX^2 + eX^2 - aX^2 \\
&\quad - abX - aeX - bcX - dX^2 - bdX - deX + adX + abd + ade + dbc \\
&= X^3 + X^2(b+e-a-d) + X(-ad - ab - ae - bc - bd - de + ad) \\
&\quad - adb - ade + abd + ade + dbc \\
&= X^3 + X^2(b+e-a-d) + X(-ab - ae - bc - bd - de) + dbc
\end{aligned}$$

We use the Routh-Hurwitz Criterion, [79], to check, if real parts of eigenvalues have negative sign. To obtain eigenvalues, which all have negative real parts it is necessary and sufficient that

(i) $b + e - a - d > 0$,

(ii) $(b + e - a - d)(-ab - ae - bc - bd - de) - dbc > 0$,

(iii) $dbc > 0$.

We note that (iii) is true, since

$$dbc = [-\bar{d}'\bar{l}_1][-2a_1^c p_1^c k\bar{s}^2\bar{c}_1][2(1 - a_1^c\bar{s})p_1^c] = 4\bar{d}'\bar{l}_1(1 - a_1^c\bar{s})(p_1^c)^2 a_1^c k\bar{s}^2\bar{c}_1 > 0.$$

We now check (i). We note that

$$\begin{aligned} b + e &= -2a_1^c p_1^c k\bar{s}^2\bar{c}_1 + d_2^c \\ &= -2a_1^c p_1^c k\left(\frac{\xi_l + p_1^c}{2a_1^c p_1^c}\right)^2 \frac{d_2^c}{p_1^c - \xi_l}\frac{1}{k}\frac{\xi_c - \xi_l}{\xi_l + p_1^c} + d_2^c \\ &= -\frac{(\xi_l + p_1^c)^2}{2a_1^c p_1^c}\frac{d_2^c}{p_1^c - \xi_l}\frac{\xi_c - \xi_l}{\xi_l + p_1^c} + d_2^c \\ &= -\frac{\xi_l + p_1^c}{2a_1^c p_1^c}\frac{\xi_c - \xi_l}{p_1^c - \xi_l}d_2^c + d_2^c. \end{aligned}$$

$$\begin{aligned} & b + e > 0 \\ \Leftrightarrow\quad & 1 > \frac{\xi_l + p_1^c}{2a_1^c p_1^c}\frac{\xi_c - \xi_l}{p_1^c - \xi_l} \\ \Leftrightarrow\quad & 2a_1^c p_1^c(p_1^c - \xi_l) > (\xi_l + p_1^c)(\xi_c - \xi_l) \\ \Leftrightarrow\quad & 2a_1^c(p_1^c)^2 - 2a_1^c p_1^c\xi_l > \xi_l\xi_c - \xi_l\xi_l + p_1^c\xi_c - p_1^c\xi_l \\ \Leftrightarrow\quad & 2a_1^c(p_1^c)^2 + \xi_l\xi_l - p_1^c\xi_c > \underbrace{(2a_1^c - 1)p_1^c}_{=\xi_c}\xi_l + \xi_l\xi_c \\ \Leftrightarrow\quad & \underbrace{(2a_1^c p_1^c - \xi_c)}_{=p_1^c}p_1^c + \xi_l\xi_l - 2\xi_l\xi_c > 0. \end{aligned}$$

We know that $\xi_c = (2a_1^c - 1)p_1^c \leq p_1^c$, therefore, $(p_1^c)^2 + \xi_l\xi_l - 2\xi_l\xi_c > \xi_c\xi_c + \xi_l\xi_l - 2\xi_l\xi_c = (\xi_l - \xi_c)^2 > 0$. Therefore, $b + e > 0$, since $-a > 0$ and $-d > 0$ statement (i) follows.

We expand (ii):

$$\begin{aligned}
&(b+e-a-d)(-ab-ae-bc-bd-de)-dbc\\
&=-ab^2-abe-b^2c-b^2d-bde-abe-ae^2-bce-bde-de^2\\
&\quad+a^2b+a^2e+abc+abd+ade+abd+ade+bcd+bd^2+d^2e-dbc\\
&=\underbrace{a^2b+2abd+bd^2+a^2e+2ade+d^2e}_{=:\alpha}\\
&\quad\underbrace{-ab^2-abe-ae^2-abe-bde-b^2d-bde-de^2}_{=:\beta}\\
&\quad\underbrace{+abc-b^2c-bce}_{=abc-bc(b+e)}
\end{aligned}$$

We obtain

$$\begin{aligned}
\alpha &= a^2b+2abd+bd^2+a^2e+2ade+d^2e\\
&= a^2(b+e)+2ad(b+e)+d^2(b+e)\\
&= (a+d)^2(b+e)>0,
\end{aligned}$$

since we have shown above that $b+e>0$. It holds

$$\begin{aligned}
\beta &= -ab^2-abe-ae^2-abe-bde-b^2d-bde-de^2\\
&= -ab(b+e)-ae(e+b)-bd(e+b)-de(b+e)\\
&= -a(b+e)^2-d(b+e)^2>0,
\end{aligned}$$

since $-a=\bar{d}'\bar{c}_1>0$ and $-d=\bar{d}'\bar{l}_1>0$.
Furthermore,

$$abc-bc(b+e)>0,$$

since $(b+e)>0$, as shown above. It holds

$$-bc=-[-2a_1^cp_1^ck\bar{s}^2\bar{c}_1][2(1-a_1^c\bar{s})p_1^c]=4(1-a_1^c\bar{s})a_1^c(p_1^c)^2k\bar{s}^2\bar{c}_1>0$$

and

$$abc=[-\bar{d}'\bar{c}_1][-2a_1^cp_1^ck\bar{s}^2\bar{c}_1][2(1-a_1^c\bar{s})p_1^c]=4(1-a_1^c\bar{s})a_1^c(p_1^c)^2k\bar{s}^2(\bar{c}_1)^2\bar{d}'>0.$$

This yields (ii). We conclude that all eigenvalues have negative real parts.

For the instability of the full leukemic steady state, we calculate the following linearization:

$$\mathcal{L}=\begin{pmatrix}
(2a_1^c-1)p_1^c-(2a_1^l-1)p_1^l & 0 & 0 & 0\\
2(1-a_1^c)p_1^c & -d_2^c & 0 & 0\\
-\bar{d}'\bar{l}_1 & 0 & -\bar{d}'\bar{l}_1 & 0\\
0 & 0 & 2(1-a_1^l)p_1^l & -d_2^l
\end{pmatrix},$$

where $2(1-a_1^c)p_1^c-(2a_1^l-1)p_1^l > 0$ is a positive eigenvalue. We have used $\bar{s}=1$ and $d(\bar{l}_1+\bar{c}_1) = d(\bar{l}_1) = (2a_1^l-1)p_1^l$. The latter follows from $\frac{d}{dt}l_1 = 0$ and $\bar{l}_1 > 0$.

Instability of the purely hematopoietic steady state follows from Lemma 4.31. ■

We now consider the case $m = 2$, $n = 2$ and $(2a_1^c-1)p_1^c = (2a_1^l-1)p_1^l$.

Proposition 4.42 (Case $[2a_1^c-1]p_1^c = [2a_1^l-1]p_1^l$)
Let $m = 2$, $n = 2$ and $(2a_1^c-1)p_1^c = (2a_1^l-1)p_1^l$. Let Assumptions 4.36 hold. Then, there exists no mixed steady state of system (4.7)-(4.9)*. The purely leukemic steady state is locally asymptotically stable. The purely hematopoietic steady state is unstable.*

Remark 4.43
In this case, there exists one zero eigenvalue and we have to reduce the system to a center manifold.

Example 4.44
Figure 4.7 illustrates the dynamics in a vicinity of a center manifold.

PROOF of Proposition 4.42

We denote the steady state value of d_c as $\bar{d}_c$. The steady state condition for l_1 implies that $\bar{d}_c = (2a_1^l-1)p_1^l$. Then, the steady state condition for c_1 yields either $\bar{c}_1 = 0$ or $\bar{s} = 1$. The latter implies that $\bar{c}_2 = 0$ and, consequently, $\bar{c}_1 = 0$. Therefore, $\bar{c}_1 = \bar{c}_2 = 0$. The value $\bar{l}_1$ is uniquely defined by $\bar{d}_c(\bar{l}_1) = (2a_1^l-1)p_1^l$. The value $\bar{l}_2$ is obtained from the steady state condition of l_2 and the value for $\bar{l}_1$.

We now linearize around this steady state and obtain

$$\mathcal{L} = \begin{pmatrix} (2a_1^c-1)p_1^c-(2a_1^l-1)p_1^l & 0 & 0 & 0 \\ 2(1-a_1^c)p_1^c & -d_2^c & 0 & 0 \\ -\bar{d}'\bar{l}_1 & 0 & -\bar{d}'\bar{l}_1 & 0 \\ 0 & 0 & 2(1-a_1^l)p_1^l & -d_2^l \end{pmatrix}$$
$$=: \begin{pmatrix} 0 & 0 & 0 & 0 \\ a & b & 0 & 0 \\ c & 0 & c & 0 \\ 0 & 0 & g & e \end{pmatrix}.$$

We note that $b < 0, c < 0, e < 0$ are eigenvalues. Therefore, the system approaches a center manifold. We are interested in the dynamics in the vicinity of the center manifold.

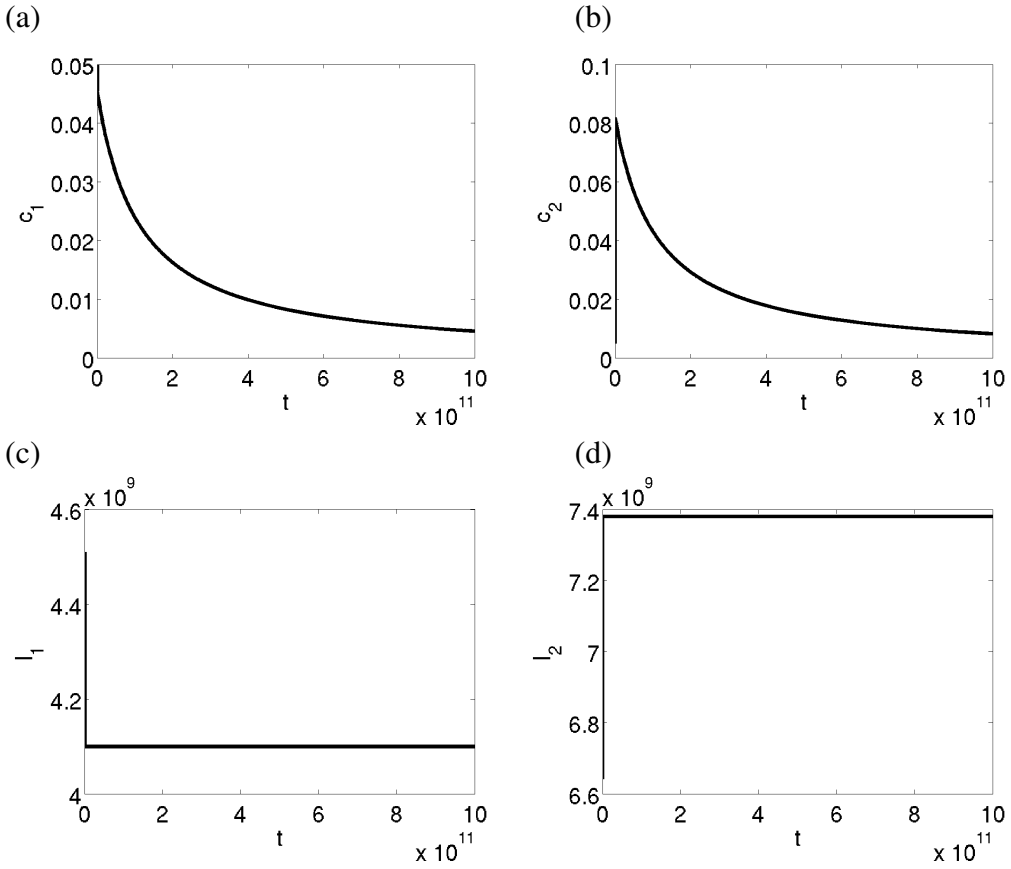

Figure 4.7: Case $(2a_1^l - 1)p_1^l - d_1^l = (2a_1^c - 1)p_1^c - d_1^c$**.** The Figure depicts the behavior in a vicinity of the center manifold. Panels (a)-(d) depict time evolution of different cell types. Parameters: $k = 10^{-10}$, $a_1^c = a_1^l = 0.55$, $p_1^l = p_1^c = 1$, $d_1^c = d_1^l = 0$, $d_2^c = d_2^l = 0.5$ and $d_c(x) = \max(0, x - 4 \cdot 10^9)10^{-9}$.

We set

$$\mathcal{T} := \begin{pmatrix} 1 & 0 & 0 & 0 \\ -a/b & 1 & 0 & 0 \\ -1 & 0 & 1 & 0 \\ g/e & 0 & 0 & 1 \end{pmatrix},$$

and notice

$$\mathcal{T}^{-1}\mathcal{L}\mathcal{T} := \begin{pmatrix} 0 & 0 & 0 & 0 \\ 0 & b & 0 & 0 \\ 0 & 0 & c & 0 \\ 0 & 0 & g & e \end{pmatrix}. \tag{4.10}$$

This implies the coordinate change

$$\begin{pmatrix} c_1 \\ c_2 \\ l_1 \\ l_2 \end{pmatrix} := \begin{pmatrix} 1 & 0 & 0 & 0 \\ -a/b & 1 & 0 & 0 \\ -1 & 0 & 1 & 0 \\ g/e & 0 & 0 & 1 \end{pmatrix} \begin{pmatrix} \tilde{c}_1 \\ \tilde{c}_2 \\ \tilde{l}_1 \\ \tilde{l}_2 \end{pmatrix} = \begin{pmatrix} \tilde{c}_1 \\ -\frac{a}{b}\tilde{c}_1 + \tilde{c}_2 \\ -\tilde{c}_1 + \tilde{l}_1 \\ \frac{g}{e}\tilde{c}_1 + \tilde{l}_2 \end{pmatrix}.$$

The inverse transformation yields

$$\begin{pmatrix} \tilde{c}_1 \\ \tilde{c}_2 \\ \tilde{l}_1 \\ \tilde{l}_2 \end{pmatrix} := \begin{pmatrix} 1 & 0 & 0 & 0 \\ a/b & 1 & 0 & 0 \\ 1 & 0 & 1 & 0 \\ -g/e & 0 & 0 & 1 \end{pmatrix} \begin{pmatrix} c_1 \\ c_2 \\ l_1 \\ l_2 \end{pmatrix} = \begin{pmatrix} c_1 \\ \frac{a}{b}c_1 + c_2 \\ c_1 + l_1 \\ -\frac{g}{e}c_1 + l_2 \end{pmatrix}.$$

We notice that $c_1 + l_1 = \tilde{l}_1$. We now transform the system:

$$\begin{aligned} \frac{d}{dt}\tilde{c}_1 &= \frac{d}{dt}c_1 = \left(\frac{2a_1^c}{1+kc_2} - 1\right) p_1^c c_1 - d(c_1 + l_1)c_1 \\ &= \left(\frac{2a_1^c}{1+k(-a\tilde{c}_1/b + \tilde{c}_2)} - 1\right) p_1^c \tilde{c}_1 - d(\tilde{l}_1)\tilde{c}_1 \qquad (4.11) \\ \frac{d}{dt}\tilde{c}_2 &= \frac{a}{b}\frac{d}{dt}c_1 + \frac{d}{dt}c_2 \\ &= \frac{a}{b}\left(\frac{2a_1^c}{1+k(-a\tilde{c}_1/b + \tilde{c}_2)} - 1\right) p_1^c \tilde{c}_1 - \frac{a}{b}d(\tilde{l}_1)\tilde{c}_1 \\ &\quad + 2\left(1 - \frac{a_1^c}{1+kc_2}\right) p_1^c c_1 - d_2^c c_2 \\ &= \frac{a}{b}\left(\frac{2a_1^c}{1+k(-a\tilde{c}_1/b + \tilde{c}_2)} - 1\right) p_1^c \tilde{c}_1 - \frac{a}{b}d(\tilde{l}_1)\tilde{c}_1 \\ &\quad + 2\left(1 - \frac{a_1^c}{1+k(-a\tilde{c}_1/b + \tilde{c}_2)}\right) p_1^c \tilde{c}_1 - d_2^c \tilde{c}_2 + \frac{a}{b}d_2^c \tilde{c}_1 \end{aligned}$$

$$
\begin{aligned}
\frac{d}{dt}\tilde{l}_1 &= \frac{d}{dt}c_1 + \frac{d}{dt}l_1 \\
&= \left(\frac{2a_1^c}{1+k(-a\tilde{c}_1/b+\tilde{c}_2)} - 1\right) p_1^c\tilde{c}_1 - d(\tilde{l}_1)\tilde{c}_1 \\
&\quad + (2a_1^l - 1)p_1^l l_1 - d(\tilde{l}_1)l_1 \\
&= \left(\frac{2a_1^c}{1+k(-a\tilde{c}_1/b+\tilde{c}_2)} - 1\right) p_1^c\tilde{c}_1 - d(\tilde{l}_1)\tilde{c}_1 \\
&\quad + (2a_1^l - 1)p_1^l(\tilde{l}_1 - \tilde{c}_1) - d(\tilde{l}_1)(\tilde{l}_1 - \tilde{c}_1) \\
\frac{d}{dt}\tilde{l}_2 &= -\frac{g}{e}\frac{d}{dt}c_1 + \frac{d}{dt}l_2 = -\frac{g}{e}\frac{d}{dt}c_1 + 2(1-a_1^l)p_1^l l_1 - d_2^l l_2 \\
&= -\frac{g}{e}\left(\frac{2a_1^c}{1+k(-a\tilde{c}_1/b+\tilde{c}_2)} - 1\right) p_1^c\tilde{c}_1 + \frac{g}{e}d(\tilde{l}_1)\tilde{c}_1 \\
&\quad + 2(1-a_1^l)p_1^l(\tilde{l}_1 - \tilde{c}_1) - d_2^l(\frac{g}{e}\tilde{c}_1 + \tilde{l}_2)
\end{aligned}
$$

We transform the steady state to the new coordinates and obtain $\bar{\tilde{c}}_1 = 0$, $\bar{\tilde{c}}_2 = 0$, $\bar{\tilde{l}}_1 = \bar{l}_1$ and $\bar{\tilde{l}}_2 = \bar{l}_2$. We now introduce the coordinate change

$$
\begin{aligned}
\hat{c}_1 &= \tilde{c}_1, \\
\hat{c}_2 &= \tilde{c}_2, \\
\hat{l}_1 &= \tilde{l}_1 - \bar{\tilde{l}}_1, \\
\hat{l}_2 &= \tilde{l}_2 - \bar{\tilde{l}}_2.
\end{aligned}
$$

Then, it holds for the steady state $\bar{\hat{c}}_1 = \bar{\hat{c}}_2 = \bar{\hat{l}}_1 = \bar{\hat{l}}_2 = 0$. The linearization around this steady state has the form as given by equation (4.10). Exactly one eigenvalue is zero and the other eigenvalues are negative. Therefore, there exists a center manifold, that is tangent to $(1,0,0,0)^T$ in the origin, [39, 87, 92].

The center manifold can be given as a graph of $\hat{c}_1$. If there exists a Taylor expansion of the center manifold, this is given by

$$
\hat{c}_2 = q(\hat{c}_1) := \alpha\hat{c}_1^2 + \mathcal{O}(\hat{c}_1^3), \tag{4.12}
$$

$$
\hat{l}_1 = r(\hat{c}_1) := \beta\hat{c}_1^2 + \mathcal{O}(\hat{c}_1^3), \tag{4.13}
$$

$$
\hat{l}_2 = w(\hat{c}_1) := \gamma\hat{c}_1^2 + \mathcal{O}(\hat{c}_1^3). \tag{4.14}
$$

We now reduce the dynamic to the center manifold. We notice that time evolution of $\hat{c}_1$ is independent of $\hat{l}_2$ but dependent on $\hat{c}_2$ and $\hat{l}_1$. Therefore, we calculate α and β. On the center manifold it holds

$$\frac{d}{dt}\hat{c}_2 = q'(\hat{c}_1)\frac{d}{dt}\hat{c}_1,$$
$$\frac{d}{dt}\hat{l}_1 = r'(\hat{c}_1)\frac{d}{dt}\hat{c}_1.$$

We expand the ODE for $\hat{c}_1$ near the center manifold and obtain:

$$\begin{aligned}\frac{d}{dt}\hat{c}_1 &= \left(\frac{2a_1^c}{1+k(-a\hat{c}_1/b+\hat{c}_2)} - 1\right) p_1^c\hat{c}_1 - d(\hat{l}_1+\bar{l}_1)\hat{c}_1 \\ &= (2a_1^c - 1)\, p_1^c\hat{c}_1 + 2a_1^c p_1^c k(a\hat{c}_1/b - \hat{c}_2)\hat{c}_1 - d(\bar{l}_1)\hat{c}_1 - d'(\bar{l}_1)\hat{l}_1\hat{c}_1 + \mathcal{O}(\hat{c}_1^3) \\ &= 2a_1^c p_1^c k\frac{a}{b}\hat{c}_1^2 + \mathcal{O}(\hat{c}_1^3).\end{aligned}$$

We used $(2a_1^c - 1)p_1 = d(\bar{l}_1)$ and the expansions (4.12)-(4.14). We, therefore, obtain $q'(\hat{c}_1)\frac{d}{dt}\hat{c}_1 = \mathcal{O}(\hat{c}_1^3)$ and $r'(\hat{c}_1)\frac{d}{dt}\hat{c}_1 = \mathcal{O}(\hat{c}_1^3)$.
We reduce the ODE for $\hat{c}_2$ to the center manifold and obtain:

$$\begin{aligned}\frac{d}{dt}\hat{c}_2 &= \frac{a}{b}\left(\frac{2a_1^c}{1+k(-a\hat{c}_1/b+\hat{c}_2)} - 1\right) p_1^c\hat{c}_1 - \frac{a}{b}d(\hat{l}_1+\bar{l}_1)\hat{c}_1 \\ &\quad + 2\left(1 - \frac{a_1^c}{1+k(-a\hat{c}_1/b+\hat{c}_2)}\right) p_1^c\hat{c}_1 - d_2^c\hat{c}_2 + \frac{a}{b}d_2^c\hat{c}_1 \\ &= \frac{a}{b}2a_1^c p_1^c k\frac{a}{b}\hat{c}_1^2 - 2a_1^c p_1\hat{c}_1 k\frac{a}{b}\hat{c}_1 - d_2^c\alpha\hat{c}_1^2 + \mathcal{O}(\hat{c}_1^3) \\ &= 2a_1^c p_1^c k\frac{a}{b}\hat{c}_1^2\left(\frac{a}{b} - 1\right) - d_2^c\alpha\hat{c}_1^2 + \mathcal{O}(\hat{c}_1^3).\end{aligned}$$

We used that $\frac{a}{b}d_2^c = -2(1-a_1^c)p_1^c$. For $\alpha = \frac{2a_1^c p_1^c k\frac{a}{b}\left(\frac{a}{b}-1\right)}{d_2}$ it holds

$$\begin{aligned}q'(\hat{c}_1)\frac{d}{dt}\hat{c}_1 &= \frac{a}{b}\left(\frac{2a_1^c}{1+k(-a\hat{c}_1/b+\hat{c}_2)} - 1\right) p_1^c\hat{c}_1 - \frac{a}{b}d(\hat{l}_1+\bar{l}_1)\hat{c}_1 \\ &\quad + 2\left(1 - \frac{a_1^c}{1+k(-a\hat{c}_1/b+\hat{c}_2)}\right) p_1^c\hat{c}_1 - d_2^c\hat{c}_2 + \frac{a}{b}d_2^c\hat{c}_1,\end{aligned}$$

up to terms of order $\mathcal{O}(\hat{c}_1^3)$.

For the dynamics of $\hat{l}_1$ on the center manifold we obtain:

$$\begin{aligned}\frac{d}{dt}\hat{l}_1 &= \left(\frac{2a_1^c}{1+k(-a\hat{c}_1/b+\hat{c}_2)}-1\right)p_1^c\hat{c}_1 - d(\hat{l}_1+\bar{l}_1)\hat{c}_1 \\ &\quad + (2a_1^l-1)p_1^l(\hat{l}_1+\bar{l}_1-\hat{c}_1) - d(\hat{l}_1+\bar{l}_1)(\hat{l}_1+\bar{l}_1-\hat{c}_1) \\ &= (2a_1^c-1)\,p_1^c\hat{c}_1 + 2a_1^cp_1^c\frac{a}{b}k\hat{c}_1^2 - d(\bar{l}_1)\hat{c}_1 \\ &\quad + (2a_1^l-1)p_1^l(\hat{l}_1+\bar{l}_1-\hat{c}_1) - d(\bar{l}_1)(\hat{l}_1+\bar{l}_1-\hat{c}_1) - \hat{l}_1d'(\bar{l}_1)(\hat{l}_1+\bar{l}_1-\hat{c}_1) \\ &\quad + \mathcal{O}(\hat{c}_1^3) \\ &= 2a_1^cp_1^c\frac{a}{b}k\hat{c}_1^2 - d'(\bar{l}_1)\bar{l}_1\beta c_1^2 + \mathcal{O}(\hat{c}_1^3).\end{aligned}$$

We used that $(2a_1^c-1)p_1^c = (2a_1^l-1)p_1^l = d_c(\bar{l}_1)$.
For $\beta = \frac{2a_1^cp_1^c\frac{a}{b}k}{d'(\bar{l}_1)\bar{l}_1}$ we obtain

$$\begin{aligned}r'(\hat{c}_1)\frac{d}{dt}\hat{c}_1 &= \left(\frac{2a_1^c}{1+k(-a\hat{c}_1/b+\hat{c}_2)}-1\right)p_1^c\hat{c}_1 - d(\hat{l}_1+\bar{l}_1)\hat{c}_1 \\ &\quad + (2a_1^l-1)p_1^l(\hat{l}_1+\bar{l}_1-\hat{c}_1) - d(\hat{l}_1+\bar{l}_1)(\hat{l}_1+\bar{l}_1-\hat{c}_1),\end{aligned}$$

up to order $\mathcal{O}(\hat{c}_1^3)$.
Insertion of the expansions into equation (4.11) and Taylor expansion yields

$$\begin{aligned}\frac{d}{dt}\hat{c}_1 &= \left(\frac{2a_1^c}{1+k(-a\hat{c}_1/b+\hat{c}_2)}-1\right)p_1^c\hat{c}_1 - d(\hat{l}_1+\bar{l}_1)\hat{c}_1 \\ &= (2a_1^c-1)\,p_1^c\hat{c}_1 + 2a_1^cp_1^ck(a\hat{c}_1/b-\hat{c}_2)\hat{c}_1 - d(\bar{l}_1)\hat{c}_1 - d'(\bar{l}_1)\hat{l}_1\hat{c}_1 + \mathcal{O}(\hat{c}_1^3) \\ &= 2a_1^cp_1^ck\frac{a}{b}\hat{c}_1^2 + \mathcal{O}(\hat{c}_1^3).\end{aligned}$$

Consequently, the dynamics on the central manifold is given by

$$\frac{d}{dt}\hat{c}_1 = 2a_1^cp_1^ck\frac{a}{b}\hat{c}_1^2 + \mathcal{O}(\hat{c}_1^3).$$

Since $2a_1^cp_1^ck\frac{a}{b} < 0$, $\hat{c}_1$ converges to zero and also $\hat{c}_2$, $\hat{l}_1$, $\hat{l}_2$ for $t\to\infty$. If we start near the origin, then $\hat{c}_2,\ \hat{l}_1, \hat{l}_2$ approach the center manifold, due to the negative real parts of the eigenvalues. The dynamics on the center manifold approaches $(0,0,0,0)$ for $t\to\infty$. Therefore, $(0,0,\bar{l}_1,\bar{l}_2)^T$ is locally asymptotically stable.

Instability of the purely hematopoietic steady state follows from Lemma 4.31, since in the purely hematopoietic steady state $\bar{d}_c = 0$ and $(2a_1^l-1)p_1^l - d_1^l > 0$.

■

Biological Remark 4.45
Propositions 4.38-4.42 suggest that the mixed steady state is linearly stable whenever it exists and that the purely leukemic steady state is unstable, if a mixed steady state exists. This finding might have treatment implications, since stable coexistence may, dependent on the healthy blood cell counts, be compatible with patients' survival. If it is possible to modify leukemic or hematopoietic cell properties, e.g., by drug application, such that coexistence of both cell lines is possible, patient survival could be achieved, even if leukemic cells cannot be eradicated. The model considered in this chapter exhibits mixed steady states for wide parameter ranges.

4.7 Further dynamic properties

Example 4.46
In Corollary 4.6 and Remark 4.7 we noticed that the properties of the leukemic stem cell population determine, which cell population of the hematopoietic lineage can act as a stem cell population. In Figures 4.8 and 4.9 we present a numerical example. We note that properties of the hematopoietic lineage are identical in both Figures. The only difference in parameters is that in Figure 4.8 we have $p_1^l = 0.3$ *and in Figure 4.9 we have* $p_1^l = 0.35$*. This difference is sufficient that cell population* c_1 *looses its stemness properties and that in Figure 4.9 there exists no steady state with* $\bar{c}_1 > 0$*.*

The following Lemma shows that the case observed in Figures 4.8 and 4.9 can happen for a wide range of parameters.

Lemma 4.47
Let $a_i > \frac{1}{2}$, $p_i > 0$ *be given. Choose* $a_j \in (a_i, 1)$ *and* $\tilde{d} \in (0, (2a_i - 1)p_i)$*. Then, there exists* $p_j > 0$ *such that* $\frac{p_i+d}{2a_ip_i} > \frac{p_j+d}{2a_jp_j}$ *for* $d \in (0, \tilde{d})$ *and* $\frac{p_i+d}{2a_ip_i} < \frac{p_j+d}{2a_jp_j}$ *for* $d \in (\tilde{d}, \infty)$.

PROOF
For fixed $a_i,\ p_i,\ a_j,\ p_j$ we set $f_1(d) := \frac{p_i+d}{2a_ip_i}$ and $f_2(d) := \frac{p_j+d}{2a_jp_j}$. Both, f_1 and f_2, are linear functions in d with slope $\frac{1}{2a_ip_i}$ and $\frac{1}{2a_jp_j}$ (resp.) and y-intercepts at $\frac{1}{2a_i}$ and $\frac{1}{2a_j}$ (resp.). We search $p_j > 0$ such that the two linear functions intersect at $d = \tilde{d}$.

We define $\tilde{s} := \frac{p_i+\tilde{d}}{2a_ip_i}$. We note that $\tilde{s} < \frac{p_i+(2a_i-1)p_i}{2a_ip_i} = 1$. Then, the slope $\frac{1}{2a_jp_j}$ has to fulfill (see picture) $\frac{1}{2a_jp_j} := \left(\tilde{s} - \frac{1}{2a_j}\right)\frac{1}{\tilde{d}}$, which yields $p_j = \frac{\tilde{d}}{2a_j\tilde{s}-1} > 0$. The positivity follows from $\tilde{s} > \frac{1}{2a_i}$.

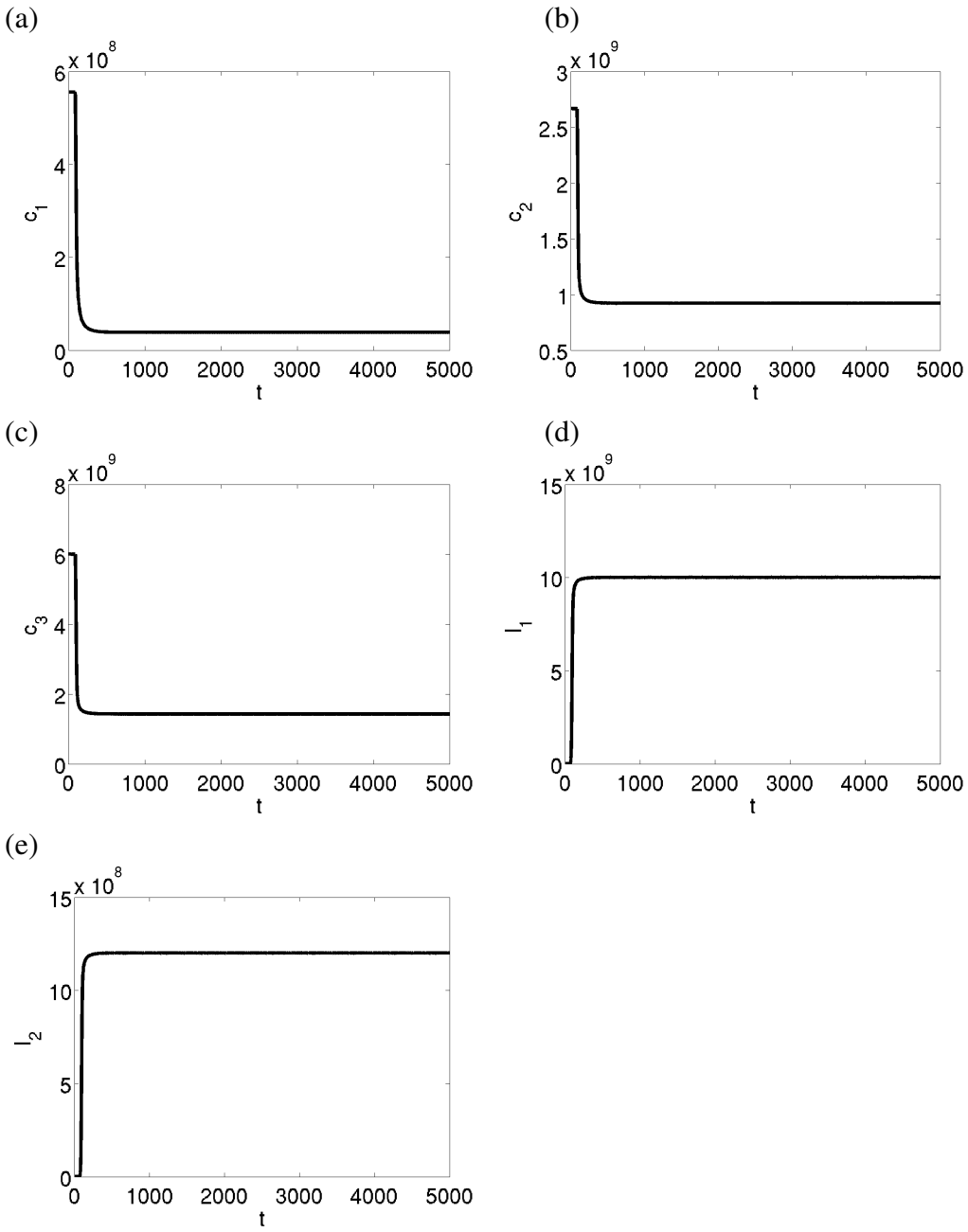

Figure 4.8: Influence of parameters p_1^l, a_1^l and d_1^l on stemness of hematopoietic cells. The Figure shows existence of a mixed steady state for $n = 3$, $m = 2$, where all $\bar{c}_i$ are positive. Parameters: $a_1^c = 0.8$, $p_1^c = 0.6$, $a_2^c c = 0.7$, $p_2^c = 1$ $a_1^l = 0.9$, $p_1^l = 0.3$, $d_3^c = 0.5$, $d_2^l = 0.5$, $d_1^l = d_1^c = d_2^c = 0$, $k = 10^{-10}$ and $d_c(x) = \max(x - 10^{10}) \cdot 10^{-10}$. Different panels show different cell populations.

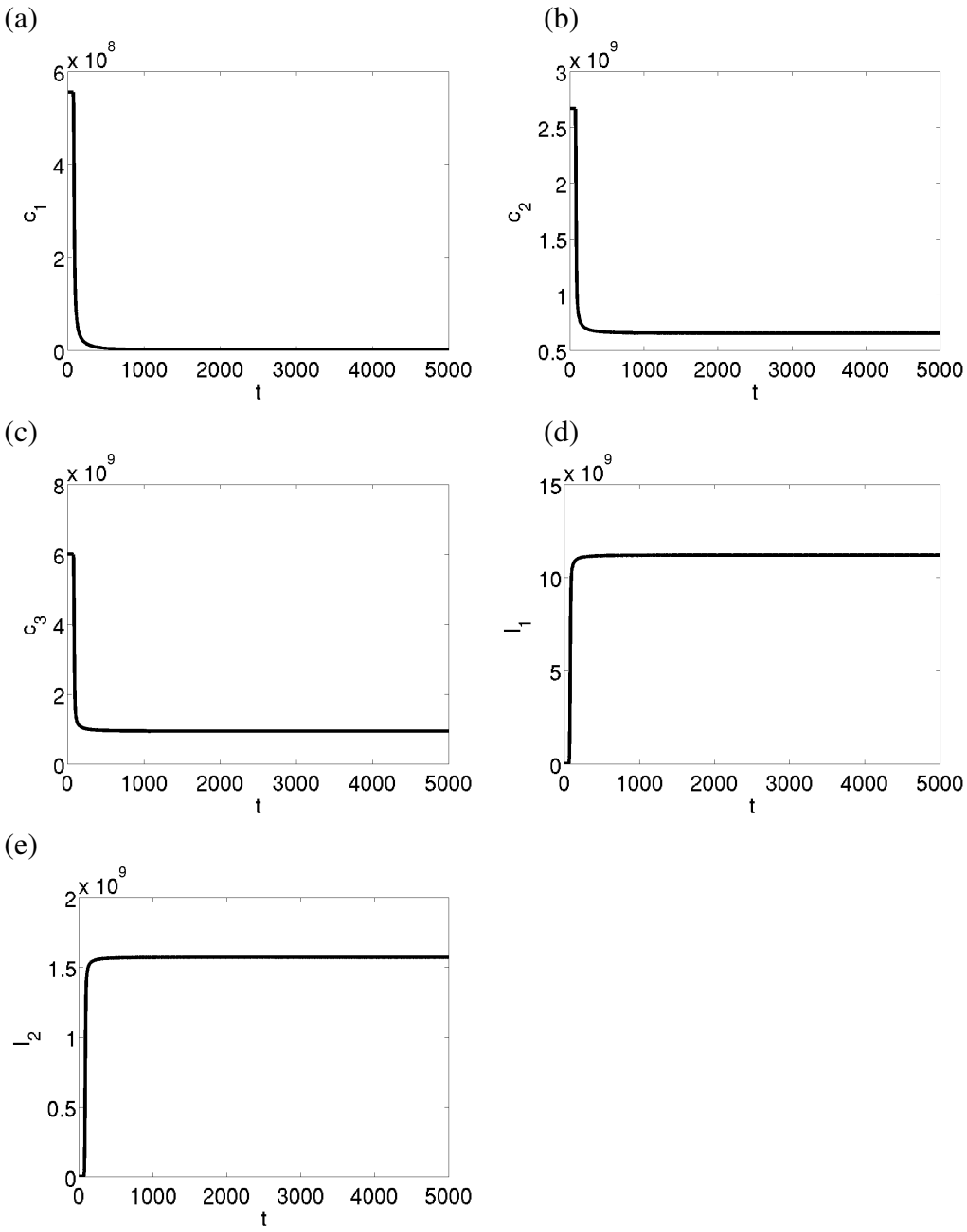

Figure 4.9: Influence of parameters p_1^l, a_1^l and d_1^l on stemness of hematopoietic cells. The Figure shows existence of a mixed steady state, where $\bar{c}_1 = 0$. In this case, there exists no steady state, where all $\bar{c}_i$ are positive. Parameters are as specified in Figure 4.8, except $p_1^l = 0.35$. This change is sufficient that c_1 looses stemness properties. Different panels show different cell populations.

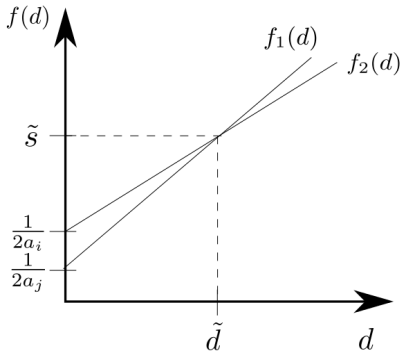

■

Corollary 4.48
Let a_2^c, p_2^c be given such that $(2a_2^c - 1)p_2^c > 0$. Let $d_1^c = d_2^c = 0$. Choose $\tilde{d} \in (0, (2a_2^c - 1)p_2^c)$. Then, there exist $a_1^c > a_2^c$ and a positive p_1^c such that $\frac{p_2^c+d}{2a_2^c p_2^c} > \frac{p_1^c+d}{2a_1^c p_1^c}$ for $d < \tilde{d}$ and $\frac{p_2^c+d}{2a_2^c p_2^c} < \frac{p_1^c+d}{2a_1^c p_1^c}$ for $d > \tilde{d}$. This means that as long as $0 < (2a_1^l - 1)p_1^l - d_1^l < \tilde{d}$, c_1 can act as stem cell population but it looses its stemness as soon as $(2a_1^l - 1)p_1^l - d_1^l > \tilde{d}$. For $d_1^c > 0$ and $d_2^c > 0$ a similar construction is possible.

4.8 Summary

In this Chapter, we analyze a new mathematical model describing interaction of hematopoietic and growth-factor independent leukemic cells. In this model, the cells compete for bone marrow space. This model exhibits equilibria with coexistence of leukemic and hematopoietic cells for wide parameter ranges. Unlike in the model of signal-dependent leukemias, these steady states are isolated (Proposition 4.19). Linearized stability analysis of a minimal system (two hematopoietic and two leukemic compartments) suggests that the purely leukemic steady state and the purely hematopoietic steady state are unstable, if a steady state with coexisting hematopoietic and leukemic cells exists. This mixed steady state is linearly stable (Propositions 4.38, 4.40, 4.42). For appropriate parameters and if the number of hematopoietic cell compartments n is greater than 2, the considered model possesses multiple purely hematopoietic steady states maintained by the same stem cell population (Remark 4.25, Example 4.27, Figure 4.3, Biological Remarks 4.26 and 4.29). These steady states can lead to high hematopoietic cell densities in marrow space that out-compete leukemic cells (Figure 4.3, Biological Remarks 4.26 and 4.29). The analytical results imply that death rates caused by presence of leukemic cells may influence stem cell function: The stem cell population of the healthy hematopoietic equilibrium may become extinct in presence of leukemia, but a downstream hematopoietic cell type may overtake stem cell function (Corollary 4.6, Biological Remark 4.7, Example 4.46).

CHAPTER 5

COMPARISON OF MODEL 1 AND MODEL 2

In this Chapter, we compare the properties of Models 1 and 2 proposed in Chapter 2 and analyzed in Chapters 3 and 4. We will introduce a general framework that allows convenient comparison of both models.

5.1 Framework

Both models fit into the following structure.

$$\begin{aligned}
\frac{d}{dt}c_1 &= f_1^c(c_1, \cdots, c_n) - g_1^c(c_1, \cdots, c_n) - h_1^c(c_1, \cdots, c_n, l_1, \cdots, l_m) \\
&\vdots \quad \vdots \quad \vdots \\
\frac{d}{dt}c_n &= f_n^c(c_1, \cdots, c_n) - g_n^c(c_1, \cdots, c_n) - h_n^c(c_1, \cdots, c_n, l_1, \cdots, l_m) \\
\frac{d}{dt}l_1 &= f_1^l(c_1, \cdots, c_n) - g_1^l(l_1, \cdots, l_n) - h_1^l(c_1, \cdots, c_n, l_1, \cdots, l_m) \\
&\vdots \quad \vdots \quad \vdots \\
\frac{d}{dt}l_m &= f_m^l(c_1, \cdots, c_n) - g_m^l(l_1, \cdots, l_n) - h_m^l(c_1, \cdots, c_n, l_1, \cdots, l_m)
\end{aligned} \tag{5.1}$$

Assumptions 5.1
Let f_i^c, f_i^l, g_i^c, g_i^l, h_i^c and h_i^l be locally Lipschitz continuous functions.
We assume that

(i) the subsystem

$$\begin{aligned}\frac{d}{dt}c_1 &= f_1^c(c_1,\ \cdots,\ c_n)\\ &\vdots \quad \vdots \quad \vdots\\ \frac{d}{dt}c_n &= f_n^c(c_1,\ \cdots,\ c_n)\end{aligned}$$

has a unique positive steady state $(\bar{c}_1,\ \cdots,\ \bar{c}_n)$.

(ii) $g_i^c(c_1,\ \cdots,\ c_n) = 0$, *if* $c_k \leq \bar{c}_k + c$ *for all* $k \in \{1,\ \cdots,\ n\}$ *and for a positive constant* c,

(iv) $h_i^c(c_1,\ \cdots,\ c_n, 0,\ \cdots,\ 0) = 0$ *and* $h_n^l(0,\ \cdots,\ 0, l_1,\ \cdots,\ l_m) = 0$.

Remark 5.2 (Interpretation)

(i) The quantities c_i *describe densities of physiological cell populations. The steady state* $(\bar{c}_1,\ \cdots,\ \bar{c}_n)$ *is considered to be the physiological (healthy) steady state of these cells.*

(ii) The quantities l_i *describe densities of malignant cells that compete with the healthy cells.*

(iii) The functions f_i^c *describe expansion or decline of hematopoietic cells of type* i*. It depends on counts of hematopoietic cells of all types. The functions* g_i^c *have the analogous meaning for the leukemic cells.*

(iv) There exist resources that are not limiting under steady state conditions, such as space or oxygen supply. Only if cell densities increase above a certain threshold, these resources become limiting and decrease cell expansion. The functions g_i^c, g_i^l *model the impact of these resources on cell dynamics. It can be interpreted as auto-inhibition in case of high cell densities.*

(v) Competition between healthy and malignant cells can inhibit expansion of cells of both types. This is modeled using the functions h_i^c *and* h_i^l.

Remark 5.3 (Models of Leukemia)

(i) In case of the model of signal-dependent leukemia (Model 1) it holds:

$f_1^c = \left(\frac{2a_1^c}{1+k^c c_n} - 1\right) p_1^c c_1 - d_1^c c_1,$
$g_1^c = 0,$
$h_1^c = \left(\frac{2a_1^c}{1+k^c c_n} - 1\right) p_1^c c_1 - \left(\frac{2a_1^c}{1+k^c c_n + k^l l_m} - 1\right) p_1^c c_1,$
$f_2^c = 2\left(1 - \frac{2a_1^c}{1+k^c c_n}\right) p_1^c c_1 + \left(\frac{2a_2^c}{1+k^c c_n} - 1\right) p_2^c c_2 - d_2^c c_2,$
$g_2^c = 0,$
$h_2^c = 2\left(1 - \frac{2a_1^c}{1+k^c c_n}\right) p_1^c c_1 + \left(\frac{2a_2^c}{1+k^c c_n} - 1\right) p_2^c c_2 - 2\left(1 - \frac{2a_1^c}{1+k^c c_n + k^l l_m}\right) p_1^c c_1$

$-\left(\frac{2a_2^c}{1+k^c c_n+k^l l_m}-1\right)p_2^c c_2$, *etc.*
$f_1^l=\left(\frac{2a_1^l}{1+k^l l_m}-1\right)p_1^l l_1-d_1^l l_1$,
$g_1^l=0$,
$h_1^l=\left(\frac{2a_1^l}{1+k^l l_m}-1\right)p_1^l l_1-\left(\frac{2a_1^l}{1+k^c c_n+k^l l_m}-1\right)p_1^l l_1$,
$f_2^l=2\left(1-\frac{2a_1^l}{1+k^l l_m}\right)p_1^l l_1+\left(\frac{2a_2^l}{1+k^l l_m}-1\right)p_2^l l_2-d_2^l l_2$,
$g_2^c=0$,
$h_2^l=2\left(1-\frac{2a_1^l}{1+k^l l_m}\right)p_1^l l_1+\left(\frac{2a_2^l}{1+k^l l_m}-1\right)p_2^l l_2-2\left(1-\frac{2a_1^l}{1+k^c c_n+k^l l_m}\right)p_1^l l_1-\left(\frac{2a_2^l}{1+k^c c_n+k^l l_m}-1\right)p_2^l l_2$, *etc.*

(ii) In case of the model of signal-independent leukemia (Model 2) it holds:
$f_1^c=\left(\frac{2a_1^c}{1+k^c c_n}-1\right)p_1^c c_1-d_1^c c_1$,
$g_1^c=d_c(c_1+\cdots+c_{n-1})$, *where* d_c *has been defined in Section 2.4*
$h_1^c=d_c(c_1+\cdots+c_{n-1}+l_1+\cdots+l_{m-1}+\chi l_m)-d_c(c_1+\cdots+c_{n-1})$,
$f_2^c=2\left(1-\frac{2a_1^c}{1+k^c c_n}\right)p_1^c c_1+\left(\frac{2a_2^c}{1+k^c c_n}-1\right)p_2^c c_2-d_2^c c_2$,
$g_2^c=g_1^c$,
$h_2^c=h_1^c$, *etc.*
$f_1^l=\left(2a_1^l-1\right)p_1^l l_1-d_1^l l_1$,
$g_1^l=d_c(l_1+\cdots+l_{m-1}+\chi l_m)$,
$h_1^l=d_c(c_1+\cdots+c_{n-1}+l_1+\cdots+l_{m-1}+\chi l_m)-d_c(l_1+\cdots+l_{m-1}+\chi l_m)$,
$f_2^l=2\left(1-2a_1^l\right)p_1^l l_1+\left(2a_2^l-1\right)p_2^l l_2-d_2^l l_2$,
$g_2^l=g_1^l$,
$h_2^l=h_1^l$, *etc.*

5.2 Steady states

We now define in analogy to Definition 3.4.

Definition 5.4 (Purely leukemic steady state)
Let $(\bar{l}_1,\ \cdots,\ \bar{l}_m)$ *be a nontrivial non-negative steady states of the subsystem*

$$\begin{aligned}\frac{d}{dt}l_1&=f_1^l(c_1,\ \cdots,\ c_n)-g_1^l(l_1,\ \cdots,\ l_n)\\ &\vdots\quad\vdots\quad\vdots\\ \frac{d}{dt}l_m&=f_n^l(c_1,\ \cdots,\ c_n)-g_n^l(l_1,\ \cdots,\ l_n).\end{aligned}$$

Then, $(0,\ \cdots,\ 0,\bar{l}_1,\ \cdots,\ \bar{l}_m)$ *is denoted as purely leukemic steady state of system* (5.1).

The following definitions are analogous to Definition 3.2.

Definition 5.5 (Purely hematopoietic steady state)
Let $(\bar{c}_1, \cdots, \bar{c}_n)$ *be a nontrivial non-negative steady state of the subsystem*

$$\begin{aligned}
\frac{d}{dt}c_1 &= f_1^c(c_1, \cdots, c_n) - g_1^c(c_1, \cdots, c_n) \\
&\vdots \quad \vdots \quad \vdots \\
\frac{d}{dt}c_n &= f_n^c(c_1, \cdots, c_n) - g_n^c(c_1, \cdots, c_n)
\end{aligned}$$

Then, $(\bar{c}_1, \cdots, \bar{c}_n, 0, \cdots, 0)$ *is denoted as purely hematopoietic steady state of system* (5.1)*.*

We consider two special cases:

Definition 5.6 (Healthy steady state)
Let $(\bar{c}_1, \cdots, \bar{c}_n)$ *be the unique positive steady state of the subsystem*

$$\begin{aligned}
\frac{d}{dt}c_1 &= f_1^c(c_1, \cdots, c_n) \\
&\vdots \quad \vdots \quad \vdots \\
\frac{d}{dt}c_n &= f_n^c(c_1, \cdots, c_n).
\end{aligned}$$

This steady state exists, due to Assumption 5.1 (i). Then, $(\bar{c}_1, \cdots, \bar{c}_n, 0, \cdots, 0)$ *is denoted as healthy steady state of system* (5.1)*. It fulfills* $g_i^c(\bar{c}_1, \cdots, \bar{c}_n) = 0$ *for all* $1 \leq i \leq n$*, due to Assumption 5.1 (ii).*

Definition 5.7 (Hyper-crowded hematopoietic steady state)
Let $(\hat{c}_1, \cdots, \hat{c}_n)$ *be a nontrivial non-negative steady state of the subsystem*

$$\begin{aligned}
\frac{d}{dt}c_1 &= f_1^c(c_1, \cdots, c_n) - g_1^c(c_1, \cdots, c_n) \\
&\vdots \quad \vdots \quad \vdots \\
\frac{d}{dt}c_n &= f_n^c(c_1, \cdots, c_n) - g_n^c(c_1, \cdots, c_n)
\end{aligned}$$

and let there exist i *such that* $g_i^c(\hat{c}_1, \cdots, \hat{c}_n) > 0$*. Then,* $(\hat{c}_1, \cdots, \hat{c}_n, 0, \cdots, 0)$ *is denoted as hematopoietic hyper-crowded steady state of system* (5.1)*.*

The following definition is analogous to Definition 3.6.

Definition 5.8 (Mixed steady state)
Let $(\bar{c}_1, \cdots, \bar{c}_n, \bar{l}_1, \cdots, \bar{l}_m)$ *be a non-negative steady state of the system* (5.1)*. If there exist* i, j *such that* $\bar{c}_i > 0$ *and* $\bar{l}_j > 0$*, the steady state is denoted as mixed steady state.*

Definition 5.9 (Maximal mixed steady state)
Let $(\bar{c}_1, \cdots, \bar{c}_n, \bar{l}_1, \cdots, \bar{l}_m)$ *be a non-negative steady state of the system* (5.1)*. If all* $\bar{c}_i > 0$ *and all* $\bar{l}_j > 0$*, the steady state is denoted as maximal mixed steady state.*

5.3 Selection properties

Definition 5.10 (Coexistence property)
The system (5.1) *has the coexistence property, if there exist mixed steady states.*

Definition 5.11 (Inter-lineage selection property)
The system (5.1) *has the inter-lineage selection property, if* $\bar{l}_1 > 0$ *in a steady state implies* $\bar{c}_1 = \cdots = \bar{c}_n = 0$, $\bar{l}_1 > 0, \ldots, \bar{l}_m > 0$ *and if* $\bar{c}_1 > 0$ *in a steady state implies that* $\bar{l}_1 = \cdots = \bar{l}_m = 0$, $\bar{c}_1 > 0, \ldots, \bar{c}_n > 0$.

Remark 5.12
Inter-lineage selection means that either only the hematopoietic or only the leukemic lineage survives.

Definition 5.13 (Hematopoietic intra-lineage selection property)
The system (5.1) *has the hematopoietic intra-lineage selection property, if there exist no mixed steady states with* $\bar{c}_1 > 0$, *but if there exist steady states where* $\bar{c}_i > 0$ *for an* $i > 1$ *and simultaneously* $\bar{l}_j > 0$ *for all* $j \in \{1, \cdots, m\}$.

Remark 5.14
Hematopoietic intra-lineage selection property means that, dependent on the properties of the leukemic cells, some stages of the hematopoietic lineage become extinct, while others survive.

Lemma 5.15
Let exist a healthy steady state of the model of signal-dependent leukemia (Model 1). Then, all mixed steady states of Model 1 with $\bar{c}_1 = 0$ *are unstable.*

PROOF
Existence of the healthy steady state requires $\frac{d_1^c + p_1^c}{2a_1^c p_1^c} < \frac{d_i^c + p_i^c}{2a_1^c p_i^c}$ for all $i > 1$, see Proposition A.1. Existence of a mixed steady state with $\bar{c}_1 = 0$ requires that $\frac{d_i^c + p_i^c}{2a_i^c p_i^c} = \frac{d_j^l + p_j^l}{2a_j^l p_j^l}$ for an index $i > 1$, and a $j \in \{1, \cdots, m\}$. This leads to $\bar{s} = \frac{d_j^l + p_j^l}{2a_j^l p_j^l}$ where $\bar{s}$ denotes the steady state value of s. Consequently, since $\frac{d_1^c + p_1^c}{2a_1^c p_1^c} < \frac{d_i^c + p_i^c}{2a_i^c p_i^c} = \bar{s}$, it follows $2(a_1^c \bar{s} - 1)p_1^c - d_1^c > 0$. Therefore, the linearization around the mixed steady state has a positive eigenvalue. ■

Remark 5.16 (Linearly stable hematopoietic intra-selection property)
For the model of signal-independent leukemias (Model 2), there exist linearly stable steady states fulfilling the hematopoietic intra-lineage selection property, i.e. $\bar{c}_1 = 0$, $\bar{c}_i > 0$ *for an* $i > 1$ *and* $\bar{l}_j > 0$ *for all* $1 \leq j \leq m$. *Below we give an example (Example 5.17).*

Example 5.17
Choose $n = 3$, $m = 2$, $d_1^c = d_2^c = d_1^l = 0$, $\chi = 0$, $a_1^c > a_2^c$, $(2a_2^c - 1)p_2^c > (2a_1^l - 1)p_1^l > (2a_1^c - 1)p_1^c > 0$. *Then, there exists a healthy steady state, due to Proposition A.1. If in a steady state* $\bar{l}_1 > 0$, *then it has to hold* $\bar{d}_c = (2a_1^l - 1)p_1^l$, *where* $\bar{d}_c$ *is the steady state value of the function* d_c *from Section 2.4. Consequently,* $(2a_1^c - 1)p_1^c - \bar{d}_c < 0$, *which implies that* $\bar{c}_1 = 0$. *There exists a steady state with* $\bar{c}_2 > 0$, $\bar{c}_3 > 0$, $\bar{l}_1 > 0$, $\bar{l}_2 > 0$ *as we see by applying Proposition 4.19 (b1) to the ODE system consisting of ODEs for* c_2, c_3, l_1, l_2. *We note that case* $(b2)$ *cannot occur for only 2 non-negative hematopoietic compartments, due to Lemma 4.8 (a). We linearize around the mixed steady state. Set* $f := \left(\frac{2a_1^c}{1+kc_3} - 1\right) p_1^c c_1 - d_c(c_1 + l_1)c_1$. *Then, we obtain using that* $\bar{c}_1 = 0$*:* $\frac{\partial}{\partial c_1} f|_{c_i=\bar{c}_i, l_i=\bar{l}_i} = \left(\frac{2a_1^c}{1+k\bar{c}_3} - 1\right) p_1^c - \bar{d}_c < 0$, $\frac{\partial}{\partial c_2} f|_{c_i=\bar{c}_i, l_i=\bar{l}_i} = 0$, $\frac{\partial}{\partial c_3} f|_{c_i=\bar{c}_i, l_i=\bar{l}_i} = 0$, $\frac{\partial}{\partial l_1} f|_{c_i=\bar{c}_i, l_i=\bar{l}_i} = 0$, $\frac{\partial}{\partial l_2} f|_{c_i=\bar{c}_i, l_i=\bar{l}_i} = 0$. *Therefore,* $\left(\frac{2a_1^c}{1+k\bar{c}_3} - 1\right) p_1^c - \bar{d}_c < 0$ *is an eigenvalue of the linearization. The remaining two eigenvalues are eigenvalues of the linearization of the subsystem consisting of ODEs for* c_2, c_3, l_1, l_2 *around the mixed steady state. These are negative, due to Proposition 4.40.*

The properties of the considered Models 1 and 2 are compared in Tables 5.1 and 5.2

	Signal-dependent Leukemia (Model 1)	**Signal-independent Leukemia (Model 2)**
Healthy steady state	exists, parameter ranges given in Prop A.1 and 3.16	exists, parameter ranges given in Prop A.1 and 4.19
Purely leukemic steady state	exists, parameter ranges given in Prop 3.16	exists, parameter ranges given in Prop 4.19
Hyper-crowded hematopoietic steady states	none	exist for proper dimension and parameter choice, Prop 4.19 (b2), Rem 4.25, Lemma 4.8
Coexistence	exists, always manifold of steady states, parameters allowing for coexistence have Lebesgue measure zero in parameter space, cf Prop. 3.16 (a)	exists, steady states are isolated and parameters allowing for coexistence have positive Lebesgue measure in parameter space, cf Prop 4.19 (b)
Inter-lineage selection	exists, parameters given in Prop. 3.16 (b)	exists, Parameters given in Prop. 4.19 (a)
Intra-lineage selection	exists, always unstable (Lemma 5.15), parameters: $\exists i > 1 : \frac{d_i^c+p_i^c}{2a_i^c p_i^c} = \frac{d_1^l+p_1^l}{2a_1^l p_1^l}$ and $\frac{d_1^c+p_1^c}{2a_1^c p_1^c} \neq \frac{d_1^l+p_1^l}{2a_1^l p_1^l}$, Prop. 3.16 (b). Parameters allowing for intra-lineage selection have Lebesgue measure zero in parameter space.	exists, parameters allowing for intra-lineage selection have positive Lebesgue measure in parameter space, Corollary 4.6, Lemma 4.47.

Table 5.1: Comparison of steady states and selection properties of the proposed leukemia models.

	Signal-dependent Leukemia (Model 1)	**Signal-independent Leukemia (Model 2)**
Healthy steady state	lin. stable, if leukemic cells cannot expand, i.e., $\frac{d_i^l+p_i^l}{2a_i^l p_i^l} > \frac{d_1^c+p_1^c}{2a_1^c p_1^c}$ for all $1 \leq i \leq m$, otherwise unstable, Prop. 3.30	lin. stable, if leukemic cells cannot expand, i.e., $(2a_i^l - 1)p_i^l - d_i^l < 0$ for all $1 \leq i \leq m$, otherwise unstable, Prop 4.38
Purely leukemic steady state	lin. stable, if leukemic cells can expand, otherwise unstable, Prop. 3.30	Linearly stable, if leukemic cells can expand and if there exists no mixed steady state, Prop.4.40
Mixed steady states	Depending on parameters the manifold of mixed steady states is either attractive or repulsive, Prop. 3.42	Lin. stable whenever it exists, Prop.4.40
Steady states with less than the maximal number of positive components	unstable, Prop 3.29	unstable, Prop. 4.34

Table 5.2: Comparison of linear stability results of a minimal version of the proposed leukemia models (4 equations).

Part II

Numerical study and applications to medicine and biology

CHAPTER 6

IMPACTS OF CELL PROPERTIES ON CLINICAL COURSE OF LEUKEMIAS

6.1 Outline of the chapter

This Chapter is devoted to numerical studies of the model of signal-dependent leukemia (Model 1), which was derived in Chapter 2.3. We are interested in the impact of proliferation and self-renewal of the different leukemic cell types on the clinical course of the disease. As a marker for the speed of disease progression, we consider the time interval from appearance of a LSC (leukemic stem cell) until mature blood cell counts have decreased by a certain percentage. We show that for parameters from a biologically relevant range, proliferation rate and fraction of self-renewal of the LPC (leukemic progenitor cell) compartment exert negligible influence on the speed of disease progression in comparison to proliferation rate and fraction of self-renewal of LSC (Section 6.3, Figures 6.1, 6.2). This finding allows to estimate LSC properties based on clinical data. We show that estimated LSC parameters vary among individuals (Section 6.4.1, Figures 6.4, 6.5) and that they correlate with survival of patients (Section 6.4.2, Figure 6.4).

6.2 Assumptions and simulations

In the following, we focus on Model 1. If the described simulations are repeated for Model 2, analogous results are obtained. We consider the case $n = m = 3$, i.e., the leukemic and the hematopoietic lineage consist each of three cell types. We denote the cell types of the hematopoietic lineage as hematopoietic stem cells (HSCs), hematopoietic progenitor cells (HPCs) and mature blood cells. Mature

blood cells are post-mitotic, i.e., they do not divide. The stages of the leukemic cell line are denoted as leukemic stem cells (LSCs), leukemic progenitor cells (LPCs), i.e., dividing leukemic non-stem cells and post-mitotic leukemic blasts.

Let the Assumptions 2.3 hold. Furthermore, we make the following Assumptions motivated by biological findings.

Assumptions 6.1

(i) All mitotic cell types have the ability to self-renew, the self-renewal potential of stem cells is higher than that of non-stem cells, [31, 35, 44, 100, 147]. Consequently, we assume $a_1^c > a_2^c$, $a_1^l > a_2^l$.

(ii) Stem cells divide less frequently than progenitor cells, [35,44,147]. Consequently, we assume $p_1^c < p_2^c$, $p_1^l < p_2^l$.

(iii) We neglect death rates of dividing cells, i.e., $d_1^c = d_1^l = d_2^c = d_2^l = 0$. *We assume that death rates of post-mitotic cells are constant over time. Blast half life is chosen between* 25% *and* 100% *of mature blood cell half-life, [152, 195].*

(iv) Leukemias can only originate from leukemic stem cells, leukemic progenitor cells are unable to out-compete hematopoieis. Consequently, we assume that $a_2^l < a_1^c$, *[35,44]. Due to Proposition 3.21, this assumption means that leukemic progenitor cells are unable to destabilize the healthy equilibrium.*

We calibrate the hematopoietic branch of the model to data from literature. The calibration is described in the Appendix C. We then fix the parameters of the hematopoietic cells and vary parameters of the different leukemic cell types. We simulate the following scenarios:

(A) Variation of LSC parameters

- We fix properties of LPCs.
- As initial conditions we choose the unique positive steady state values for c_1 to c_3 and $l_1(0) = 1$, $l_2(0) = l_3(0) = 0$.
- We vary p_1^l between $0.5 \times p_1^c$ and $10 \times p_1^c$ and a_1^l between $1.05 \times a_1^c$ and a value close to the maximal possible fraction of self renewal, which is 1, namely 0.999.
- We record how long it takes until the mature blood cell counts are reduced by 20%. Choosing different cutoff-values between 10% and 90% does not

change the presented results; alternatively marrow blast fractions can be used to define the time point of diagnosis.

- We repeat the simulations for different values of LPC parameters.

(B) Variation of LPC parameters

- We fix properties of LSCs.
- As initial conditions we choose the unique positive steady state values for c_1 to c_3 and $l_1(0) = 1$, $l_2(0) = l_3(0) = 0$.
- We vary p_2^l between $0.5 \times p_2^c$ and $20 \times p_2^c$ and a_2^l between $0.01 \times a_1^c$ and $0.99 \times a_1^c$. The biological interpretation of the latter condition is that leukemia can only originate from LSC and not from LPC, [35, 44].
- We record how long it takes until the mature blood cell counts are reduced by 20%. Choosing different cutoff-values between 10% and 90% does not change the presented results; alternatively marrow blast fractions can be used to define the time point of diagnosis.
- We repeat the simulations for different values of LSC parameters.

6.3 Simulation results

Simulation results are depicted in Figure 6.1. Simulations suggest that LSC properties have a strong impact on clinical dynamics. The time needed for 20% reduction of mature cell counts varies by more than 250% for the chosen set of LSC properties (Figure 6.1 (a)). Fast impairment of healthy hematopoiesis requires large LSC self-renewal rate or fast LSC divisional kinetics or a combination of both. Figure 6.1 (a) further suggests that the mapping linking LSC properties to the time required to reduce mature cell counts by 20% is not bijective.

On the other hand, simulations indicate that variations of LPC properties have little impact on dynamics of the disease. Only if the self-renewal capacity of leukemic progenitor cells approaches the self-renewal capacity of HSC or LSC, the influence of LPC properties on leukemia dynamics becomes visible. For the chosen parameter ranges, the time needed for reduction of mature cells by 20% changes by less than 15%, if LPC properties are varied. This value is small in comparison to the impact of LSC described above. Figure 6.1 (b)-(d) shows the impact of LPC properties for different fixed sets of LSC parameters. Figure 6.2 shows example time dynamics of the marrow blast fraction $((l_1(t) + l_2(t) + l_3(t))/(c_1(t) + c_2(t) + l_1(t) + l_2(t) + l_3(t)))$. The Figure shows that also dynamics of marrow blast fractions are determined by LSC properties and that LPC properties or death rates of post-mitotic blast excert negligible influence.

Remark 6.2
Computer simulations suggest that within biologically relevant parameter ranges LPC properties exert negligible influence on the clinical dynamics of acute leukemias.

6.4 Application to patient data

Remark 6.2 suggests that it could be possible to estimate LSC properties based on the clinical course. Since leukemic stem cells are considered as the origin for relapses, [31, 35, 88, 100, 147, 148], the estimated LSC properties should correlate with patient prognosis, [88]. The aim of the following Sections is to estimate LSC parameters based on clinical data and to correlate them with patient prognosis.

6.4.1 Estimation of surrogate LSC parameters

To estimate LSC parameters based on clinical observations, we use bone marrow aspiration data from individual patients participating in clinical trials at the University Hospital of Heidelberg (Department of Medicine V). Written consent for usage of clinical data for scientific purposes was obtained from each patient. The data are contributed by Prof. Dr. Anthony Ho and Natalia Baran (Medical Clinic V, University Hospital of Heidelberg). We consider data of 41 randomly chosen

Figure 6.1 ***(facing page)*****: Impact of LSC and LPC dynamics on clinical course.** (a) Impact of LSC properties on impairment of hematopoiesis. The vertical axis depicts the time elapsed between appearance of one LSC per kg of body weight with the properties indicated on the x axis (self-renewal) and y axis (proliferation) and reduction of mature healthy cell counts by 20%. Time T is defined as the time coordinate of the minimum of the depicted graph. We introduce this time unit to compare impact of stem and progenitor cell properties on leukemia dynamics. The time scale of the vertical axis is the same in panels (a)-(e). (b)-(e): Impact of LPC properties on impairment of hematopoiesis. The vertical axis depicts the time elapsed between appearance of one LSC per kg of body weight and reduction of mature healthy cell counts by 20%, the x and y axes indicate properties of the LPC population. For each of panels (b)-(e), LSC properties have been set to different fixed values: (b) LSC proliferation: 0.5 x HSC proliferation, LSC self-renewal: 0.87; (c) LSC proliferation: 5 x HSC proliferation, LSC self-renewal: 0.9; (d) LSC proliferation: 10 x HSC proliferation, LSC self-renewal: 0.99; (e) LSC proliferation: 1 x HSC proliferation, LSC self-renewal: 0.86. The Figure shows that the impact of LPC properties is small in comparison to that of LSC properties, while the range of parameter variation is similar for LSC and LPC.

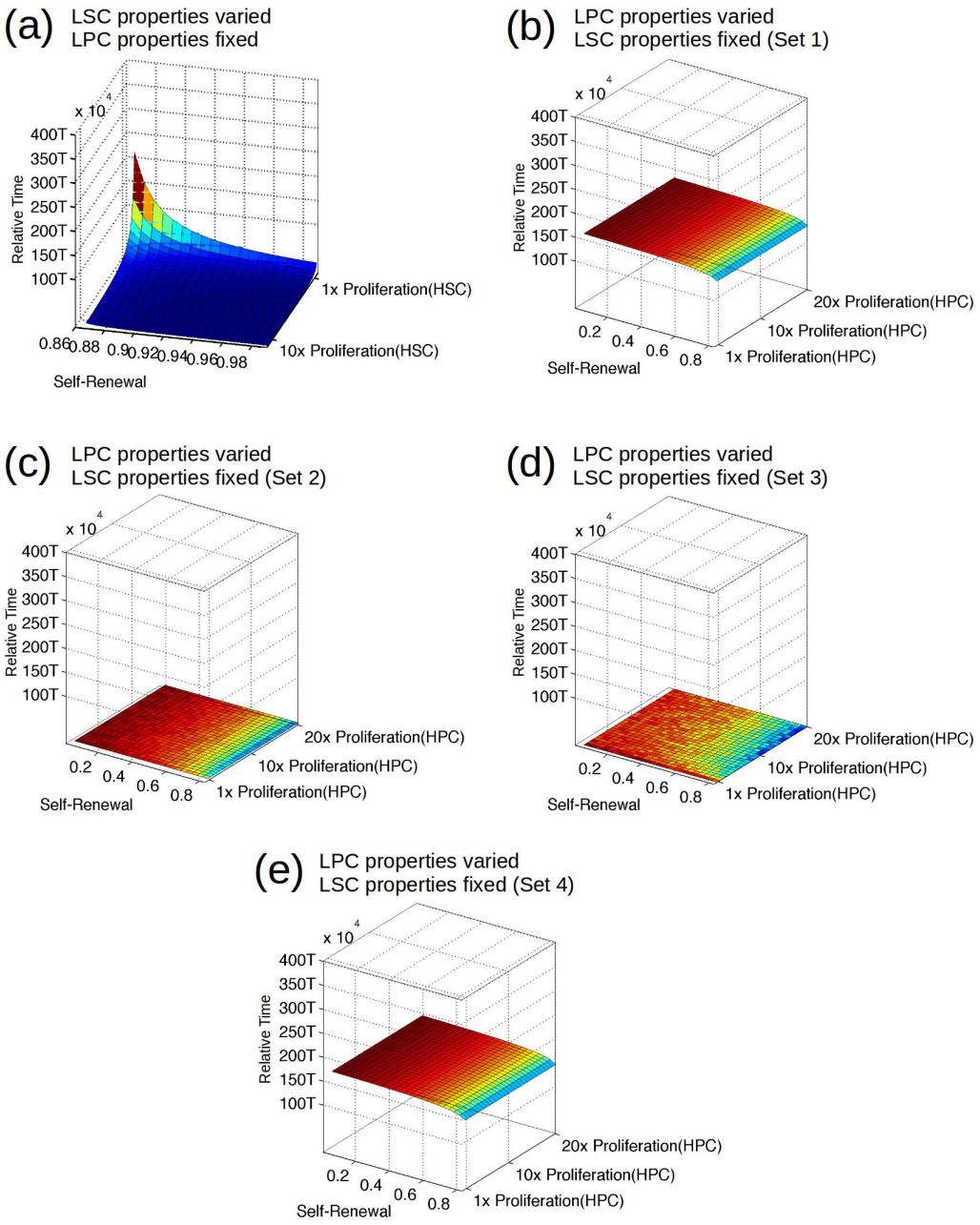
(a)
LSC properties varied
LPC properties fixed
x 10^4
400T
350T
300T
250T
200T
150T
100T
Relative Time
0.86 0.88 0.9 0.92 0.94 0.96 0.98
Self-Renewal
1x Proliferation(HSC)
10x Proliferation(HSC)
(b)
LPC properties varied
LSC properties fixed (Set 1)
x 10^4
400T
350T
300T
250T
200T
150T
100T
Relative Time
0.2 0.4 0.6 0.8
Self-Renewal
20x Proliferation(HPC)
10x Proliferation(HPC)
1x Proliferation(HPC)
(c)
LPC properties varied
LSC properties fixed (Set 2)
x 10^4
400T
350T
300T
250T
200T
150T
100T
Relative Time
0.2 0.4 0.6 0.8
Self-Renewal
20x Proliferation(HPC)
10x Proliferation(HPC)
1x Proliferation(HPC)
(d)
LPC properties varied
LSC properties fixed (Set 3)
x 10^4
400T
350T
300T
250T
200T
150T
100T
Relative Time
0.2 0.4 0.6 0.8
Self-Renewal
20x Proliferation(HPC)
10x Proliferation(HPC)
1x Proliferation(HPC)
(e)
LPC properties varied
LSC properties fixed (Set 4)
x 10^4
400T
350T
300T
250T
200T
150T
100T
Relative Time
0.2 0.4 0.6 0.8
Self-Renewal
20x Proliferation(HPC)
10x Proliferation(HPC)
1x Proliferation(HPC)

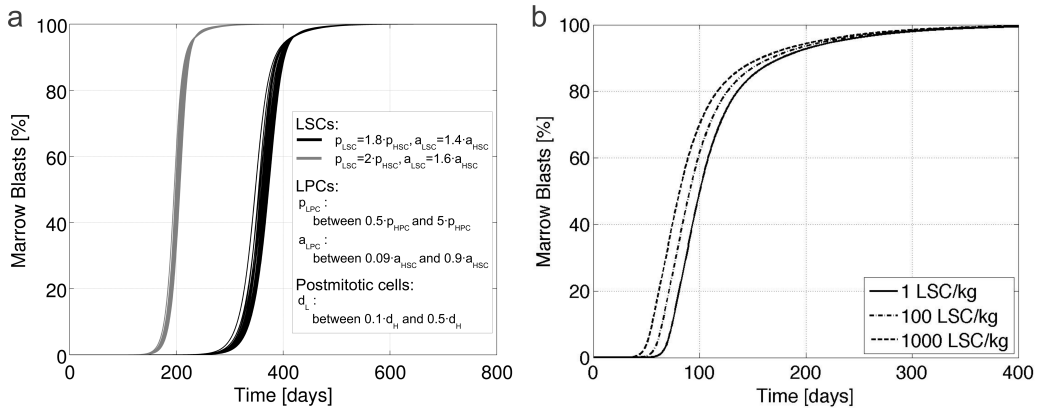

Figure 6.2: Impact of LSC and LPC dynamics on clinical course. (a) The Figure shows time evolution of bone marrow blast fractions in dependence of LSC, LPC and post-mitotic cell properties. Curves corresponding to the same LSC properties have the same color (black: LSC proliferation equals 1.8 x HSC-proliferation, LSC self-renewal equals 1.4 x HSC self-renewal, gray: LSC proliferation equals 2 x HSC-proliferation, LSC self-renewal equals 1.6 x HSC self-renewal) but differ with respect to LPC and post-mitotic cell properties (LPC properties are varied by a factor of ten, LPC proliferation is between 0.5 x HPC proliferation and 5x HPC proliferation, LPC self-renewal is varied between 0.09 x HPC self-renewal and 0.9 HPC self-renewal, death rate of post-mitotic leukemic cells varies between 0.1 x death rate of mature hematopoietic cells and 0.5 x death rate of mature hematopoietic cells). The Figure shows that curves of the same color are very similar, although HPC properties vary by a factor of 10, while black curves differ strongly from gray curves, although LSC properties differ only by 15%. This shows that small variations of LSC properties have a large influence on clinical course, while changes of LPC and post-mitotic cell properties exert much less influence. (b) Minimal time from remission to relapse, given that a small number of LSC survived chemotherapy and that hematopoiesis fully recovered after therapy. The curve depicts the maximal possible bone marrow blast count depending on the time elapsed since complete remission. The number of surviving LSC had little impact as long as it was smaller than 100 LSC per kg of body weight. The curves were obtained for LSC self-renewal of 0.999 and LSC division rate of approximately two divisions per day, which we considered as an upper bound of division frequency; p_{LSC}, p_{HSC}, p_{LPC}, p_{HPC}: proliferation rates of LSC, HSC, LPC, HPC respectively; a_{LSC}, a_{HPC}, a_{LPC}: fractions of self-renewal of LSC, HSC, LPC respectively; d_H, d_L: clearance rates of postmitotic hematopoietic or leukemic cells respectively.

patients suffering from relapse of acute myeloid leukemias (AMLs).

From the data we obtain the time elapsed between successfully treatment of primary disease and first relapse as well as the marrow blast fractions at the time, when relapse is diagnosed (Figure 6.3). For each individual patient we then systematically search for parameters (LSC proliferation rates and fractions of self-renewal) compatible with the clinical observations. We make additional assumptions that LSC number at complete remission is small (less than 100 per kg of body weight) and that hematopoietic recovery occurs fast in comparison to relapse. To identify LSC parameters we vary LSC generation time between half a day and several months and self-renewal fraction between 0.501 and 0.999 (a fraction of self-renewal equal to 1 means that all daughter cells are of the same type as the mother cell). Within this parameter range we find all possible combinations compatible with clinical data. Blast fractions are calculated by dividing the number of all leukemic cell types by the number of all hematopoietic cell types residing in bone marrow. The system is initialized with steady state hematopoietic cell counts and a small number of LSCs (approx. 1 LSC per kg of body weight). Other choices of initial LSC counts lead to similar dynamics, see Figure 6.2.

Above we have noted that the function relating LSC parameters to blast dynamics is not bijective, therefore, we obtain for each patient a one dimensional manifold of parameters that are compatible with the observed clinical dynamics of the respective patient. The results are depicted in Figure 6.4 (a), the parameters compatible with the observed clinical dynamics of an individual patient are represented by a line in parameter space.

For 31 out of 41 patients LSC parameters could be identified. Ten of the 41 patients included in this analysis showed fast expansion of leukemic cell mass that was incompatible with the assumption that a small number of LSC survived under complete reconstitution of hematopoiesis upon induction chemotherapy. The following reasons could lead to fast increase of leukemic cell burden: (1) impairment of hematopoiesis or micro-environment, [211], (2) inefficiency of therapy or resistant LSC, [33, 188], (3) autonomous cell expansion, i.e., expansion of cells independently of environmental signals, [54, 193]. Details on these patients are given in Appendix D.

Biological Remark 6.3
Figure 6.4 shows that estimated LSC parameters differ between individual patients, this even holds for patients carrying the same leukemogenetic mutations, see Figure 6.5. This is in line with the clinically observed heterogeneity of acute myeloid leukemias, [64, 117].

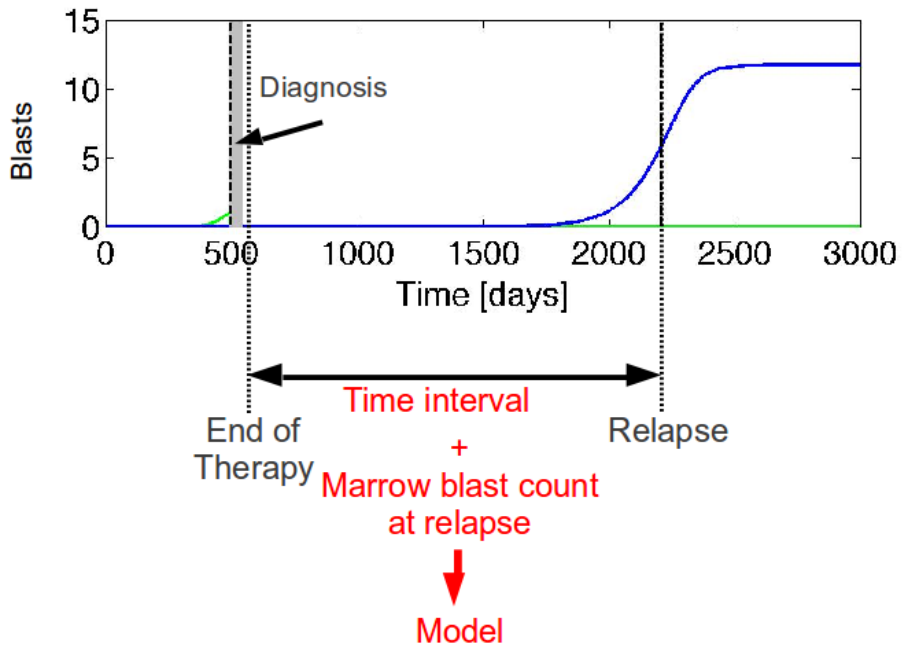

Figure 6.3: Patient data used to estimate LSC properties. Duration of chemotherapies is indicated by gray areas. Estimation of LSC parameters is based on time between successful treatment and diagnosis of relapse and bone marrow blast fraction at relapse.

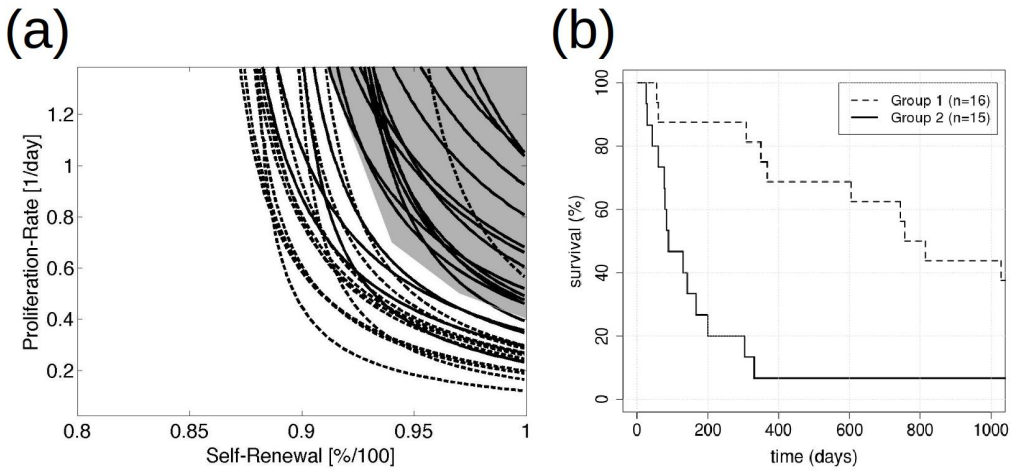

Figure 6.4: Estimated LSC properties and prognosis. (a) The Figure shows possible combinations of proliferation rates and self-renewal fractions of 31 relapsing AML (M1 & M2) patients. The estimation is not unique, i.e., different combinations of self-renewal and proliferation fit equally well. To take this into account each patient is represented by a line connecting possible combinations of self-renewal fractions and proliferation rates of the LSC population responsible for relapse in the respective patient. Estimated properties correlate with overall survival after first relapse. Continuous lines: survival shorter than one year, dotted lines: survival longer than one year. Cell parameters located in the gray area correlate with bad prognosis. FLT3-ITD is a key mutation detected in many acute myeloid leukemia patients, [78, 178]. The corresponding picture for the subset of FLT3-ITD positive patients can be found in Figure 6.5. The plot shows that LSC properties vary among different patients and that high self-renewal can partially compensate for slow proliferation and vice versa. (b) 31 Patients (13 of them are FLT3-ITD positive) were subdivided into 2 groups based on the estimated LSC parameters. If estimated LSC parameters were located in the gray area of panel (a), the corresponding patient was assigned to the poor prognosis group otherwise the patient was assigned to the good prognosis group. The plot shows the survival curves of the good (Group 1) and the bad (Group 2) prognosis group. Survival was measured from diagnosis of the first relapse until death. The difference between the two groups is significant (p=0.003 by the logrank test). Data from A.D. Ho, N. Baran, University Hospital of Heidelberg.

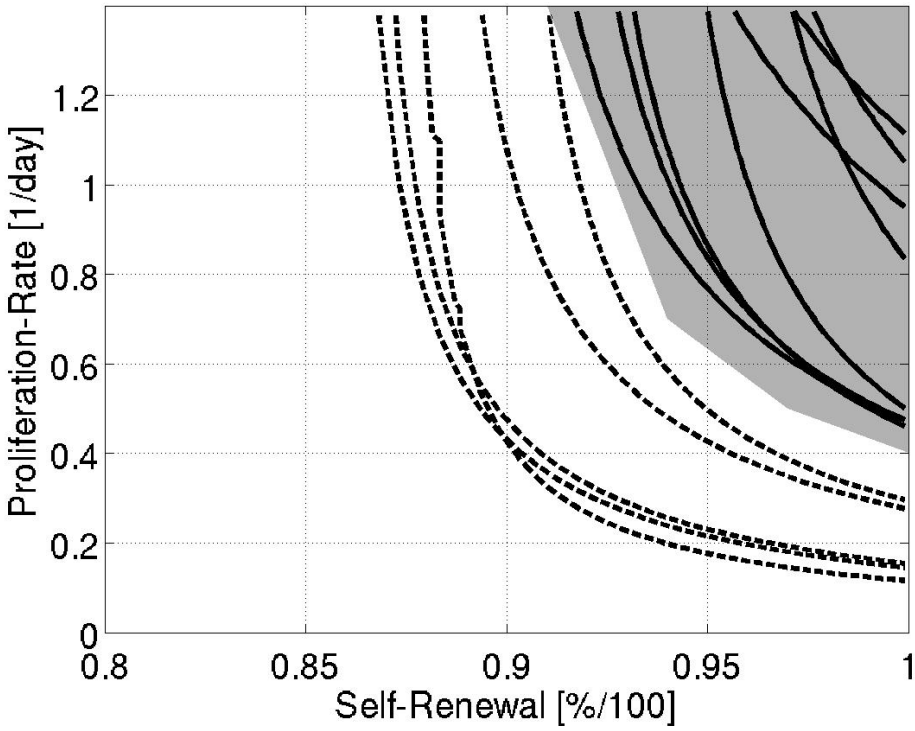

Figure 6.5: Estimated LSC properties for patients carrying the same type of mutation (FLT3-ITD). Data from A.D. Ho, N. Baran, University Hospital of Heidelberg. For explanation see Figure 6.4.

Remark 6.4
If multiple bone marrow aspirations are taken into account, the model is in good agreement with clinical data. For example patients with more than one bone marrow aspiration, comparison of model and data is shown in Figure 6.6.

6.4.2 Impact of LSC properties on survival

Grouping patients based on the estimated LSC self-renewal and proliferation rates (i.e., assigning patients with "high" estimated LSC self-renewal and proliferation rates to one group and patients with "low" estimated LSC self-renewal and proliferation rates to a second group) reveals that patients surviving more than one year after the first relapse have different estimated LSC self-renewal and proliferation rates than patients surviving less than one year. Figure 6.4 (a, b) provides evidence that patients could be categorized into good prognosis versus poor prognosis groups. The parameter ranges for both groups were defined based on a test group. Survival curves of the two groups differ significantly (p=0.003 by the log-rank test, [12, 28, 65, 66, 105]. Figure 6.4 (b) shows survival curves for both prognostic groups. In the subgroup with good prognosis median overall survival after the first relapse was approximately 2 years, while in the subgroup with bad prognosis it was approximately 3 months. The correlation between the estimated LSC parameters and survival suggests that the estimated LSC self-renewal and proliferation rates might serve as clinically meaningful parameters to predict relapses.

Biological Remark 6.5
In recent years a growing number of genetic, [56, 64, 117], epigenetic, [90], and regulatory aberrations, [81, 159], relevant for leukemogenesis and risk stratification has been described. Despite this knowledge the impact of these factors on clinical course and on cell properties is not well-defined, [64, 88, 208]. In general the impact of a given parameter may depend on the absence or presence of other, still unknown, parameters, [17, 64, 78, 179]. Genetic studies suggest that leukemogenetic hits may vary considerably among patients, [109, 110, 196]. Variability in survival of patients with the same risk factors underscores the complexity of the interplay of different detected aberrations. For this reason model based estimation of LSC parameters might constitute a more direct complementary approach to risk stratification.

Biological Remark 6.6
Due to the complexity of the mechanisms leading to evolution of AML and simplifications in the models, the estimated LSC parameters, i.e., divisional kinetics and self-renewal rates, should be understood as surrogate markers for LSC behavior that correlate with clinical outcome. As such, they should not be regarded as quantitative estimates of the kinetic properties of LSCs.

Biological Remark 6.7
The model allows to compare estimated LSC properties of different relapses in the same patient. In most cases self-renewal and/or proliferation increase between first and second relapse. An example is shown in Figure 6.7, further examples are provided in Appendix G.

6.5 Summary

In this Chapter, we study dynamical properties of a version of the model of signal-dependent leukemias (Model 1) including three hematopoietic (HSC, HPC, mature cells) and three leukemic cell types (LSC, LPC, post-mitotic blasts). We calibrate the hematopoietic branch of the model to data from literature (Appendix C). We then study the impact of proliferation rates and fractions of self-renewal of LPCs and LSCs on the time elapsing between appearance of one LSC per kg of body weight and reduction of mature cell counts by 20%. Simulation results for parameters from a biologically reasonable range show that LPC parameters have a negligible influence on the considered quantity in comparison to LSC parameters (Section 6.3, Figures 6.1, 6.2). These results hold under the assumptions that stem cells have higher self-renewal potential than progenitor cells and that death rates of immature cell types are small. Based on this finding, we estimate LSC parameters from clinical data of individual patients. Using the time elapsing between successful treatment and relapse and the marrow blast fraction at relapse, we can restrict LSC parameters to a one dimensional manifold in the two dimensional parameter space (Section 6.4). This approach shows that LSC parameters vary considerably between different patients, even if they carry the same leukemogenetic key mutation FLT3-ITD (Section 6.4.1, Figures 6.4, 6.5, Remark 6.3). Also between different relapses in the same patient, LSC parameters change, mostly to higher self-renewal and proliferation (Biological Remark 6.7, Figure 6.7). We use the log-rank test to show that the estimated LSC parameters correlate with patient survival (Section 6.4.2, Figure 6.4). This demonstrates that the estimated parameters might serve as surrogates for LSC dynamics. The proposed frameworks offers a complementary and straightforward approach to risk-stratification and design of follow-up schedules (Section 6.4.2, Biological Remark 6.5). The model, furthermore, proposes that impairment of hematopoiesis, inefficiency of therapy and autonomous cell expansion lead to early relapses after treatment (Section 6.4).

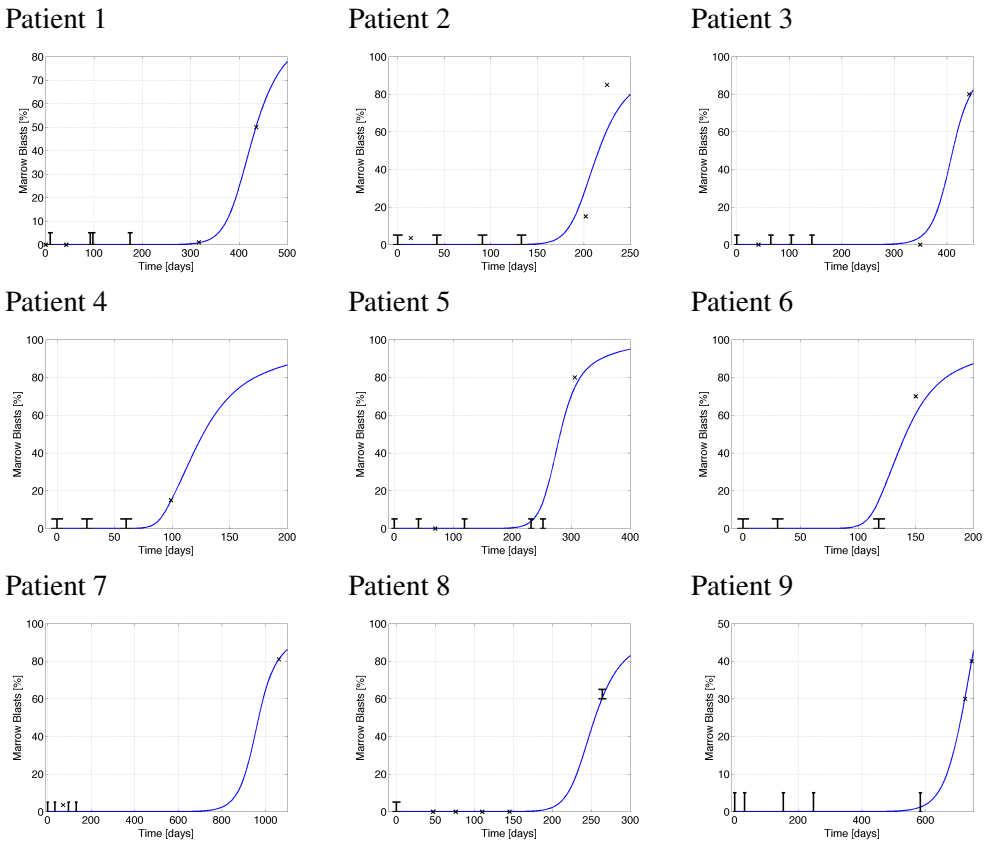

Figure 6.6: Fit of model to individual patient marrow blast fractions. The Figure compares model fits to data of example patients. The depicted simulations are based on the LSC parameters minimizing the squared difference between model simulations and clinical data. Parameter values of more mature cell types have little impact on the outcome. Data from A.D. Ho, N. Baran, University Hospital of Heidelberg. Blue lines: simulation, black symbols: data (with error bars, if available).

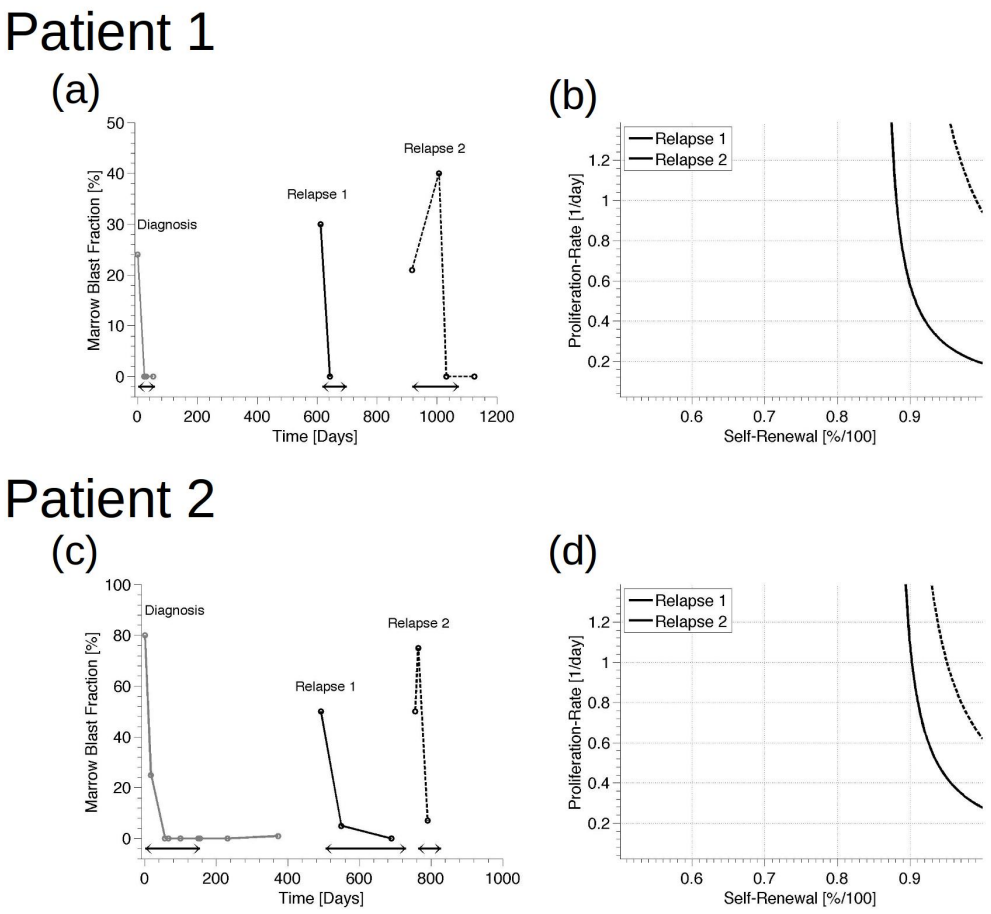

Figure 6.7: Estimated LSC properties in the first and second relapse. (a, c) Marrow blast dynamics of two patients experiencing two relapses. Horizontal arrows at the bottom of the graph denote treatment duration (in the case of chemotherapy from the beginning of the first until end of last cycle, in the case of targeted therapy from the beginning until the end of drug administration). (b, d) Estimated properties of the LSC responsible for the first and second relapse. Figure (b) corresponds to the patient data in (a), Figure (d) to that in (c). The results demonstrate that LSC properties changed between the relapses. Higher self-renewal and / or proliferation in the second relapse correspond to selection of more aggressive, faster expanding, LSC than in the first relapse.

CHAPTER 7

MODELS OF CLONAL SELECTION IN ACUTE LEUKEMIAS

7.1 Outline of the chapter

This Chapter is devoted to numerical studies of clonal evolution and selection in acute leukemias. Recent experimental results suggest that the leukemic cell mass consists of multiple, heterogeneous clones, the size of which changes over time, [56]. In this Chapter, we investigate, which cell properties in terms of proliferation and self-renewal are selected for during early phases of the disease and during chemotherapy. For this task, we use multi-lineage versions of the models introduced in Chapter 2 (Sections 7.2.1 and 7.2.2). We, furthermore, include a simple model of chemotherapy to simulate selection processes under treatment conditions (Section 7.2.3). Numerical simulations are described in Section 7.3. The models are calibrated to data from literature and compared to clinical data (Section 7.4.9) and to data from sequencing studies (Section 7.4.10).

We show that genetic differences between cells detected at primary diagnosis and cells detected at relapse can be explained by clonal selection mechanisms and do not necessarily require new mutations. Furthermore, clonal competition is an efficient mechanisms to limit the number of clones contributing to leukemic cell mass (Sections 7.4.1, 7.4.3). The models suggest that cells at primary diagnosis have high proliferation rates and high self-renewal potential, whereas cells at relapse have high self-renewal potential and small proliferation rates (Section 7.4.2, 7.4.5). Implications of this finding on patient prognosis and treatment strategies are discussed in Section 7.4. Finally, we provide a mathematical analysis of simplified versions of both models to show, which cell properties lead to long-term survival of leukemic clones and which cell properties lead to out-competition (Section 7.6).

The content of this Chapter, except mathematical analysis, has been published as *Stiehl, Baran, Ho, Marciniak-Czochra: Clonal selection and therapy resistance in acute leukemias: Mathematical modelling explains different proliferation patterns at diagnosis and relapse, 2014*, [213].

7.2 Models

The considered models are multi-lineage versions of the models introduced in Chapter 2. For simplicity, we consider only two stages per lineage, i.e., stem and non-stem cells. A schematic representation of the models is given in Fig 7.1.

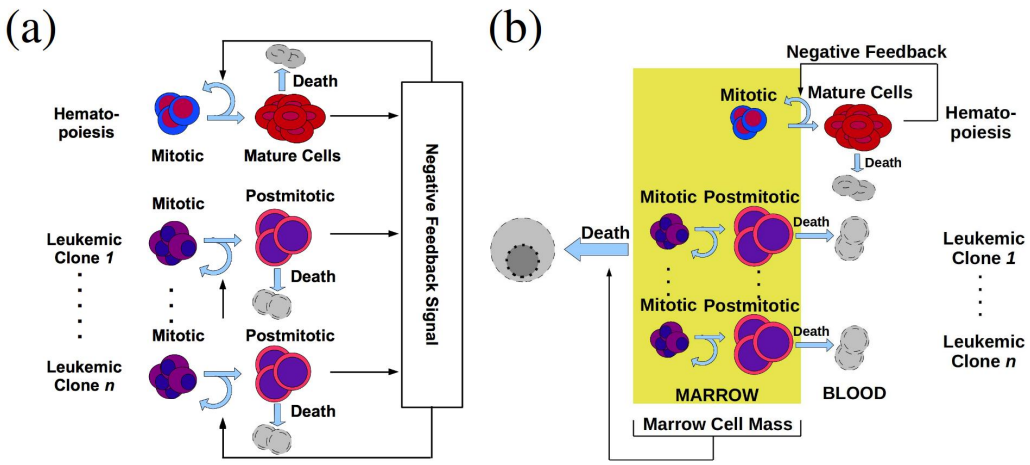

Figure 7.1: Schematic Representation of the Models. In Model 1 (a) self-renewal of leukemic and hematopoietic cells depends on the total number of post-mitotic cells via negative feedback. In Model 2 (b) self-renewal of hematopoietic cells depends on mature blood cell counts. Leukemic cells are independent of hematopoietic feedback signals. Increasing cell numbers in bone marrow space lead to increasing death rates of all bone marrow cell types, namely mitotic hematopoietic and all leukemic cells.

Definition 7.1 (Clone)
As a clone we understand all genetically identical cells originating from a single cell, [56].

7.2.1 Multi-clonal signal-dependent leukemia

We extend the model introduced in Chapter 2.3 to account for the interaction of one hematopoietic cell line and n ($n \in \mathbb{N}$) leukemic clones. We consider mitotic and post-mitotic cell compartments for each leukemic clone and for the

hematopoietic lineage. Let p^{l^i} denote the proliferation rate of mitotic cells in leukemic clone i and $a^{l^i}_{max}$ the corresponding maximal fraction of self-renewal. By $d^{l^i}_2 > 0$ we denote the clearance rate of post-mitotic cells of clone i. Moreover, we denote by $l^i_1(t)$ the level of mitotic cells of clone i and by $l^i_2(t)$ the level of post-mitotic cells at time t. Cell densities of the hematopoietic lineage are denoted as c_1 and c_2, the respective properties are denoted as p^c, a^c_{max} and d^c_2. For simplicity, we assume that mitotic cells do not die. These assumptions result in the following system of ordinary differential equations.

$$\begin{aligned}
\frac{d}{dt}c_1(t) &= \big(2a^c_{max}s(t) - 1\big)p^c c_1(t) \\
\frac{d}{dt}c_2(t) &= 2\big(1 - a^c_{max}s(t)\big)p^c c_1(t) - d^c_2 c_2(t) \\
\frac{d}{dt}l^1_1(t) &= \big(2a^{l^1}_{max}s(t) - 1\big)p^{l^1} l^1_1(t) \\
\frac{d}{dt}l^1_2(t) &= 2\big(1 - a^{l^1}_{max}s(t)\big)p^{l^1} l^1_1(t) - d^{l^1}_2 l^1_2(t) \\
\quad\vdots \quad & \quad\vdots \quad\quad \vdots \\
\frac{d}{dt}l^n_1(t) &= \big(2a^{l^n}_{max}s(t) - 1\big)p^{l^n} l^n_1(t) \\
\frac{d}{dt}l^n_2(t) &= 2\big(1 - a^{l^n}_{max}s(t)\big)p^{l^n} l^n_1(t) - d^{l^n}_2 l^n_2(t) \\
s(t) &= \frac{1}{1 + k^c c_2(t) + k^l \sum_{i=1}^n l^i_2(t)}.
\end{aligned} \tag{7.1}$$

We assume $1 > a^c_{max} > 0.5$, $p^c > 0$, $d^c_2 > 0$, $a^{l^i} \in (0,1)$, $p^{l^i} > 0$, $d^{l^i}_2 > 0$ for $1 \le i \le n$, $k^c > 0$, $k^l > 0$, $c_1(0) > 0$, $c_2(0) \ge 0$ and $l^i_1(0) > 0$, $l^i_2(0) \ge 0$ for $1 \le i \le n$.

Biological Remark 7.2
The expression for $s(t)$ is a special case of $\tilde{s}(t) = 1/\big(1 + k^c c_2(t) + \sum_{i=1}^n k^l_i l^i_2(t)\big)$, where we assume that $k^l_i = k^l$ for all i. This simplification corresponds to the observation that the density of cytokine receptors is similar on cells of all leukemic clones. For the major cytokine of the myeloid line, G-CSF, [160], this is is true for many patients, [206]. Since there is evidence that in some patients receptor densities may differ between different leukemic clones, [206], we have repeated all simulations with a randomly chosen k^l_i value for each clone, ranging from 30% of k^c to 100% of k^c. This heterogeneity had no significant impact on the model dynamics. Since in many cases the receptor density on leukemic cells is of the same order of magnitude as that on hematopoietic cells, [126, 206], we assume also $k^l = k^c$ for the remainder of this Chapter.

7.2.2 Multi-clonal signal-independent leukemia

We extend the model introduced in Chapter 2.4 to account for the interaction of one hematopoietic cell line and n leukemic clones. As above, we consider mitotic and post-mitotic cell compartments for each leukemic clone and for the hematopoietic lineage. Let $p^{\tilde{l}^i}$ denote the proliferation rate of mitotic cells in leukemic clone i and $a^{\tilde{l}^i}$ the corresponding fraction of self-renewal. By $d_2^{\tilde{l}^i} > 0$ we denote the clearance rate of post-mitotic cells of clone i. Denote by $\tilde{l}_1^i(t)$ the level of mitotic cells of clone i and by $\tilde{l}_2^i(t)$ the level of post-mitotic cells at time t. Cell densities of the hematopoietic lineage are denoted as c_1 and c_2, the respective properties are denoted as p^c, a_{max}^c and d_2^c. We assume that all leukemic cells are located in bone marrow, corresponding to $\chi = 1$ in the notation from Chapter 2.4. As specified in Chapter 2.4, the death rate caused by marrow crowding is denoted by d. It is assumed to affect all cell populations in marrow space. We assume that $d \equiv 0$ for arguments smaller than a threshold $\bar{x}$ and strictly monotonically increasing for arguments larger than $\bar{x}$. Especially, we assume that $d(\bar{c}_1) = 0$, where $\bar{c}_1$ is the unique positive steady state value of c_1 for $\bar{l}_1^i = \bar{l}_2^i = 0$ for all i. These assumptions result in the following system of ordinary differential equations:

$$
\begin{aligned}
\frac{d}{dt}c_1(t) &= \big(2a_{max}^c s(t) - 1\big)p^c c_1(t) - d(x(t))c_1(t) \\
\frac{d}{dt}c_2(t) &= 2\big(1 - a_{max}^c s(t)\big)p^c c_1(t) - d_2^c c_2(t) \\
s(t) &= \frac{1}{1 + k^c c_2(t)} \\
\frac{d}{dt}\tilde{l}_1^1(t) &= \big(2a^{\tilde{l}^1} - 1\big)p^{\tilde{l}^1}\tilde{l}_1^1(t) - d(x(t))\tilde{l}_1^1(t) \\
\frac{d}{dt}\tilde{l}_2^1(t) &= 2\big(1 - a^{\tilde{l}^1}\big)p^{\tilde{l}^1}\tilde{l}_1^1(t) - d_2^{\tilde{l}^1}\tilde{l}_2^1(t) - d(x(t))\tilde{l}_2^1(t) \\
&\vdots \quad \vdots \quad \vdots \\
\frac{d}{dt}\tilde{l}_1^n(t) &= \big(2a^{\tilde{l}^n} - 1\big)p^{\tilde{l}^n}\tilde{l}_1^n(t) - d(x(t))\tilde{l}_1^n(t) \\
\frac{d}{dt}\tilde{l}_2^n(t) &= 2\big(1 - a^{\tilde{l}^n}\big)p^{\tilde{l}^n}\tilde{l}_1^n(t) - d_2^{\tilde{l}^n}\tilde{l}_2^n(t) - d(x(t))\tilde{l}_2^n(t) \\
x(t) &= c_1(t) + \sum_{i=1}^{n}\tilde{l}_1^i(t) + \sum_{i=1}^{n}\tilde{l}_2^i(t).
\end{aligned}
\tag{7.2}
$$

We assume $1 > a_{max}^c > 0.5$, $p^c > 0$, $d_2^c > 0$, $a^{l^i} \in (0,1)$, $p^{l^i} > 0$, $d_2^{l^i} > 0$ for $1 \le i \le n$, $k^c > 0$, $k^l > 0$, $c_1(0) > 0$, $c_2(0) \ge 0$ and $l_1^i(0) > 0$, $l_2^i(0) \ge 0$ for $1 \le i \le n$.

7.2.3 Chemotherapy

We focus on classical cytotoxic therapy acting on fast dividing cells. Therapy is introduced to the models by adding a death rate proportional to the proliferation rate. The assumption is motivated by the fact that many of the classical therapeutic agents used for treatment of leukemias act on cells in the phase of division or DNA replication, [26]. Consequently, the higher the fraction of mitotic cells at the time of treatment, the higher the proportion of killed cells. Therefore, the rate of induced cell death is proportional to the number of mitotic cells. We assume that the linear factor, denoted by k_{chemo}, is identical for all mitotic cells. Under chemotherapy, the equation for mitotic hematopoietic cells in Model 1 takes the form

$$\frac{d}{dt}c_1(t) = \big(2a^c_{max}s(t) - 1\big)p^c c_1(t) - k_{chemo} \cdot p^c \cdot c_1(t). \tag{7.3}$$

Similarly, we obtain for mitotic cells of leukemic clone i

$$\frac{d}{dt}l^i_1(t) = \big(2a^{l^i}_{max}s(t) - 1\big)p^{l^i} l^i_1(t) - k_{chemo} \cdot p^{l^i} \cdot l^i_1(t). \tag{7.4}$$

Chemotherapy in Model 2 is introduced analogously:

$$\frac{d}{dt}c_1(t) = \big(2a^c_{max}s(t) - 1\big)p^c c_1(t) - d(x(t))c_1(t) - k_{chemo} \cdot p^c \cdot c_1(t), \tag{7.5}$$

$$\frac{d}{dt}l^i_1(t) = \big(2a^{l^i} - 1\big)p^{l^i} l^i_1(t) - d(x(t))l^i_1(t) - k_{chemo} \cdot p^{l^i} \cdot l^i_1(t). \tag{7.6}$$

7.3 Simulation of clonal selection during early disease and treatment

In this Section, we solely focus on the selection process of preexisting leukemic clones. Therefore, we do not consider new mutations. We initialize simulations with a fixed number of leukemic clones (e.g., 50), equal in size, with randomly chosen parameters. To understand, which leukemic cell properties lead to survival advantage during evolution of leukemias and relapse after chemotherapy, we observe how the size of the respective clones changes over time.

Initial conditions for computer simulations are equilibrium cell counts in the hematopoietic cell lineage and a small cell number for different leukemic clones (1 per kg of body weight).

We calibrate the model of the hematopoietic system based on data from bone marrow histology. The calibration is described in the Appendix E. This allows to fix parameters for the hematopoietic line. Parameters of leukemic clones are

chosen randomly (fraction self-renewal uniformly from $(0.6, 0.999)$, proliferation rate uniformly from $(0.01, 1.2)$). Details of model parameters are described in the Appendix E.

We assume that primary diagnosis and diagnosis of relapse occur, when healthy blood cell counts are decreased by 50% of their steady state value. We perform simulations for 50 patients, i.e., 50 different sets of initial data and model parameters, with 50 leukemic clones per patient. The growth properties of leukemic clones are chosen randomly within certain ranges. The simulations are done using the following algorithm:

(i) We assume that in healthy individuals the hematopoietic cells are in a dynamic equilibrium, i.e., production of each cell type equals its clearance. We, therefore, start from healthy equilibrium in the hematopoietic lineage and one mitotic cell per kg of body weight for each leukemic clone. We assume that the initial number of leukemic clones in each patient is 50. This number is arbitrarily chosen. All presented simulations are repeated for different numbers of leukemic clones (between 3 and 100), which leads to comparable results.

(ii) We run simulations until the number of healthy mature blood cells has decreased by 50%. We consider this point as the time-point of diagnosis. The sensitivity of standard methods to detect clones has been reported to be around 1%, [161], i.e., clones consisting of less than 1% of total cell mass are not detected. At the time-point of diagnosis we record cell properties, i.e., proliferation and self-renewal of all clones consisting of more than 1% of total cell mass. In the following, we denote these clones as '*significantly contributing clones*'.

(iii) Next, we simulate chemotherapy. For simplification, we consider seven applications of cytotoxic drugs (one per day during seven following days, corresponding to standard inductions). Simulations show that the number of drug applications has no influence on the presented qualitative results. As proposed in literature, [182], we define that a cell population has become extinct, if it consists of less than one cell. Initial conditions for the post-therapy period are obtained from cell counts after therapy, where counts of extinct populations are set to zero. We continue simulations until mature blood cell counts decrease by 50% and then assess the cell properties of the significantly contributing clones contributing at relapse, as described in (ii).

Simulations are performed using standard ODE-solvers from the Matlab-software package (Version 7.8, The MathWorks, Inc, Natic, MA), which are based on Runge-Kutta schemes.

7.4 Results

7.4.1 Clonality at diagnosis

Simulations indicate that at diagnosis rarely more than 3-4 clones significantly contribute to the total leukemic cell mass. In most cases more than 40-50% of the total leukemic cell mass originates from a single leukemic clone. This finding is identical for both considered models.

7.4.2 Properties of clones at diagnosis

Simulations indicate that the clones significantly contributing to the leukemic cell mass have high proliferation rates and high self-renewal potential. Such configuration of parameters leads to an efficient cell expansion. The properties of clones contributing significantly to leukemic cell mass at diagnosis of 50 virtual patients are depicted in Figure 7.2. This finding is identical for both considered models.

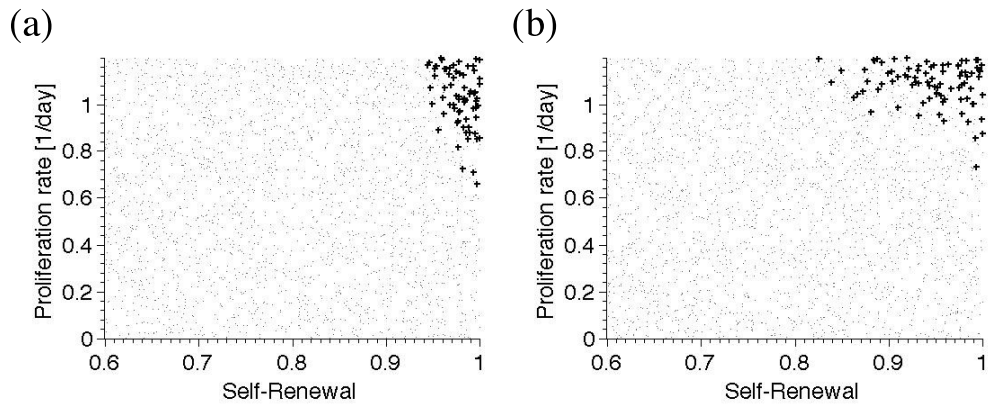

Figure 7.2: Impact of growth properties on clonal selection. The Figures depict clonal selection in 50 simulated patients. Each black '.' marks cellular properties of a leukemic clone present at the beginning of the simulations in at least one patient. Each '+' marks properties of a leukemic clone contributing significantly to the leukemic cell mass at diagnosis in at least one patient. Leukemic cells present at diagnosis have high proliferation rates and high self-renewal potential. (a): Model 1, (b): Model 2.

Remark 7.3 (Testable Prediction 1)
A testable prediction of the models is that more sensitive methods should reveal larger numbers of different clones that exist but do not significantly contribute to the leukemic cell mass at the time of diagnosis. In the next Section, we will see that this is also true at the time of relapse.

7.4.3 Clonality at relapse

The clonality at relapse is comparable to the clonality at diagnosis. Rarely more than three clones significantly contribute to the total leukemic cell mass. This finding is the same for both considered models.

Biological Remark 7.4
In most cases of acute lymphoblastic leukemia (ALL) the clones dominating relapse have already been present at diagnosis but undetectable by routine methods, [46, 148, 227]. Due to quiescence, very slow cycling or other intrinsic mechanisms, [46, 148] these clones survive chemotherapy and eventually expand, [46, 148]. This implies that the main mechanism of relapse in ALL is based on a selection of existing clones and not an acquisition of therapy-specific mutations, [46]. Similar mechanisms have been described for acute myeloid leukemia (AML), where clones at relapse are genetically closely related to clones at primary diagnosis, [56, 109], and did not have to acquire additional mutations during the course of disease, [16, 171].

7.4.4 Selection processes limit the number of significantly contributing clones

Figures 7.3 and 7.4 show that variation of the initial number of clones has little effect on the number of significantly contributing clones at diagnosis.

Biological Remark 7.5
This result is in agreement with data from recent gene sequencing studies and allows to explain these data. In these studies, [9,56], at most 4 contributing clones were detected in case of AML and at most 10 in case of ALL. In many patients this number was even smaller. Our study implies that clonal selection, due to different growth characteristics, is an efficient mechanism to reduce the number of clones contributing to leukemic cell burden.

7.4.5 Properties of clones at relapse

The properties of leukemic clones responsible for relapse depend on the efficiency of chemotherapy. We run computer simulations for varied efficiency of chemotherapy, namely different death rates imposed on mitotic cell compartments. In the case of inefficient chemotherapy, i.e., killing rates of mitotic cells being relatively small, the clones present at diagnosis are also responsible for relapse. These clones have high proliferation rates and high self-renewal potential. In the case of more efficient chemotherapy, i.e., killing rates of mitotic cells being higher, the clones responsible for primary presentation differ from the clones responsible for relapse. Compared to the clones leading to primary presentation, the clones responsible for relapse have low proliferation rates but high self-renewal

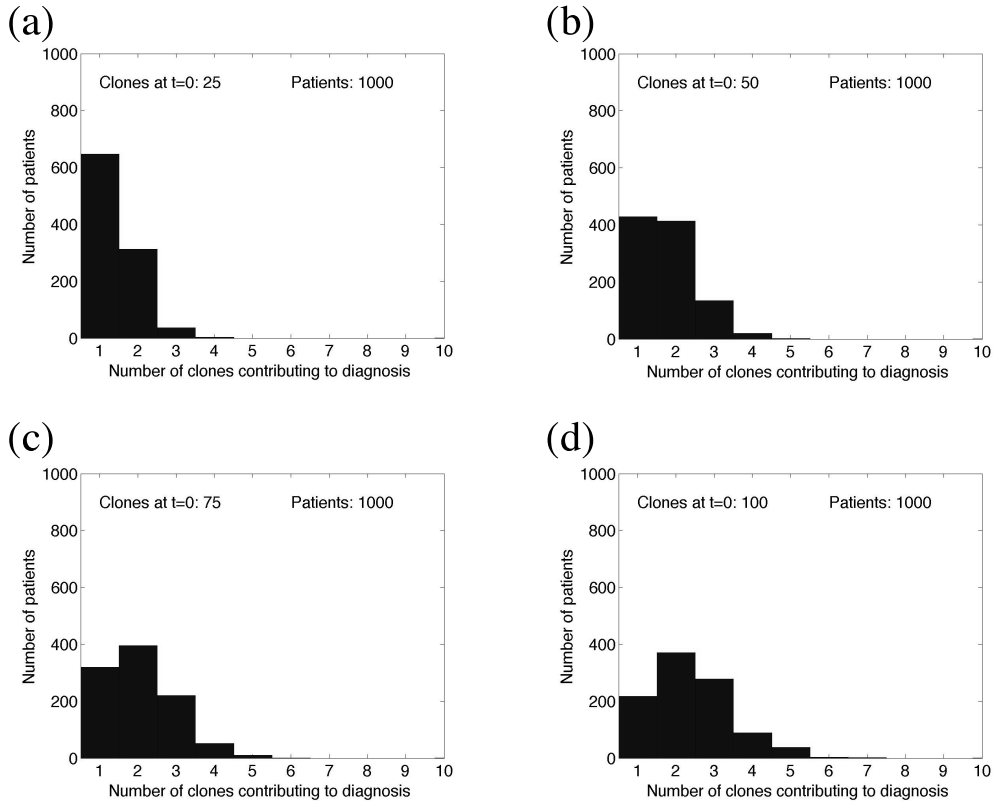

Figure 7.3: Clones contributing to diagnosis (Model 1). The Figure shows the distribution of the number of clones that contribute to diagnosis. The number of clones present at the beginning is 25 (a), 50 (b), 75 (c) or 100 (d). The simulations include 1000 patients. The Figure shows that for all initial conditions (a)-(d) the number of contributing clones is relatively constant (3 or less for more than 80% of the patients).

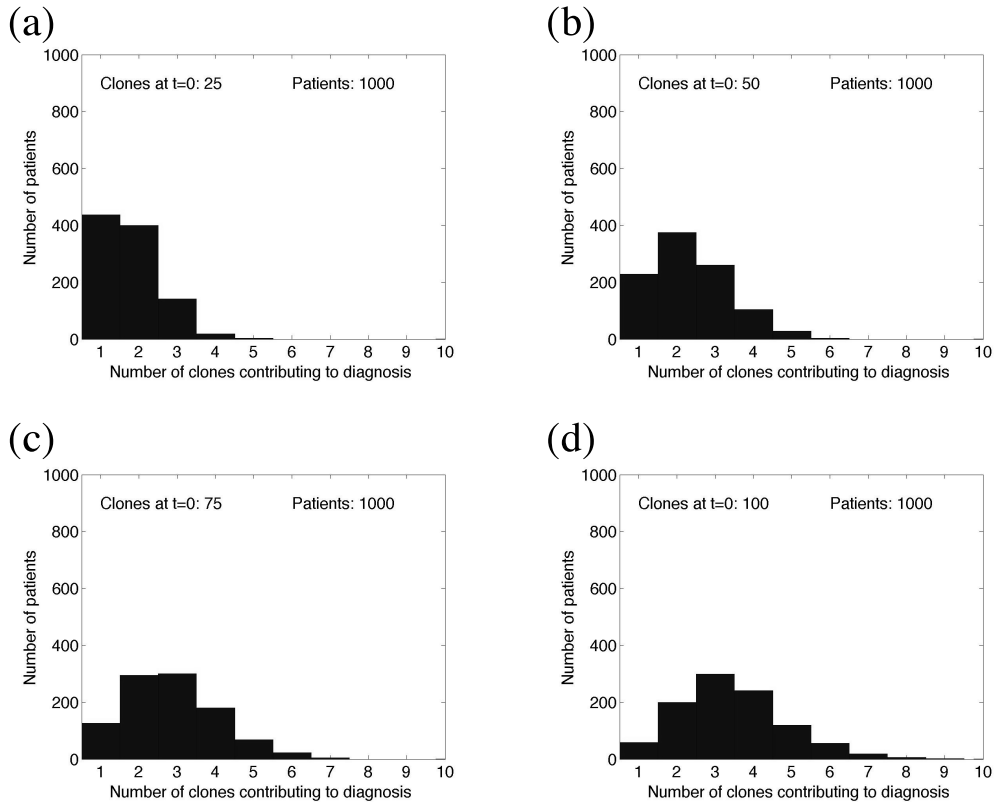

Figure 7.4: Clones contributing to diagnosis (Model 2). The Figure shows the distribution of the number of clones that contribute to diagnosis. The number of clones present at the beginning is 25 (a), 50 (b), 75 (c) or 100 (d). The simulations include 1000 patients. The Figure shows that for all initial conditions (a)-(d) the number of contributing clones is relatively constant (5 or less for more than 80% of the patients). In Model 2 the average number of clones contributing to relapse is slightly higher than in Model 1.

potential. The properties of clones contributing significantly to leukemic cell mass at diagnosis and at relapse are depicted in Figure 7.5. Both models lead to similar results.

Remark 7.6
The results suggest that observation of leukemic clones with different properties at different time-points does not necessarily require occurrence of new mutations. It can be a result of a selection process.

Remark 7.7 (Testable Prediction 2)
A prediction of the model is that cells present at relapse show mutations responsible for high self-renewal. Especially mutations present in dominant clones at relapse but not at primary diagnosis should be linked to high self-renewal.

Biological Remark 7.8 (Mutations leading to high self-renewal)
Remark 7.7 provides an algorithm to search for combinations of mutations that could enhance self-renewal. This might be important from a biological point of view. Deep sequencing techniques allow detection of a large number of somatic and leukemic mutations, nevertheless, their impact on functional properties is not well understood, [56]. Simulation results presented above might help to link the mutations detected at diagnosis and relapse to cellular properties, namely either high proliferation, high self-renewal (diagnosis) or high self-renewal, low proliferation (relapse). In this sense, the proposed model helps to close the gap between genetic markers and functional cell properties.

Remark 7.9 (Robustness to model assumptions)
The fact that both models lead to similar results suggest that even if the exact mechanism of interaction between leukemic and hematopoietic cells is not known, conclusions about the selected cell properties might be possible, since these seem to be robust with respect to model assumptions.

Biological Remark 7.10
The result that slow cycling is an important selective mechanism is compatible with the finding that cells in minimal residual disease samples are highly quiescent, [148]. It is further supported by the fact that addition of anthracyclines, which act independent of cell cycle, [62], leads to improved outcome of relapse therapies in ALL, [45].

Biological Remark 7.11 (Driving mechansism behind clonal selection)
The principle of clonal competition in leukemia evolution and the fact that resistant sub-clones might be responsible for relapse have been discussed for a long time, [46]. The developed models provide for the first time evidence that self-renewal potential is a major force behind this mechanism. High self-renewal can lead to rapid cell expansion, even in case of slow proliferation. This finding is new and cannot be concluded from biological data so far.

Biological Remark 7.12 (High resistance and fast expansion)
Slow proliferation and high self-renewal allow to achieve high therapy resistance (due to slow proliferation) and fast expansion (due to high stem cell self-renewal) at the same time. This might explain why relapsed diseases are very resistant to a broad spectrum of cytotoxic agents. This finding is in agreement with data from clinical practice in ALL suggesting that the clones selected for at relapse possess inherently reduced sensitivity to treatment, [46].

Remark 7.13 (Testable Prediction 3)
A prediction of the model is that cells present at relapse could originate from small clones already present at diagnosis. Since relapses are a frequent and severe complication of acute leukemias, [70, 74, 142, 177, 189], mutations in small clones at diagnosis could be better prognostic markers that that detected clones dominating cell mass at primary diagnosis. A main challenge in the interpretation of sequencing data may, therefore, be the task to detect prognostically significant small clones among the potentially high number of small clones present at diagnosis.

Biological Remark 7.14 (Resistance of relapsing disease)
Clonal selection processes under chemotherapy leading to high self-renewal and slow proliferation may explain the observed resistance of relapsing disease. Since in acute leukemias the time interval of drug application is relatively short (weeks), occurrence of new mutations leading to resistance during the treatment period is relatively improbable in comparison to treatment of chronic leukemias with drug application over years.

7.4.6 Treatment of relapse

If the same treatment strategy as in case of primary treatment is applied to a relapsed patient, remission time is significantly shorter (Fig. 7.6). Second relapse is

---

Figure 7.5 *(facing page)*: Impact of growth properties on clonal selection. The Figures depict clonal selection in 50 simulated patients. Each black '.' marks cellular properties of a leukemic clone present at the beginning of the simulations in at least one patient. Each '+' marks properties of a leukemic clone contributing significantly to the leukemic cell mass at diagnosis in at least one patient. Gray squares mark properties of cell clones contributing significantly to relapse after chemotherapy in at least one patient. In comparison to leukemic cells present at diagnosis, clones at relapse have lower proliferation rates. (a): Model 1, strong chemotherapy, (b): Model 1, weak chemotherapy, (c): Model 2, strong chemotherapy, (d): Model 2, weak chemotherapy. (e) Example of the dynamics of hematopoietic (left) and leukemic (right) cells in one simulated patient. Vertical dotted lines mark primary diagnosis and relapse. Therapy is indicated by a gray rectangle. In the given example primary manifestation and relapse of the disease are diagnosed when mature blood cells decreased by 50%.

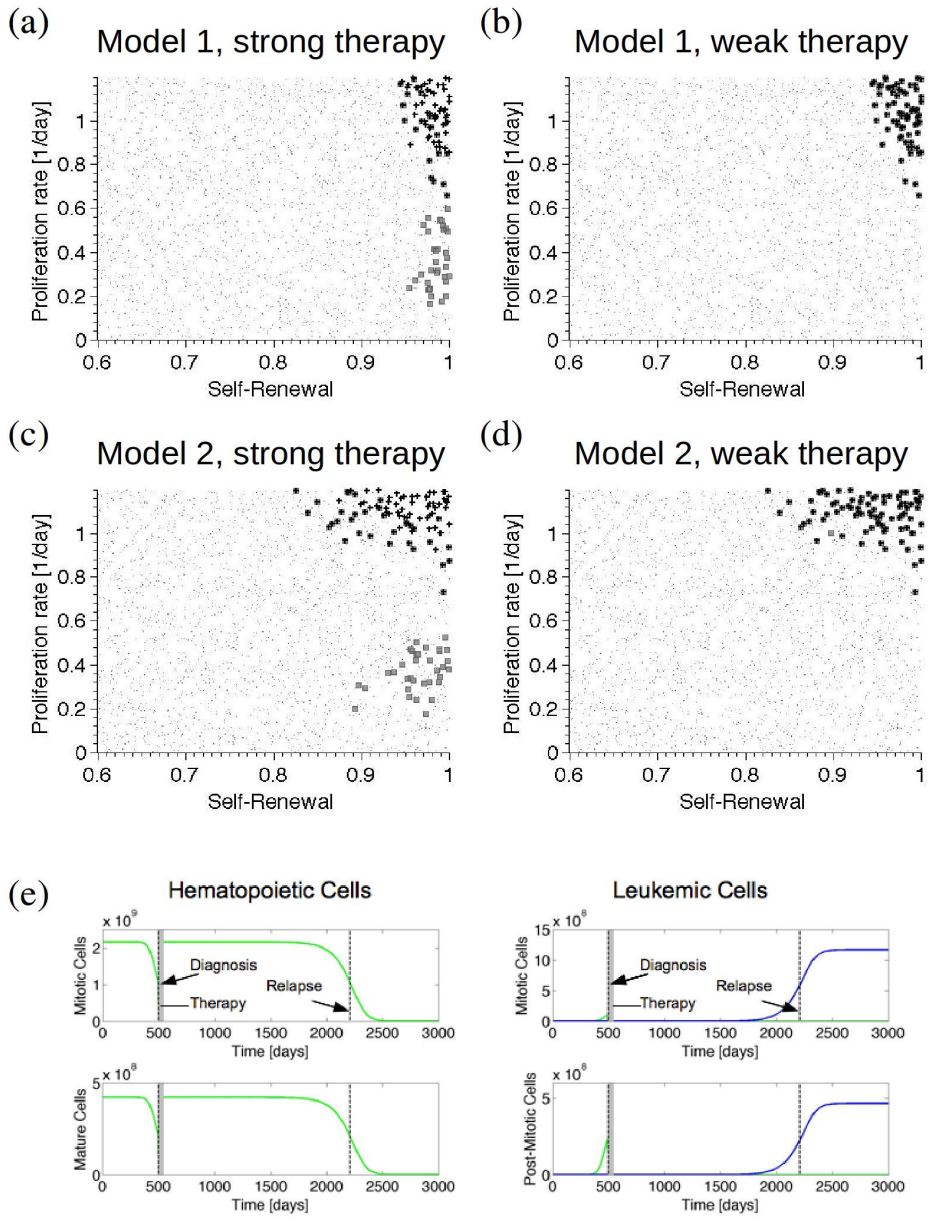
(a)
Model 1, strong therapy
(b)
Model 1, weak therapy
(c)
Model 2, strong therapy
(d)
Model 2, weak therapy
Proliferation rate [1/day]
Self-Renewal
(e)
Hematopoietic Cells
Leukemic Cells
Mitotic Cells
Mature Cells
Post-Mitotic Cells
Diagnosis
Relapse
Therapy
Time [days]

mostly triggered by the same clones as primary relapse. With repeated chemotherapy, clonal composition changes in favor of the clones with minimal proliferation (Clone 5 in Fig. 7.6).

Biological Remark 7.15
This finding is in agreement with data from clinical practice in ALL suggesting that the clones selected for at relapse possess inherently reduced sensitivity to treatment, [46], and may be also responsible for second relapse, [46]. The dynamics of leukemic cells in our model are in good agreement with data from clinical practice: Chemotherapy is able to reduce leukemic cell load after relapses, [227], nevertheless, this reduction does not lead to durable remission, [45]. This reflects the poor prognosis of relapsed patients, [29, 45, 122]. The increasing fraction of cells with reduced drug sensitivity predicted by the simulations explains the experimental finding that cells present at relapse are more resistant to chemotherapy than cells present at initial diagnosis, [29, 122]. It also shows that repetition of the same induction therapy leads to worse results in relapse compared to primary manifestation, [45]. The selection of slowly cycling cells predicted by our model seems to be an important mechanism in AML. It it was demonstrated that induction of cell cycling enhances chemo-sensitivity of leukemic cells, [194], and improves patient outcome after therapy, [144]. The models suggest that repeated chemotherapy can lead to the selection of clones that are not competitive in natural environment, i.e., that can be out-competed by clones sensitive to chemotherapy after cessation of the treatment.

7.4.7 Short term expansion efficiency does not correlate with long term self-maintenance

If leukemic cell behavior depends on hematopoietic cytokines (Model 1), the current signaling environment influences expansion of leukemic clones. In this scenario, it is possible that fast proliferating cells with low self-renewal potential dominate the leukemic cell mass during an initial phase. If, with increasing leukemic cell mass, self-renewal becomes down-regulated, e.g., due to occupation of bone marrow niche, eventually the cell clone with the highest affinity to self-renewal survives, although its proliferation might be slow. An example of time evolution during an early phase is depicted in Fig. 7.7.

7.4.8 Late relapses can originate from clones that were already present at diagnosis

Simulations of Model 1 indicate that late relapses, e.g., relapses after more than 3 years, can originate from clones that were already present at diagnosis but did not significantly contribute to the leukemic cell mass at that time. These relapses are triggered by very slowly proliferating cells, which survive chemotherapy and

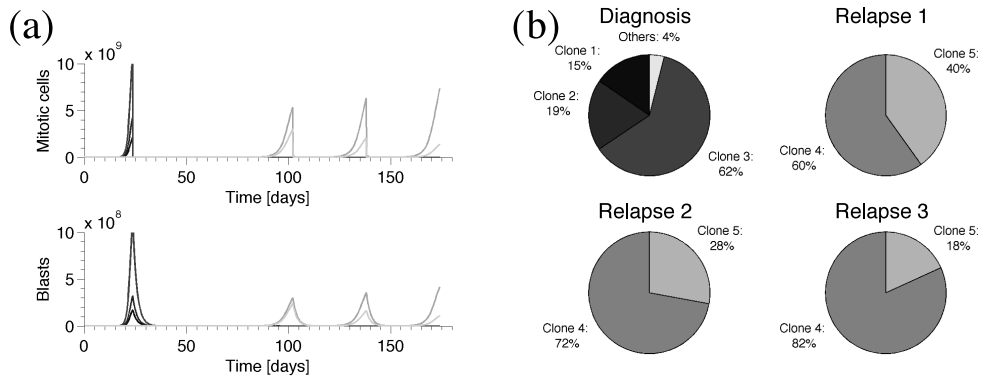

Figure 7.6: Time dynamics and clonal composition of subsequent relapses. The Figure depicts an example of multiple relapses after chemotherapy. Relapses are treated using the same strategy as primary presentation. A: Leukemic cell counts, each color indicates a different clone. Time between relapses 2, 3 and 4 is shorter than remission after first treatment. This demonstrates that the selected clones are not fully responsive to the applied therapy. B: Clonal composition of leukemic cell mass at the primary diagnosis and at relapses. Charts depict the contribution of major clones to the total leukemic cell mass. Clones responsible for relapse are present at very small fractions at primary diagnosis ($<< 5\%$). Relapses are triggered by the same clones, but their relative contribution to the leukemic cell mass change in favor of the slowly proliferating highly self-renewing cells.

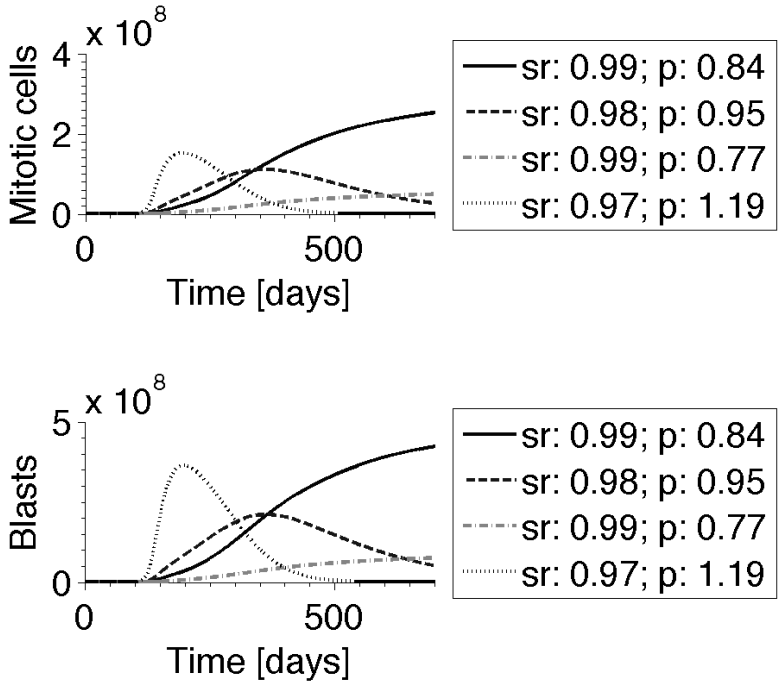

Figure 7.7: First phase of leukemic clone evolution. At the beginning, fast proliferating clones with low self-renewal can dominate. They are later out-competed by clones with high self-renewal, which is an advantage under high competition for niche spaces, needed for self-renewal. If there exist clones with high self-renewal and high proliferation, they will dominate during this first phase of leukemic evolution. Each line type corresponds to one leukemic clone. Blasts are immature cells used for diagnosis of leukemias. In the course of the disease blasts accumulate and out-compete hematopoiesis. Blast counts greater than 5% are considered as pathological, [139]. The simulations are based on Model 1.

then slowly grow. At primary diagnosis fast proliferating clones dominate. The slowly proliferating clones are then selected by chemotherapy. This finding is able to explain relapses without additional mutations occurring after primary diagnosis. Thus, temporary risk factor exposure (e.g., chemicals or radiation) can be responsible also for very late relapses and presentations.

7.4.9 Comparison of simulations to clinical data

To check if the proposed modelling framework is consistent with the observed dynamics of leukemia, we calibrate the model to data of two patients with multiple relapses. Since in clinical routine only few key mutations are monitored, we choose patient examples with different key mutations detected at diagnosis and at relapses. Such data are relatively rare, therefore, we focus on two patients. The selected two patients showed different AML-typical mutations. The available data include time periods between induction/consolidation chemotherapy and relapse as well as the percentages of leukemic blasts in the bone marrow at diagnosis, follow-ups and relapse. In addition, emergence and subsequent elimination of leukemia driving mutations (FLT3, MLL-PTD) in the bone marrow cells were precisely monitored using molecular biology methods, [198, 220, 237]. We verify if, and under which assumptions, the proposed model is compatible with clinical observations. This can serve as a qualitative 'proof of principle' and leads to hypotheses concerning changes in cell properties induced by the respective mutations. We assume that each mutation is associated with one leukemic cell clone. We interpret differences at diagnosis and at relapse as the result of a clonal selection process, due to chemotherapy and cell properties. For this study we apply Model 2, since simulations over a large range of parameters showed that remissions shorter than 150 days are only compatible with Model 2.

Simulations of the evolution of leukemic clones in the two patients are depicted in Figures 7.8 and 7.9. The results show that bone marrow blast fraction can be well described by the model. In Patient 1 a leukemia specific mutation (FLT3-ITD of a length of 39 bp) is detected at diagnosis. This mutation becomes extinct and the relapse is triggered by two different leukemia specific mutations (FLT3-ITD of length 42 bp and 63 bp). This behavior is reproduced in the model simulation. At diagnosis leukemic cell mass is mainly derived from one clone, whereas at relapse two different clones contribute to leukemic cell mass.

In Patient 2 FLT3-ITD mutation and MLL-PTD-mutation were both detected at diagnosis. The MLL-PTD mutation practically did not contribute to relapse. The model reflects this scenario. At diagnosis two different clones contribute to leukemic cell mass, one of which becomes extinct and is not detected at the relapse. In this patient, the clone responsible for relapse behaves similarly to the HSC lineage. Thus, classical cytotoxic treatment would not lead to its eradication. This is an indication for application of new anti-leukemic drugs, if feasible,

or for bone marrow transplantation.

7.4.10 Comparison of model to sequencing data

Recent sequencing studies allow to measure the number of clones and their contribution to leukemic cell mass at different time-points of the disease. In the following, we use sequencing data from ALL patients published in [9]. For simplicity, we only count the number of different clones and neglect the genetic interdependence between them. Figure 7.10 compares the pattern of clonal evolution in model simulations and in the example data sets. The Figure shows that the model is able to cover qualitative observations in the patient examples. More examples are presented in Appendix G. The model suggests that if the number of patients investigated in sequencing studies increases, more patterns could be detected. Figure 7.11 gives examples for patterns observed in model simulations but not in the 5 relapsing patients from the study in [9].

7.5 A model with mutations

In this Section, we describe an extension of Model 1, which includes mutations. An analogous extension is also possible for Model 2.

7.5.1 Biological background

There is evidence that a preleukemic HSC compartment serves as a reservoir of accumulated mutations, [110]. This hypothesis is supported by the finding that some of the mutations recurrently observed in leukemia already exist in the HSC compartment of a majority of leukemia patients, [110]. These preleukemic HSC seem to behave similarly to normal HSC, [110]. The hypothesis is that a relatively small number of additional hits may transform these preleukemic HSC into LSC. Nevertheless, details of the underlying dynamics are not well understood, [110].

We make the following assumptions:

- LSC with new properties can be generated either from preleukemic HSC or from LSC, due to acquisition of mutations. This is in line with the current knowledge, [109, 238].

- For simplicity, we assume that the influx of new LSC from the preleukemic compartment is constant in time. This assumption is made, due to simplicity, since at the moment the dynamics of the preleukemic compartment is not well understood, [110]. We neglect mutations leading from normal HSC, i.e., non-preleukemic HSC to LSC.

(a)

	Diagnosis t=0		Control t=150		Relapse t=200
Clone 1 (FLT3-ITD, 39 bp)	present	↘	0	→	0
Clone 2 (FLT3-ITD, 42 bp)	0	↗	present	↗	present
Clone 3 (FLT3-ITD, 63 bp)	0	→	0	↗	present

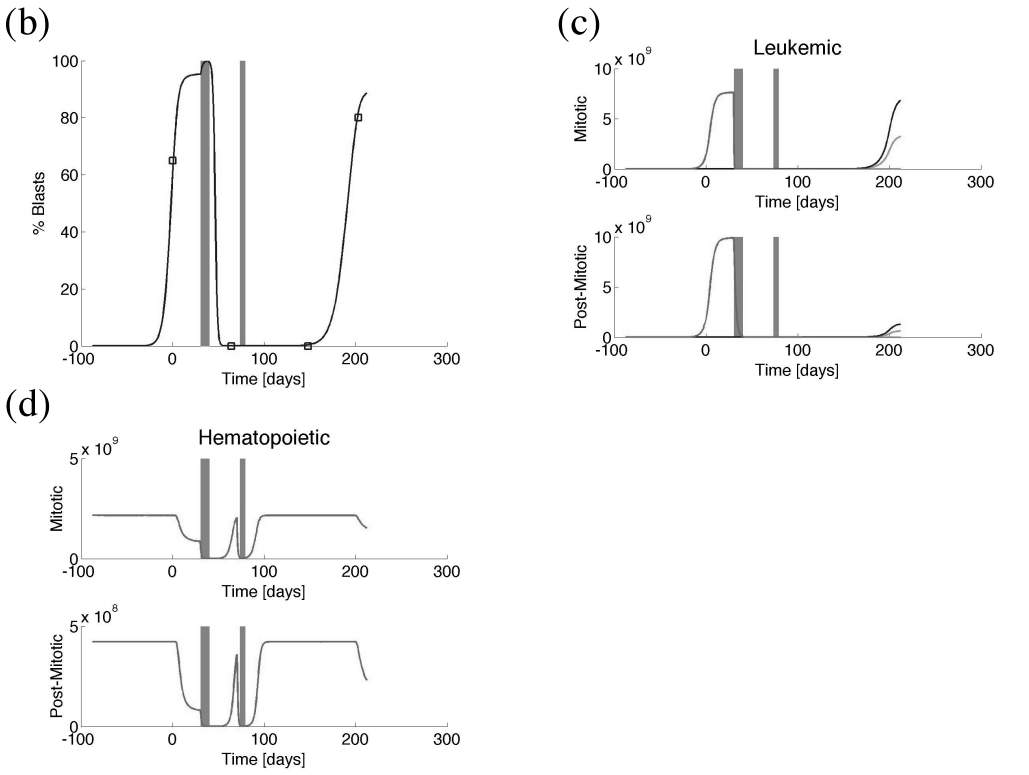

Figure 7.8: Fitting of model to patient data (Patient 1). Different leukemic mutations are used to distinguish between different clones. (a) The table indicates presence and absence of different leukemic clones at different time-points of the disease. Arrows indicate, if the respective clones increased or decreased during the time interval between the measurements. The depicted data are based on PCR analysis of bone marrow cells. (b) Comparison of simulated blast counts to data. Data are indicated as squares. (c) Evolution of leukemic populations. Each clone is indicated by a different line type. (d) Simulated counts of healthy leukocytes. Chemotherapy cycles are indicated by gray rectangles. Data from A.D. Ho, N. Baran (Medical Clinics V, University Hospital of Heidelberg). By "% Blasts", we denote the sum of leukemic cells of all clones divided by the total number of bone marrow cells.

(a)

	Diagnosis t=0	Control t=50	Control t=140	Relapse t=245
Clone 1 (MLL-PTD)	Present (low)	0	0	Present (high)
Clone 2 (FLT3-ITD)	Present (high)	0	0	Present (low)

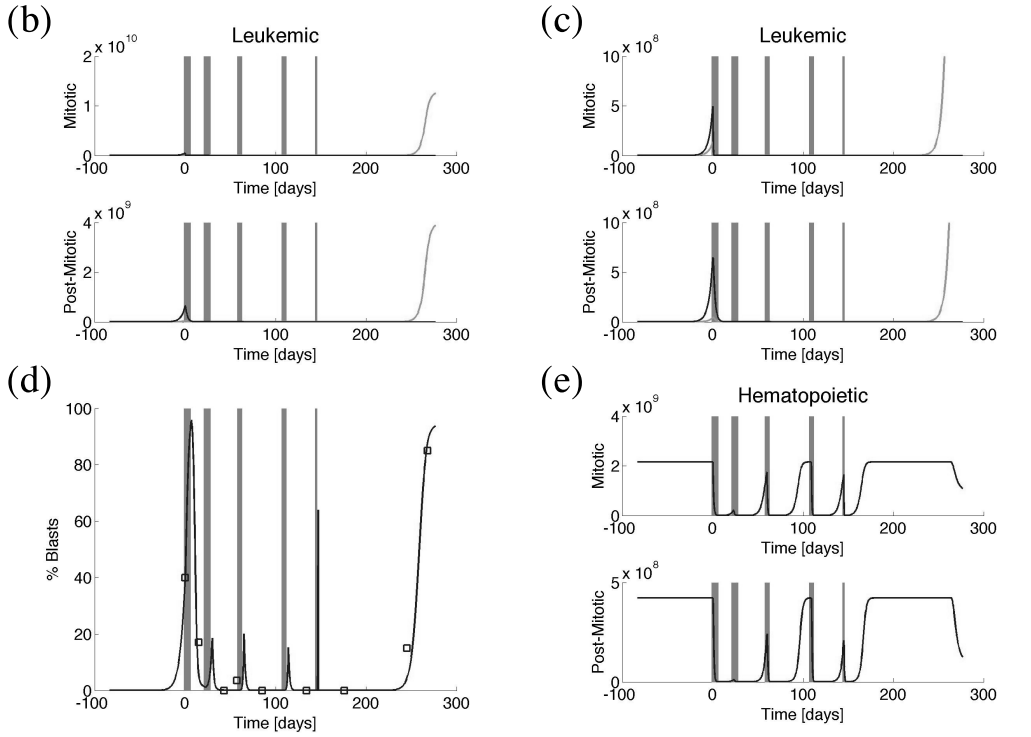

Figure 7.9: Fitting of model to patient data (Patient 2). Different leukemic mutations are used to distinguish between different clones. (a) The table indicates presence and absence of different leukemic clones at different time-points of the disease. Arrows indicate, if the respective clones increased or decreased during the time interval between the measurements. Small arrows indicate small changes, large arrows large changes. The depicted data are based on PCR analysis of bone marrow cells. (b)-(c): Evolution of leukemic populations with differently scaled vertical axis (cells per kg of body weight). Each clone is indicated by a different line type. (d): Comparison of simulated blast counts to data. Data are indicated as squares. (e): Simulated counts of healthy leukocytes in cells per kg of body weight. Chemotherapy cycles are indicated by gray rectangles. Data from A.D. Ho, N. Baran (Medical Clinics V, University Hospital of Heidelberg).

- We assume that most mutations in LSC are acquired during replication of the genome and neglect other possible origins. In line with [109] we neglect mutations leading to dedifferentiation of non-LSC leukemic cells.

7.5.2 Model

Let $l_1^i(t)$ be the concentration of LSC of clone i at time t. The flux to mitosis is then $l_1^i(t)p^{l^i}(t)$. From mitosis we obtain $2a^{l^i}(t)p^{l^i}(t)l_1^i(t)$, where $a^{l^i}(t)$ is the fraction of LSC self-renewal of clone i at time t. We assume that the fraction ν of these cells is mutated, ν takes into account replication errors in relevant genes and is assumed to be constant. The influx $\alpha_i(t)$ of mutated LSCs, due to new mutations occurring in clone i at time t is, therefore, $2a^{l^i}(t)p^{l^i}(t)l_1^i(t)\nu$.
We obtain the following set of equations describing dynamics of clone i:

$$\begin{aligned}
\frac{d}{dt}l_1^i(t) &= 2a^{l^i}(t)p^{l^i}(t)l_1^i(t)(1-\nu) - p^{l^i}(t)l_1^i \\
\frac{d}{dt}l_2^i(t) &= 2(1-a^{l^i}(t))p^{l^i}(t)l_1^i(t) - d_2^{l^i}l_2^i(t) \\
\alpha_i(t) &= 2a^{l^i}(t)p^{l^i}(t)l_1^i(t)\nu
\end{aligned}$$

A similar system of equations has been obtained in [225]. Since l_2^i is considered to be post-mitotic, we do not distinguish between cells that acquired a mutation during the divisions and those that did not.

The influx $\alpha(t)$ of mutated cells at time t is given by

$$\alpha(t) = \gamma + \sum_{i=1}^{N(t)} \alpha_i(t),$$

Figure 7.10 ***(facing page)*****: Patterns of clonal evolution - comparison of model and data.** Panel (a) illustrates how data on clonal evolution is obtained and visualized. For each patient clonal composition of the leukemic cell mass, i.e., number and size of clones, at primary diagnosis and at relapse is recorded using sequencing technology. Clonal size is measured in % of total leukemic cell mass, 100% means that all leukemic cells originate from one clone. Sensitivity of methods is around 1%. Size 0% means that the corresponding clone could not be detected at the respective time-point. The diagrams depict clonal size for each clone detected at primary diagnosis and/or relapse, i.e., for each clone there exist two measurements. Panels (b) -(d): Comparison of experimental measurements to model simulations. Red curves correspond to measurements, black curves in the same row to model simulations with similar behavior. The two measurements referring to the same clone are connected by a line to visualize changes in clonal contribution. The data were taken from [9].

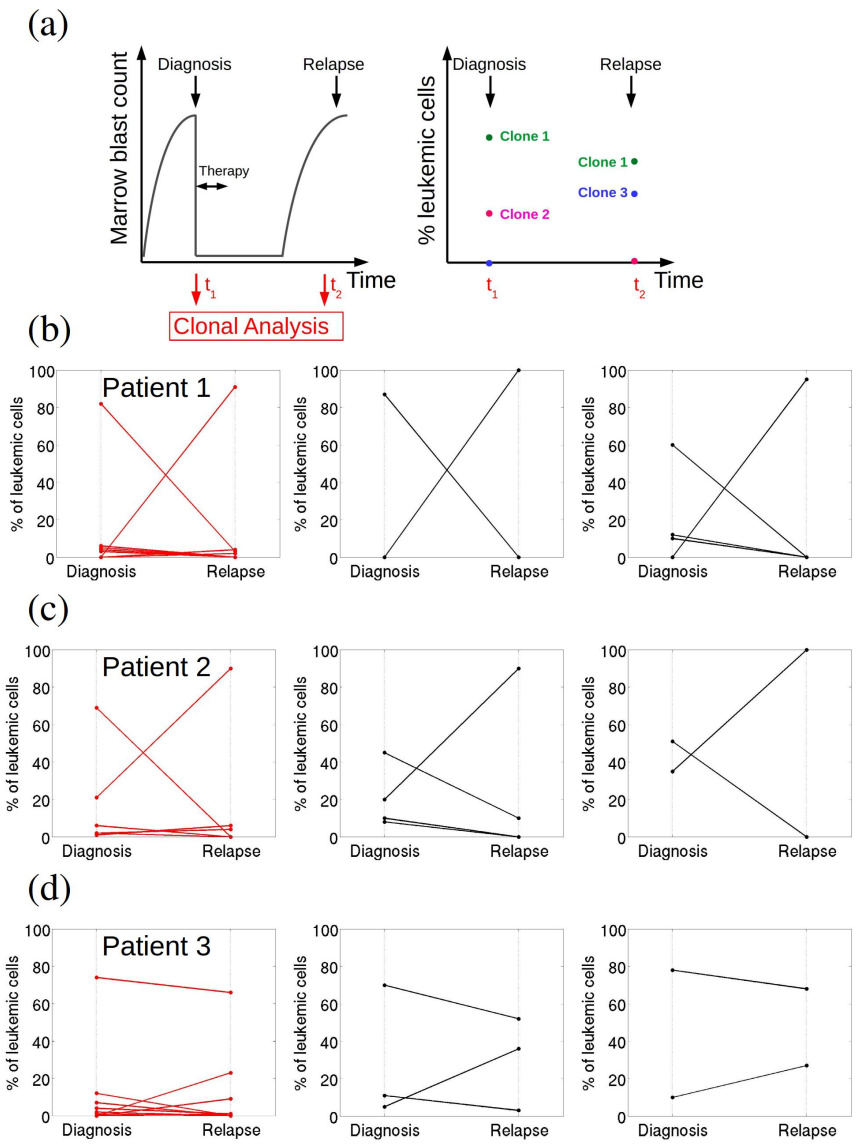
(a)
Marrow blast count
Diagnosis
Relapse
Therapy
Time
t1
t2
Clonal Analysis
% leukemic cells
Diagnosis
Relapse
Clone 1
Clone 1
Clone 3
Clone 2
Time
t1
t2
(b)
Patient 1
% of leukemic cells
Diagnosis
Relapse
(c)
Patient 2
(d)
Patient 3

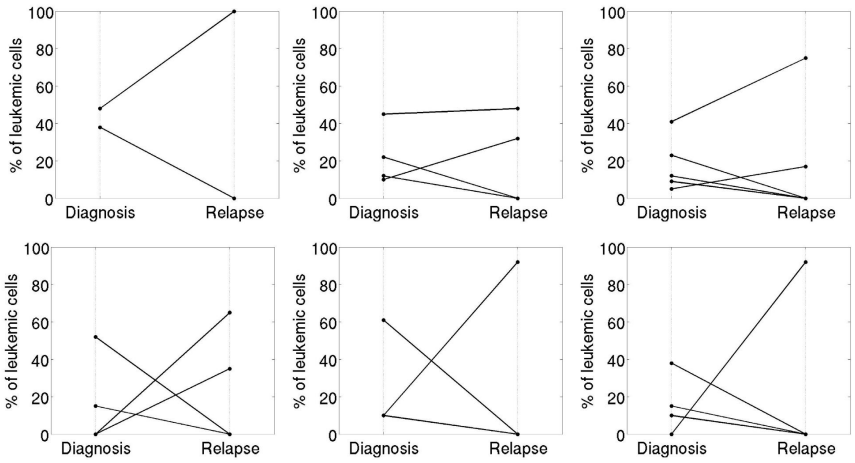

Figure 7.11: Patterns of clonal evolution. The Figure shows patterns of clonal evolution beyond those depicted in Figure 7.10. The patterns depicted here have not yet been observed in patient data. For explanation of the graphs see caption of Figure 7.10.

where γ is the constant influx from the preleukemic compartment and $N(t)$ the number of leukemic clones present at time t. We interpret the rate $\alpha(t)$ as the rate of an inhomogeneous Poisson process. Poisson processes describe rare events, [186,187], therefore, they are a suitable tool to model mutations. It is known from probability theory that, if τ_1 is a jump time of the inhomogeneous Poisson process with rate $\lambda(t)$, then the next jump time τ_2 can be generated by solving the equation $\int_{\tau_1}^{\tau_2} \lambda(t)dt = -\log(1-u)$ for τ_2. Here, u is an uniformly distributed random variable $u \in [0,1]$, [121]. We further know that if u is uniformly distributed in $u \in [0,1]$, then $-\log(1-u)$ is exponentially distributed with parameter 1, [186].

7.5.3 Simulations

We simulate the system with mutations as follows:

(i) We start simulations from the equilibrium counts of hematopoietic cells, one LSC per kg of body weight and no post-mitotic leukemic cells. LSC properties are chosen randomly from uniform distributions (proliferation rate between 0.01 and 0.9, self-renewal between 0.5 and 1).

(ii) At time $t_0 = 0$ we draw an exponentially distributed random number r_1 with parameter 1. We simulate the system until the time-point t_1, which fulfills $\int_{t_0}^{t_1} \lambda(t)dt = r_1$.

(iii) At time-point t_1 a mutation occurs that gives rise to a new LSC. This is modeled by adding to the system a new LSC clone, consisting of one LSC and no less primitive leukemic cells. We assume that the mutation occurs

in a random gene position, therefore, we assign random cell properties to the new clone, i.e., self-renewal and proliferation chosen randomly from uniform distributions (proliferation rate between 0.01 and 0.9, self-renewal between 0.5 and 1). This choice is made for the sake of simplicity, since details about the impact of mutations on cell behavior and the underlying probability distributions are not known, [56]. We then draw another random number r_2 and continue simulations until time-point t_2 fulfilling $\int_{t_1}^{t_2} \lambda(t)dt$, etc.

The results obtained from these simulations are similar to the results from the model without mutations. At primary diagnosis cells show high self-renewal and high proliferation, while at relapse cells show high self-renewal and reduced proliferation (Figure 7.12). The proliferation rates differ significantly between diagnosis and relapse ($p < 10^{-6}$ in Kruskal-Wallis Test), while self-renewal does not differ significantly ($p \approx 0.7$ in Kruskal-Wallis test).

7.6 Mathematical analysis

In this Section, we give analytical results for simplified versions of Models (7.1) and (7.2). The proofs are deferred to Appendix F. The analytical methods used are taken from [61, 91].

7.6.1 Model 1

Proposition 7.16 (Selection and coexistence in Model 1)
Consider system (7.1) *with positive initial conditions. Assume that death rates of mitotic cells are zero. Let all fractions of self-renewal be greater than 0.5.*

(i) Let proliferation rates of all clones be equal. Then, all populations with non-maximal fraction of self-renewal tend to zero for t tending to infinity. All populations with maximal self-renewal are bounded away from zero.

(ii) Let fractions of self-renewal of all clones be equal. Then, all cell populations are bounded away from zero and infinity.

The proof is given in Section F.1.

Remark 7.17
Proposition 7.16 is the discrete version of the results presented in [91] for a continuous version of Model 1.

Remark 7.18
The proposition shows that self-renewal is important for clonal selection processes. If clones differ in self-renewal, then some clones tend to zero, while others survive. If clones only differ in proliferation rates, all clones survive.

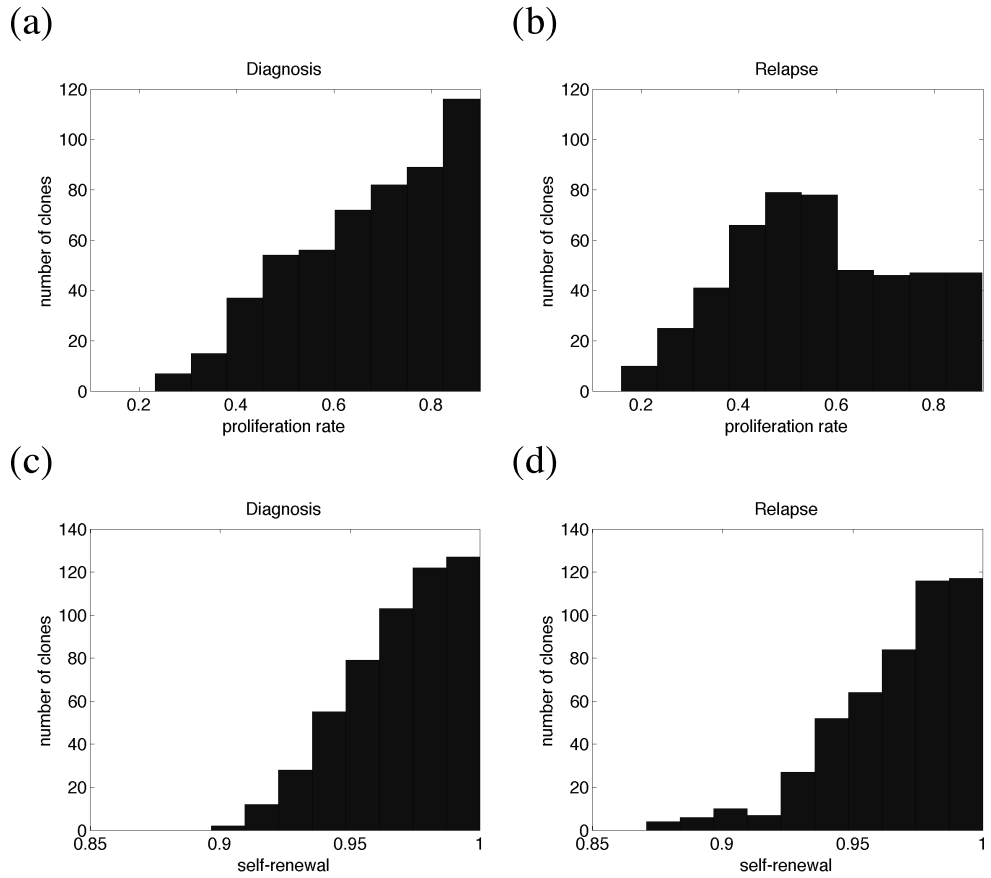

Figure 7.12: Clonal properties at diagnosis and at relapse in a model with mutations. The Figure shows the distribution of self-renewal and proliferation rate of leukemic clones present at diagnosis and at relapse. The plots include data of 500 simulated patients. As in the models without mutations, proliferation is reduced at relapse in comparison to diagnosis, while self-renewal is high at both time-points. (a) proliferation rate at diagnosis, (b) proliferation rate at relapse, (c) self-renewal at diagnosis, (d) self-renewal at relapse. The simulations are for $\gamma = 0.02/days$ and for $\nu = 5 \cdot 10^{-8}$, $k_{chemo} = 60$. Similar results are obtained for different values, e.g., if γ and ν are varied by a factor of 10.

7.6.2 Model 2

For simplicity, we assume that post-mitotic leukemic cells do not stay in bone marrow, i.e., we replace x in system (7.2) by $x(t) = c_1(t) + \sum_{i=1}^{n} \tilde{l}_1^i(t)$. We, furthermore, assume that mitotic cells do not die. For the modified system we obtain the following proposition.

Proposition 7.19 (Selection and coexistence in Model 2)
Assume we have positive initial conditions. Set $\zeta^i := (2a^{\tilde{l}^i} - 1)p^{\tilde{l}^i}$ *and* $\zeta := \max_{1\leq i\leq N} \zeta^i$. *Denote by* K_1 *a global upper bound for* c_1, *which exists, due to Lemma F.9. It holds*

(i) All $\tilde{l}_1^j$ *with* $\zeta^j < \zeta$ *tend to zero for* t *tending to infinity.*

(ii) If, additionally, $\min_{1\leq i\leq N} \zeta^i > d(K_1)$, *then* $\tilde{l}_1^j$ *with* $\zeta^j = \zeta$ *are bounded away from zero for all times.*

(iii) If, additionally, there exists $0 < \hat{s} < 1$ *such that* $(2a_{max}^c \hat{s} - 1)p^c - \zeta > 0$, *then* c_1 *is bounded away from zero.*

The proof is given in Section F.2.

Biological Remark 7.20
Statements (i) and (ii) describe the selection process, only cell populations with maximal expansion rates can survive for long times. Statement (iii) describes coexistence of leukemic and hematopoietic cells, if stimulation of hematopoietic cells leads to an expansion rate that is larger than that of leukemic cells.

Remark 7.21
Figure 4.2 in Chapter 4 shows for a version of the model with more than two compartments that, if $\min_{1\leq i\leq N}\{(2a^{\tilde{l}^i} - 1)p^{\tilde{l}^i}\} > d(K_1)$ *is not fulfilled, all* $\tilde{l}_1^i$ *may tend to zero.*

Remark 7.22
Proposition 7.19 shows that in Model 2 only leukemic clones with maximal $\zeta := (2a_1^l - 1)p_1^l$ *can coexist. This behavior is very similar to Model 1, where only clones with maximal self-renewal can coexist. The analytical result from Propositions 7.16 and 7.19 explain, why the selection dynamics observed in numerical simulations are very similar for both models. An important difference between both Models is that in Model 2 healthy and leukemic cells can coexist for wide parameter ranges, even if LSC self-renewal is higher than steady state self-renewal of HSCs. In Model 1 this is not possible.*

7.7 Summary

In this Chapter, we extend the models from Chapter 2 to account for competition between multiple leukemic clones (Sections 7.2.1 and 7.2.2). The individual clones differ with respect to the parameters describing their dynamic properties. We neglect occurrence of new mutations, instead, we study evolution of different clones that have equal size at the initial time zero. We define the time-points of diagnosis of primary disease and relapse when healthy cell counts have decreased by 50% of their steady state value. We, furthermore, include a simple model of classical chemotherapy assuming that killing efficiency of the drug increases with proliferation rates (Section 7.2.3). Numerical studies suggest that the number of clones contributing to more than 1% of the total leukemic cell mass is rarely higher than 5. This holds for both considered models at primary diagnosis and at relapse and approximately independently of the number of clones present at time zero (Sections 7.4.1, 7.4.3, Figures 7.3, 7.4). This finding suggests that competition is a mechanism that limits the number of detectable clones (Section 7.4.4). The cells present at diagnosis have high proliferation rates and high self-renewal potential (Section 7.4.2,Figure 7.2), the cells responsible for relapse have slow proliferation rates and high self-renewal (Section 7.4.5,Figure 7.5). This finding is new and could not be concluded from experimental data so far. These insights in cell properties can help to understand the impact of newly detected mutations on dynamic cell properties (Remarks 7.7, 7.8). The proposed model is compatible with clinical data of individual patients (Section 7.4.9) and data from sequencing studies (Section 7.4.10). The model suggests that presence of genetically different cells at diagnosis and relapse does not necessarily require new mutations between diagnosis and relapse, instead, it can be explained by clonal selection mechanisms (Remark 7.6). The work presented in this Chapter has led to the following new hypotheses:

(1) More sensitive methods may detect large numbers of relatively small clones at diagnosis and relapse of acute leukemias (Remarks 7.3).

(2) Clones dominating at relapse may be already present at diagnosis, but undetectable by routine methods (Remark 7.13).

(3) Mutations detected in cells present at relapse may increase self-renewal (Remark 4.7).

(4) Presence of small clones carrying mutations leading to small proliferation and high self-renewal at the time-point of diagnosis may correlate with the risk for relapse and the time of disease free survival (Remark 7.13).

(5) The combination of slow proliferation and high self-renewal leads to resistance to classical cytotoxic drugs but allows a relatively efficient expansion of cells. This could explain the observed resistance of relapsing disease.

Since the time interval of drug application is short in acute leukemias, the occurrence of new drug specific mutations is relatively improbable (Remark 7.14).

(6) Properties of cells detected at second relapse compared to properties of cells detected at first relapse show more similarities that properties of cells detected at primary diagnosis compared to cells detected at first relapse (Section 7.4.6).

Finally, we show analytically that in case of signal-dependent leukemia only clones with maximal self-renewal survive for long times. If all clones have identical self-renewal and differ only with respect to proliferation rates, no selection is observed and all clones show long-term survival (Proposition 7.16). In case of signal-independent leukemia only clones with maximal expansion rates $(2a-1)p$ can survive. Coexistence is established, whenever signal stimulation can increase expansion rates of hematopoietic cells to larger values than expansion rates of leukemic clones (Proposition 7.19).

Part III

Model reduction

CHAPTER 8

TIKHONOV REDUCTION

8.1 Outline of the chapter

Tikhonov's Theorem is a classical tool to study reduction of ODE systems, where derivatives are multiplied with a small parameter, [19]. The models of stem cell dynamics considered in this thesis are examples for such problems, since cell division and differentiation take place at different time scales than signal dynamics, [30,160,203]. Tikhonov's theorem provides conditions under which solutions of the reduced system (quasi-steady state reduction) approximate solutions of the original system for the parameter tending to zero. Tikhonov-reductions are only valid on *finite* time intervals. In Section 8.2, we recapitulate the theorem and its assumptions according to [19]. In Section 8.3, we apply the Tikonov Theorem to a minimal version of the stem cell model (2.3) introduced in Chapter 2. We obtain that the quasi stead state approximation of the stem cell model is close to the original system on finite time intervals, if cytokine dynamics are fast enough compared to cell divisions (Theorem 8.13). In the next Chapter, we will study the approximation on the infinite time interval.

8.2 Tikhonov's Theorem

We cite Tikhonov's Theorem from [19]. We consider a system

$$\begin{aligned} \frac{d}{dt}\mathbf{u}_\varepsilon &= \mathbf{f}(t,\mathbf{u}_\varepsilon,\mathbf{v}_\varepsilon,\varepsilon), \qquad \mathbf{u}(0)=\mathbf{u}^0 \\ \varepsilon\frac{d}{dt}\mathbf{v}_\varepsilon &= \mathbf{g}(t,\mathbf{u}_\varepsilon,\mathbf{v}_\varepsilon,\varepsilon), \qquad \mathbf{v}(0)=\mathbf{v}^0 \end{aligned} \tag{8.1}$$

The following assumptions are required.

Definition 8.1 (Lipschitz condition (from [221], p. 184))
Let $X \subset \mathbb{R}^n$, $T > 0$, $\varepsilon > 0$. A function

$$\mathbf{f} : [0,T] \times X \times [-\varepsilon, \varepsilon],\ (t, \mathbf{x}, \mu) \mapsto \mathbf{f}(t, \mathbf{x}, \mu)$$

fulfills the Lipschitz condition with respect to $\mathbf{x}$, if for all $\mathbf{x}_1, \mathbf{x}_2 \in X$

$$|\mathbf{f}(t, \mathbf{x}_1, \mu) - \mathbf{f}(t, \mathbf{x}_2, \mu)| \leq L|\mathbf{x}_1 - \mathbf{x}_2|, \tag{8.2}$$

where L is a positive constant independent of μ and t.

Assumption 8.2 (Lipschitz continuity of right hand-side)
Let $\bar{\mathcal{U}} \subset \mathbb{R}^n$ be a compact set and $\mathcal{V} \in \mathbb{R}^m$ be a bounded open set. Let $T > 0$, $\varepsilon_0 > 0$. Let

$$\mathbf{f} : [0,T] \times \bar{\mathcal{U}} \times \mathcal{V} \times [0, \varepsilon_0] \to \mathbb{R}^n, \quad (t, \mathbf{u}, \mathbf{v}, \varepsilon) \mapsto \mathbf{f}(t, \mathbf{u}, \mathbf{v}, \varepsilon) \tag{8.3}$$

$$\mathbf{g} : [0,T] \times \bar{\mathcal{U}} \times \mathcal{V} \times [0, \varepsilon_0] \to \mathbb{R}^m, \quad (t, \mathbf{u}, \mathbf{v}, \varepsilon) \mapsto \mathbf{g}(t, \mathbf{u}, \mathbf{v}, \varepsilon) \tag{8.4}$$

be continuous functions that fulfill the Lipschitz condition with respect to the variables $(\mathbf{u}, \mathbf{v})$ in $\bar{\mathcal{U}} \times \mathcal{V}$.

Assumption 8.3 (Isolated root of the fast equation)
Consider the reduced system

$$\frac{d}{dt}\mathbf{u} = \mathbf{f}(t, \mathbf{u}, \mathbf{v}, 0), \qquad \mathbf{u}(0) = \mathbf{u}^0, \tag{8.5}$$

$$0 = \mathbf{g}(t, \mathbf{u}, \mathbf{v}, 0). \tag{8.6}$$

Assume that there exists a solution $\Phi \in C^0([0,T] \times \bar{\mathcal{U}}, \mathcal{V})$ of equation (8.6). Furthermore, there exists $\delta > 0$ such that for all $(t, \mathbf{u}) \in [0,T] \times \bar{\mathcal{U}}$ fulfilling $0 < |\mathbf{v} - \Phi(t, \mathbf{u})| < \delta$, it holds $\mathbf{g}(t, \mathbf{u}, \mathbf{v}, 0) \neq 0$.

Assumption 8.4
(Local asymptotic stability of the fast equation for fixed slow variables)

Consider the system

$$\frac{d}{d\tau}\tilde{\mathbf{v}}^{(\mathbf{t},\mathbf{u})} = \mathbf{g}(t, \mathbf{u}, \tilde{\mathbf{v}}^{(\mathbf{t},\mathbf{u})}, 0), \tag{8.7}$$

where $\tilde{\mathbf{v}}^{(\mathbf{t},\mathbf{u})}(0)$ is given and t and $\mathbf{u}$ are treated as parameters. Assume that $\forall \eta > 0\ \exists \delta > 0$ such that $\forall (t, \mathbf{u}) \in [0,T] \times \bar{\mathcal{U}}$ it holds

$$|\tilde{\mathbf{v}}^{(\mathbf{t},\mathbf{u})}(0) - \Phi(t, \mathbf{u})| < \delta \Rightarrow \begin{cases} \forall \tau > 0 \text{ it holds } |\tilde{\mathbf{v}}^{(\mathbf{t},\mathbf{u})}(\tau) - \Phi(t, \mathbf{u})| < \eta \quad \text{and} \\ \lim_{\tau \to \infty} \tilde{\mathbf{v}}^{(\mathbf{t},\mathbf{u})}(\tau) = \Phi(t, \mathbf{u}) \end{cases} \tag{8.8}$$

Assumption 8.5
(Lipschitz continuity and unique solution of the reduced system)

Consider the reduced system

$$\frac{d}{dt}\hat{\mathbf{u}} = \mathbf{f}(t, \hat{\mathbf{u}}, \Phi(t, \hat{\mathbf{u}}), 0), \quad \hat{\mathbf{u}}(0) = \mathbf{u}^0. \tag{8.9}$$

Assume that the function $(t, \mathbf{u}) \mapsto \mathbf{f}(t, \mathbf{u}, \Phi(t, \mathbf{u}), 0)$ *satisfies the Lipschitz condition* (8.2) *with respect to* $\mathbf{u}$*. Furthermore, assume that there exists a unique solution* $\hat{\mathbf{u}}$ *of the reduced system* (8.9) *such that* $\hat{\mathbf{u}}(t) \in Int\,\bar{\mathcal{U}},\ \forall t \in]0, T[$.

Assumption 8.6
(Attractivity of the root corresponding to initial data of slow variables)

Consider the system

$$\frac{d}{d\tau}\check{\mathbf{v}} = \mathbf{g}(0, \mathbf{u}^0, \check{\mathbf{v}}, 0), \ \ \check{\mathbf{v}}(0) = \mathbf{v}^0. \tag{8.10}$$

Assume $\lim_{\tau\to\infty} \check{\mathbf{v}}(\tau) = \Phi(0, \mathbf{u}^0)$*, i.e.,* $\mathbf{v}^0$ *belongs to the basin of attraction of* $\Phi(0, \mathbf{u}^0)$*. Furthermore,* $\check{\mathbf{v}}(\tau) \in \mathcal{V}$ *for all* $\tau \geq 0$*.*

Theorem 8.7 (Tikhonov's Theorem)
Let Assumptions 8.2-8.6 hold. Then, there exists $\varepsilon_0 > 0$ *such that for any* $\varepsilon \in]0, \varepsilon_0]$ *there exists a unique solution* $(\mathbf{u}_\varepsilon, \mathbf{v}_\varepsilon)$ *of system* (8.1) *on* $[0, T]$ *and*

$$\begin{aligned} &\lim_{\varepsilon\to 0} \mathbf{u}_\varepsilon(t) = \hat{\mathbf{u}}(t) && \forall t \in]0, T], \\ &\lim_{\varepsilon\to 0} \mathbf{v}_\varepsilon(t) = \Phi(t, \hat{\mathbf{u}}(t)) =: \hat{\mathbf{v}}(t) && \forall t \in]0, T], \end{aligned}$$

where $\hat{\mathbf{u}}$ *is the solution of the reduced system* (8.9)*.*

8.3 Tikhonov reduction of stem cell model

We now apply Tikhonov's Theorem to the model (2.3) of hematopoiesis from Chapter 2.

Definition 8.8 (Unreduced stem cell model)
The unreduced stem cell model has the following form.

$$\begin{aligned}
\frac{d}{dt}c_{1,\varepsilon} &= (2a_1 s_\varepsilon - 1)p_1 c_{1,\varepsilon}, \quad c_{1,\varepsilon}(0) = c_1^0 \\
\frac{d}{dt}c_{2,\varepsilon} &= 2(1 - a_1 s_\varepsilon)p_1 c_{1,\varepsilon} - d_2 c_{2,\varepsilon}, \quad c_{2,\varepsilon}(0) = c_2^0 \\
\varepsilon\frac{d}{dt}s_\varepsilon &= 1 - kc_{2,\varepsilon}s_\varepsilon - s_\varepsilon, \quad s_\varepsilon(0) = s^0
\end{aligned} \tag{8.11}$$

Remark 8.9 (Biological Motivation)
The third ODE is a modification of equation (2.2) *on page 26. To take into account that signal dynamics is arbitrarily fast, we multiply the left hand-side of equation* (2.2) *by* ε*. We, furthermore, set* $\alpha = \beta$ *to have a signal concentration equal to* 1 *in the steady state without cells. This is convenient, since then we can interpret* a_1 *as self-renewal fraction under maximal endogenous stimulation.*

Definition 8.10 (Reduced stem cell model)
The following system describes the reduced version of Model (8.11)*.*

$$\begin{aligned}
\frac{d}{dt}c_1 &= (2a_1 s - 1)p_1 c_1, \quad c_1(0) = c_1^0 \\
\frac{d}{dt}c_2 &= 2(1 - a_1 s)p_1 c_1 - d_2 c_2, \quad c_2(0) = c_2^0 \\
s &= \frac{1}{1 + kc_2}
\end{aligned} \tag{8.12}$$

In the following, we check the assumptions of Tikhonov's Theorem.

Lemma 8.11
Let $0 < \varepsilon < 1$ *and* $0 \leq s_\varepsilon(0) < 1/a_1$*. For non-negative initial conditions of* $c_{1,\varepsilon}$*,* $c_{2,\varepsilon}$*, the solutions of system* (8.11) *are unique, exist globally in time, stay non-negative and are uniformely bounded. The bounds are uniform in* ε*.*

PROOF
To simplify notation, we write a instead of a_1 and p instead of p_1. Local existence and uniqueness follow from Picard-Lindelöf's theorem, [21, 97], since the right hand-side is locally Lipschitz continuous. It holds

$$\varepsilon \frac{d}{dt} s_\varepsilon = 1 - k c_{2,\varepsilon} s_\varepsilon - s_\varepsilon \leq 1 - s_\varepsilon. \tag{8.13}$$

This implies that

$$s_\varepsilon \leq \max\{1, s_\varepsilon(0)\} =: S \tag{8.14}$$

Therefore, if $s_\varepsilon(0) < 1/a$, it follows that $as(t) < 1$ for all $t > 0$. Consequently, $2(1 - as)pc_1 \geq 0$ for non-negative c_1. This implies $\frac{d}{dt} c_{2,\varepsilon}|_{c_{2,\varepsilon}=0} \geq 0$. We, furthermore, see that $\frac{d}{dt} c_{1,\varepsilon}|_{c_{1,\varepsilon}=0} \geq 0$ and $\frac{d}{dt} s_\varepsilon|_{s_\varepsilon=0} \geq 0$. This implies non-negativity of solutions.

We now show uniform boundedness of solutions. Statement (8.14) and the assumption $s_\varepsilon(0) < 1/a$ imply that there exists $\delta > 0$ such that $s_\varepsilon(t) < \frac{1}{a} - \delta$ for all $t > 0$. We note that δ does not depend on ε. It holds:

$$\begin{aligned} \frac{d}{dt} \frac{c_{1,\varepsilon}}{c_{2,\varepsilon}} &= ((2as_\varepsilon - 1)p + d_2) \frac{c_{1,\varepsilon}}{c_{2,\varepsilon}} - 2(1 - as_\varepsilon) p \frac{c_{1,\varepsilon}^2}{c_{2,\varepsilon}^2} \\ &\leq (p + d_2) \frac{c_{1,\varepsilon}}{c_{2,\varepsilon}} - 2\delta p \frac{c_{1,\varepsilon}^2}{c_{2,\varepsilon}^2}. \end{aligned} \tag{8.15}$$

This implies that $\frac{d}{dt} \frac{c_{1,\varepsilon}}{c_{2,\varepsilon}} < 0$, if $\frac{c_{1,\varepsilon}}{c_{2,\varepsilon}} > \frac{p+d_2}{2p\delta}$, consequently, $\frac{c_{1,\varepsilon}}{c_{2,\varepsilon}} \leq \max\{\frac{c_{1,\varepsilon}(0)}{c_{2,\varepsilon}(0)}, \frac{p+d_2}{2p\delta}\} =: M$. We note that M does not depend on ε.

We obtain $c_{2,\varepsilon} \geq \frac{c_{1,\varepsilon}}{M}$. We assume that $\varepsilon < 1$. Then, it holds

$$\begin{aligned} \frac{d}{dt} \left(2ap\varepsilon s_\varepsilon + \frac{k}{M} c_{1,\varepsilon} \right) &= 2ap(1 - kc_{2,\varepsilon} s_\varepsilon - s_\varepsilon) + \frac{k}{M} (2as_\varepsilon - 1) pc_{1,\varepsilon} \\ &\leq 2ap(1 - k\frac{c_{1,\varepsilon}}{M} s_\varepsilon - s_\varepsilon) + \frac{k}{M} (2as_\varepsilon - 1) pc_{1,\varepsilon} \\ &= 2ap - 2aps_\varepsilon - \frac{k}{M} pc_{1,\varepsilon} \\ &\leq 2ap - 2aps_\varepsilon\varepsilon - \frac{k}{M} pc_{1,\varepsilon} \\ &\leq \begin{cases} 2ap - \left(2aps_\varepsilon\varepsilon + \frac{k}{M} c_{1,\varepsilon}\right) & p \geq 1 \\ 2ap - p\left(2aps_\varepsilon\varepsilon + \frac{k}{M} c_{1,\varepsilon}\right) & p < 1. \end{cases} \end{aligned}$$

In both cases we obtain ODEs of the type $\frac{d}{dt} x = \alpha - \beta x$ for constants $\alpha, \beta > 0$. This implies $x \leq \max\{\frac{\alpha}{\beta}, x(0)\}$. It holds $\alpha = 2ap$ and $\beta = \min\{p, 1\}$. Therefore, $\left(2ap\varepsilon s_\varepsilon + \frac{k}{M} c_{1,\varepsilon}\right) \leq \max\{\left(2aps_\varepsilon(0) + \frac{k}{M} c_{1,\varepsilon}(0)\right), \frac{2ap}{\min\{p,1\}}\} =: L$. We note that

L does not depend on ε. We used non-negativity of s_ε and $0 < \varepsilon \leq 1$. This implies boundedness of $c_{1,\varepsilon}$. Due to non-negativity of $c_{1,\varepsilon}$ and s_ε, we obtain $c_{1,\varepsilon} \leq L$.

$$\frac{d}{dt}c_{2,\varepsilon} \leq 2\delta pL - d_2 c_{2,\varepsilon}.$$

This implies $c_{2,\varepsilon} \leq \max\{c_{2,\varepsilon}(0), \frac{2\delta pL}{d_2}\}$. We now have uniform bounds for the solutions. Local existence and uniform bounds imply global existence, [106]. ■

Lemma 8.12
Let $\frac{1}{2} < a_1 < 1$, $p_1 > 0$, $d_2 > 0$. *For* $0 \leq s_\varepsilon(0) < 1/a_1$, *non-negative* $c_{1,\varepsilon}(0)$, $c_{2,\varepsilon}(0)$ *and* $\varepsilon \leq 1$, *system* (8.11) *fulfills Assumptions 8.2-8.6.*

PROOF

It holds for $\mathbf{u} = (c_{1,\varepsilon}, c_{2,\varepsilon})^T$ and $v = s_\varepsilon$:

$$\mathbf{f}(t, \mathbf{u}, v, \varepsilon) = \begin{pmatrix} (2av - 1)pu_1 \\ 2(1 - av)pu_1 - d_2 u_2 \end{pmatrix},$$
$$g(t, \mathbf{u}, v, \varepsilon) = 1 - ku_2 v - v.$$

We check Assumption 8.2. Due to Lemma 8.11, solutions of system (8.11) are globally bounded and bounds do not depend on ε. Therefore, solutions stay within compact sets. Thus, without changing solutions of the system, we can define $\mathbf{f}$ and $\mathbf{g}$ on $[0, T] \times \bar{\mathcal{U}} \times \mathcal{V} \times [0, 1]$ with a bounded set $\mathcal{V}$ and a compact set $\bar{\mathcal{U}}$, e.g., $\mathcal{V} :=]-\delta, v_{max} + \delta[$, where δ is a small positive constant and v_{max} the upper bound of v existing due to Lemma 8.11 and $\bar{\mathcal{U}} := [0, U_1] \times [0, U_2]$, where U_1, U_2 are greater than the upper bounds from Lemma 8.11.

If two functions fulfill the Lipschitz condition, then their sum and their difference also fulfill the Lipschitz condition. We note that the function $(x, y) \mapsto xy$ fulfills the Lipschitz condition, if x and y come from bounded domains. Since $\mathcal{U}$ and $\mathcal{V}$ are bounded sets, $\mathbf{f}$ and g fulfill the Lipschitz condition. Hence, Assumption 8.2 is fulfilled.

We check Assumption 8.3. It holds

$$g(t, \mathbf{u}, v, 0) = 1 - ku_2 v - v = 0 \Leftrightarrow v = \frac{1}{1 + ku_2} =: \Phi(t, \mathbf{u}).$$

Thus, Assumption 8.3 is fulfilled.

We check Assumption 8.4. System (8.7) has the form $\frac{d}{d\tau}\tilde{v}^{(l)} = 1 - kl\tilde{v}^{(l)} - \tilde{v}^{(l)}$, where l is a parameter from the range of u_2. Consequently, $\tilde{v}^{(l)}(\tau) = \frac{1}{1+kl} + (\tilde{v}^{(l)}(0) - \frac{1}{1+kl})e^{-(1+kl)\tau}$. We see that $\lim_{\tau\to\infty} \tilde{v}^{(l)}(\tau) = \frac{1}{1+kl}$. With $\Phi(t, l) = \frac{1}{1+kl}$

we have $|\tilde{v}^{(l)}(\tau) - \Phi(t,l)| = |(\tilde{v}^{(l)}(0) - \frac{1}{1+kl})e^{-(1+kl)\tau}| \leq |(\tilde{v}^{(l)}(0) - \frac{1}{1+kl})|$. This holds for all non-negative l. Therefore, for each given η, the choice $\delta = \eta$ fulfills Assumption 8.4: $|(\tilde{v}^{(l)}(0) - \frac{1}{1+kl})| < \eta \Rightarrow |\tilde{v}^{(l)}(\tau) - \Phi(t,l)| \leq \eta$.

We check Assumption 8.5. We consider the function

$$(t, \mathbf{u}) \mapsto \begin{pmatrix} (2a\frac{1}{1+ku_2} - 1)pu_1 \\ 2(1 - a\frac{1}{1+ku_2})pu_1 - d_2u_2 \end{pmatrix} = \mathbf{f}(t, \mathbf{u}, \Phi(t, \mathbf{u}), 0)$$

for $(t, \mathbf{u}) \in [0, T] \times \bar{\mathcal{U}}$. We note that

$$\left| \frac{1}{1+ku_2} - \frac{1}{1+k\tilde{u}_2} \right| = \left| k \frac{\tilde{u}_2 - u_2}{(1+k\tilde{u}_2)(1+ku_2)} \right| \leq k|\tilde{u}_2 - u_2|.$$

Since $\frac{1}{1+ku_2}$, u_2 and u_1 are bounded, $\mathbf{f}(t, \mathbf{u}, \Phi(t, \mathbf{u}), 0)$ fulfills the Lipschitz condition. Uniqueness of solutions of system and $\mathbf{u}(t) \in Int\, \bar{\mathcal{U}}$ follow from Lemma A.8 for $\mathcal{U}$ and $\mathcal{V}$ chosen appropriately. We note that all quantities decrease at most exponentially, therefore, they stay positive on finite intervals, if their initial conditions are positive.
We check Assumption 8.6. We consider the equation

$$\frac{d}{d\tau}\check{v} = 1 - ku_2(0)\check{v} - \check{v}, \quad \check{v}(0) = \mathbf{v}^0. \tag{8.16}$$

The solution is $\check{v}(\tau) = \frac{1}{1+ku_2(0)} + \left(v^0 - \frac{1}{1+ku_2(0)}\right) e^{-(ku_2(0)+1)\tau}$, which converges to $\frac{1}{1+ku_2(0)}$ and stays in $\mathcal{V}$ for appropriate choice of $\mathcal{V}$.

■

We, therefore, obtain the following Theorem.

Theorem 8.13 (Reduction for finite times)
Let $\frac{1}{2} < a_1 < 1$, $p_1 > 0$, $d_2 > 0$, $T < \infty$. For non-negative initial conditions, $s_\varepsilon(0) < \frac{1}{a_1}$ and $\varepsilon > 0$ small enough, solutions $(c_{1,\varepsilon}, c_{2,\varepsilon}, s_\varepsilon)$ of system (8.11) exist and fulfill

$$\begin{aligned} \lim_{\varepsilon \to 0} c_{1,\varepsilon}(t) &= c_1(t), \quad \textit{for } t \in]0, T] \\ \lim_{\varepsilon \to 0} c_{2,\varepsilon}(t) &= c_2(t), \quad \textit{for } t \in]0, T] \\ \lim_{\varepsilon \to 0} s_\varepsilon(t) &= \frac{1}{1 + kc_2(t)}, \quad \textit{for } t \in]0, T], \end{aligned}$$

where (c_1, c_2) are the solution of the reduced system (8.12) for the same initial conditions.

8.4 Summary

In this Chapter, we show that a minimal version of the stem cell model (2.3) introduced in Chapter 2 fulfills assumptions of the Tikhonov Theorem. We obtain that the solutions of the reduced system (8.10) (quasi steady state approximation) are close to the solutions of the singular perturbation problem (8.11) on finite intervals and for small ε (Theorem 8.13).

CHAPTER 9

REDUCTION ON UNBOUNDED TIME INTERVALS

9.1 Outline of the chapter

This Chapter is devoted to reductions of mathematical models describing processes taking place at different time scales (fast time, τ, slow time, $t = \tau\varepsilon$, $\varepsilon > 0$ small, [69, 113]). We consider the following Cauchy problem

$$\frac{d\mathbf{u}_\varepsilon}{dt} = \mathbf{f}(\mathbf{u}_\varepsilon, v_\varepsilon),\ t > 0, \quad \mathbf{u}_\varepsilon(0) = \mathbf{u}^0; \tag{9.1}$$

$$\varepsilon\frac{dv_\varepsilon}{dt} = -\alpha v_\varepsilon + \Phi(\mathbf{u}_\varepsilon, v_\varepsilon),\ t > 0, \quad v_\varepsilon(0) = v^0. \tag{9.2}$$

This system is a special autonomous case of system (8.1), where the non-linearity in the second equation has a specific form, namely $g(t, \mathbf{u}_\varepsilon, v_\varepsilon, \varepsilon) = -\alpha v_\varepsilon + \Phi(\mathbf{u}_\varepsilon, v_\varepsilon)$.

In Section 9.4, we show that the difference of the solutions of system (9.1) - (9.2) and of the solutions of the reduced system (quasi-steady state approximation) is of order $\mathcal{O}(\varepsilon)$ on the infinite time interval. Assumptions and technical preliminaries are introduced in Sections 9.2 and 9.3.

The main assumptions are regularity of the right hand-side (Assumption 9.1), existence of an isolated stable root of equation (9.2) (Assumption 9.3), location of initial data in the basin of attraction of this root, boundedness of solutions of the quasi steady state approximation (Assumption 9.2), and that the linearization of

equation (9.1) along solutions of the reduced system has only exponentially decaying solutions (Assumption 9.4).

In Section 9.5, we apply the obtained results to the stem cell model (2.3) introduced in Chapter 2.

The results of this Chapter are submitted for publication as *" Marciniak-Czochra, A., Mikelic, A., and Stiehl, T. A rigorous renormalization group second order approximation for singularly perturbed nonlinear ODEs".*

9.2 Definitions and assumptions

Assumption 9.1 (Regularity and existence of isolated real root)

(i) Let $\mathbf{f} \in C^3(\mathbb{R}^n \times \mathbb{R}, \mathbb{R}^n)$, $(\mathbf{u}, v) \mapsto \mathbf{f}(\mathbf{u}, v)$, $\Phi \in C^3(\mathbb{R}^n \times \mathbb{R}, \mathbb{R})$, $(\mathbf{u}, v) \mapsto \Phi(\mathbf{u}, v)$.

(ii) Let $\alpha \in \mathbb{R}^+$ *and let the algebraic equation* $0 = -\alpha v + \Phi(\mathbf{u}, v)$ *have at least one isolated real root* $v = v(\mathbf{u}) = \varphi(\mathbf{u})$*, i.e.,* $0 = -\alpha\varphi(\mathbf{u}) + \Phi(\mathbf{u}, \varphi(\mathbf{u}))$ *for all* $\mathbf{u} \in \mathbb{R}^n$*. Moreover, it exists* $\delta > 0$ *such that* $0 \neq -\alpha v + \Phi(\mathbf{u}, v)$ *for all* $\mathbf{u}, v$ *with* $0 < |v - \varphi(\mathbf{u})| < \delta$*.*

Assumption 9.2 (Solvability of reduced problem)
We suppose that the reduced problem

$$-\alpha v + \Phi(\mathbf{A}, v) = 0, \quad \frac{d}{dt}\mathbf{A} = \mathbf{f}(\mathbf{A}, v),\ t > 0, \quad \textit{and} \quad \mathbf{A}(0) = \mathbf{u}^0, \tag{9.3}$$

has a smooth bounded solution $\{\mathbf{A}, v\}$ *on* $\mathbb{R}^+$*, where* $v = \varphi(\mathbf{A})$ *is the isolated real root from Assumption 9.1 (ii).*

Assumption 9.3 (Stability and attractivity of the isolated root)

(i) We suppose that the considered real isolated root $\varphi(\mathbf{A})$ *and the solution* $\mathbf{A}$ *from Assumption 9.2 satisfy* $\xi(\mathbf{A}) := \alpha - \partial_y\Phi(\mathbf{x}, y)|_{(\mathbf{x}=\mathbf{A}, y=\varphi(\mathbf{A}))} \geq M_0 > 0$ *for all* $t \geq 0$*. This means that the root* φ *is a locally stable root.*

(ii) Let the initial datum v^0 *be in the basin of attraction of the root* $v = \varphi(\mathbf{A})$ *from problem* (9.3)*, i.e., for all for all* $\delta > 0$*, there exists* $t(\delta) > 0$ *such that the solution* w *of the initial value problem* $\frac{d}{dt}w = -\alpha w + \Phi(\mathbf{A}(t), w)$*,* $w(0) = v^0$ *satisfies* $|w(t) - \varphi(\mathbf{A}(t))| \leq \delta$ *for* $t > t(\delta)$*.*

(iii) Let $\alpha - \partial_y\Phi(\mathbf{x}, y)|_{(\mathbf{x}=\mathbf{u}^0, y\in\mathcal{I})} \geq \frac{M_0}{2} > 0$ *for* $\mathcal{I} = [\min\{\varphi(\mathbf{u}^0), v^0\}, \max\{\varphi(\mathbf{u}^0), v^0\}]$.

Assumption 9.4 (Fundamental solution for linearized system)
Let fundamental solutions S*,* $S(0) = \mathrm{id}$ *of the problem*

$$\frac{d}{dt}\mathbf{w} = \Big(D_x\mathbf{f}(\mathbf{x}, y) + \partial_y\mathbf{f}(\mathbf{x}, y) \otimes \nabla\varphi(\mathbf{x})\Big)\Big|_{(\mathbf{x}=\mathbf{A}, y=\varphi(\mathbf{A}))}\mathbf{w} \tag{9.4}$$

fulfill $||S(t)S^{-1}(\tau)|| \leq Ce^{-k(t-\tau)}$ *for constants* $C > 0$, $k > 0$ *and* $t \geq \tau$. *Here* $||\cdot||$ *is e.g., the matrix norm induced by the Euclidean norm.* $D_x\mathbf{f}(\mathbf{x}, y)$ *denotes the Jacobian of* $\mathbf{f}(\mathbf{x}, y)$ *with respect to its first* n*-dimensional variable.*

Remark 9.5 (Exponential dichotomy)
Assumption 9.4 is a special case of the exponential dichotomy assumption, stating that there exists a projection P *such that* $||S(t)PS^{-1}(\tau)|| \leq Ke^{-\kappa(t-s)}$ *for* $s \leq t < \infty$ *and* $||S(t)(I-P)S^{-1}(\tau)|| \leq Le^{\mu(t-s)}$ *for* $s \geq t > -\infty$ *for appropriate positive constants* K, L, κ, μ, *[140].*

Definition 9.6
(i) (Exact solution) The solution of the system

$$\frac{d\mathbf{u}_\varepsilon}{dt} = \mathbf{f}(\mathbf{u}_\varepsilon, v_\varepsilon),\ t > 0, \quad \mathbf{u}_\varepsilon(0) = \mathbf{u}^0; \tag{9.5}$$

$$\varepsilon\frac{dv_\varepsilon}{dt} = -\alpha v_\varepsilon + \Phi(\mathbf{u}_\varepsilon, v_\varepsilon),\ t > 0, \quad v_\varepsilon(0) = v^0. \tag{9.6}$$

is referred to as "exact solution".

(ii) (Quasi-steady state approximation, Reduced system) The solution of the system

$$\frac{d\mathbf{A}}{dt} = \mathbf{f}(\mathbf{A}, v),\ t > 0, \quad \mathbf{A}(0) = \mathbf{u}^0; \tag{9.7}$$

$$0 = -\alpha v + \Phi(\mathbf{A}, v) \tag{9.8}$$

is referred to as "quasi-steady state approximation" or as "solution of the reduced system". The isolated real root of (9.8) *is denoted as* $\varphi(\mathbf{A})$.

9.3 Preliminaries

Existence of exponentially decaying fundamental solutions is robust in the following sense:

Lemma 9.7
Let $M : \mathbb{R}^+ \to \mathbb{R}^{n,n}$, $t \mapsto M(t)$ *be continuous. Let the fundamental solution* Y *of the problem*

$$\begin{aligned} \frac{d}{dt}\mathbf{x} &= M(t)\mathbf{x} \\ \mathbf{x}(\nu) &= \mathbf{x}_\nu \end{aligned} \tag{9.9}$$

fulfill $||Y(t)Y^{-1}(s)|| \leq Ke^{-\alpha(t-s)}$ *for all* $t \geq s$ *and positive constants* α *and* K. *Let* $B : \mathbb{R}^+ \to \mathbb{R}^{n,n}$, $t \mapsto B(t)$ *be continuous. Let exist a real finite* $t_1 > 0$ *and a positive real constant* C *such that* $||B(t)|| \leq C$ *for* $0 \leq t < t_1$ *and* $||B(t)|| \leq c < \frac{\alpha}{K}$ *for all* $t \geq t_1$. *Then, there exist real constants* $\hat{K} > 0$ *and* $\hat{\alpha} > 0$ *such that a fundamental solution* $\tilde{Y}$ *of the initial value problem*

$$\begin{aligned} \frac{d}{dt}\mathbf{x} &= (M(t) + B(t))\mathbf{x} \\ \mathbf{x}(0) &= \mathbf{x}_0 \end{aligned} \tag{9.10}$$

fulfills $||\tilde{Y}(t)\tilde{Y}^{-1}(s)|| \leq \hat{K}e^{-\hat{\alpha}(t-s)}$ *for all* $s \leq t$.

The constants $\hat{K}$ *and* $\hat{\alpha}$ *depend only on* $K,\ C,\ c,\ \alpha,\ t_1$.

The proof is given in Appendix H on pp. 275.

Corollary 9.8 (Existence of tubular domain)
Let Assumptions 9.1 to 9.4 hold. Let $\mathbf{A}$, φ, v^0 *be defined as in Definition 9.6. Then, there exist real positive constants* b, t_0, λ_0, *and two smooth curves* $\lambda^a, \lambda^b : \mathbb{R}_0^+ \to \mathbb{R}$, $t \mapsto \lambda^a(t)$, $t \mapsto \lambda^b(t)$, *fulfilling*

(i) $\lambda^a(t) > \lambda^b(t)$, *for all* $t \geq 0$,

(ii) $v^0 \in (\lambda^b(0), \lambda^a(0))$, $\varphi(\mathbf{A}(t)) \in (\lambda^b(t), \lambda^a(t))$, *for all* $t \geq 0$,

(iii) $\lambda^a(t) = \varphi(\mathbf{A}(t)) + \lambda_0$, $\lambda^b(t) = \varphi(\mathbf{A}(t)) - \lambda_0$, *for* $t \geq t_0$.

Define a tubular domain by

$$\mathcal{T}_{b,\lambda} := \mathit{Int}\ \cup_{t\in\mathbb{R}^+} \{(\mathbf{x}, y, t)\}_{\{|x_j - A_j(t)|<b,\ j=1,\ldots,n,\ y\in(\lambda^b(t),\lambda^a(t))\}}. \tag{9.11}$$

Then, for all continuous functions $(\mu, \nu) : \mathbb{R}_0^+ \to \mathbb{R}^n \times \mathbb{R}$, $t \mapsto (\mu(t), \nu(t))$ *in the interior of* $\mathcal{T}_{b,\lambda}$, *fundamental systems* S *of the initial value problem*

$$\frac{d}{dt}\mathbf{w} = \left(D_x\mathbf{f}(\mathbf{x}, y) + \partial_y\mathbf{f}(\mathbf{x}, y) \otimes \nabla\varphi(\mathbf{x}) \right)\Big|_{(\mathbf{x}=\mu, y=\nu)} \mathbf{w},\ \ \mathbf{w}(0) = \mathbf{w}^0 \tag{9.12}$$

fulfill $||S(t)S^{-1}(\tau)|| \leq \hat{C}e^{-\hat{k}(t-\tau)}$ *for* $t \geq \tau \geq 0$. *The constants* $\hat{C}$ *and* $\hat{k}$ *are positive and depend only on* $\mathcal{T}_{b,\lambda}$. *Furthermore, it holds* $\alpha - \partial_y\Phi(\mathbf{x}, y)|_{(\mathbf{x}=\mu,y=\nu)} \geq \frac{M_0}{4} > 0$ *for all* $(x, y) \in \mathcal{T}_{b,\lambda}$.

A scheme of $\mathcal{T}_{b,\lambda}$ *is depicted in Figure 9.1*

Remark 9.9
We say a function $(\mu, \nu) : \mathbb{R}^+ \to \mathbb{R}^n \times \mathbb{R}$ *lies in the interior of* $\mathcal{T}_{b,\lambda}$, *if* $(\mu(t), \nu(t), t) \in \mathcal{T}_{b,\lambda}$ *for all* $t \in \mathbb{R}^+$.

Remark 9.10
We can choose b *such that* $|\mathbf{u} - \mathbf{A}(t)| \leq b$ *implies* $\varphi(\mathbf{u}) \in (\lambda^b(t), \lambda^a(t))$

A proof of Corollary 9.8 and Remark 9.10 is given in Appendix H pp. 278.

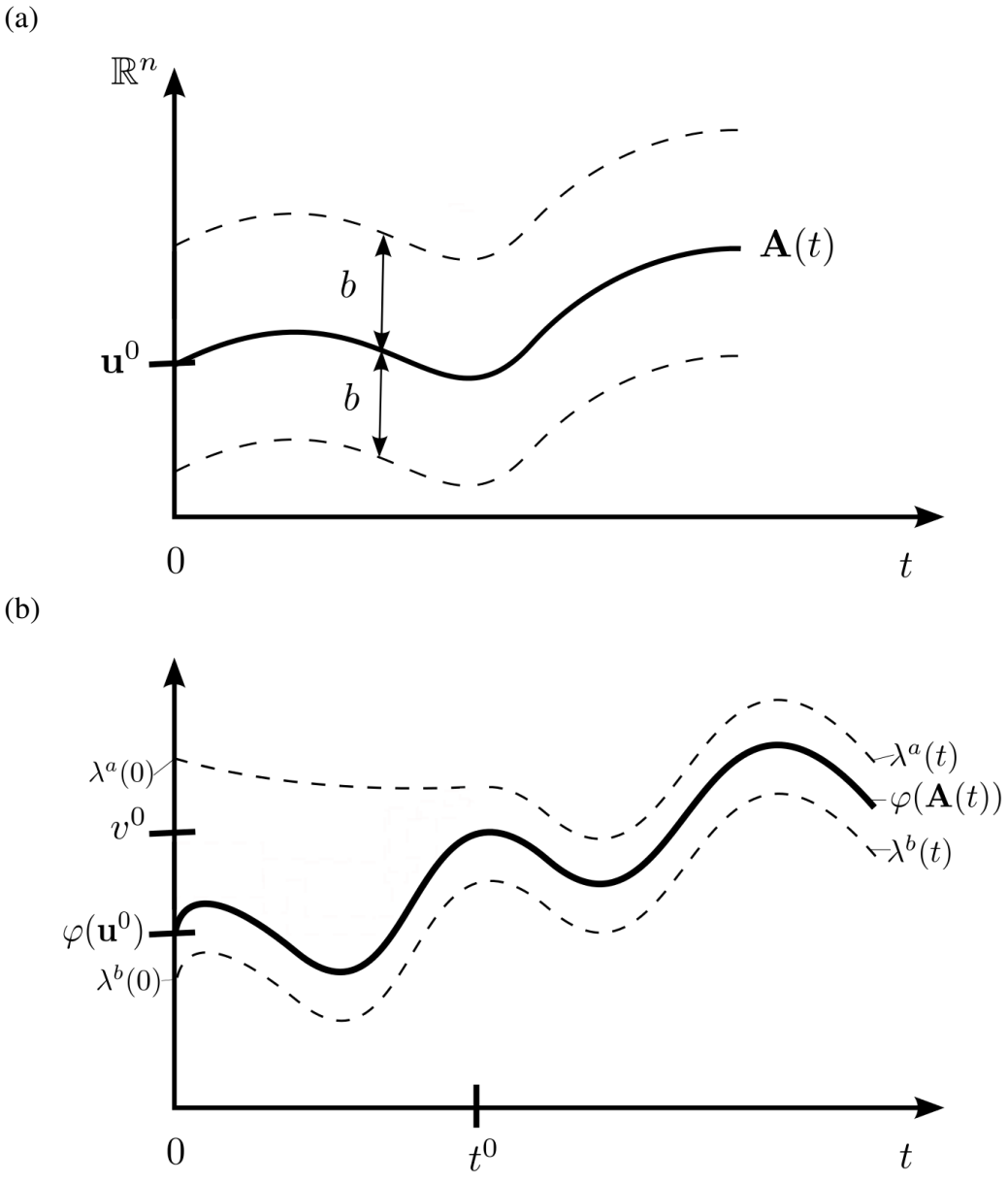

Figure 9.1: Scheme of $\mathcal{T}_{b,\lambda}$. For details see Corollary 9.8.

9.4 Proofs of approximation properties

For technical convenience, we introduce the functions $\tilde{\mathbf{f}}$, $\tilde{\Phi}$, which we consider instead of $\mathbf{f}$, Φ. In a neighborhood of $(\mathbf{A}, \varphi(\mathbf{A}))$, $\tilde{\mathbf{f}}$ coincides with $\mathbf{f}$ and $\tilde{\Phi}$ coincides with Φ. In the following, the functions $\tilde{\mathbf{f}}$, $\tilde{\Phi}$ are referred to as "extensions of $\mathbf{f}$, Φ".

Definition 9.11 (Extensions $\tilde{\mathbf{f}}$ and $\tilde{\Phi}$)
Denote by $\lambda^a, \lambda^b : \mathbb{R}_0^+ \to \mathbb{R}$ the smooth functions with the properties stated in Corollary 9.8 and by b the constant b from Corollary 9.8. Let $\mathbf{A}$, φ be defined as in Definition 9.6.

(i) We set for $j = 1, \cdots, n$

$$\tilde{x}_j(x_j, t) = \begin{cases} x_j, & \text{if} \quad |A_j(t) - x_j| < b; \\ A_j(t) + b, & \text{if} \quad x_j - A_j(t) \geq b; \\ A_j(t) - b, & \text{if} \quad x_j - A_j(t) \leq -b. \end{cases} \tag{9.13}$$

and

$$\tilde{y}(y, t) = \begin{cases} y, & \text{if} \quad y \in (\lambda^b(t), \lambda^a(t)); \\ \lambda^a(t), & \text{if} \quad y \geq \lambda^a(t); \\ \lambda^b(t), & \text{if} \quad y \leq \lambda^b(t). \end{cases} \tag{9.14}$$

(ii) We define

$$\tilde{\mathbf{f}}(\mathbf{x}, y, t) \equiv \tilde{\mathbf{f}}(x_1, \cdots, x_m, y, t) := \mathbf{f}(\tilde{x}_1(x_1, t), \cdots, \tilde{x}_n(x_n, t), \tilde{y}(y, t))$$
$$\tilde{\Phi}(\mathbf{x}, y, t) \equiv \tilde{\Phi}(x_1, \cdots, x_m, y, t) := \Phi(\tilde{x}_1(x_1, t), \cdots, \tilde{x}_n(x_n, t), \tilde{y}(y, t))$$

Remark 9.12

(i) The functions $\tilde{\Phi}$ and $\tilde{\mathbf{f}}$ are globally Lipschitz continuous.

(ii) Let $(\mathbf{x}, y, t) \in \mathbb{R}^n \times \mathbb{R} \times \mathbb{R}^+$. For all $(\mathbf{x}, y, t) \in \mathcal{T}_{b,\lambda}$ the functions $\mathbf{f}$, Φ coincide with $\tilde{\mathbf{f}}$, $\tilde{\Phi}$.

(iii) The functions $\tilde{\Phi}$ and $\tilde{\mathbf{f}}$ are differentiable but the derivatives can be discontinuous in boundary points of $\mathcal{T}_{b,\lambda}$.

Lemma 9.13
If we choose b according to Remark 9.10, there exists a function $\tilde{\varphi} : \mathbb{R}^n \times \mathbb{R}_0^+ \to \mathbb{R}$, $(\mathbf{x}, t) \mapsto \tilde{\varphi}(\mathbf{x}, t)$ fulfilling $0 = -\alpha\tilde{\varphi}(\mathbf{x}, t) + \tilde{\Phi}(\mathbf{x}, \tilde{\varphi}(\mathbf{x}, t), t)$ for all $(\mathbf{x}, t) \in \mathbb{R}^n \times \mathbb{R}_0^+$. The function $\tilde{\varphi}$ is differentiable but the derivative is discontinuous at the boundary of $\mathcal{T}_{b,\lambda}$. In the interior of $\mathcal{T}_{b,\lambda}$ the functions φ and $\tilde{\varphi}$ coincide.

The proof is given in Appendix H on page 281.

Definition 9.14 (Simplified problem)

(i) Using the extensions $\tilde{\mathbf{f}}$ *and* $\tilde{\Phi}$ *from above, we define the following initial value problem as "simplified problem":*

$$\frac{d\tilde{\mathbf{u}}_\varepsilon}{dt} = \tilde{\mathbf{f}}(\tilde{\mathbf{u}}_\varepsilon, \tilde{v}_\varepsilon, t),\ t > 0, \quad \tilde{\mathbf{u}}_\varepsilon(0) = \mathbf{u}^0; \tag{9.15}$$

$$\varepsilon\frac{d\tilde{v}_\varepsilon}{dt} = -\alpha\tilde{v}_\varepsilon + \tilde{\Phi}(\tilde{\mathbf{u}}_\varepsilon, \tilde{v}_\varepsilon, t),\ t > 0, \quad \tilde{v}_\varepsilon(0) = v^0. \tag{9.16}$$

(ii) (Solution for the reduced simplified problem) The solution of the system

$$\frac{d\tilde{\mathbf{A}}}{dt} = \tilde{\mathbf{f}}(\tilde{\mathbf{A}}, \tilde{v}, t),\ t > 0, \quad \tilde{\mathbf{A}}(0) = \mathbf{u}^0; \tag{9.17}$$

$$0 = -\alpha\tilde{v} + \Phi(\tilde{\mathbf{A}}, \tilde{v}) \tag{9.18}$$

is referred to as "solution of the reduced simplified problem". The isolated real root of (9.18) *is denoted as* $\tilde{\varphi}(\tilde{\mathbf{A}}, t)$.

Remark 9.15

The functions $\tilde{\mathbf{f}}$ *and* $\tilde{\Phi}$ *are globally Lipschitz continuous. Due to Picard-Lindelöf-Theorem (global version), [219], the simplified problem* (9.15)-(9.16) *has a unique* C^1 *solution on* $[0,\ T]$ *for all* $0 < T < \infty$.

Definition 9.16 (Initial layers)

(i) The initial layer ζ_0 *for problem* (9.7)-(9.8) *is defined by*

$$\begin{aligned}\frac{d\zeta_0}{dt} &= -\alpha\zeta_0 + \Phi(\mathbf{u}^0, \varphi(\mathbf{u}^0) + \zeta_0) - \Phi(\mathbf{u}^0, \varphi(\mathbf{u}^0)),\\ \zeta_0(0) &= v^0 - \varphi(\mathbf{u}^0).\end{aligned} \tag{9.19}$$

(ii) The initial layer $\tilde{\zeta}_0$ *for the simplified problem* (9.17)-(9.18) *is defined by*

$$\begin{aligned}\frac{d\tilde{\zeta}_0}{dt} &= -\alpha\tilde{\zeta}_0 + \tilde{\Phi}(\mathbf{u}^0, \tilde{\varphi}(\mathbf{u}^0, t) + \tilde{\zeta}_0, t) - \tilde{\Phi}(\mathbf{u}^0, \tilde{\varphi}(\mathbf{u}^0, t), t),\\ \tilde{\zeta}_0(0) &= v^0 - \tilde{\varphi}(\mathbf{u}^0, t).\end{aligned} \tag{9.20}$$

Lemma 9.17 (Asymptotic behavior of initial layers)

The initial layers exist and fulfill the estimates $|\zeta_0(t)| \leq Ce^{-M_0 t/4}$, $|\tilde{\zeta}_0(t)| \leq Ce^{-M_0 t/4}$. M_0 *is the constant introduced in Assumption 9.3.*

The proof is given in Appendix H on page 283.

Proposition 9.18
Let Assumptions 9.1-9.4 be fulfilled. Then, for

$$\tilde{\mathcal{V}}_\varepsilon(t) := \tilde{v}_\varepsilon(t) - \tilde{\varphi}(\tilde{\mathbf{u}}_\varepsilon, t) - \tilde{\zeta}_0(\frac{t}{\varepsilon}), \tag{9.21}$$

it holds

$$|\tilde{\mathcal{V}}_\varepsilon(t)| \leq C \min\{e^{-kt/\varepsilon} + \varepsilon, \varepsilon \log \frac{1}{\varepsilon} + \varepsilon\}, \tag{9.22}$$

for an appropriate $k > 0$ and all $t \geq 0$.

PROOF
The function $\partial_v \tilde{\Phi}$ is identical to $\partial_v \Phi$ inside $\mathcal{T}_{b,\lambda}$ and equal to 0 outside. Therefore, $\alpha - \partial_y \Phi(\mathbf{x}, y)|_{\mathbf{x}=\mathbf{A}, y=\varphi(\mathbf{A})} \geq \min\{\frac{M_0}{4}, \alpha\}$ everywhere. We can always choose M_0 in Assumption 9.3 such that $M_0 \leq \alpha$.

By definition, it holds $\tilde{\mathcal{V}}_\varepsilon(0) = 0$. We note that, due to Lemma 9.13, $\alpha\tilde{\varphi}(\mathbf{x}, t) = \tilde{\Phi}(\mathbf{x}, \tilde{\varphi}(\mathbf{x}, t), t)$ for all $\mathbf{x} \in \mathbb{R}^n$. We obtain

$$\begin{aligned}
\varepsilon\frac{d}{dt}\tilde{\mathcal{V}}_\varepsilon &= -\alpha\tilde{v}_\varepsilon + \tilde{\Phi}(\tilde{\mathbf{u}}_\varepsilon, \tilde{v}_\varepsilon, t) - \varepsilon\frac{d}{dt}\tilde{\varphi}(\tilde{\mathbf{u}}_\varepsilon, t) + \alpha\tilde{\zeta}_0(t/\varepsilon) + \tilde{\Phi}(\mathbf{u^0}, \tilde{\varphi}(\mathbf{u^0}, t), t) \\
&\quad -\tilde{\Phi}\big(\mathbf{u^0}, \tilde{\varphi}(\mathbf{u^0}, t) + \tilde{\zeta}_0(t/\varepsilon), t\big) \\
&= -\alpha\tilde{v}_\varepsilon + \alpha\tilde{\zeta}_0(t/\varepsilon) + \alpha\tilde{\varphi}(\tilde{\mathbf{u}}_\varepsilon, t) - \alpha\tilde{\varphi}(\tilde{\mathbf{u}}_\varepsilon, t) + \tilde{\Phi}(\tilde{\mathbf{u}}_\varepsilon, \tilde{v}_\varepsilon, t) - \varepsilon\frac{d}{dt}\tilde{\varphi}(\tilde{\mathbf{u}}_\varepsilon, t) \\
&\quad +\tilde{\Phi}(\mathbf{u^0}, \tilde{\varphi}(\mathbf{u^0}, t), t) - \tilde{\Phi}\big(\mathbf{u^0}, \tilde{\varphi}(\mathbf{u^0}, t) + \tilde{\zeta}_0(t/\varepsilon), t\big) \\
&= -\alpha\tilde{\mathcal{V}}_\varepsilon - \alpha\tilde{\varphi}(\tilde{\mathbf{u}}_\varepsilon, t) + \tilde{\Phi}(\tilde{\mathbf{u}}_\varepsilon, \tilde{v}_\varepsilon, t) - \varepsilon\frac{d}{dt}\tilde{\varphi}(\tilde{\mathbf{u}}_\varepsilon, t) + \tilde{\Phi}(\mathbf{u^0}, \tilde{\varphi}(\mathbf{u^0}, t), t) \\
&\quad -\tilde{\Phi}\big(\mathbf{u^0}, \tilde{\varphi}(\mathbf{u^0}, t) + \tilde{\zeta}_0(t/\varepsilon), t\big) \\
&= -\alpha\tilde{\mathcal{V}}_\varepsilon - \alpha\tilde{\varphi}(\tilde{\mathbf{u}}_\varepsilon, t) + \tilde{\Phi}(\tilde{\mathbf{u}}_\varepsilon, \tilde{v}_\varepsilon, t) - \varepsilon\frac{d}{dt}\tilde{\varphi}(\tilde{\mathbf{u}}_\varepsilon, t) + \alpha\tilde{\varphi}(\mathbf{u^0}, t) + \tilde{\Phi}\big(\tilde{\mathbf{u}}_\varepsilon, \tilde{\varphi}(\tilde{\mathbf{u}}_\varepsilon, t) \\
&\quad +\tilde{\zeta}_0(t/\varepsilon), t\big) - \tilde{\Phi}\big(\tilde{\mathbf{u}}_\varepsilon, \tilde{\varphi}(\tilde{\mathbf{u}}_\varepsilon, t) + \tilde{\zeta}_0(t/\varepsilon), t\big) - \tilde{\Phi}(\mathbf{u^0}, \tilde{\varphi}(\mathbf{u^0}, t) + \tilde{\zeta}_0(t/\varepsilon), t) \\
&= -\alpha\tilde{\mathcal{V}}_\varepsilon + \tilde{\Phi}(\tilde{\mathbf{u}}_\varepsilon, \tilde{v}_\varepsilon, t) - \tilde{\Phi}(\tilde{\mathbf{u}}_\varepsilon, \tilde{\varphi}(\tilde{\mathbf{u}}_\varepsilon, t) + \tilde{\zeta}_0(t/\varepsilon), t) \\
&\quad -\varepsilon\frac{d}{dt}\tilde{\varphi}(\tilde{\mathbf{u}}_\varepsilon, t) + \alpha\big(\tilde{\varphi}(\mathbf{u^0}, t) + \tilde{\zeta}_0(t/\varepsilon)\big) \\
&\quad +\tilde{\Phi}(\tilde{\mathbf{u}}_\varepsilon, \tilde{\varphi}(\tilde{\mathbf{u}}_\varepsilon, t) + \tilde{\zeta}_0(t/\varepsilon), t) - \alpha\big(\tilde{\varphi}(\tilde{\mathbf{u}}_\varepsilon, t) + \tilde{\zeta}_0(t/\varepsilon)\big) - \tilde{\Phi}\big(\mathbf{u^0}, \tilde{\varphi}(\mathbf{u^0}, t) + \tilde{\zeta}_0(t/\varepsilon), t\big) \\
&= -(\alpha - \frac{\partial\tilde{\Phi}^\star}{\partial v})\tilde{\mathcal{V}}_\varepsilon - \varepsilon\frac{d}{dt}\tilde{\varphi}(\tilde{\mathbf{u}}_\varepsilon, t) + \tilde{I}(t)
\end{aligned} \tag{9.23}$$

with

$$\begin{aligned}
\tilde{I}(t) := \tilde{\Phi}(\tilde{\mathbf{u}}_\varepsilon, \tilde{\varphi}(\tilde{\mathbf{u}}_\varepsilon, t) + \tilde{\zeta}_0(t/\varepsilon), t) - \alpha(\tilde{\varphi}(\tilde{\mathbf{u}}_\varepsilon, t) + \tilde{\zeta}_0(t/\varepsilon)) \\
-\tilde{\Phi}\big(\mathbf{u^0}, \varphi(\mathbf{u^0}, t) + \tilde{\zeta}_0(t/\varepsilon), t\big) + \alpha(\tilde{\varphi}(\mathbf{u^0}, t) + \tilde{\zeta}_0(t/\varepsilon))
\end{aligned} \tag{9.24}$$

and $\dfrac{\partial\tilde{\Phi}^\star}{\partial v} := \dfrac{\partial\tilde{\Phi}(\tilde{\mathbf{u}}_\varepsilon, v^\star)}{\partial v}$. Here, $v^\star$ is an intermediate value between $\tilde{v}_\varepsilon$ and $\tilde{\varphi}(\tilde{\mathbf{u}}_\varepsilon, t) + \tilde{\zeta}_0(t/\varepsilon)$.

Note that extended non-linearities $\tilde{\Phi}$ and $\tilde{\mathbf{f}}$ are only Lipschitz continuous and their partial derivatives are bounded but discontinuous. Therefore, we estimate $\tilde{I}(t)$ without using higher order derivatives. It holds

$$\begin{aligned}\tilde{I}(t) =&\tilde{\Phi}(\tilde{\mathbf{u}}_\varepsilon, \tilde{\varphi}(\tilde{\mathbf{u}}_\varepsilon, t) + \tilde{\zeta}_0(t/\varepsilon), t) - \tilde{\alpha}(\tilde{\varphi}(\tilde{\mathbf{u}}_\varepsilon, t) + \tilde{\zeta}_0(t/\varepsilon))\\ &- \tilde{\Phi}\big(\mathbf{u^0}, \tilde{\varphi}(\mathbf{u^0}, t) + \tilde{\zeta}_0(t/\varepsilon), t\big) + \alpha(\tilde{\varphi}(\mathbf{u^0}, t) + \tilde{\zeta}_0(t/\varepsilon))\\ =&\tilde{\Phi}(\tilde{\mathbf{u}}_\varepsilon, \tilde{\varphi}(\tilde{\mathbf{u}}_\varepsilon, t) + \tilde{\zeta}_0(t/\varepsilon), t) - \tilde{\Phi}(\tilde{\mathbf{u}}_\varepsilon, \tilde{\varphi}(\tilde{\mathbf{u}}_\varepsilon, t), t)\\ &- \tilde{\Phi}\big(\mathbf{u^0}, \tilde{\varphi}(\mathbf{u^0}, t) + \tilde{\zeta}_0(t/\varepsilon), t\big) + \tilde{\Phi}\big(\mathbf{u^0}, \tilde{\varphi}(\mathbf{u^0}, t), t\big). \end{aligned} \tag{9.25}$$

Consequently,

$$\begin{aligned}|\tilde{I}(t)| \leq&|\tilde{\Phi}(\tilde{\mathbf{u}}_\varepsilon, \tilde{\varphi}(\tilde{\mathbf{u}}_\varepsilon, t) + \tilde{\zeta}_0(t/\varepsilon), t) - \tilde{\Phi}(\tilde{\mathbf{u}}_\varepsilon, \tilde{\varphi}(\tilde{\mathbf{u}}_\varepsilon, t), t)|\\ &+ |\tilde{\Phi}\big(\mathbf{u^0}, \tilde{\varphi}(\mathbf{u^0}, t) + \tilde{\zeta}_0(t/\varepsilon), t\big) - \tilde{\Phi}\big(\mathbf{u^0}, \tilde{\varphi}(\mathbf{u^0}, t), t\big)|\\ \leq&C\tilde{\zeta}_0(\frac{t}{\varepsilon}) \leq Ce^{-\frac{M_0}{4}t/\varepsilon}, \end{aligned} \tag{9.26}$$

due to the Lipschitz property. The constant C depends only on the derivatives of Φ in $\bar{\mathcal{T}}_{b,\lambda}$. C is independent of t and ε. Then,

$$|\tilde{I}(t)| \leq C\varepsilon \text{ for } t > C\varepsilon\log(\frac{1}{\varepsilon}). \tag{9.27}$$

We now consider the case $t \leq C\varepsilon\log(\frac{1}{\varepsilon})$. We use Tailor expansion to obtain:

$$\begin{aligned}|\tilde{I}(t)| \leq& |\tilde{\Phi}(\tilde{\mathbf{u}}_\varepsilon, \tilde{\varphi}(\tilde{\mathbf{u}}_\varepsilon, t) + \tilde{\zeta}_0(t/\varepsilon), t) - \tilde{\Phi}(\mathbf{u}^0, \tilde{\varphi}(\mathbf{u}^0, t) + \tilde{\zeta}_0(t/\varepsilon), t)|+\\ &|\tilde{\Phi}(\tilde{\mathbf{u}}_\varepsilon, \tilde{\varphi}(\tilde{\mathbf{u}}_\varepsilon, t), t) - \tilde{\Phi}(\mathbf{u}^0, \varphi(\mathbf{u}^0, t), t)|\\ =& \left|(\tilde{\mathbf{u}}_\varepsilon - \mathbf{u^0})\cdot\nabla_x\,\tilde{\Phi}\Big(\mathbf{x}, \tilde{\varphi}(\mathbf{x}, t) + \tilde{\zeta}_0(t/\varepsilon)\Big)\Big|_{\mathbf{x}=\mathbf{u^0}+\eta(\tilde{\mathbf{u}}_\varepsilon-\mathbf{u^0})}\right|\\ &+\left|(\tilde{\mathbf{u}}_\varepsilon - \mathbf{u^0})\cdot\nabla_x\,\tilde{\Phi}\Big(\mathbf{x}, \tilde{\varphi}(\mathbf{x}, t)\Big)\Big|_{\mathbf{x}=\mathbf{u^0}+\eta^*(\tilde{\mathbf{u}}_\varepsilon-\mathbf{u^0})}\right|\\ \leq\ & t\sum_{i=1}^m\left\|\frac{d}{dt}\tilde{u}^i_\varepsilon\right\|_{L^\infty(\mathbb{R}^+)}\left(\left\|\nabla_{x^i}\tilde{\Phi}\Big(\mathbf{x}, \tilde{\varphi}(\mathbf{x}, t) + \zeta_0(t/\varepsilon)\Big)\right\|_{L^\infty(\mathbb{R}^+)}\right.\\ &\left.+\left\|\nabla_{x^i}\tilde{\Phi}\Big(\mathbf{x}, \tilde{\varphi}(\mathbf{x}, t)\Big)\right\|_{L^\infty(\mathbb{R}^+)}\right)\\ &\leq C\varepsilon\log(\frac{1}{\varepsilon}), \end{aligned} \tag{9.28}$$

if $t \leq C\varepsilon \log(\frac{1}{\varepsilon})$. Here $\eta,\ \eta^* \in (0,1)$ are time dependent functions. The constant C depends only on derivatives of $\mathbf{f}$ and Φ in $\bar{\mathcal{T}}_{b,\lambda}$. By $\nabla_x \tilde{\Phi}\Big(\mathbf{x}, \tilde{\varphi}(\mathbf{x},t)\Big)$, we denote the total derivative with respect to $\mathbf{x}$. It holds

$$\varepsilon \frac{d}{dt}\tilde{\varphi}(\tilde{\mathbf{u}}_\varepsilon, t) = \varepsilon \nabla\tilde{\varphi}(\tilde{\mathbf{u}}_\varepsilon, t)\cdot \tilde{\mathbf{f}}(\tilde{\mathbf{u}}_\varepsilon, \tilde{v}_\varepsilon) \leq C\varepsilon, \tag{9.29}$$

since $\tilde{\mathbf{f}}$ is bounded and $\nabla\tilde{\varphi}$ is bounded ($\nabla\varphi$ is bounded in $\bar{\mathcal{T}}_{b,\lambda}$ and $\nabla\tilde{\varphi} = \nabla\varphi$ in $\bar{\mathcal{T}}_{b,\lambda}$ and zero outside). Again, C depends only on properties of the functions $\mathbf{f}$, Φ in $\bar{\mathcal{T}}_{b,\lambda}$ and is especially independent of t and ε.

In summary, we obtain

$$\varepsilon \frac{d}{dt}\tilde{\mathcal{V}}_\varepsilon = -(\alpha - \frac{\partial\tilde{\Phi}^\star}{\partial v})\tilde{\mathcal{V}}_\varepsilon + g(t), \tag{9.30}$$

with $g(t) := \tilde{I}(t) - \varepsilon\frac{d}{dt}\tilde{\varphi}(\mathbf{u}_\varepsilon)$. Due to (9.27), (9.28) and (9.29), $|g| \leq C\varepsilon + C\varepsilon\log(\frac{1}{\varepsilon})$. Since $-(\alpha - \frac{\partial\tilde{\Phi}^\star}{\partial v}) \leq -\frac{M_0}{4}$, we obtain

$$\begin{aligned}|\tilde{\mathcal{V}}_\varepsilon| \leq& \int_0^t e^{-(\alpha - \frac{\partial\tilde{\Phi}^\star}{\partial v})(t-\tau)/\varepsilon}\left(C + C\log\left(\frac{1}{\varepsilon}\right)\right)d\tau \\ \leq& C\left(\varepsilon + \varepsilon\log\left(\frac{1}{\varepsilon}\right)\right).\end{aligned}$$

We also have:

$$\varepsilon \frac{d}{dt}\tilde{\mathcal{V}}_\varepsilon = -(\alpha - \frac{\partial\tilde{\Phi}^\star}{\partial v})\tilde{\mathcal{V}}_\varepsilon + g(t), \tag{9.31}$$

with $g(t) := \tilde{I}(t) + \varepsilon\frac{d}{dt}\tilde{\varphi}(\tilde{\mathbf{u}}_\varepsilon)$ and $|g| \leq C\varepsilon + Ce^{-\frac{M_0}{4}t/\varepsilon}$, due to (9.26) and (9.29).

Therefore,

$$\begin{aligned}|\tilde{\mathcal{V}}_\varepsilon| \leq& \int_0^t e^{-(\alpha - \frac{\partial\tilde{\Phi}^\star}{\partial v})(t-\tau)/\varepsilon}(C + \frac{1}{\varepsilon}Ce^{-\frac{M_0}{4}\tau/\varepsilon})d\tau \\ \leq& C\varepsilon + \frac{C}{\varepsilon}e^{-\min\{\frac{M_0}{8},\alpha\}(t/\varepsilon)}\int_0^t Ce^{\min\{\frac{M_0}{8},\alpha\}\tau/\varepsilon - \frac{M_0}{4}\tau/\varepsilon}d\tau \\ \leq& C\varepsilon + \frac{C}{\min\{\frac{M_0}{8},\alpha\} - M_0/4}e^{-\min\{\frac{M_0}{8},\alpha\}(t/\varepsilon)}(e^{\min\{\frac{M_0}{8},\alpha\}t/\varepsilon - \frac{M_0}{4}t/\varepsilon} - 1)d\tau \\ \leq& C\varepsilon + Ce^{-kt/\varepsilon},\end{aligned}$$

for a constant $k > 0$. ■

Proposition 9.19
Let Assumptions 9.1-9.4 be fulfilled.

(i) Then, there exists ε_0 such that for all $0 < \varepsilon \leq \varepsilon_0$ the error $\tilde{\delta}_\varepsilon(t) := \tilde{\mathbf{u}}_\varepsilon(t) - \tilde{\mathbf{A}}(t)$ satisfies $|\delta_\varepsilon(t)| \leq C\varepsilon$ for all $t > 0$. The constant C only depends on $\mathbf{f}$ and Φ.

(ii) For $\varepsilon \leq \varepsilon_0$, $(\tilde{\mathbf{u}}_\varepsilon, \tilde{v}_\varepsilon) \in \mathcal{T}_{b,\lambda}$ for all $t \geq 0$, therefore, $\tilde{\mathbf{f}} = \mathbf{f}$ and $\tilde{\Phi} = \Phi$ in a neighborhood of the solution $(\tilde{\mathbf{u}}_\varepsilon, \tilde{v}_\varepsilon)$. Hence the solutions to problem (9.15)-(9.16) coincide with the solution to problem (9.5)-(9.6). They exist for all times.

PROOF
We use the notation "$\mathbf{u}_\varepsilon \in \mathcal{T}_{b,\lambda}$ for $t \leq T$" to denote that $|\mathbf{u}_\varepsilon(t) - \mathbf{A}(t)| < b$ for $t \leq T$. We use the notation "$v_\varepsilon \in \mathcal{T}_{b,\lambda}$ for $t \leq T$" to denote that $v_\varepsilon(t) \in (\lambda^b(t), \lambda^a(t))$ for $t \leq T$. We set $\tilde{\delta}_\varepsilon := \tilde{\mathbf{u}}_\varepsilon - \tilde{\mathbf{A}}$. We consider the initial value problem

$$\begin{aligned} \frac{d\tilde{\delta}_\varepsilon}{dt} &= \tilde{\mathbf{f}}(\tilde{\mathbf{A}} + \tilde{\delta}_\varepsilon, \tilde{\varphi}(\tilde{\mathbf{A}} + \tilde{\delta}_\varepsilon, t) + \tilde{\zeta}_0(\frac{t}{\varepsilon}) + \tilde{\mathcal{V}}_\varepsilon, t) - \tilde{\mathbf{f}}(\tilde{\mathbf{A}}, \tilde{\varphi}(\tilde{\mathbf{A}}, t), t) \\ \tilde{\delta}_\varepsilon(0) &= 0. \end{aligned} \tag{9.32}$$

Due to Lipschitz continuity of the right hand side, there exists a unique solution to this problem.

From Corollary 9.8 we know that there exists a tubular domain $\mathcal{T}_{b,\lambda}$, such that for all continuous functions (μ, ν) in $\bar{\mathcal{T}}_{b,\lambda}$ the system

$$\frac{d}{dt}w = \left(D_x\mathbf{f}(\mathbf{x}, y) + \partial_y\mathbf{f}(\mathbf{x}, y) \otimes \nabla\varphi(\mathbf{x}) \right)|_{(\mathbf{x}=\mu, y=\nu)} w$$

has an exponential dichotomy. $\mathcal{T}_{b,\lambda}$ is chosen such that $\mathbf{u}_\varepsilon(0) = \tilde{\mathbf{u}}_\varepsilon(0)$ and $v_\varepsilon(0) = \tilde{v}_\varepsilon(0)$ are in the interior of $\mathcal{T}_{b,\lambda}$. Due to continuity, the functions $\tilde{\mathbf{u}}_\varepsilon$ and $\tilde{v}_\varepsilon$ will stay in $\mathcal{T}_{b,\lambda}$ for some time. As long as $\tilde{\mathbf{u}}_\varepsilon$ and $\tilde{v}_\varepsilon$ stay in $\bar{\mathcal{T}}_{b,\lambda}$, it holds $\tilde{\delta}_\varepsilon = \delta_\varepsilon := \mathbf{u}_\varepsilon - \mathbf{A}$. The error δ_ε fulfills the following initial value problem:

$$\begin{aligned} \frac{d\delta_\varepsilon}{dt} &= \mathbf{f}(\mathbf{A} + \delta_\varepsilon, \varphi(\mathbf{A} + \delta_\varepsilon) + \zeta_0(\frac{t}{\varepsilon}) + \mathcal{V}_\varepsilon, t) - \mathbf{f}(\mathbf{A}, \varphi(\mathbf{A})), \\ \delta_\varepsilon(0) &= 0. \end{aligned} \tag{9.33}$$

We will now derive estimates valid as long as the solutions stay in $\bar{\mathcal{T}}_{b,\lambda}$. We obtain

$$\mathbf{f}(\mathbf{A} + \delta_\varepsilon, \varphi(\mathbf{A} + \delta_\varepsilon)) - \mathbf{f}(\mathbf{A}, \varphi(\mathbf{A}) = (D_x\mathbf{f} + \partial_y\mathbf{f} \otimes \nabla\varphi)(\eta(t))\delta_\varepsilon, \tag{9.34}$$

where $\eta(t)$ is between $\mathbf{A}(t)$ and $\mathbf{A}(t) + \delta_\varepsilon(t) = \mathbf{u}_\varepsilon(t)$. Since $\mathbf{f}$ is continuously differentiable, η is continuous. Furthermore, $\eta(t) \in \bar{\mathcal{T}}_{b,\lambda}$, as long as $\mathbf{u}_\varepsilon \in \bar{\mathcal{T}}_{b,\lambda}$. Due to Remark 9.10, this implies that $\varphi(\eta(t)) \in (\lambda^b(t), \lambda^a(t))$.

The function $\eta(t)$ depends only on $\mathbf{f}$, $\mathbf{u}_\varepsilon, v_\varepsilon, \mathbf{A}, \Phi$. Since it is in $\bar{\mathcal{T}}_{b,\lambda}$, Corollary 9.8 implies that there exist constants $C > 0, \beta > 0$, depending only on $\mathbf{A}$ and $\mathcal{T}_{b,\lambda}$ such that all fundamental solutions S of

$$\frac{d}{dt}\mathbf{w} = \left(D_x\mathbf{f}(\mathbf{x}, y) + \partial_y \mathbf{f}(\mathbf{x}, y) \otimes \nabla\varphi(\mathbf{x}) \right)|_{(\mathbf{x}=\eta, y=\varphi(\eta))}\mathbf{w}$$

fulfill $||S(t)S^{-1}(\tau)|| \leq Ce^{-\beta(t-\tau)}$, for $t \geq \tau$. The constants $C,\ \beta$ do not depend on η or ε.

Furthermore, it holds

$$\begin{aligned} ||\mathbf{f}(\mathbf{A} + \delta_\varepsilon, \varphi(\mathbf{A} + \delta_\varepsilon) + \zeta_0(\frac{t}{\varepsilon}) + \mathcal{V}_\varepsilon, t) - \mathbf{f}(\mathbf{A} + \delta_\varepsilon, \varphi(\mathbf{A} + \delta_\varepsilon)||_2 \\ \leq \tilde{C}e^{-Lt/\varepsilon} + \tilde{C}\varepsilon, \end{aligned} \tag{9.35}$$

where L is a positive constant. For the latter estimate we used Proposition 9.18 and boundedness of derivatives of $\mathbf{f}$ in $\bar{\mathcal{T}}_{b,\lambda}$. The constants L and $\tilde{C}$ do not depend on ε. We obtain:

$$\frac{d\delta_\varepsilon}{dt} = (D_x\mathbf{f} + \partial_y\mathbf{f} \otimes \nabla\varphi)(\eta(t))\delta_\varepsilon + \mathbf{g_2}(t)$$

with $|\mathbf{g}_2| \leq \tilde{C}e^{-Lt/\varepsilon} + \tilde{C}\varepsilon$. Then, Assumption 9.4 implies

$$\begin{aligned} ||\delta_\varepsilon(t)||_2 \leq& \int_0^t C\tilde{C}e^{-\beta(t-\tau)}(\varepsilon + e^{-L\tau/\varepsilon})\, d\tau \\ \leq& C\tilde{C}\varepsilon \int_0^t e^{-\beta(t-\tau)}\, d\tau + C\tilde{C}\int_0^\infty e^{-L\tau/\varepsilon} d\tau \\ \leq& C\tilde{C}\varepsilon\left(\frac{1}{\beta} + \frac{1}{L}\right). \end{aligned} \tag{9.36}$$

Since $C,\ \tilde{C},\ \beta,\ L$ do not depend on ε, we can choose ε such small that $C\tilde{C}\varepsilon\left(\frac{1}{\beta} + \frac{1}{L}\right) \leq b/2$, where b is the radius of the tube $\mathcal{T}_{b,\lambda}$ in direction of $\mathbf{A}$ (Corollary 9.8). Then $\tilde{\mathbf{u}}_\varepsilon$ can never leave $\mathcal{T}_{b,\lambda}$ as long as $\tilde{v}_\varepsilon \in \bar{\mathcal{T}}_{b,\lambda}$.

We now study the behavior of v_ε, as long as $(\mathbf{u}_\varepsilon, v_\varepsilon) \in \bar{\mathcal{T}}_{b,\lambda}$. We assume for the moment that $v^0 \geq \varphi(\mathbf{u}_\varepsilon(0)) = \varphi(\mathbf{A}(0))$. The opposite case works analogously.

In the case $v_\varepsilon(0) = v^0 \geq \varphi(\mathbf{u}_\varepsilon(0)) = \varphi(\mathbf{A}(0))$, it holds $\zeta_0 \geq 0$, since $\zeta_0(0) \geq 0$ and since ζ_0 does not change sign. By Proposition 9.18, we obtain

$$\begin{aligned} & |v_\varepsilon - \varphi(\mathbf{u}_\varepsilon) - \zeta_0(t/\varepsilon)| < C\varepsilon\log(1/\varepsilon) + C\varepsilon \\ \Leftrightarrow \quad & -C\varepsilon\log(1/\varepsilon) - C\varepsilon < v_\varepsilon - \varphi(\mathbf{u}_\varepsilon) + \varphi(\mathbf{A}) - \varphi(\mathbf{A}) - \zeta_0(t/\varepsilon) \\ & < C\varepsilon\log(1/\varepsilon) + C\varepsilon \end{aligned}$$

As long as we stay inside $\bar{\mathcal{T}}_{b,\lambda}$, we get by estimate (9.36) $|\varphi(\mathbf{u}_\varepsilon) - \varphi(\mathbf{A})| \leq ||\nabla\varphi||C\varepsilon$ and $\nabla\varphi$ is bounded for $\mathbf{u}_\varepsilon \in \bar{\mathcal{T}}_{b,\lambda}$. Therefore, $|\varphi(\mathbf{u}_\varepsilon) - \varphi(\mathbf{A})| \leq D\varepsilon$. Thus, we obtain

$$-C\varepsilon\log(1/\varepsilon) - \tilde{C}\varepsilon + \zeta_0(t/\varepsilon) < v_\varepsilon - \varphi(\mathbf{A}) < C\varepsilon\log(1/\varepsilon) + \tilde{C}\varepsilon + \zeta_0(t/\varepsilon)$$

Since we assumed $\zeta_0(t/\varepsilon) \geq 0$, we obtain

$$-C\varepsilon\log(1/\varepsilon) - \tilde{C}\varepsilon < v_\varepsilon - \varphi(\mathbf{A}) < C\varepsilon\log(1/\varepsilon) + \tilde{C}\varepsilon + \zeta_0(t/\varepsilon),$$

which yields

$$-C\varepsilon\log(1/\varepsilon) - \tilde{C}\varepsilon < v_\varepsilon - \varphi(\mathbf{A}) < C\varepsilon\log(1/\varepsilon) + \tilde{C}\varepsilon + \zeta_0(0), \tag{9.37}$$

since ζ_0 is exponentially decaying.

Due to the construction of $\mathcal{T}_{b,\lambda}$, we have $\varphi(\mathbf{A}) \in (\lambda^b(t), \lambda^a(t))$ for all $t \geq 0$ and $[\varphi(\mathbf{A}(0)), v^0 = \zeta_0(0) + \varphi(\mathbf{A}(0))] \subset (\lambda^b(0), \lambda^a(0))$. Due to the continuity of the involved functions, there exists $\theta > 0$ such that $[\varphi(\mathbf{A}(t)), \zeta_0(0) + \varphi(\mathbf{A}(t))] \subset (\lambda^b(t), \lambda^a(t))$ for $0 \leq t \leq \theta$. Note that θ does not depend on ε. We define $Q^b := \min_{0\leq t\leq\theta} \varphi(\mathbf{A}(t)) - \lambda^b(t) > 0$ and $Q^a := \min_{0\leq t\leq\theta} \lambda^a(t) - \varphi(\mathbf{A}(t)) - \zeta_0(0) > 0$.

We now choose $\bar{\varepsilon}_0 > 0$ such that $C\varepsilon\log(1/\varepsilon) + \tilde{C}\varepsilon < \frac{\min\{Q^a,Q^b\}}{2} =: \frac{Q}{2}$. Due to estimate (9.37), we then have $\operatorname{dist}(v_\varepsilon, \partial\mathcal{T}_{b,\lambda}) \geq \frac{Q}{2}$, for $0 \leq t \leq \theta$ for $\varepsilon < \bar{\varepsilon}_0$.

Let $d > 0$ be given. Since $|\zeta_0(t/\varepsilon)| \leq |\zeta_0(0)|e^{-Lt/\varepsilon}$, we can choose $\hat{\varepsilon}_0(d) \leq \bar{\varepsilon}_0$ such that $|\zeta_0(t/\varepsilon)| < d$ for all $t \geq \theta$, $\varepsilon \leq \hat{\varepsilon}_0(d)$. We now consider $\theta \leq t$. Due to construction of $\mathcal{T}_{b,\lambda}$, it holds $\varphi(\mathbf{A}) \in (\lambda^b(t), \lambda^a(t))$ for all t and $R_1 := \inf_{t\in\mathbb{R}^+}(\lambda^a(t) - \varphi(\mathbf{A})) > 0$, $R_2 := \inf_{t\in\mathbb{R}^+}(\varphi(\mathbf{A}) - \lambda^b(t)) > 0$. We set $R := \min\{R_1, R_2\}$.

We obtain $|v_\varepsilon - \varphi(\mathbf{A})| = |v_\varepsilon - \varphi(\mathbf{u}_\varepsilon) + \varphi(\mathbf{u}_\varepsilon) - \varphi(\mathbf{A}) + \zeta_0(t/\varepsilon) - \zeta_0(t/\varepsilon)| \leq |\mathcal{V}_\varepsilon| + |\zeta_0(t/\varepsilon)| + |\varphi(\mathbf{u}_\varepsilon) - \varphi(\mathbf{A})|$. As long as we stay inside $\bar{\mathcal{T}}_{b,\lambda}$, we get by estimate (9.36) that $|\varphi(\mathbf{u}_\varepsilon) - \varphi(\mathbf{A})\| \leq ||\nabla\varphi||C\varepsilon = D\varepsilon$ (note that $\nabla\varphi$ is bounded for $\mathbf{u}_\varepsilon \in \bar{\mathcal{T}}_{b,\lambda}$). Consequently, by Proposition 9.18: $|v_\varepsilon - \varphi(\mathbf{A})| \leq C\varepsilon\log(1/\varepsilon) + D\varepsilon + |\zeta_0(t/\varepsilon)|$.

We now choose $\hat{\varepsilon}_0$ (see above) such that $|\zeta_0(t/\varepsilon)| < R/4$ for all $t \geq \theta, \varepsilon \leq \hat{\varepsilon}_0$. We choose $\tilde{\varepsilon}_0$ such that $D\tilde{\varepsilon}_0 + C\tilde{\varepsilon}_0\log(1/\tilde{\varepsilon}_0) \leq R/4$. This implies that for $\varepsilon < \varepsilon_0 :=$

$\min\{\hat{\varepsilon}_0, \tilde{\varepsilon}_0, \bar{\varepsilon}_0\}$ we have $|v_\varepsilon - \varphi(\mathbf{A})| \leq R/2$ for $\theta \leq t$, i.e., $v_\varepsilon \in (\lambda^b(t), \lambda^a(t))$. This means that as long as $\mathbf{u}_\varepsilon \in \bar{\mathcal{T}}_{b,\lambda}$, v_ε cannot reach the boundary of $\mathcal{T}_{b,\lambda}$.

At $t = 0$ it holds $(\tilde{\mathbf{u}}_\varepsilon(0), \tilde{v}_\varepsilon(0)) = (\mathbf{u}_\varepsilon, v_\varepsilon) \in \mathcal{T}_{b,\lambda}$. Assume at $t = t^*$ the solutions leave $\mathcal{T}_{b,\lambda}$ for the first time. This means that either ($\mathbf{u}_\varepsilon(t^*) \in \partial\mathcal{T}_{b,\lambda}$ and $v_\varepsilon(t^*) \in \bar{\mathcal{T}}_{b,\lambda}$) or ($v_\varepsilon(t^*) \in \partial\mathcal{T}_{b,\lambda}$ and $\mathbf{u}_\varepsilon(t^*) \in \bar{\mathcal{T}}_{b,\lambda}$). In both cases it follows from the reasoning above $|\mathbf{u}_\varepsilon(t^*) - \mathbf{A}(t^*)| \leq \frac{b}{2}$ and $v_\varepsilon(t^*) \in (\lambda^b(t^*), \lambda^a(t^*))$ as shown above, which is a contradiction. Therefore, v_ε, $\mathbf{u}_\varepsilon$ stay in the interior of $\mathcal{T}_{b,\lambda}$. This yields (ii). Consequently, estimate (9.36) holds for all times, this yields (i).

■

Since we do not need extensions any more, we can get a better estimate for $\mathcal{V}_\varepsilon$.

Proposition 9.20
Let Assumptions 9.1-9.4 be fulfilled. Let ε be small enough. Then, for

$$\mathcal{V}_\varepsilon(t) := v_\varepsilon(t) - \varphi(\mathbf{u}_\varepsilon, t) - \zeta_0(\frac{t}{\varepsilon}), \tag{9.38}$$

it holds

$$|\mathcal{V}_\varepsilon(t)| \leq C\varepsilon, \quad 0 \leq t. \tag{9.39}$$

PROOF
It holds $\mathcal{V}_\varepsilon(0) = 0$ and $\mathcal{V}_\varepsilon$ satisfies equation

$$\varepsilon\frac{d}{dt}\mathcal{V}_\varepsilon = -(\alpha - \frac{\partial\Phi^\star}{\partial v})\mathcal{V}_\varepsilon - \varepsilon\frac{d}{dt}\varphi(\mathbf{u}_\varepsilon, t) + I(t) \tag{9.40}$$

with

$$\begin{aligned} I(t) :=& \Phi(\mathbf{u}_\varepsilon, \varphi(\mathbf{u}_\varepsilon, t) + \zeta_0(t/\varepsilon), t) - \alpha(\varphi(\mathbf{u}_\varepsilon, t) + \zeta_0(t/\varepsilon)) \\ & - \Phi\big(\mathbf{u}^{\mathbf{0}}, \varphi(\mathbf{u}^{\mathbf{0}}, t) + \zeta_0(t/\varepsilon), t\big) + \alpha(\varphi(\mathbf{u}^{\mathbf{0}}, t) + \zeta_0(t/\varepsilon)). \end{aligned} \tag{9.41}$$

We set $\dfrac{\partial\Phi^\star}{\partial v} := \dfrac{\partial\Phi(\mathbf{u}_\varepsilon, v^\star)}{\partial v}$, where $v^\star$ is an appropriate value between v_ε and $\varphi(u_\varepsilon)$.

Equations (9.40) and (9.41) correspond to equations (9.23) and (9.24) without wiggles "˜".

We note that

$$\begin{aligned}
0 =& \frac{d}{d\eta}(-\alpha\varphi(\mathbf{u}_\varepsilon(\eta t)) + \Phi(\mathbf{u}_\varepsilon(\eta t), \varphi(\mathbf{u}_\varepsilon(\eta t))))\\
=& -\alpha\nabla\varphi(\mathbf{u}_\varepsilon(\eta t)) \cdot \frac{d}{d\tau}\mathbf{u}_\varepsilon(\tau)|_{\tau=\eta t} t\\
&+ \nabla_u \Phi(\mathbf{u}, v)|_{\mathbf{u}=\mathbf{u}_\varepsilon(\eta t), v=\varphi(\mathbf{u}_\varepsilon(\eta t))} \cdot \frac{d}{d\tau}\mathbf{u}_\varepsilon(\tau)|_{\tau=\eta t} t\\
&+ \partial_v \Phi(\mathbf{u}, v)|_{\mathbf{u}=\mathbf{u}_\varepsilon(\eta t), v=\varphi(\mathbf{u}_\varepsilon(\eta t))} \nabla\varphi(\mathbf{u}_\varepsilon(\eta t)) \cdot \frac{d}{d\tau}\mathbf{u}_\varepsilon(\tau)|_{\tau=\eta t} t
\end{aligned} \tag{9.42}$$

We used that $\alpha\varphi(\cdot) = \Phi(\cdot, \varphi(\cdot))$.
Now we give a better estimate for $I(t)$ using the second order derivatives:

$$\begin{aligned}
|I(t)| =& \left| \int_0^1 \frac{d}{d\eta} \big[\Phi\big(\mathbf{u}_\varepsilon(\eta t), \varphi(\mathbf{u}_\varepsilon(\eta t)) + \zeta_0(t/\varepsilon)\big) - \alpha\big(\varphi(\mathbf{u}_\varepsilon(\eta t)) + \zeta_0(t/\varepsilon)\big)\big] d\eta \right|\\
=& \Bigg| \int_0^1 t\nabla_u \Phi(\mathbf{u}, v)|_{\mathbf{u}=\mathbf{u}_\varepsilon(\eta t), v=\varphi(\mathbf{u}_\varepsilon(\eta t))+\zeta_0(t/\varepsilon))} \cdot \frac{d}{d\tau}\mathbf{u}_\varepsilon(\tau)|_{\tau=\eta t}\\
&+ t\partial_v \Phi(\mathbf{u}, v)|_{\mathbf{u}=\mathbf{u}_\varepsilon(\eta t), v=\varphi(\mathbf{u}_\varepsilon(\eta t))+\zeta_0(t/\varepsilon))} \nabla\varphi(\mathbf{u}_\varepsilon(\eta t)) \cdot \frac{d}{d\tau}\mathbf{u}_\varepsilon(\tau)|_{\tau=\eta t}\\
&- t\alpha\nabla\varphi(\mathbf{u}_\varepsilon(\eta t)) \cdot \frac{d}{d\tau}\mathbf{u}_\varepsilon(\tau)|_{\tau=\eta t} \Bigg|\\
\overset{(*)}{=}& \Bigg| \int_0^1 t\nabla_u \Phi(\mathbf{u}, v)|_{\mathbf{u}=\mathbf{u}_\varepsilon(\eta t), v=\varphi(\mathbf{u}_\varepsilon(\eta t))+\zeta_0(t/\varepsilon))} \cdot \frac{d}{d\tau}\mathbf{u}_\varepsilon(\tau)|_{\tau=\eta t}\\
&- t\nabla_u \Phi(\mathbf{u}, v)|_{\mathbf{u}=\mathbf{u}_\varepsilon(\eta t), v=\varphi(\mathbf{u}_\varepsilon(\eta t))} \cdot \frac{d}{d\tau}\mathbf{u}_\varepsilon(\tau)|_{\tau=\eta t}\\
&+ t\partial_v \Phi(\mathbf{u}, v)|_{\mathbf{u}=\mathbf{u}_\varepsilon(\eta t), v=\varphi(\mathbf{u}_\varepsilon(\eta t))+\zeta_0(t/\varepsilon))} \nabla\varphi(\mathbf{u}_\varepsilon(\eta t)) \cdot \frac{d}{d\tau}\mathbf{u}_\varepsilon(\tau)|_{\tau=\eta t}\\
&- t\partial_v \Phi(\mathbf{u}, v)|_{\mathbf{u}=\mathbf{u}_\varepsilon(\eta t), v=\varphi(\mathbf{u}_\varepsilon(\eta t))} \nabla\varphi(\mathbf{u}_\varepsilon(\eta t)) \cdot \frac{d}{d\tau}\mathbf{u}_\varepsilon(\tau)|_{\tau=\eta t}\\
&- t\alpha\nabla\varphi(\mathbf{u}_\varepsilon(\eta t)) \cdot \frac{d}{d\tau}\mathbf{u}_\varepsilon(\tau)|_{\tau=\eta t} + t\alpha\nabla\varphi(\mathbf{u}_\varepsilon(\eta t)) \cdot \frac{d}{d\tau}\mathbf{u}_\varepsilon(\tau)|_{\tau=\eta t} d\eta \Bigg|\\
=& t\Bigg| \int_0^1 \partial_v \nabla_u \Phi(\mathbf{u}, v)|_{\mathbf{u}=\mathbf{u}_\varepsilon(\eta t), v=\varphi(\mathbf{u}_\varepsilon(\eta t))+\zeta^*)} \zeta_0(t/\varepsilon) \cdot \frac{d}{d\tau}\mathbf{u}_\varepsilon(\tau)|_{\tau=\eta t}\\
&+ \partial_{vv}^2 \Phi(\mathbf{u}, v)|_{\mathbf{u}=\mathbf{u}_\varepsilon(\eta t), v=\varphi(\mathbf{u}_\varepsilon(\eta t))+\zeta^{**})} \nabla\varphi(\mathbf{u}_\varepsilon(\eta t))\zeta_0(t/\varepsilon) \cdot \frac{d}{d\tau}\mathbf{u}_\varepsilon(\tau)|_{\tau=\eta t} \Bigg|\\
\leq& tC \int_0^1 |\zeta_0(t/\varepsilon)|\, d\eta \leq tCe^{-\frac{M_0}{4\varepsilon}t}
\end{aligned} \tag{9.43}$$

In step $(*)$ we subtracted (9.42). We use that $\mathbf{f}$, Φ, φ and their derivatives are bounded in $\mathcal{T}_{b,\lambda}$. Due to Proposition 9.19 (ii), solutions do not leave $\mathcal{T}_{b,\lambda}$ for $\varepsilon \leq \varepsilon_0$. We, furthermore, used Lemma 9.17. Insertion of (9.43) into (9.40) yields

$$\varepsilon\frac{d}{dt}\mathcal{V}_\varepsilon = -(\alpha - \frac{\partial\Phi^\star}{\partial v})\mathcal{V}_\varepsilon + g_1(t)$$

with $g_1(t) := -\varepsilon\frac{\nabla_u\Phi(\mathbf{u}_\varepsilon,\varphi(\mathbf{u}_\varepsilon))}{\alpha-\frac{\partial\Phi}{\partial v}(\mathbf{u}_\varepsilon,\varphi(\mathbf{u}_\varepsilon))} \cdot \mathbf{f}(\mathbf{u}_\varepsilon, v_\varepsilon) + I(t)$. It holds $|g_1| \leq C(te^{-\frac{M_0}{4\varepsilon}t} + \varepsilon) \leq C\varepsilon$. The latter estimate holds, since for $k > 0$, $|te^{-kt}| \leq \frac{1}{ek}$. Assumption 9.3, Proposition 9.19 (ii) and Corollary 9.8 imply $-(\alpha - \frac{\partial\Phi^\star}{\partial v}) < -\frac{M_0}{4} < 0$.

We, therefore, obtain using Young's inequality, [20],

$$\begin{aligned}|\mathcal{V}_\varepsilon(t)| &\leq \int_0^t e^{-\frac{M_0}{4\varepsilon}(t-\tau)}\frac{|g_1(\tau)|}{\varepsilon}d\tau \\ &\leq C\int_0^t e^{-\frac{M_0}{4\varepsilon}(t-\tau)}\,d\tau \leq C\varepsilon. \end{aligned} \tag{9.44}$$

■

We summarize the results in the following Theorem.

Theorem 9.21 (Approximation at order ε)
Let ε be small enough. Let Assumptions 9.1-9.4 be fulfilled. Then,

$$\sup_{0\leq t\leq+\infty} ||\mathbf{u}_\varepsilon(t) - \mathbf{A}(t)||_2 \leq C\varepsilon, \tag{9.45}$$

$$|v_\varepsilon(t) - \varphi(\mathbf{A}(t))| \leq C(\varepsilon + e^{-M_0 t/\varepsilon}), \quad \forall t \in \mathbb{R}^+. \tag{9.46}$$

PROOF
The first statement is identical to Proposition 9.19 (i). The second statement follows from $|v_\varepsilon - \varphi(\mathbf{A})| - |\varphi(\mathbf{u}_\varepsilon) - \varphi(\mathbf{A}) + \zeta_0(t/\varepsilon)| \leq |v_\varepsilon - \varphi(\mathbf{A}) - \big(\varphi(\mathbf{u}_\varepsilon) - \varphi(\mathbf{A}) + \zeta_0(t/\varepsilon)\big)| = |\mathcal{V}_\varepsilon| \leq C\varepsilon$ using Proposition 9.20. This implies that $|v_\varepsilon - \varphi(\mathbf{A})| \leq C\varepsilon + |\zeta_0(t/\varepsilon)| + |\varphi(\mathbf{u}_\varepsilon) - \varphi(\mathbf{A})|$. The first statement of the Theorem and boundedness of the derivatives of φ in $\mathcal{T}_{b,\lambda}$ imply $|\varphi(\mathbf{u}_\varepsilon) - \varphi(\mathbf{A})| \leq D\varepsilon$. ■

9.5 Application to the stem cell model

We consider the minimal version of stem cell model (8.11) and its reduced counterpart (8.12). We now check the assumptions of Theorem 9.21. For that purpose we need Lemmas 9.22 and 9.23.

Lemma 9.22
Let $a_1 \in (0.5, 1)$, $p_1 > 0$, $d_2 > 0$ and $k > 0$ be real constants. Then, problem (8.12) *has a unique positive equilibrium* $(\bar{c}_1, \bar{c}_2)$.

PROOF
It holds $\frac{d}{dt}c_1 = 0 \Leftrightarrow \bar{s} = \frac{1}{2a_1}$, since we assume that $\bar{c}_1 > 0$. Therefore, $\bar{c}_2 = \frac{2a_1-1}{k}$. The constraint $\frac{d}{dt}c_2 = 0$ is equivalent to $p_1\bar{c}_1 = d_2\bar{c}_2$, which implies $\bar{c}_1 = \frac{(2a_1-1)d_2}{kp_1}$. Assumptions on parameters assure positivity of this steady state. ■

Lemma 9.23
Let $\bar{\mathbf{A}}$ be a steady state of the reduced system from Definition 9.6. Let $\mathbf{A^0}$ be in the basin of attraction of $\bar{\mathbf{A}}$.

Let all eigenvalues of $D_x\mathbf{f}(\mathbf{x}, y) + \partial_y\mathbf{f}(\mathbf{x}, y) \otimes \nabla\varphi(\mathbf{x})|_{\mathbf{x}=\bar{\mathbf{A}}, y=\varphi(\bar{\mathbf{A}})}$ have negative real part. Then, there exist positive constants c, C such that fundamental solutions S of the initial value problem

$$\frac{d}{dt}\mathbf{x} = \left(\nabla_u\mathbf{f}(\mathbf{x}, y) + \partial_v\mathbf{f}(\mathbf{x}, y) \otimes \nabla\varphi(\mathbf{x})|_{\mathbf{x}=\mathbf{A}(\mathbf{t}), y=\varphi(\mathbf{A}(\mathbf{t}))}\right)\mathbf{x} \tag{9.47}$$

$$\mathbf{x}(0) = \mathbf{x}^0 \tag{9.48}$$

fulfill $||S(t)S^{-1}(\tau)|| \leq Ce^{-c(t-\tau)}$ for all $t \geq \tau$.

The proof is given on page 284 in Appendix H, it is based on Lemma 9.7.

Lemma 9.24
Let $a_1 \in (0.5, 1)$, $p_1 > 0$, $d_2 > 0$ and $k > 0$ be real constants. We set $\Phi((c_1, c_2), s) := 1 - kc_2s$, $\alpha = 1$, $\mathbf{f}((c_1, c_2), s) := \begin{pmatrix}(2a_1s - 1)p_1c_1 \\ 2(1 - a_1s)p_1c_1 - d_2c_2\end{pmatrix}$. Then, it holds:

(i) $-\alpha s + \Phi((c_1, c_2), s) = 0$ *has exactly one real root, which is* $\varphi((c_1, c_2)) := s(c_2) := \frac{1}{1+kc_2}$.

(ii) The reduced problem (8.12) *has a smooth bounded solution for positive $c_1(0)$ and non-negative $c_2(0)$. The solution is unique and exists for all $t > 0$.*

(iii) (a) $\alpha - \partial_s\Phi|_{c_1=x, c_2=y, s=s(y)} \geq 1$, *for all non-negative real (x, y).*

(b) Let $c_1(0)$, $c_2(0)$ be in the basin of attraction of the unique positive steady state $(\bar{c}_1, \bar{c}_2)$. Let w be a solution of

$$\frac{d}{dt}w = -\alpha w + \Phi((c_1(t), c_2(t)), w)$$
$$w(0) = v_0.$$

Then, for each $\delta > 0$ there exists $t(\delta) > 0$ such that

$$|w(t) - \varphi((c_1(t), c_2(t))^T)| \leq \delta \text{ for } t > t(\delta).$$

(iv) Let additionally $c_1(0)$, $c_2(0)$ be in the basin of attraction of the positive steady state $(\bar{c}_1, \bar{c}_2)$. Then fundamental systems S of the the initial value problem

$$\frac{d}{dt}\mathbf{y} = \Big(D_x\mathbf{f}(\mathbf{x}, y) + \partial_y\mathbf{f}(\mathbf{x}, y) \otimes \nabla\varphi(\mathbf{x})|_{\mathbf{x}=\mathbf{A}(t), y=\varphi(\mathbf{A}(t))} \Big)\, \mathbf{y}, \quad \mathbf{y}(0) = \mathbf{y}^0$$

fulfill $||S(t)S^{-1}(\tau)|| \leq Ke^{-k(t-\tau)}$ for $t \geq \tau$ and appropriate positive constants k, K. Here $\mathbf{A}(t) = \begin{pmatrix} c_1(t) \\ c_2(t) \end{pmatrix}$.

PROOF

(i) $-s + 1 - kc_2 s = 0 \Leftrightarrow s = \frac{1}{1+kc_2}$.

(ii) follows from Lemma A.8 and Picard-Lindelöf's Theorem, [97].

(iii) It holds $\alpha - \partial_s\Phi|_{c_1=x, c_2=y, s=s(y)} = 1 + ky$. This yields (a).
We know that, due to the assumptions, $c_2(t) \to \bar{c}_2$ for $t \to \infty$. Since the linearization around the positive equilibrium has only eigenvalues with negative real part, we know that $|c_2(t) - \bar{c}_2| \leq L|c_2(0)|e^{-lt}$ for appropriate positive constants L, l, (see Theorem 9.3 in [92]). We are interested in behavior of solutions of the problem

$$\begin{aligned} &\frac{d}{dt}w = -\alpha w + \Phi((c_1(t), c_2(t)), w) = -(1 + kc_2(t))w + 1, \\ &w(0) = v_0. \end{aligned} \tag{9.49}$$

First, we consider the problem

$$\begin{aligned} &\frac{d}{dt}\tilde{w} = -(1 + kc_2)\tilde{w} \\ &\tilde{w}(0) = v_0, \end{aligned} \tag{9.50}$$

the linearization of which around its steady state (which is zero) has eigenvalue $-(1 + k\bar{c}_2) < -1$. We then know that solutions of problem (9.50) fulfill $|\tilde{w}| \leq C|\tilde{w}_0|e^{-kt}$ for appropriate positive C, k. Let S be a fundamental solution of (9.50). We set $\bar{w} = \frac{1}{1+k\bar{c}_2}$ and make a coordinate transformation ($\hat{w} = w - \bar{w}$) to obtain

$$\begin{aligned} \frac{d}{dt}\hat{w} &= -(1 + kc_2(t))(\hat{w} + \bar{w}) + 1 \\ &= -(1 + kc_2(t))\hat{w} + \frac{k(\bar{c}_2 - c_2(t))}{1 + k\bar{c}_2} \\ \hat{w}(0) &= v_0 + \bar{w}. \end{aligned} \tag{9.51}$$

The homogeneous parts of problems (9.50) and (9.51) are identical. We, therefore, obtain using the variation of constants formula, [234]:

$$\hat{w}(t) = \hat{w}(0)S(t) + \int_0^t S(t)S(-\tau)\frac{k(\bar{c}_2 - c_2(t))}{1+k\bar{c}_2}d\tau$$

and

$$\begin{aligned}
|\hat{w}(t)| \leq & Ce^{-kt} + \int_0^t Ce^{-k(t-\tau)}\frac{k(|\bar{c}_2 - c_2(t)|)}{1+k\bar{c}_2}d\tau \\
\leq & Ce^{-kt} + \int_0^t Ce^{-k(t-\tau)}\frac{k(Le^{-l\tau})}{1+k\bar{c}_2}|c_2(0)|d\tau \\
\leq & Ce^{-kt} + C'\int_0^t e^{-k(t-\tau)}e^{-l\tau}d\tau \\
\leq & Ke^{-\kappa t},
\end{aligned}$$

for $K,\ \kappa > 0$ chosen appropriately (see Lemma H.4). Consequently, $w(t) \to \frac{1}{1+k\bar{c}_2}$ for $t \to \infty$. It also holds $\varphi((c_1(t), c_2(t))^T) \to \varphi(\bar{c}_1, \bar{c}_2) = \frac{1}{1+k\bar{c}_2}$ for $t \to \infty$.

Let $\delta > 0$ be given. Choose $t(\delta)$ such that $|w(t) - \frac{1}{1+k\bar{c}_2}| \leq \delta/2$ for $t > t(\delta)$ and $|\varphi((c_1(t), c_2(t))^T) - \frac{1}{1+k\bar{c}_2}| \leq \delta/2$ for $t > t(\delta)$. Then, for $t > \delta(t)$ it holds $|w(t) - \varphi((c_1(t), c_2(t))^T)| \leq |w(t) - \frac{1}{1+k\bar{c}_2}| + |\varphi((c_1(t), c_2(t))^T) - \frac{1}{1+k\bar{c}_2}| \leq \delta$. This yields (b).

(iv) We calculate eigenvalues of $\Big(D_x\mathbf{f}(\mathbf{x}, y) + \partial_y\mathbf{f}(\mathbf{x}, y) \otimes \nabla\varphi(\mathbf{x})|_{\mathbf{x}=(\bar{c}_1,\bar{c}_2), y=s(\bar{c}_2)}\Big)$. It holds

$$\begin{aligned}
&\Big(D_x\mathbf{f}(\mathbf{x}, y) + \partial_y\mathbf{f}(\mathbf{x}, y) \otimes \nabla\varphi(\mathbf{x})|_{\mathbf{x}=(c_1,c_2), y=s(c_2)}\Big) \\
&\qquad = \begin{pmatrix} \left(\frac{2a_1}{1+kc_2} - 1\right)p_1 & -\frac{2ka_1p_1c_1}{(1+kc_2)^2} \\ 2\left(1 - \frac{a_1}{1+kc_2}\right)p_1 & \frac{2ka_1p_1c_1}{(1+kc_2)^2} - d_2 \end{pmatrix}
\end{aligned}$$

Therefore,

$$\Big(D_x\mathbf{f}(\mathbf{x}, y) + \partial_y\mathbf{f}(\mathbf{x}, y) \otimes \nabla\varphi(\mathbf{x})|_{\mathbf{x}=(\bar{c}_1,\bar{c}_2), y=s(\bar{c}_2)}\Big) = \begin{pmatrix} 0 & -\frac{(2a_1-1)d_2}{2a_1} \\ p_1 & -\frac{d_2}{2a_1} \end{pmatrix} \tag{9.52}$$

Since trace is negative and determinant positive, both eigenvalues have negative real parts. Lemma 9.23 implies (iv).

■

We now have the following result.

Proposition 9.25
Let (c_1, c_2) denote the solutions of system (8.12)*, let $(c_{1,\varepsilon}, c_{2,\varepsilon}, s_\varepsilon)$ denote the solution of system* (8.11)*. Let c_1^0, c_2^0 denote the initial conditions for $c_1,\ c_2$ and $c_{1,\varepsilon}, c_{2,\varepsilon}$. Let $a_1 \in (0.5, 1)$, $p_1 > 0$, $d_2 > 0$ and $k > 0$ be real constants. Let c_1^0, c_2^0 be in the basin of attraction of the unique positive steady state of system* (8.12)*. Then, for ε small enough it holds*

(i) $\sup_{0\le t\le\infty} \left\| \begin{pmatrix} c_1 \\ c_2 \end{pmatrix} - \begin{pmatrix} c_{1,\varepsilon} \\ c_{2,\varepsilon} \end{pmatrix} \right\|_2 \le C\varepsilon,$

(ii) $\left| \frac{1}{1+kc_2(t)} - s_\varepsilon(t) \right| \le C(\varepsilon + e^{-kt/\varepsilon}) \quad$ *for* $t \in \mathbb{R}^+$

(iii) $\sup_{T_0\le t\le\infty} \left\| \frac{1}{1+kc_2} - s_\varepsilon \right\|_2 \le C\varepsilon \quad$ *for* $T_0 = \mathcal{O}(1)$,

(iv) $\sup_{0\le t\le\infty} \left\| \frac{1}{1+kc_2} + \zeta_0\left(\frac{t}{\varepsilon}\right) - s_\varepsilon \right\|_2 \le C\varepsilon,$

where $\zeta_0(t) = \left(v^0 - \frac{1}{1+ku_2^0}\right) e^{-(1+ku_2^0)t}$.

PROOF
Due to Lemma 9.24, Assumptions 9.1-9.4 are fulfilled. Statements (i)-(iii) follow from Theorem 9.21. Statement (iv) follows from Proposition 9.20.
It holds for the initial layer ζ_0:

$$\begin{aligned} \zeta_0(0) &= v^0 - \frac{1}{1+ku_2^0} \\ \frac{d}{dt}\zeta_0 &= -\zeta_0 + 1 - ku_2^0\left(\frac{1}{1+ku_2^0} + \zeta_0\right) - \left(1 - ku_2^0\left(\frac{1}{1+ku_2^0}\right)\right) \\ &= -(1+ku_2^0)\zeta_0 \end{aligned}$$

This implies that $\zeta_0(t) = \left(v^0 - \frac{1}{1+ku_2^0}\right) e^{-(1+ku_2^0)t}$.

■

Example 9.26
A numerical example for Proposition 9.25 is given in Figure 9.2.

Example 9.27
A numerical example for the time dynamics of the exact solution $(c_{1,\varepsilon}, c_{2,\varepsilon}, s_\varepsilon)$, the quasi steady state approximation with initial layer correction $(c_1, c_2, s + \zeta_0(t/\varepsilon))$ and the quasi steady state approximation without initial layer (c_1, c_2, s) is given in Figure 9.3.

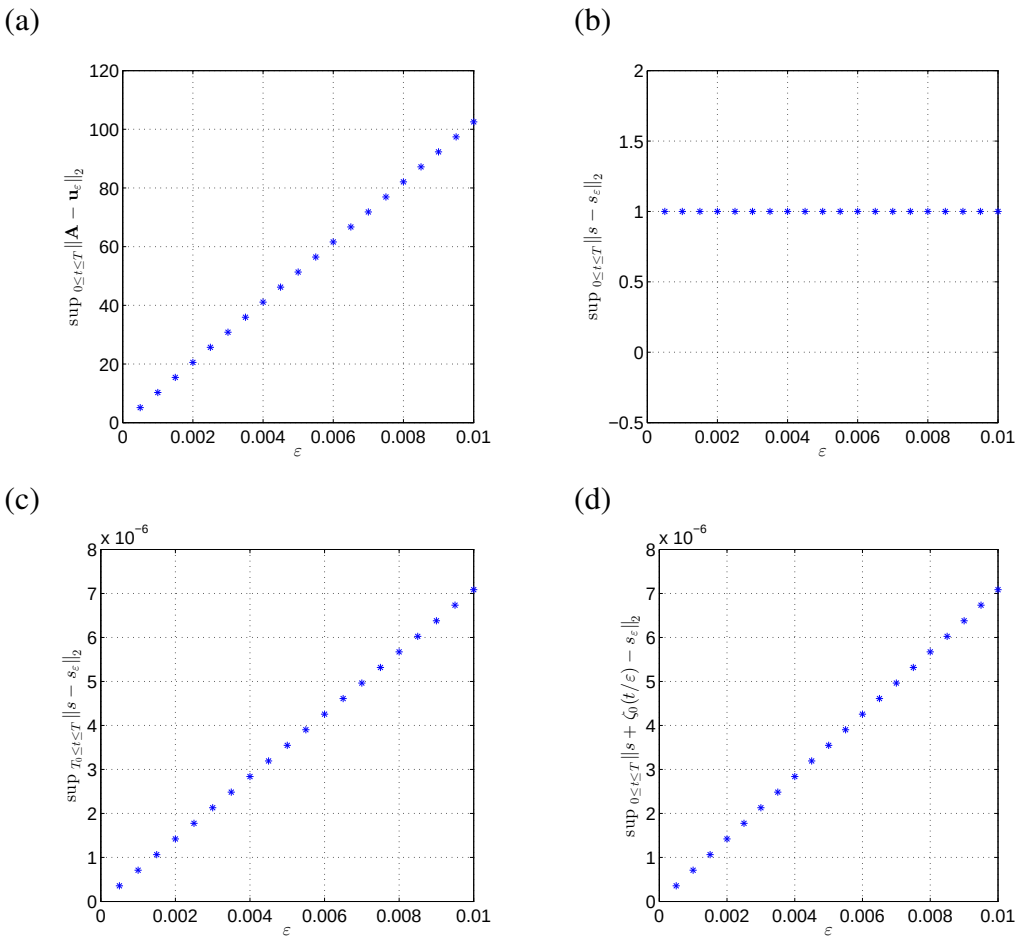

Figure 9.2: Approximation properties. Panel (a) shows distance of quasi steady state approximation of the slow components $\mathbf{A} = (c_1, c_2)^T$ from the exact solution $\mathbf{u}_\varepsilon = (c_{1,\varepsilon}, c_{2,\varepsilon})^T$, which is of order ε, cf. Proposition 9.25 (i). Panels (b-d) show distance of quasi steady state approximation of the slow component $\varphi(\mathbf{A}) = s$ from the exact solution s_ε, which is of order $\mathcal{O}(1)$ on $[0, T]$, Panel (b), cf. Proposition 9.25 (ii), but of order ε on $[T_0, T]$ for $T_0 = \mathcal{O}(1)$, Panel (c), cf. Proposition 9.25 (iii), and of order ε on $[0, T]$, if initial layer correction is added, Panel (d), cf. Proposition 9.25 (iv). In all Panels $a_1 = 0.55$, $p_1 = 0.5$, $d_2 = 0.5$, $k = 10^{-7}$, $c_{1,\varepsilon}(0) = c_{2,\varepsilon}(0) = 100$, $s_\varepsilon(0) = 0$ and $T = 100$. In Panel (c) $T_0 = 1$.

The following Proposition generalizes the result of Proposition 9.25 to versions of the model with more than 2 cell types.

Definition 9.28
The stem cell model with n cell types has the following form.

$$\begin{aligned}
\frac{d}{dt}c_{1,\varepsilon}(t) &= \big(2a_1 s_\varepsilon(t) - 1\big)p_1 c_{1,\varepsilon}(t) - d_1 c_{1,\varepsilon}(t),\\
&\vdots \quad \vdots \quad \vdots\\
\frac{d}{dt}c_{i,\varepsilon}(t) &= 2\big(1 - a_{i-1}s_\varepsilon(t)\big)p_{i-1}c_{i-1,\varepsilon}(t) + \big(2a_i s_\varepsilon(t) - 1\big)p_i(t)c_{i,\varepsilon}(t)\\
&\quad -d_i^c c_i(t), \quad 1 < i < n,\\
&\vdots \quad \vdots \quad \vdots\\
\frac{d}{dt}c_{n,\varepsilon}(t) &= 2\big(1 - a_{n-1}s_\varepsilon(t)\big)p_{n-1}c_{n-1,\varepsilon}(t) - d_n c_{n,\varepsilon}(t),\\
\varepsilon\frac{d}{dt}s_\varepsilon &= 1 - kc_{n,\varepsilon}s_\varepsilon - s_\varepsilon.
\end{aligned} \tag{9.53}$$

Its reduced counterpart is given in Chapter 2, system (2.3).

Proposition 9.29
Consider system (9.53). *Let* $(2a_1 - 1)p_1 - d_1 > 0$, $d_n > 0$, $d_i \geq 0$ *for* $i = 1, \cdots, n-1$, $p_i > 0$, *and* $a_i \in (0,1)$ *for* $i = 1, \cdots, n-1$, $c_1(0) > 0$, $c_i(0) \geq 0$ *for* $i = 2, \cdots, n$. *Let parameters be chosen such that there exists a locally asymptotically stable positive steady state. Let* c_i^0 *be in the basin of attraction of this steady state, then estimates of Theorem 9.25 hold also for* $n > 2$.

Figure 9.3 *(facing page)*: Comparison of exact solution and quasi steady state approximation. Panel (a) shows the exact solution $c_{1,\varepsilon}$ together with the quasi steady state approximation. Panel (b) shows an enlargement taken from the dashed box in Panel (a). Panels (c) and (d): analogous visualization for $c_{2,\varepsilon}$. Panels (e) and (f) compare time evolution of s_ε and the corresponding quasi-steady state approximation for different time scales. Panels (g) and (h) show correction of quasi steady state approximation s using the initial layer $\zeta_0(t/\varepsilon)$. In all Panels: $a_1 = 0.6$, $p_1 = 1$, $d_2 = 0.1$, $k = 10^{-7}$.

(a)

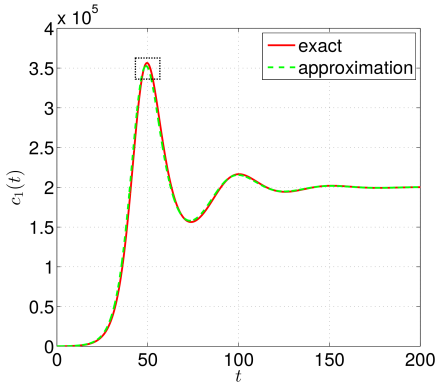
x 10^5
exact
approximation
$c_1(t)$
t

(b)

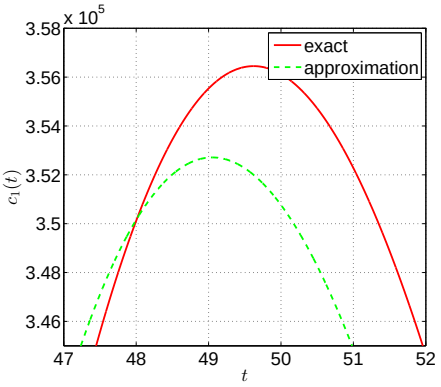
x 10^5
exact
approximation
$c_1(t)$
t

(c)

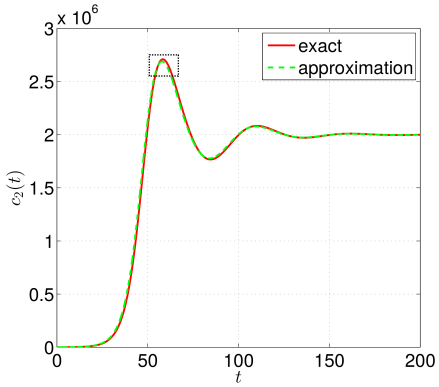
x 10^6
exact
approximation
$c_2(t)$
t

(d)

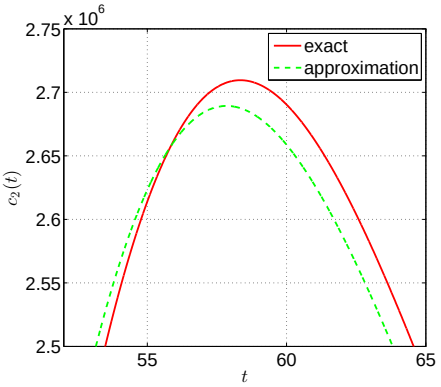
x 10^6
exact
approximation
$c_2(t)$
t

(e)

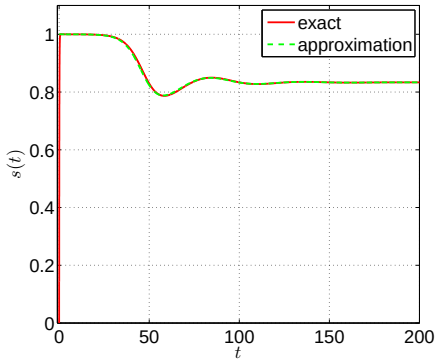
exact
approximation
$s(t)$
t

(f)

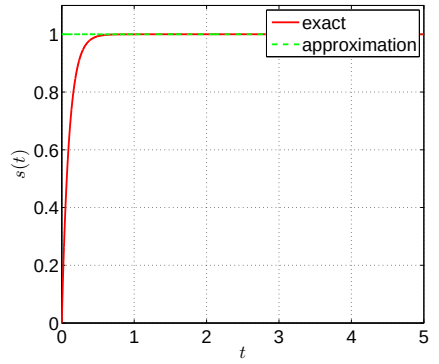
exact
approximation
$s(t)$
t

(g)

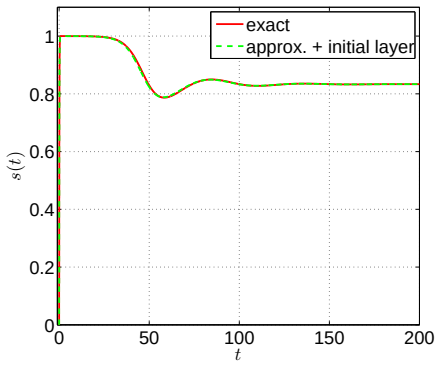
exact
approx. + initial layer
$s(t)$
t

(h)

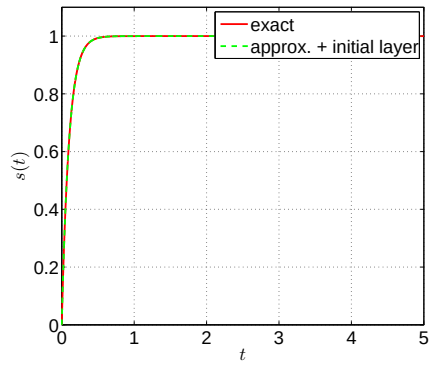
exact
approx. + initial layer
$s(t)$
t

PROOF
Statements (i) and (iii) from Lemma 9.24 are independent of n. The analogue to statement (ii) follows from Lemma A.8. The analogue to statement (iv) follows from the assumptions on linear stability of the equilibrium. ■

Remark 9.30
We notice that the reduced system (8.12) *and the unreduced system* (8.11) *possess the same steady states. Propositions 9.25 and 9.29 imply that if a steady state of the reduced system is linearly stable, then the corresponding steady state for the unreduced system is also linearly stable.*

Since (in)stability of the equilibrium with zero cell counts is of special biological interest, we note following.

Remark 9.31
The trivial steady state ($\bar{c}_1 = ... = \bar{c}_n = 0$) of the reduced system is linearly (un)stable, if and only if the corresponding semi-trivial equilibrium ($\bar{c}_{1,\varepsilon} = ... = \bar{c}_{n,\varepsilon} = 0$, $\bar{s}_\varepsilon = 1$) of the unreduced system is linearly (un)stable. Therefore, linear stability of the reduced system corresponds to linear stability of the full system. For more details refer to Appendix H.

Remark 9.32
(Comparison of assumptions 9.1-9.4 to assumptions of Tikhonov's Theorem)

In this Remark, we compare the assumptions of Theorem 9.21 from this Chapter to the Assumptions of Tikhonov's Theorem.

(i) *Regularity of the right hand-side: Tikhonov's Theorem requires that the right hand-side is continuous and fulfills the Lipschitz-condition from Definition 8.1 on the finite interval $[0, T]$ (Assumption 8.2). In the proof of Tihkonov's Theorem, the singular perturbation problem is reformulated as a regular perturbation problem. The Lipschitz condition is required to obtain existence of solutions of the regular perturbation problem for small positive ε. In Theorem 9.21, we assume higher regularity of the right hand-side, namely C^3 (Assumption 9.1 (i)). We do not explicitly assume the Lipschitz condition. To obtain existence and uniqueness of solutions for small $\varepsilon > 0$, we construct the extended functions $\tilde{\mathbf{f}}$, $\tilde{\Phi}$ (Definition 9.11), which fulfill a Lipschitz condition (Remark 9.12). The Assumptions of Theorem 9.21 guarantee that the solutions of the studied singular perturbation problem problem stay in a region, where $\mathbf{f}$, Φ and the extensions $\tilde{\mathbf{f}}$, $\tilde{\Phi}$ coincide.*

(ii) *Existence of isolated root: Theorem 9.21 and Tikhonov's Theorem require that the fast equation possesses a real isolated root (Assumptions 9.1 (ii) and 8.3).*

(iii) *Existence of solution of the reduced problem: Theorem 9.21 and Tikhonov's Theorem require that the reduced problem possesses a unique solution, which is bounded (on [0,T] in case of Tikhonov's Theorem and on the infinite time interval in case of Theorem 9.21), see Assumptions 9.2 and 8.5.*

(iv) *Attractiveness of the root: If we restrict ourselves to autonomous systems, the fast equation has the form* $\varepsilon \frac{d}{dt} v = g(\mathbf{u}, v)$. *Here,* $\mathbf{u} \in \mathcal{U}$ *denotes the slow variable and* $v \in \mathcal{V}$ *denotes the fast variable. The root of the fast equation is a function* $\Psi : \mathcal{U} \to \mathcal{V}$ *fulfilling* $g(\mathbf{u}, \Psi(\mathbf{u})) = 0$, *for all* $\mathbf{u} \in \mathcal{U}$. *In the context of Tikhonov's Theorem,* Ψ *is denoted as* Φ *(Assumption 8.3), in case of Theorem 9.21, it is denoted as* φ *(Assumption 9.1 (ii)). Both theorems require that, if we fix* $\mathbf{u}$ *from a predefined set, the root* $\Psi(\mathbf{u}) \equiv const$ *is a locally asymptotically stable equilibrium of* $\frac{d}{dt} v = g(\mathbf{u}, v)$. *In case of Tikhonov's Theorem, this is formulated in Assumption 8.4. In case of Theorem 9.21, this is formulated in Assumption 9.3(i). Assumption 9.3(i) requires that the eigenvalue of the linearization* $\partial_v g(\mathbf{u}, v)$ *is negative and bounded away from zero on the set* $\{(\mathbf{A}(t), \Psi(\mathbf{A}(t))) \mid t \geq 0\}$, *where* $\mathbf{A}$ *is the solution of the reduced problem.*

(v) *Initial conditions from the basin of attraction: Both Theorems require assumptions on the initial data of the fast variable* v^0. *In case of Tikhonov's Theorem, it is sufficient to fix the slow variable at its initial value* $\mathbf{u}^0$ *and to let the fast variable evolve under this condition. In detail, we assume that* v^0 *is in the basin of attraction of the steady state* $\Psi(\mathbf{u}^0)$ *of the equation* $\varepsilon \frac{d}{dt} v = g(\mathbf{u}^0, v)$. *In case of Theorem 9.21, we need more. Since we consider an infinite time interval, it is not enough to fix the slow variable at its initial condition* $\mathbf{u}^0$ *to study dynamics of the fast variable. Instead, we study dynamics of the fast variable in the neighborhood of the trajectory of the reduced system. Denote the trajectory of the reduced system as* $\{(\mathbf{A}(t), \Psi(\mathbf{A}(t))) \mid t \in \mathbb{R}_0^+\}$. *Assumption 9.3 (ii) requires that the trajectory* $\Psi(\mathbf{A}(t))$ *is attractive, in the sense, that the solution of the non-autonomous system* $\frac{d}{dt} v = g(\mathbf{A}(t), v)$ *for initial condition* v^0 *approaches the curve* $\Psi(\mathbf{A}(t))$ *for* $t \to \infty$.

(vi) *Attractiveness of the solution of the reduced system: Theorem 9.21 requires one assumption that has no counterpart in the Tikhonov setting. We consider the right hand-side of the reduced slow equation* $\mathbf{f}(\mathbf{u}, \Psi(\mathbf{u}))$. *It is required that fundamental solutions of its linearization along trajectories of the reduced system for initial condition* $\mathbf{u}^0$ *are exponentially decaying. This means that the linear non-autonomous system with right hand-side* $D_u \mathbf{f}(\mathbf{u}, \Psi(\mathbf{u}))|_{\mathbf{u}=\mathbf{A}(t)}$ *has only decaying solutions. Here,* $\mathbf{A}(t)$ *is the solution of the reduced system for initial data* $\mathbf{u}^0$. *Practically, this means that trajectories of the reduced system starting in the neighborhood of* $\mathbf{u}^0$ *approach* $\mathbf{A}(t)$ *for long times.*

9.6 Summary

In this Chapter, we prove that solutions of system (9.1)-(9.2) are close to solutions of the reduced system (quasi steady state approximation) under Assumptions 9.1-9.4. In the proof, we first analyze the approximation of the fast equation by the quasi steady state approximation and standard initial layers (Proposition 9.18). For technical convenience, we first use a localized version of the right hand-side (Definition 9.11). Based on the approximation result for v_ε, we prove approximation of $\mathbf{u}_\varepsilon$ (Proposition 9.20). Combination of both yields that the difference of solutions of the reduced system and solutions of (9.1)-(9.2) is of order ε on the infinite time interval (Theorem 9.21). We finally apply the proved theorem to the stem cell model (2.3) introduced in Chapter 2. The model fulfills assumptions of Theorem 9.21 for initial data in the basin of attraction of a linearly stable positive equilibrium (Lemma 9.24). Application of the theorem then yields that solutions of the reduced system are close to exact solutions for such initial data (Theorems 9.25 and 9.29).

CHAPTER 10

CONCLUDING REMARKS

In this thesis, new models of acute leukemias have been developed. New features of the models are

(i) Leukemic stem cells and leukemic non-stem cells are able to perform self-renewal. This assumption is based on experimental knowledge showing that besides HSCs also healthy non-stem cells can perform self-renewal under stress conditions, such as after bone marrow transplantation, [14, 185, 214].

(ii) The models implement and compare different aspects of interaction between leukemic and healthy cells. These are competition for survival factors or increased death rates in case of overcrowded marrow space. Furthermore, the models take into account that leukemic cells can either respond to hematopoietic growth factors or expand independently of them. These assumptions are based on experimental data showing that cells from different patients may behave differently under signal stimulation, [8, 54, 55, 93, 137, 146, 192, 206, 229]. Independence of cell expansion from regulatory factors is considered to be one important hallmark of cancers, [94].

(iii) The models can be extended to account for the competition between multiple leukemic clones. Recent experimental data show that leukemias are multi-clonal diseases and that contribution of individual clones to total cell mass changes over time, [9, 56].

Two different models have been analyzed in detail. Both models have the form of systems of nonlinear ordinary differential equations describing dynamics of the different hematopoietic and leukemic cell types. Each cell type is characterized by (a) proliferation rate, (b) fraction of self-renewal, describing, which fraction of the cells originating from a division is of the same type as the parent cell, (c) death rate. Behavior of leukemic cells and their interaction with hematopoietic cells differ in both models as follows:

- **Model 1**: Leukemic and hematopoietic cells depend on stimulation by hematopoietic cytokines. Differentiation of cells of both lineages increases, if cytokine stimulation decreases. Post-mitotic leukemic and hematopoietic cells absorb cytokine molecules, as motivated by data on receptor expression, [126, 206].

- **Model 2**: Only hematopoietic cells depend on cytokines. Leukemic cells expand independently of environmental factors, [98]. Overcrowding of marrow niche space causes cell death in healthy and leukemic cells, [34,67,107, 128,243]. Only post-mitotic hematopoietic cells absorb cytokine molecules.

The two models can be seen as two extreme cases of a continuum: In Model 1, leukemic cells are fully dependent on hematopoietic growth factors, whereas in Model 2 they are fully independent. Cytokine dynamics in both models are described using a Hill-function increasing for decreasing concentrations of the cell types absorbing cytokines. This approach is based on a quasi-steady state approximation motivated by the different time scales of cell division and cytokine kinetics, [30]. Alternatively, cytokine dynamics can be described using an additional ODE. In Chapters 8 and 9 it has been shown rigorously that solutions of the model with explicit cytokine dynamics converge to solutions of the model based on the quasi-steady state approximation, if cytokine dynamics is fast enough. We first studied the approximation on a finite time interval using Tikhonov's Theorem and then we extended the approximation result to the infinite time interval using additional assumptions.

Although the presented results are robust with respect to model assumptions and parameters, the models include important simplifications. The first simplification is neglecting of space and physical interactions between cells. It is known that immature cells grow in specialized niches within bone marrow, [136, 166, 180, 205], where cell-cell contacts, mechanical interactions, [136, 205], and interaction with the nervous system, [95], play an important role. Up to now the complexity of these micro-environments is not well understood. For this reason, the considered models take into account only one cytokine. The developed models focus on the dynamics of large populations of cells. For this reason, individual cells and physical interaction between them are not explicitly considered. A second simplification is neglecting of replicative senescence (Hayflick limit). This allows stem cells to divide infinitely many times. Nevertheless, models of the blood system suggest that even if Hayflick limit is considered, dynamic properties of the system remain similar, [158]. The consideration of multiple clones is a first step to include inter-cellular variability into the models. Recent experiments, although mainly performed in non-hematopoietic tissues, suggest that even genetically identical cells may behave differently, [32, 89]. One possible explanation for this is the so called phenotypic switching describing non-genetic mechanisms leading to adaptation of cell behavior to environmental influences. Nevertheless, these findings

are still under debate, [245], and, therefore, not considered in the current versions of the model.

In the following, we discuss important conclusions form the work presented in this thesis and relate them to biological and clinical questions.

Mathematical study: The two considered models show common features as well as important differences. Both models possess uniformely bounded, unique, non-negative solutions for non-negative initial conditions. In both models, there exists a healthy steady state with positive hematopoietic cell concentrations and absence of leukemic cells. Similarly, for both models there exist steady states characterized by positive leukemic cell counts and absence of hematopoietic cells, provided that parameters of leukemic stem cells allow for their expansion. For suitable parameters, both models further exhibit steady states, where leukemic and hematopoietic cells can coexist. Nevertheless, in Model 1 the subspace of parameters compatible with coexistence has Lebesgue-measure zero in parameter space. In this case, there always exists a one dimensional manifold of steady states, which is a center manifold. Depending on parameters, the center manifold can either be attractive or repulsive. In Model 2, there exists a wide parameter range leading to isolated steady states, where healthy and malignant cells can coexists. The presence of leukemic cells and consecutive overcrowding of marrow space impose increased death rates on the healthy cell population. The coexistence is observed, if and only if this cell loss can be compensated by increased cytokine stimulation of healthy cells. Naturally, in Model 1 such a behavior is not possible, since both, healthy and leukemic cells, respond to the same cytokine. Therefore, increased cytokine levels lead to stimulation of hematopoietic and leukemic cells, which results in out-competition of hematopoietic cells, due to the intrinsic growth advantages of leukemic cells. The steady states with coexisting hematopoietic and leukemic cells can be interpreted as chronic hematopoietic diseases such as MGUS or Waldenström's disease, [129, 226]. Also in Model 2, there exists a parameter subspace of Lebesgue measure zero leading to existence of a center manifold. Differently from Model 1, these parameters do not imply existence of a manifold of steady states. In the minimal case (4 equations) the center manifold is always attractive. Model 2 exhibits further steady states without leukemic cells, where overcrowding of hematopoietic cells leads to increased apoptosis rates. These steady states show high counts of immature cells as it is observed for example in myelodysplastic syndromes, [53]. For proper parameters, both models show dynamics consistent with acute leukemias, i.e., increase of bone marrow blast fractions from 5% to 90% within some weeks. For a version of the models including multiple leukemic clones, we show analytically that in case of Model 1 only clones with maximal self-renewal survive for long times. If all clones have identical self-renewal and differ only with respect to proliferation rates, no selection is observed and all clones show long-term survival. In case

of Model 2, only clones with maximal expansion rates can survive. Coexistence with hematopoietic cells is established, whenever signal stimulation can increase expansion rates of hematopoietic cells to larger values than expansion rates of leukemic clones. Finally, we have shown that solutions of the reduced model systems, which are based on a quasi-steady state approximation of cytokine dynamics, are close to solutions of a singular perturbation problem, where cytokine dynamics are modeled by an additional ODE. We provide bounds for the difference of solutions of both systems with respect to the L^∞ norm on the *infinite* time interval and under the assumption that cytokine dynamics are fast enough compared to cell proliferation and differentiation.

A combination of mathematical analysis and application of the proposed models to patient data has led to new insight into different open questions of acute leukemias.

Dynamic properties of leukemic stem cells: In primates, dynamics of stem cells of the hematopoietic system is not directly observable, due to unavailability of appropriate stem cell markers, [68, 104, 147, 202]. The proposed models allow to systematically characterize leukemic stem cell properties leading to expansion of malignant cells. Both models suggest that an increase of self-renewal is always sufficient for that purpose, whereas an increased proliferation alone is in general not sufficient. This finding challenges the classical paradigm of cancer biology assuming that high proliferation is a hallmark of malignant cells, [94, 204]. For both models, it is possible to find parameter regimes, where malignant cells of all stages proliferate slower than their benign counterparts. Nevertheless, the exact conditions leading to leukemia stem cell expansion differ for both models. In case of Model 1, under the additional assumptions that stem cells do not die, it is necessary and sufficient that LSCs possess higher self-renewal than HSCs. Under the same assumptions, higher proliferation of LSCs alone does not lead to out-competition of the healthy cells. In case of positive death rates for stem cells, it is sufficient that either LSCs have smaller death rates, higher proliferation or higher self-renewal than HSCs, provided that HSCs and LSCs differ only with respect to one parameter. In Model 2, it is necessary and sufficient for LSC expansion that LSC self-renewal is larger than one half, provided that LSCs do not die. If LSCs have positive death rates, then this condition is necessary but not sufficient, since either self-renewal or proliferation have to be high enough to compensate for cell loss due to death. In Model 2, it is assumed that leukemic cells are independent of hematopoietic factors. Therefore, it is intuitive that, different from Model 1, conditions leading to LSC expansion do not depend on parameters describing hematopoietic cell dynamics. The scenario that leukemic cells are totally independent of hematopoietic growth factors allows feedback mechanisms of the hematopoietic system to selectively increase hematopoietic cell production. This may lead to coexistence of hematopoietic and leukemic cells with reason-

able steady state hematopoietic cell concentrations. In this respect, independence of leukemic cells on cytokines may be advantageous for patient survival. Nevertheless, independence of hematopoietic growth factors leads to fast expansion of leukemic cells, since they do not respond to limitations of environmental factors. In this sense, such leukemias are more aggressive. Many of the predicted LSC parameter constellations allowing for leukemic cell expansion can be linked to observed dynamics of different hematological diseases such as different AML, [216], (smoldering) macroglobulinemia Waldenström, [129, 226], smoldering myeloma or MGUS, [23, 127].

Stemness property: As the stemness property of a cell population we understand the ability of this population to give rise to a cell line and to maintain this cell line in a steady state. There is increasing evidence that the stemness property depends on cell intrinsic determinants, such as gene expression networks leading to self-renewal, and on cell extrinsic factors, such as environmental signals and mechanical contact to neighbor cells. Experimental results suggest that leukemic cells influence the micro-environment in a way that the hematopoietic stem cell population cannot efficiently fulfill their function and eventually decline, [15, 50, 197]. The models proposed in this thesis support the idea that stemness is a relative property, emerging from environmental features and from competition between cell lines. Presence of leukemic cells changes the environment in a way that hematopoietic stem cells do not possess the stemness property under the altered conditions: In Model 1, the existence of leukemic cell alters cytokine concentrations in a way that stimulation of HSCs is to weak to induce sufficient self-renewal. In this model, either all hematopoietic cell types survive or all of them go extinct in a steady state. This is different in Model 2, where, in dependence of LSC parameters, it is possible that HSCs go extinct, while a downstream hematopoietic progenitor cell type acquires stemness properties and maintains the lineage. This observation demonstrates how leukemic cell properties determine, which hematopoietic cell type can act as stem cell population. In vivo this phenomenon would lead to decline of hematopoietic cell counts, since progenitor cells only possess the ability to divide a finite number of times. These implications raise the question, whether it could be possible to treat leukemias using interventions that modify the micro-environment.

Heterogeneity of the disease: The clinical picture of acute leukemias is very heterogeneous. The proposed models suggest different origins of this heterogeneity. The first source of inter-individual heterogeneity might be the mode of competition between leukemic cells and hematopoietic cells. This follows from the above comparison of dynamic properties of Model 1 and Model 2. A second source of heterogeneity are dynamic properties of leukemic cells such as proliferation rates and fractions of self-renewal and their relation to the respective quantities of hematopoietic cells. Model analysis and simulations imply that parameters of

leukemic cells decide, whether the system converges to states, where both lineages can coexist, whether one of the lineages goes extinct or whether the system shows complex dynamic behavior including oscillations. A further implication of the models is that similar dynamic features may originate from different parameter regimens and different modes of interaction. For this reason, similar clinical pictures do not allow to conclude about similar mechanisms of disease and similar adequate treatment strategies. Fitting of a six-equation version of Model 1 to patient data shows that self-renewal and proliferation of LSCs differ strongly between patients, even if patients carry the same leukemogenetic key mutation (FLT3-ITD). For the considered group of 40 patients the estimated leukemic stem cell properties correlate with patient prognosis. This finding underlines that stem cell properties may have a strong impact on clinical course and outcome of the disease. A third source of heterogeneity may originate from clonal selection processes. The models suggest that intrinsically different leukemic cell clones compete with each other. During the course of the disease the contribution of the different clones to the leukemic cell mass changes. This may explain why properties of the leukemic cell mass change over time. Depending on the properties of the individual clones, different clinical pictures with different numbers of contributing clones can be observed.

Impact of stem cells on clinical dynamics: Division kinetics and self-renewal rates of LSCs and less primitive leukemia blast cells are poorly understood, since these parameters cannot be monitored in vivo, [56, 68, 104, 147, 202, 208]. This issue is however, of biological and clinical significance as not only the absolute number of leukemic cells may determine the clinical course but also the number of LSCs among them and their dynamical properties such as proliferation and self-renewal rates. This is illustrated by the following two hypothetical scenarios. (1) A small number of LSCs surviving induction chemotherapy may drastically reduce overall survival, if they rapidly expand after cessation of the treatment. (2) A small number of LSCs surviving induction therapy but remaining dormant or slowly cycling after cessation of therapy may lead to relapse after many years and a longer period of survival than in scenario (1). This reasoning underlines, that even if it were possible to directly measure LSC numbers, e.g., based on surface markers, it would be important to know their dynamic behavior. The proposed models allow to simulate, which impact properties of different cell types have on the dynamics of the disease. Simulations using a calibrated version of Model 1 (3 hematopoietic and 3 leukemic cell types) suggest that properties of the leukemic mitotic non-stem cell compartment have little impact on the time elapsing before detection of the disease compared to properties of LSCs. This finding implies that LSC properties are a major determinant of the clinical course. Consequently, it should be possible to draw conclusions about LSC behavior based on clinical observations. In Chapter 6, we have estimated LSC properties based on bone marrow aspiration data of patients with relapsing leukemias. The estimation procedure

allows to restrict LSC proliferation rates and self-renewal to a one dimensional manifold in the two dimensional parameter space. Although estimated stem cell parameters can only be treated as surrogate markers of stem cell behavior due to simplifications in the model, the estimated LSC properties correlate with patient survival. This finding is in line with the hypothesis that leukemic stem cells trigger relapse and that, consequently, their dynamic behavior influences the dynamic of the disease, [35,41,47,88,210].

Mechanisms of clonal selection and relapse: The proposed models are extended to describe dynamics of multiple leukemic clones. This approach is motivated by recent genetic studies showing that leukemic cells originate from multiple clones with different mutation profiles, [9,56]. Nevertheless, the impact of the mutations detected in the leukemic cells is not well understood, [56, 208]. The proposed mathematical models help to understand how dynamic properties of individual clones can influence the selection process. Simulations of multi-clonal versions of both models suggest that at primary diagnosis cells with high self-renewal and high proliferation dominate, whereas at relapse cells with high self-renewal and slow proliferation are present. This finding seems plausible, since during the early phase of disease high self-renewal and high proliferation lead to rapid expansion of cells. Since cycling cells have a higher probability of being killed by classical chemotherapy, they are preferentially eliminated by the treatment. In relapse dominating clones show high self-renewal and slow proliferation. The considered models as well as other works e.g., [83, 131, 157, 170] suggest that high self-renewal of immature cells leads to fast expansion of a cell population in comparison to low self-renewal. In this sense, high self-renewal can partially compensate for disadvantages caused by slow proliferation and is, therefore, a driving force of relapse. Interestingly, in model simulations the number of leukemic clones contributing at least 1% to the total leukemic cell mass is rarely higher than 5, even if the number of clones present at the beginning of simulations is higher than 50. This finding is in line with data from recent sequencing studies, [9, 56]. This result demonstrates that the dynamic interaction between the different clones restricts the number of clones significantly contributing to the total cell mass. The models predict that more sensitive methods may detect high numbers of small clones, which serve as a reservoir of cells that can trigger relapse. This finding is in line with the hypothesis that relapse might be triggered by clones already present at diagnosis and does not require occurrence of additional mutations, [46, 148, 227]. Fitting of the model to patient data supports this view. Especially in cases of acute leukemias duration of treatment is relatively short. Establishment of treatment-related mutations leading to drug resistance is less probable than in chronic leukemias, where drugs are administered over months or years. Comparison of simulation results of both models reveals that these conclusions are robust with respect to the assumptions made on interactions between the different cell lines. The reported findings may be applied to better under-

stand functional consequences of detected mutations, since they suggest that the combination of genetic hits present at relapse leads to high self-renewal and slow proliferation.

Clinical applications and new hypotheses: This work has led to the following new hypotheses and possible clinical implications:

(1) The proposed models allow to derive estimates for LSC proliferation and self-renewal based on clinical data, which correlate with clinical prognosis of individual patients. In recent years a growing number of genetic, [56, 64, 117], epigenetic, [90] and regulatory aberrations, [81, 159] relevant risk stratification has been described. Despite this knowledge the impact of these factors on clinical course and on cell properties is not well-defined [56, 64, 88, 208]. In general, the impact of a given parameter may depend on the absence or presence of other, still unknown, parameters, [17, 64, 78, 179]. Genetic studies suggest that leukemogenetic hits may vary considerably among patients, [109, 110, 196]. Variability in survival of patients with the same risk factors underscores the complexity of the interplay of different detected aberrations. Model based estimation of LSC parameters might be a complementary and more direct approach to risk-stratification of patients, which allows to optimize treatment and follow-up strategies.

(2) The models suggest that cells at relapse of acute leukemias show high self-renewal and slow proliferation. The slow proliferation leads to resistance to classical cytotoxic drugs, while high self-renewal results in efficient expansion of cell populations. Selection of such cells under treatment explains the observed resistance of relapsed diseases to multiple therapeutic agents after relatively short treatment periods. This view does not require occurrence of new mutations under treatment to explain resistance.

(3) The models provide insights in dynamic cell properties at different time-points of the disease, namely high proliferation and self-renewal at primary diagnosis and slow proliferation but high self-renewal at relapse. This finding may help to assign functional consequences to mutations observed at different stages of the disease, which are yet unknown, [56, 208].

(4) The models suggest that clonal competition limits the number of large clones. Nevertheless, small clones may persist and serve as a reservoir of cells that trigger relapse. This view suggests that assessment of genetic aberrations of small clones may be a better prognostic marker, than assessment of aberrations of the clones that dominate at diagnosis, as it is current practice.

BIBLIOGRAPHY

[1] ABKOWITZ, J. L., CATLIN, S. N., MCCALLIE, M. T., AND GUTTORP, P. Evidence that the number of hematopoietic stem cells per animal is conserved in mammals. *Blood 100* (2002), 2665–2667.

[2] ABLAIN, J., AND DE THE, H. Revisiting the differentiation paradigm in acute promyelocytic leukemia. *Blood 117* (2011), 5795–5802.

[3] ADIMY, M., AND CRAUSTE, F. Modeling and asymptotic stability of a growth factor- dependent stem cell dynamics model with distributed delay. *Discrete Contin. Dyn. Syst. Ser. B 8* (2007), 19–38.

[4] ADIMY, M., CRAUSTE, F., AND RUAN, S. A mathematical study of the hematopoiesis process with applications to chronic myelogenous leukemia. *SIAM J Appl Math 65* (2005), 1328–1352.

[5] ADIMY, M., CRAUSTE, F., AND RUAN, S. Modelling hematopoiesis mediated by growth factors with applications to periodic hematological diseases. *Bull Math Biol 68* (2006), 2321–2351.

[6] AGARWAL, R., AND O'REGAN, D. *An Introduction to Ordinary Differential Equations*. Springer, Heidelberg, 2008.

[7] ALARCON, T., GETTO, P., MARCINIAK-CZOCHRA, A., AND VIVANCO, M. A model for stem cell population dynamics with regulated maturation delay. *Discr. Cont. Dyn. Systems Suppl* (2011), 91–94.

[8] ALMEIDA, J., DEL CAÑIZO, C., ORFAO, A., HERNANDEZ, J., HERNANDEZ, D., GALENDE, J., CABALLERO, D., GARCIA-SANZ, R., AND SAN MIGUEL, J. In vitro autonomous proliferation in ANLL: Clinical and biological significance. *Leuk Res 19* (1995), 411–16.

[9] ANDERSON, K., LUTZ, C., VAN DELFT, F., BATEMAN, C., GUO, Y., COLMAN, S., KEMPSKI, H., MOORMAN, A., TITLEY, I., SWANSBURY, J., KEARNEY, L., ENVER, T., AND GREAVES, M. Genetic variegation of clonal architecture and propagating cells in leukaemia. *Nature 469* (2011), 356–61.

[10] ANDREY, L. Chaos in cancer. *Med. Hypotheses 28* (1989), 143–144.

[11] ARINO, O., AND KIMMEL, M. Stability analysis of models of cell production systems. *Math Modelling 7* (1986), 1269–1300.

[12] ARMITAGE, P., BERRY, G., AND MATTHEWS, J. *Statistical Methods in Medical Research, 4th ed.* Blackwell Science Ltd, Oxford, UK, 2002.

[13] ASHKENAZI, R., GENTRY, S., AND JACKSON, T. Pathways to tumorigenesis–modeling mutation acquisition in stem cells and their progeny. *Neoplasia 10* (2008), 1170–82.

[14] ASTORI, G., MALANGONE, W., ADAMI, V., RISSO, A., DOROTEA, L., AND FALASCA, E. A novel protocol that allows short-term stem cell expansion of both committed and pluripotent hematopoietic progenitor cells suitable for clinical use. *Blood Cells Mol Dis 27* (2001), 715–24.

[15] AYALA, F., DEWAR, R., KIERAN, M., AND KALLURI, R. Contribution of bone microenvironment to leukemogenesis and leukemia progression. *Leukemia 23* (2009), 2233–41.

[16] BACHAS, C., SCHUURHUIS, G., ASSARAF, Y., KWIDAMA, Z., KELDER, A., WOUTERS, F., SNEL, A., KASPERS, G., AND CLOOS, J. The role of minor subpopulations within the leukemic blast compartment of AML patients at initial diagnosis in the development of relapse. *Leukemia 26* (2012), 1313–20.

[17] BACHER, U., HAFERLACH, C., KERN, W., HAFERLACH, T., AND SCHNITTGER, S. Prognostic relevance of FLT3-TKD mutations in AML: the combination matters - an analysis of 3082 patients. *Blood 111* (2008), 2527–37.

[18] BALEA, S., HALANAY, A., JARDAN, D., NEAMTU, M., AND SAFTA, C. Stability analysis of a feedback model for the action of the immune system in leukemia. *Math. Model. Nat. Phenom. 9* (2014), 108–132.

[19] BANASIAK, J., AND LACHOWICZ, M. *Methods of Small Parameter in Mathematical Biology*. Springer, Heidelberg, 2014.

[20] BARREIRA, L., AND VALS, C. *Measure Theory, Vol 1*. Springer, Heidelberg, 2007.

[21] BARREIRA, L., AND VALS, C. *Ordinary Differential Equations - Qualitative Theory*. American Mathematical Society, Providence, RI, 2010.

[22] BAUM, M., CHAPLAIN, M., ANDERSON, A., DOUEK, M., AND VAIDYA, J. Does breast cancer exist in a state of chaos? *Eur J Cancer 35* (1999), 886–891.

[23] BEJAR, R., LEVINE, R., AND EBERT, B. Unraveling the molecular pathophysiology of myelodysplastic syndromes. *J Clin Oncol. 29* (2011), 504–514.

[24] BELAIR, J., MACKEY, M., AND MAHAFFY, J. Age-structured and two-delay models for erythropoiesis. *Math Biosci 128* (1995), 317–346.

[25] BELLAN, C., STEFANO, L., GIULIA DE, F., ROGENA, E., AND LORENZO, L. Burkitt lymphoma versus diffuse large B-cell lymphoma: a practical approach. *Hematol Oncol. 28* (2010), 53–56.

[26] BERGER, D., ENGELHARDT, R., AND HENSS, H. Basic principles of chemotherapy. In *Concise manual of hematology and oncology.*, D. Berger, R. Engelhardt, H. Henss, and M. R, Eds. New York: Springer, 2008, pp. 65–68.

[27] BERGER, M., MOTTA, C., BOIRET, N., AUBLET-CUVELIER, B., BONHOMME, J., AND TRAVADE, P. Membrane fluidity and adherence to extracellular matrix components are related to blast cell count in acute myeloid leukemia. *Leuk Lymphoma 15* (1994), 297–302.

[28] BEWICK, V., CHEEK, L., AND BALL, J. Statistics review 12: survival analysis. *Crit Care 8* (2004), 389–394.

[29] BHATLA, T., WANG, J., MORRISON, D., RAETZ, E., BURKE, M., BROWN, P., AND CARROLL, W. Epigenetic reprogramming reverses the relapse-specific gene expression signature and restores chemosensitivity in childhood b-lymphoblastic leukemia. *Blood 119* (2012), 5201–10.

[30] BOGNER, V., KEIL, L., KANZ, K., KIRCHHOFF, C., LEIDEL, B., MUTSCHLER, W., AND BIBERTHALER, P. Very early posttraumatic serum alterations are significantly associated to initial massive RBC substitution, injury severity, multiple organ failure and adverse clinical outcome in multiple injured patients. *Eur J Med Res. 14* (2009), 284–291.

[31] BONNET, D., AND DICK, J. Human acute myeloid leukemia is organized as a hierarchy that originates from a primitive hematopoietic cell. *Nat Med. 3* (1997), 730–737.

[32] BROCK, A., CHANG, H., AND HUANG, S. Non-genetic heterogeneity—a mutation-independent driving force for the somatic evolution of tumours. *Nat Rev Genetic 10* (2009), 336–42.

[33] BUCCISANO, F., MAURILLO, L., GATTEI, V., DEL POETA, G., DEL PRINCIPE, M., COX, M., PANETTA, P., CONSALVO, M., MAZZONE, C., NERI, B., OTTAVIANI, L., FRABONI, D., TAMBURINI, A., LO-COCO, F., AMADORI, S., AND VENDITTI, A. The kinetics of reduction of minimal residual disease impacts on duration of response and survival of patients with acute myeloid leukemia. *Leukemia 20* (2006), 1783–9.

[34] BUECHNER, T., AND HEINECKE, A. The role of prognostic factors in acute myeloid leukemia. *Leukemia 10 Suppl. 1* (1996), S28–S29.

[35] BUSS, E., AND HO, A. Leukemia stem cells. *Int. J. Cancer 129* (2011), 2328–2336.

[36] BUXTON, I., AND BENET, L. Pharmacokinetics: The dynamics of drug absorption, distribution, metabolism and elimination. In *Goodman and Gilman's The Pharmacological Basis of Therapeutics.*, L. Brunton, B. Chabner, and B. Knollman, Eds. New York: McGraw Hill, 2011, pp. 17–41.

[37] CALVI, L., ADAMS, G., WEIBRECHT, K., WEBER, J., OLSON, D., KNIGHT, M., MARTIN, R., SCHIPANI, E., DIVIETI, P., BRINGHURST, F., MILNER, L., KRONENBERG, H., AND SCADDEN, D. Osteoblastic cells regulate the haematopoietic stem cell niche. *Nature 425* (2003), 841–846.

[38] CARLO-STELLA, C., CESANA, C., REGAZZI, E., FALZETTI, F., AVERSA, F., RIZZOLI, V., MARTELLI, M., AND TABILIO, A. Peripheral blood progenitor cell mobilization in healthy donors receiving recombinant human granulocyte colony-stimulating factor. *Exp Hematol. 28* (2000), 216–224.

[39] CARR, J. *Applications of Center Manifold Theory*. Springer, Heidelberg, 1981.

[40] CARTWRIGHT, G. E., ATHENS, J. W., AND WINTROBE, M. M. The kinetics of granulopoiesis in normal man. *Blood 24* (1964), 780–803.

[41] CHAN, K., HUANG, Y., AND CHEN, J. Understanding and targeting cancer stem cells: therapeutic implications and challenges. *Acta Pharmacol Sin. 34* (2013), 732–40.

[42] CHEN, L., GOLDENFELD, N., AND OONO, Y. Renormalization group theory for global asymptotic analysis. *Phys. Rev. Lett. 73* (1994), 1311–15.

[43] CHEN, L., GOLDENFELD, N., AND OONO, Y. Renormalization group and singular perturbations: Multiple scales, boundary layers, and reductive perturbation theory. *Phys. Rev. E 54* (1996), 376–394.

[44] CHEN, S., HUANG, Y., LIU, S., TSAI, F., SHYU, W., AND LIN, S. An overview of concepts for cancer stem cells. *Cell Transplant 20* (2011), 113–120.

[45] CHESSELLS, J. Relapsed lymphoblastic leukaemia in children: a continuing challenge. *Br J Haematol 102* (1998), 423–28.

[46] CHOI, S., HENDERSON, M., KWAN, E., BEESLEY, A., SUTTON, R., BAHAR, A., GILES, J., VENN, N., POZZA, L., BAKER, D., MARSHALL, G., KEES, U., HABER, M., AND NORRIS, M. Relapse in children with acute lymphoblastic leukemia involving selection of a preexisting drug-resistant subclone. *Blood 110* (2007), 632–9.

[47] CLEVERS, H. The cancer stem cell: premises, promises and challenges. *Nat Med 17* (2011), 313–319.

[48] COFFEY, D. Self-organization, complexity and chaos: the new biology for medicine. *Nat Med 4* (1998), 882–885.

[49] COLIJN, C., AND MACKEY, M. A mathematical model of hematopoiesis –i. periodic chronic myelogenous leukemia. *J Theor Biol 237* (2005), 117–132.

[50] COLMONE, A., AMORIM, M., PONTIER, A., WANG, S., JABLONSKI, E., AND SIPKINS, D. Leukemic cells create bone marrow niches that disrupt the behavior of normal hematopoietic progenitor cells. *Science 322* (2008), 1861–65.

[51] CRONKITE, E. P. Kinetics of granulopoiesis. *Clin. Haematol 8* (1979), 351–370.

[52] CROOKS, G. Lymphopoiesis. In *Williams Hematology*, K. Kaushansky, M. Lichtman, E. Beutler, T. Kipps, J. Prchal, and U. Seligsohn, Eds. McGraw Hill, New York, 2010, pp. 1095–1103.

[53] DAS, M., CHAUDHURI, S., AND LAW, S. Unveiling the paradoxical nature of myelodysplastic syndromes (MDS): Why hypercellular marrow strongly favors accelerated apoptosis. *Biochem Cell Biol. 91* (2013), 303–8.

[54] DEL CANIZO, C., GALENDE, J., ALMEIDA, J., BRUFAU, A., MOTA, A., AND SAN MIGUEL, J. In vitro growth in acute myeloblastic leukemia: clinico-biological correlations. *Leuk Lymphoma 36* (1999), 1–7.

[55] DEL CANIZO, M., BRUFAU, A., ALMEIDA, J., GALENDE, J., GARCIA MARCOS, M., MOTA, A., GARCIA R, FERNANDEZ CALVO, J., RAMOS, F., FISAC, P., ORFAO, A., AND SAN MIGUEL, J. In vitro growth in acute myeloblastic leukaemia: relationship with other clinico-biological characteristics of the disease. *Br J Haematol 103* (1998), 137–42.

[56] DING, L., LEY, T., LARSON, D., MILLER, C., KOBOLDT, D., WELCH, J., RITCHEY, J., YOUNG, M., LAMPRECHT, T., MCLELLAN, M., MCMICHAEL, J., WALLIS, J., LU, C., SHEN, D., HARRIS, C., DOOLING, D., FULTON, R., FULTON, L., CHEN, K., SCHMIDT, H., KALICKI-VEIZER, J., MAGRINI, V., COOK, L., MCGRATH, S., VICKERY, T., WENDL, M., HEATH, S., WATSON, M., LINK, D., TOMASSON, M., SHANNON, W., PAYTON, J., KULKARNI, S., WESTERVELT, P., WALTER, M., GRAUBERT, T., MARDIS, E., WILSON, R., AND DIPERSIO, J. Clonal evolution in relapsed acute myeloid leukaemia revealed by whole-genome sequencing. *Nature 481* (2012), 506–510.

[57] DINGLI, D., AND PACHECO, J. Stochastic dynamics and the evolution of mutations in stem cells. *BMC Biol 9* (2011), 41.

[58] DOMMANGE, F., CARTRON, G., ESPANEL, C., GALLAY, N., DOMENECH, J., BENBOUBKER, L., OHRESSER, M., COLOMBAT, P., BINET, C., WATIER, H., HERAULT, O., AND GOELAMS STUDY GROUP. CXCL12 polymorphism and malignant cell dissemination/tissue infiltration in acute myeloid leukemia. *FASEB J 20* (2006), 1913–1915.

[59] DOS SANTOS, R., AND DA SILVA, L. A possible explanation for the variable frequencies of cancer stem cells in tumors. *PLoS One 8* (2013), e69131.

[60] DOUMIC-JAUFFRET, M., KIM, P., AND PERTHAME, B. Stability analysis of a simplified yet complete model for chronic myelogenous leukemia. *Bull Math Biol 72* (2010), 1732–1759.

[61] DOUMIC-JAUFFRET, M., MARCINIAK-CZOCHRA, A., PERTHAME, B., AND ZUBELLI, J. A structured population model of cell differentiation. *SIAM J Appl Math 71* (2011), 1918–1940.

[62] DY, G., AND ADJEI, A. Principles of chemotherapy. In *Oncology- An Evidence-Based Approach*, A. Chang, D. Hayes, H. Pass, R. Stone, P. Ganz, T. Kinsella, J. Schiller, and V. Strecher, Eds. Heidelberg: Springer, 2006, pp. 14–40.

[63] ENGEL, C., SCHOLZ, M., AND LOEFFLER, M. A computational model of human granulopoiesis to simulate the hematotoxic effects of multicycle polychemotherapy. *Blood 104* (2004), 2323–2331.

[64] ESTEY, E. Acute myeloid leukemia: 2013 update on risk-stratification and management. *Am J Hematol 88* (2013), 318–27.

[65] EVERITT, B., AND HOTHORN, T. A lego system for conditional inference. *The American Statistician 60* (2006), 257–63.

[66] EVERITT, B., AND HOTHORN, T. *A Handbook of Statistical Analyses Using R, 2nd ed.* Chapman and Hall CRC, London, UK, 2010.

[67] FANIN, R., ZUFFA, E., FASOLA, G., DAMIANI, D., GALLIZIA, C., MICHIELI, M., MARCUZZI, P., RUSSO, D., VISANI, G., AND RESEGOTTI, L. Serum lactate dehydrogenase is an important risk determinant in acute lymphocytic leukemia. *Haematologica 74* (1989), 161–165.

[68] FELIPE RICO, J., HASSANE, D., AND GUZMAN, M. Acute myelogenous leukemia stem cells: from bench to bedside. *Cancer Lett. 338* (2013), 4–9.

[69] FENICHEL, N. Geometric singular perturbation theory for ordinary differential equations. *J Diff Eq 31* (1979), 53–98.

[70] FERRARA, F., AND SCHIFFER, C. Acute myeloid leukaemia in adults. *Lancet 381* (2013), 484–95.

[71] FLIEDNER, T. M. Kinetik und Regulationsmechanismen des Granulozytenumsatzes. *Schweiz Med Wochenschr. 104* (1974), 98–107.

[72] FOLEY, C., BERNARD, S., AND MACKEY, M. Cost-effective G-CSF therapy strategies for cyclical neutropenia: Mathematical modelling based hypotheses. *J Theor Biol 238* (2004), 754–763.

[73] FOLEY, C., AND MACKEY, M. Dynamic hematological disease: a review. *J Math Biol. 58* (2009), 285–322.

[74] FORMAN, S., AND ROWE, J. The myth of the second remission of acute leukemia in the adult. *Blood 121* (2013), 1077–82.

[75] FORSTER, O. *Analysis I, 11. Aufl.* Springer Spektrum, Wiesbaden, 2013.

[76] FRIED, W. Erythropoietin and erythropoiesis. *Exp Hematol 37* (2009), 1007–1015.

[77] FUERTINGER, D., KAPPEL, F., THIJSSEN, S., LEVIN, N., AND KOTANKO, P. A model of erythropoiesis in adults with sufficient iron availability. *J Math Biol. 66* (2013), 1209–40.

[78] GALE, R., GREEN, C., ALLEN, C., MEAD, A., BURNETT, A., HILLS, R., LINCH, D., AND MEDICAL RESEARCH COUNCIL ADULT LEUKAEMIA WORKING PARTY. The impact of FLT3 internal tandem duplication mutant level, number, size, and interaction with NPM1 mutations in a large cohort of young adult patients with acute myeloid leukemia. *Blood 111* (2008), 2776–84.

[79] GANTMACHER, F. *The theory of matrices 2*. Chelsea Publishing, 1964.

[80] GARRIDO, S., APPELBAUM, F., WILLMAN, C., AND BANKER, D. Acute myeloid leukemia cells are protected from spontaneous and drug-induced apoptosis by direct contact with a human bone marrow stromal cell line (HS-5). *Exp Hematol 29* (2001), 448–457.

[81] GENTLES, A., PLEVRITIS, S., MAJETI, R., AND ALIZADEH, A. Association of a leukemic stem cell gene expression signature with clinical outcomes in acute myeloid leukemia. *JAMA 304* (2010), 2706–15.

[82] GENTRY, S., ASHKENAZI, R., AND JACKSON, T. A maturity-structured mathematical model of mutation acquisition in the absence of homeostatic regulation. *Math. Model. Nat. Phenom 4* (2009), 156–182.

[83] GENTRY, S., AND JACKSON, T. A mathematical model of cancer stem cell driven tumor initiation: Implications of niche size and loss of homeostatic regulatory mechanisms. *PLoS One 8* (2013), e71128.

[84] GERLINGER, M., AND SWANTON, C. How Darwinian models inform therapeutic failure initiated by clonal heterogeneity in cancer medicine. *Br J Cancer 103* (2010), 1139–43.

[85] GETTO, P., MARCINIAK-CZOCHRA, A., NAKATA, Y., AND VIVANCO, M. Global dynamics of two-compartment models for cell production systems with regulatory mechanisms. *Math Biosci 245* (2013), 258–268.

[86] GRIFFIN, J., AND LOEWENBERG, B. Clonogenic cells in acute myeloblastic leukemia. *Blood 68* (1986), 1185–1195.

[87] GUCKENHEIMER, J., AND HOLMES, P. *Nonlinear Oscillations, Dynamical Systems, and Bifurcations of Vector Fields*. Springer, 2002.

[88] GUDGIN, E., AND HUNTLY, B. Acute myeloid leukemia: leukemia stem cells write a prognostic signature. *Stem Cell Research and Therapy 2* (2011), 1–3.

[89] GUPTA, P., FILLMORE, C., JIANG, G., SHAPIRA, S., TAO, K., KUPERWASSER, C., AND LANDER, E. Stochastic state transitions give rise to phenotypic equilibrium in populations of cancer cells. *Cell 146* (2011), 633–44.

[90] GUTIERREZ, S., AND ROMERO-OLIVA, F. Epigenetic changes: a common theme in acute myelogenous leukemogenesis. *J. Hematol Oncol 6* (2013), 57.

[91] GWIAZDA, P., MARCINIAK-CZOCHRA, A., AND STECHER, J. Mass concentration in a nonlocal model of clonal selection. *Preprint arXiv:1401.6043 [math.CA]* (2014), DOI:10.1112/0000/000000.

[92] HALE, J., AND KOCAK, H. *Dynamics and Bifurcations*. Springer, Heidelberg, 1991.

[93] HAN, L., WIERENGA, A., ROZENVELD-GEUGIEN, M., VAN DE LANDE, K., VELLENGA, E., AND SCHURINGA, J. Single-cell STAT5 signal transduction profiling in normal and leukemic stem and progenitor cell populations reveals highly distinct cytokine responses. *PLoS One 4* (2009), e7989.

[94] HANAHAN, D., AND WEINBERG, R. Hallmarks of cancer: the next generation. *Cell 144* (2011), 646–74.

[95] HANOUN, M., ZHANG, D., MIZOGUCHI, T., PINHO, S., PIERCE, H., KUNISAKI, Y., LACOMBE, J., ARMSTRONG, S., DÜHRSEN, U., AND FRENETTE, P. Acute myelogenous leukemia-induced sympathetic neuropathy promotes malignancy in an altered hematopoietic stem cell niche. *Cell stem cell 15* (2014), 365–375.

[96] HARRISON, W. J. The total cellularity of the bone marrow in man. *J Clin Pathol 15* (1962), 254–259.

[97] HARTMAN, P. *Ordinary Differential Equations (Classics in Applied Mathematics, Vol 38), 2nd ed.* SIAM, Phiadelphia, 1987.

[98] HAYAKAWA, F., TOWATARI, M., KIYOI, H., TANIMOTO, M., KITAMURA, T., SAITO, H., AND NAOE, T. Tandem-duplicated Flt3 constitutively activates STAT5 and MAP kinase and introduces autonomous cell growth in IL-3-dependent cell lines. *Oncogene 19* (2000), 624–631.

[99] HO, A., AND WAGNER, W. The beauty of asymmetry: asymmetric divisions and self-renewal in the haematopoietic system. *Current opinion in hematology 14* (2007), 330–36.

[100] HOPE, K., JIN, L., AND DICK, J. Acute myeloid leukemia originates from a hierarchy of leukemic stem cell classes that differ in self-renewal capacity. *Nature Immunology 5* (2004), 738–743.

[101] HOPPENSTEADT, F. Singular perturbations on the infinite interval. *Trans Amer Math Soc 123* (1966), 521–535.

[102] HOPPENSTEADT, F. Properties of solutions of ordinary differential equations with small parameters. *Comm Pure Appl Math 24* (1971), 807–840.

[103] HOPPENSTEADT, F. *Analysis and Simulation of Chaotic Systems*. Springer, New York, 2000.

[104] HORTON, S., AND HUNTLY, B. Recent advances in acute myeloid leukemia stem cell biology. *Haematologica 97* (2012), 966–74.

[105] HOTHORN, T., HORNIK, K., VAN DE WIEL, M., AND ZEILEIS, A. Implementing a class of permutation tests: The coin package. *Journal of Statistical Software 28* (2008), 1–23.

[106] HSIEH, P., AND SIBUYA, Y. *Basic Theory of Ordinary Differential Equations*. Springer, Heidelberg, 1999.

[107] IRVINE, A., MAGILL, M., SOMERVILLE, L., AND MCMULLIN, M. pontaneous intramedullary apoptosis is present in disorders other than myelodysplasia. *Exp. Hematol 26* (1998), 435–439.

[108] ITZKOVITZ, S., BLAT, I., JACKS, T., CLEVERS, H., AND VAN OUDENAARDEN, A. Optimality in the development of intestinal crypts. *Cell 148* (2012), 608–19.

[109] JAN, M., AND MAJETI, R. Clonal evolution of acute leukemia genomes. *Oncogene 32* (2013), 135–140.

[110] JAN, M., SNYDER, T., CORCES-ZIMMERMAN, M., VYAS, P., WEISSMAN, I., QUAKE, S., AND MAJETI, R. Clonal evolution of preleukemic hematopoietic stem cells precedes human acute myeloid leukemia. *Sci Transl Med 4* (2012), 149ra118.

[111] JANDL, J. H. Blood cell formation. In *Textbook of Hematology*, J. H. Jandl, Ed. Boston, MA: Little, Brown and Company, 1996, pp. 1–69.

[112] JANZ, S., POTTER, M., AND RABKIN, C. S. Lymphoma- and leukemia-associated chromosomal translocations in healthy individuals. *Genes Chromosomes Cancer. 36* (2003), 211–223.

[113] JONES, C. Geometric singular perturbation theory. In *Dynamical Systems*, L. Arnold, C. Jones, K. Mischaikow, G. Raugel, and R. Johnson, Eds. Springer, Heidelberg, 1995, pp. 44–118.

[114] KAPER, T. An introduction to geometric methods and dynamical systems theory for singular perturbation problems. *Proceedings of Symposia in Applied Mathematics 56* (1999), 85–131.

[115] KAUFMANN, W., AND KAUFMAN, D. Cell cycle control, dna repair and initiation of carcinogenesis. *FASEB J 7* (1993), 1188–91.

[116] KAUSHANSKY, K. Lineage-specific hematopoietic growth factors. *NEJM 354* (2006), 2034–45.

[117] KIHARA, R., NAGATA, Y., KIYOI, H., KATO, T., YAMAMOTO, E., SUZUKI, K., CHEN, F., ASOU, N., OHTAKE, S., MIYAWAKI, S., MIYAZAKI, Y., SAKURA, T., OZAWA, Y., USUI, N., KANAMORI, H., KIGUCHI, T., IMAI, K., UIKE, N., KIMURA, F., KITAMURA, K., NAKASEKO, C., ONIZUKA, M., TAKESHITA, A., ISHIDA, F., SUZUSHIMA, H., KATO, Y., MIWA, H., SHIRAISHI, Y., CHIBA, K., TANAKA, H., MIYANO, S., OGAWA, S., AND NAOE, T. Comprehensive analysis of genetic alterations and their prognostic impacts in adult acute myeloid leukemia patients. *Leukemia 28* (2014), 1586–95.

[118] KIM, P., LEE, P., AND LEVY, D. Dynamics and potential impact of the immune response to chronic myelogenous leukemia. *PLoS Comput Biol 4* (2008), e1000095.

[119] KIM, Y., KOO, B., JEONG, H., YOON, M., SONG, R., SHIN, J., JEONG, D., KIM, S., AND KONG, Y. Defective notch activation in microenvironment leads to myeloproliferative disease. *Blood 112* (2008), 4628–38.

[120] KLAUS, J., HERRMANN, D., BREITKREUTZ, I., HEGENBART, U., MAZITSCHEK, U., EGERER, G., CREMER, F., LOWENTHAL, R. M., HUESING, J., FRUEHAUF, S., MOEHLER, T., HO, A. D., AND GOLDSCHMIDT, H. Effect of CD34 cell dose on hematopoietic reconstitution and outcome in 508 patients with multiple myeloma undergoing autologous peripheral blood stem cell transplantation. *Eur J Haematol. 78* (2007), 21–28.

[121] KLEIN, R., AND ROBERTS, S. A time-varying poisson arrival process generator. *Simulation 43* (1984), 193–5.

[122] KLUMPER, E., PIETERS, R., VEERMAN, A., HUISMANS, D., LOONEN, A., HAEHLEN, K., KASPERS, G., VAN WERING, E., HARTMANN, R., AND HENZE, G. In vitro cellular drug resistance in children with relapsed/refractory acute lymphoblastic leukemia. *Blood 86* (1995), 3861–8.

[123] KNAUER, F. *Dynamical Behaviour of a single Feedback-Controlled Haematopoietic Model*. Diploma Thesis, University of Heidelberg, 2012.

[124] KOMAROVA, N. Principles of regulation of self-renewing cell lineages. *PLoS One 8* (2013), e72847.

[125] KOMAROVA, N., AND WODARZ, D. Evolutionary dynamics of mutator phenotypes in cancer: implications for chemotherapy. *Cancer Res 63* (2003), 6635–42.

[126] KONDO, S., OKAMURA, S., ASANO, Y., HARADA, M., AND NIHO, Y. Human granulocyte colony-stimulating factor receptors in acute myelogenous leukemia. *Eur J Hematol 46* (1991), 223–230.

[127] KORDE, N., KRISTINSSON, S., AND LANDGREN, O. Monoclonal gammopathy of undetermined significance (MGUS) and smoldering multiple myeloma (SMM): novel biological insights and development of early treatment strategies. *Blood 117* (2011), 5573–5581.

[128] KORNBERG, A., AND POLLIACK, A. Serum lactic dehydrogenase (LDH) levels in acute leukemia: marked elevations in lymphoblastic leukemia. *Blood 56* (1980), 351–355.

[129] KYLE, R., BENSON, J., LARSON, D., THERNEAU, T., DISPENZIERI, A., MELTON, L., AND RAJKUMAR, S. IgM monoclonal gammopathy of undetermined significance and smoldering Waldenstroem's macroglobulinemia. *Clin Lymphoma Myeloma 9* (2009), 17–18.

[130] LA PORTA, C., ZAPPERI, S., AND SETHNA, J. Senescent cells in growing tumors: Population dynamics and cancer stem cells. *PLoS Comput Biol. 8* (2012), e1002316.

[131] LANDER, A., GOKOFFSKI, K., WAN, F., NIE, Q., AND CALOF, A. Cell lineages and the logic of proliferative control. *PLoS biology 7* (2009), 84–100.

[132] LANGE, S., TAKATA, K., AND WOOD, R. DNA polymerases and cancer. *Nat Rev Cancer 11* (2011), 96–110.

[133] LANSDORP, P. Stem cell biology for the transfusionist. *Vox Sang. 74 Suppl 2* (1998), 91–94.

[134] LAYTON, J., HOCKMAN, H., SHERIDAN, W., AND MORSTYN, G. Evidence for a novel in vivo control mechanism of granulopoiesis: mature cell-related control of a regulatory growth factor. *Blood 74* (1989), 1303–1307.

[135] LEDER, K., HOLLAND, E., AND MICHOR, F. The therapeutic implications of plasticity of the cancer stem cell phenotype. *PLoS One 5* (2010), e14366.

[136] LEE, H., LI, N., EVANS, S., DIAZ, M., AND WENZEL, P. Biomechanical force in blood development: extrinsic physical cues drive pro-hematopoietic signaling. *Differentiation 86* (2013), 92–103.

[137] LEMOLI, R., GULATI, S., STRIFE, A., LAMBEK, C., PEREZ, A., AND CLARKSON, B. Proliferative response of human acute myeloid leukemia cells and normal marrow enriched progenitor cells to human recombinant growth factors IL-3, GM-CSF and G-CSF alone and in combination. *Leukemia 5* (1991), 386–91.

[138] LENAERTS, T., PACHECO, J., TRAULSEN, A., AND DINGLI, D. Tyrosine kinase inhibitor therapy can cure chronic myeloid leukemia without hitting leukemic stem cells. *Haematologica 95* (2010), 900–907.

[139] LIESVELD, J., AND LICHTMAN, M. Acute myelogenous leukemia. In *Williams Hematology*, K. Kaushansky, M. Lichtman, E. Beutler, T. Kipps, J. Prchal, and U. Seligsohn, Eds. McGraw Hill, New York, 2010, pp. 1095–1103.

[140] LIN, Z., AND LIN, Y. *Linear Systems Exponential Dichotomy and Structure of Sets of Hyperbolic Points*. World Scientific, Singapore, 2000.

[141] LO, W., CHOU, C., GOKOFFSKI, K., WAN, F., LANDER, A., CALOF, A., AND NIE, Q. Feedback regulation in multistage cell lineages. *Math Biosci Eng 6* (2009), 59–82.

[142] LOCATELLI, F., MORETTA, F., AND RUTELLA, S. Management of relapsed acute lymphoblastic leukemia in childhood with conventional and innovative approaches. *Curr Opin Oncol. 25* (2013), 707–15.

[143] LOEFFLER, H., RASTETTER, J., AND HAFERLACH, T. *Atlas of Clinical Hematology*. Springer, Heidelberg, 2000. p. 78.

[144] LOEWENBERG, B., VAN PUTTEN, W., THEOBALD, M., GMUER, J., VERDONCK, L., SONNEVELD, P., FEY, M., SCHOUTEN, H., DE GREEF, G., FERRANT, A., KOVACSOVICS, T., GRATWOHL, A., DAENEN, S., HUIJGENS, P., BOOGAERTS, M., DUTCH-BELGIAN HEMATO-ONCOLOGY COOPERATIVE GROUP, AND SWISS GROUP FOR CLINICAL CANCER RESEARCH. Effect of priming with granulocyte colony-stimulating factor on the outcome of chemotherapy for acute myeloid leukemia. *N Engl J Med 349* (2003), 743–52.

[145] LORD, B., BRONCHUD, M., OWENS, S., CHANG, J., HOWELL, A., SOUZA, L., AND DEXTER, T. The kinetics of human granulopoiesis following treatment with granulocyte colony-stimulating factor in vivo. *Proc Natl Acad Sci U S A 86* (1989), 9499–9503.

[146] LOWENBERG, B., VAN PUTTEN, W., TOUW, I., DELWEL, R., AND SANTINI, V. Autonomous proliferation of leukemic cells in vitro as a determinant of prognosis in adult acute myeloid leukemia. *NEJM 328* (1993), 614–19.

[147] LUTZ, C., HOANG, V., AND HO, A. Identifying leukemia stem cells - is it feasible and does it matter? *Cancer Lett 338* (2013), 10–14.

[148] LUTZ, C., WOLL, P., HALL, G., CASTOR, A., DREAU, H., CAZZANIGA, G., ZUNA, J., JENSEN, C., CLARK, S., BIONDI, A., MITCHELL, C., FERRY, H., SCHUH, A., BUCKLE, V., JACOBSEN, S., AND ENVER, T. Quiescent leukaemic cells account for minimal residual disease in childhood lymphoblastic leukaemia. *Leukemia 27* (2013), 1204–7.

[149] MACKEY, M. Unified hypothesis of the origin of aplastic anaemia and periodic hematopoiesis. *Blood 51* (1978), 941–956.

[150] MACLEAN, A., LO CELSO, C., AND STUMPF, M. Population dynamics of normal and leukaemia stem cells in the haematopoietic stem cell niche show distinct regimes where leukaemia will be controlled. *J R Soc Interface 10* (2013), 20120968.

[151] MALHOTRA, O., AND SALAM, S. Cyclic oscillations of leucocyte counts in chronic myeloid leukaemia. *Postgrad Med J 67* (1991), 87–9.

[152] MALINOWSKA, I., STELMASZCZYK-EMMEL, A., WASIK, M., AND ROKICKA-MILEWSKA, R. Apoptosis and ph of blasts in acute childhood leukemia. *Med Sci Monit 8* (2002), CR441–CR447.

[153] MANESSO, E., TELES, J., BRYDER, D., AND PETERSON, C. Dynamical modelling of haematopoiesis: an integrated view over the system in homeostasis and under perturbation. *J R Soc Interface 10* (2013), 20120817.

[154] MANGEL, M., AND BONSALL, M. Phenotypic evolutionary models in stem cell biology: Replacement, quiescence, and variability. *PLoS One. 3* (2008), e1591.

[155] MANKO, J., WALTER-CRONECK, A., JAWNIAK, D., GRZASKO, N., GORSKA-KOSICKA, M., CIOCH, M., AND DMOSZYNSKA, A. A clinical comparison of the efficacy and safety of biosimilar G-CSF and originator G-CSF in haematopoietic stem cell mobilization. *Pharmacol Rep 66* (2014), 239–242.

[156] MARCINIAK-CZOCHRA, A., AND STIEHL, T. Mathematical models of hematopoietic reconstitution after stem cell transplantation. In *Model Based Parameter Estimation: Theory and Applications.*, H. Bock, T. Carraro, W. Jaeger, and S. Koerkel, Eds. Heidelberg, Springer, 2011.

[157] MARCINIAK-CZOCHRA, A., STIEHL, T., JÄGER, W., HO, A. D., AND WAGNER, W. Modeling of asymmetric cell division in hematopoietic stem cells – regulation of self-renewal is essential for efficient repopulation. *Stem Cells Dev. 18* (2009), 377–385.

[158] MARCINIAK-CZOCHRA, A., STIEHL, T., AND WAGNER, W. Modeling of replicative senescence in hematopoietic development. *Aging (Albany NY) 1(8)* (2009), 723–732.

[159] MARCUCCI, G., MAHARRY, K., METZELER, K., VOLINIA, S., WU, Y., MROZEK, K., NICOLET, D., KOHLSCHMIDT, J., WHITMAN, S., MENDLER, J., SCHWIND, S., BECKER, H., EISFELD, A., CARROLL, A., POWELL, B., KOLITZ, J., GARZON, R., CALIGIURI, M., STONE, R., AND BLOOMFIELD, C. Clinical role of microRNAs in cytogenetically normal acute myeloid leukemia: miR-155 upregulation independently identifies high-risk patients. *J Clin Oncol 31* (2013), 2068–93.

[160] METCALF, D. Hematopoietic cytokines. *Blood 111* (2008), 485–491.

[161] MEYER, J., WANG, J., HOGAN, L., YANG, J., DANDEKAR, S., PATEL, J., TANG, Z., ZUMBO, P., LI, S., ZAVADIL, J., LEVINE, R., CARDOZO, T., HUNGER, S., RAETZ, E., EVANS, W., MORRISON, D., MASON, C., AND CARROLL, W. Relapse-specific mutations in NT5C2 in childhood acute lymphoblastic leukemia. *Nat Genet 45* (2013), 290–4.

[162] MICHOR, F., HUGHES, T., IWASA, Y., BRANFORD, S., SHAH, N., SAWYERS, C., AND NOVAK, M. Dynamics of chronic myeloid leukaemia. *Nature 435* (2005), 1267–1270.

[163] MIRAKI-MOUD, F., ANJOS-AFONSO, F., HODBY, K., GRIESSINGER, E., ROSIGNOLI, G., LILLINGTON, D., JIA, L., DAVIES, J., CAVENAGH, J., SMITH, M., OAKERVEE, H., AGRAWAL, S., GRIBBEN, J., BONNET, D., AND TAUSSIG, D. Acute myeloid leukemia does not deplete normal hematopoietic stem cells but induces cytopenias by impeding their differentiation. *PNAS 110* (2013), 13576–81.

[164] MORGAN, D., DESAI, A., EDGAR, B., GLOTZER, M., HEALD, R., KARSENTI, E., NASMYTH, K., PINES, J., AND SHERR, C. *The Cell Cycle. In: B. Alberts, A. Johnson, J. Lewis, M. Raff, K. Roberts, R. Walter (Eds): Molecular Biology of the Cell, 5th Edition*. Garland Science, 2007.

[165] MUNK PEDERSEN, I., AND REED, J. Microenvironmental interactions and survival of cll b-cells. *Leuk Lymphoma 45* (2004), 2365–2372.

[166] NAGASAWA, T., OMATSU, Y., AND SUGIYAMA, T. Control of hematopoietic stem cells by the bone marrow stromal niche: the role of reticular cells. *Trends Immunol 32* (2011), 315–320.

[167] NAKATA, Y., GETTO, P., MARCINIAK-CZOCHRA, A., AND ALARCON, T. Stability analysis of multi-compartment models for cell production systems. *J Biol Dyn 6 Suppl 1* (2012), 2–18.

[168] NEUMEISTER, B., BESENTHAL, I., AND BOEHM, B. *Klinikleitfaden Labordiagnostik*. Elsevier, Munich, 2009.

[169] O'MALLEY, R. *Singular perturbation methods for ordinary differential equations*. Springer, Heidelberg, 1991.

[170] OSTBY, I., RUSTEN, L., KVALHEIM, G., AND GROTTUM, P. A mathematical model for reconstitution of granulopoiesis after high dose chemotherapy with autologous stem cell transplantation. *J Math Biol 47* (2003), 101–36.

[171] PARKIN, B., OUILLETTE, P., LI, Y., KELLER, J., LAM, C., ROULSTON, D., LI, C., SHEDDEN, K., AND MALEK, S. Clonal evolution and devolution after chemotherapy in adult acute myelogenous leukemia. *Blood 121* (2013), 369–77.

[172] PAZDZIOREK, P. Mathematical model of stem cell differentiation and tissue regeneration with stochastic noise. *Bull Math Biol 76* (2014), 1642–1669.

[173] POLAK, R., AND BUITENHUIS, M. The PI3K/PKB signaling module as key regulator of hematopoiesis: implications for therapeutic strategies in leukemia. *Blood 119* (2012), 911–923.

[174] PUI, C. Acute lymphoblastic leukemia. In *Williams Hematology, 8th ed.*, K. Kaushansky, M. Lichtman, E. Beutler, T. Kipps, U. Seligsohn, and J. Prchal, Eds. New York: Mc Graw Hill, 2010, pp. 1409–1430.

[175] PUJO-MENJOUET, L., BERNARD, S., AND MACKEY, M. Long period oscillations in a G0 model of hematopoietic stem cells. *SIAM J Appl Dyn Syst 4* (2005), 312–332.

[176] RAAIJMAKERS, M., MUKHERJEE, S., GUO, S., ZHANG, KOBAYASHI, T., SCHOONMAKER, J., EBERT, B., AL-SHAHROUR, F., HASSERJIAN, R., SCADDEN, E., AUNG, Z., MATZA, M., MERKENSCHLAGER, M., LIN, C., ROMMENS, J., AND SCADDEN, D. Bone progenitor dysfunction induces myelodysplasia and secondary leukaemia. *Nature 464* (2010), 852–57.

[177] RAVANDI, F. Relapsed acute myeloid leukemia: why is there no standard of care? *Best Pract Res Clin Haematol. 26* (2013), 253–9.

[178] REILLY, J. FLT3 and its role in the pathogenesis of acute myeloid leukaemia. *Leuk Lymphoma 44* (2003), 1–7.

[179] RENNEVILLE, A., ROUMIER, C., BIGGIO, V., NIBOUREL, O., BOISSEL, N., FENAUX, P., AND PREUDHOMME, C. Cooperating gene mutations in

acute myeloid leukemia: a review of the literature. *Leukemia 22* (2008), 915–31.

[180] RENSTRÖM, J., KRÖGER, M., PESCHEL, C., AND OOSTENDORP, R. How the niche regulates hematopoietic stem cells. *Chem Biol Interact. 184* (2010), 7–15.

[181] REYA, T., MORRISON, S., CLARKE, M., AND WEISSMAN, I. Stem cells, cancer, and cancer stem cells. *Nature 414* (2001), 105–11.

[182] RODRIGUEZ-BRENES, I., WODARZ, D., AND KOMAROVA, N. Stem cell control, oscillations, and tissue regeneration in spatial and non-spatial models. *Front Oncol. 3* (2013), 82.

[183] ROEDER, I., HORN, M., GLAUCHE, I., HOCHHAUS, A., MUELLER, M., AND LOEFFLER, M. Dynamic modeling of imatinib-treated chronic myeloid leukemia: functional insights and clinical implications. *Nat Med 12* (2006), 1181–1184.

[184] ROEDER, I., AND LOEFFLER, M. A novel dynamic model of hematopoietic stem cell organization based on the concept of within-tissue plasticity. *Exp Hematol 30* (2002), 853–861.

[185] ROODMAN, G., LEMAISTRE, C., CLARK, G., PAGE, C., NEWCOMB, T., AND KNIGHT, W. CFU-GEMM correlate with neutrophil and platelet recovery in patients receiving autologous marrow transplantation after high-dose melphalan chemotherapy. *Bone Marrow Transplant 2* (1987), 165–73.

[186] ROSS, S. *Stochastic Processes*. New York: Wiley, 1996.

[187] ROSS, S. *Simulation*. London: Elsevier, 2006.

[188] ROSSI, G., MINERVINI, M., MELILLO, L., DI NARDO, F., DE WAURE, C., SCALZULLI, P., PERLA, G., VALENTE, D., SINISI, N., AND CACSAVILLA, N. Predictive role of minimal residual disease and log clearance in acute myeloid leukemia: a comparison between multiparameter flow in cytometry and Wilm's tumor 1 levels. *Ann Hematol 93* (2014), 1149–57.

[189] ROWE, J. Optimal management of adults with all. *Br J Haematol. 144* (2009), 468–83.

[190] RUDNICKI, R. Chaoticity of the blood cell production system. *Chaos 19* (2009), 043112.

[191] RUPEC, R., JUNDT, F., REBHOLZ, B., ECKELT, B., WEINDL, G., HERZINGER, T., FLAIG, M., MOOSMANN, S., PLEWIG, G., DOERKEN, B., FOERSTER, I., HUSS, R., AND PFEFFER, K. Stroma-mediated dysregulation of myelopoiesis in mice lacking I kappa B alpha. *Immunity 322* (2005), 479–91.

[192] RUSSELL, N., HUNTER, A., BRADBURY, D., ZHU, Y., AND KEITH, F. Biological features of leukaemic cells associated with autonomous growth and reduced survival in acute myeloblastic leukaemia. *Leuk Lymphoma 16* (1995), 223–29.

[193] RUSSELL, N., HUNTER, A., BRADBURY, D., ZHU, Y., AND KEITH, F. Biological features of leukaemic cells associated with autonomous growth and reduced survival in acute myeloblastic leukaemia. *Leuk Lymphoma 16* (1995), 223–229.

[194] SAITO, Y., UCHIDA, N., TANAKA, S., SUZUKI, N., TOMIZAWA-MURASAWA, M., SONE, A., NAJIMA, Y., TAKAGI, S., AOKI, Y., WAKE, A., TANIGUCHI, S., SHULTZ, L., AND ISHIKAWA, F. Induction of cell cycle entry eliminates human leukemia stem cells in a mouse model of AML. *Nat Biotechnol 28* (2010), 275–80.

[195] SAVITSKIY, V., SHMAN, T., AND POTAPNEV, M. Comparative measurement of spontaneous apoptosis in pediatric acute leukemia by different techniques. *Cytometry B Clin Cytom 56* (2003), 16–22.

[196] SCHAUB, F., LOOSER, R., LI, S., HAO-SHEN, H., LEHMANN, T., TICHELLI, A., AND SKODA, R. Clonal analysis of TET2 and JAK2 mutations suggests that TET2 can be a late event in the progression of myeloproliferative neoplasms. *Blood 115* (2010), 2003–7.

[197] SCHEPERS, K., PIETRAS, E., REYNAUD, DAND FLACH, J., BINNEWIES, M., GARG, T., WAGERS, A., HSIAO, E., AND PASSEGUÉ, E. Myeloproliferative neoplasia remodels the endosteal bone marrow niche into a self-reinforcing leukemic niche. *Cell stem cell 13* (2013), 285–99.

[198] SCHNITTGER, S., KERN, W., TSCHULIK, C., WEISS, T., DICKER, F., FALINI, B., HAFERLACH, C., AND HAFERLACH, T. Minimal residual disease levels assessed by NPM1 mutation-specific RQ-PCR provide important prognostic information in AML. *Blood 114* (2009), 2220–312.

[199] SCHOLZ, M., ENGEL, C., AND LOEFFLER, M. Modelling human granulopoiesis under poly-chemotherapy with G-CSF support. *J Math Biol 50* (2005), 397–439.

[200] SCHUELER, F., HIRT, C., AND DOELKEN, G. Chromosomal translocation t(14;18) in healthy individuals. *Semin Cancer Biol. 13* (2003), 203–209.

[201] SHAHRIYARI, L., AND KOMAROVA, N. Symmetric vs. asymmetric stem cell divisions: an adaptation against cancer? *PLoS One 8* (2013), e76195.

[202] SHEPHERD, B., KIEM, H., LANSDORP, P., DUNBAR, C., AUBERT, G., LAROCHELLE, A., SEGGEWISS, R., GUTTORP, P., AND ABKOWITZ,

J. Hematopoietic stem-cell behavior in nonhuman primates. *Blood 110* (2007), 1806–1813.

[203] SHEPHERD, B. E., GUTTORP, P., LANSDORP, P. M., AND ABKOWITZ, J. L. Estimating human hematopoietic stem cell kinetics using granulocyte telomere lengths. *Exp Hematol. 32* (2004), 1040–1050.

[204] SHERR, C. Cancer cell cycles. *Science 274* (1996), 1672–7.

[205] SHIN, J., SWIFT, J., IVANOVSKA, I., SPINLER, K., BUXBOIM, A., AND DISCHER, D. Mechanobiology of bone marrow stem cells: From myosin-II forces to compliance of matrix and nucleus in cell forms and fates. *Differentiation 86* (2013), 77–86.

[206] SHINJO, K., TAKESHITA, A., OHNISHI, K., AND OHNO, R. Granulocyte colony-stimulating factor receptor at various stages of normal and leukemic hematopoietic cells. *Leuk Lymphoma 25* (1997), 37–46.

[207] SHIVAMOGGI, B. *Perturbation Methods for Differential Equations*. Birkhaeuser, Basel, 2002.

[208] SHLUSH, L., ZANDI, S., MITCHELL, A., CHEN, W., BRANDWEIN, J., GUPTA, V., KENNEDY, J., SCHIMMER, A., SCHUH, A., YEE, K., MCLEOD, J., DOEDENS, M., MEDEIROS, J., MARKE, R., KIM, H., LEE, K., MCPHERSON, J., HUDSON, T., CONSORTIUM, H. P.-L. G. P., BROWN, A., YOUSIF, F., TRINH, Q., STEIN, L., MINDEN, M., WANG, J., AND DICK, J. Identification of pre-leukaemic haematopoietic stem cells in acute leukaemia. *Nature 506* (2014), 328–33.

[209] SMITH, C. Production, distribution and fate of neutrophils. In *Williams Hematology, 8th ed.*, K. Kaushansky, M. Lichtman, E. Beutler, T. Kipps, U. Seligsohn, and J. Prchal, Eds. New York: Mc Graw Hill, 2010, pp. 891–896.

[210] SOLTANIAN, S., AND MATIN, M. Cancer stem cells and cancer therapy. *Tumour Biol 32* (2011), 425–440.

[211] SPYRIDONIDIS, A., KUTTLER, T., WASCH, R., SAMEK, E., WATERHOUSE, M., BEHRINGER, D., BERTZ, H., AND FINKE, J. Reduced intensity conditioning compared to standard conditioning preserves the in vitro growth capacity of bone marrow stroma, which remains of host origin. *Stem Cells Dev 14* (2005), 213–222.

[212] STIEHL, T. *Mathematical models of hematopoietic stem cells' maintenance and differentiation*. Diploma Thesis, University of Heidelberg, 2009.

[213] STIEHL, T., BARAN, N., HO, A., AND MARCINIAK-CZOCHRA, A. Clonal selection and therapy resistance in acute leukaemias: mathematical modelling explains different proliferation patterns at diagnosis and relapse. *J. R. Soc. Interface 11* (2014), 20140079.

[214] STIEHL, T., HO, A., AND MARCINIAK-CZOCHRA, A. The impact of CD34+ cell dose on engraftment after SCTs: personalized estimates based on mathematical modeling. *Bone Marrow Transplant 49* (2014), 30–7.

[215] STIEHL, T., AND MARCINIAK-CZOCHRA, A. Characterization of stem cells using mathematical models of multistage cell lineages. *Mathematical and Computer Modelling 53* (2011), 1505–1517.

[216] STIEHL, T., AND MARCINIAK-CZOCHRA, A. Mathematical modelling of leukemogenesis and cancer stem cell dynamics. *Math. Mod. Natural Phenomena. 7* (2012), 166–202.

[217] TAVOR, S., EISENBACH, M., JACOB-HIRSCH, J., GOLAN, T., PETIT, I., BENZION, K., KAY, S., BARON, S., AMARIGLIO, N., DEUTSCH, V., NAPARSTEK, E., AND RECHAVI, G. The CXCR4 antagonist AMD3100 impairs survival of human AML cells and induces their differentiation. *Leukemia 22* (2008), 2151–2158.

[218] TAVOR, S., PETIT, I., POROZOV, S., GOICHBERG, P., AVIGDOR, A., SAGIV, S., NAGLER, A., NAPARSTEK, E., AND LAPIDOT, T. Motility, proliferation, and egress to the circulation of human AML cells are elastase dependent in NOD/SCID chimeric mice. *Blood 106* (2005), 2120–2127.

[219] TESCHL, G. *Ordinary differential equations and dynamical systems*. American Mathematical Society, Providence, RI, 2012.

[220] THIEDE, C., STEUDEL, C., MOHR, B., SCHAICH, M., SCHAEKEL, U., PLATZBECKER, U., WERMKE, M., BORNHAEUSER, M., RITTER, M., NEUBAUER, A., EHNINGER, G., AND ILLMER, T. Analysis of FLT3-activating mutations in 979 patients with acute myelogenous leukemia: association with FAB subtypes and identification of subgroups with poor prognosis. *Blood 99* (2002), 4326–35.

[221] TIKHONOV, A., VASILEVA, A., AND SVESHNIKOV, A. *Differential equations*. Springer, Heidelberg, 1985.

[222] TOMASETTI, C., AND LEVY, D. Role of symmetric and asymmetric division of stem cells in developing drug resistance. *PNAS 107* (2010), 16766–16771.

[223] TOMASETTI, C., VOGELSTEIN, B., AND PARMIGIANI, G. Half or more of the somatic mutations in cancers of self-renewing tissues originate prior to tumor initiation. *PNAS 110* (2013), 1999–2004.

[224] TORMO, M., MARUGAN, I., AND CALABUIG, M. Myelodysplastic syndromes: an update on molecular pathology. *Clin Transl Oncol 12* (2010), 652–661.

[225] TRAULSEN, A., LENAERTS, T., PACHECO, J., AND DINGLI, D. On the dynamics of neutral mutations in a mathematical model for a homogeneous stem cell population. *J R Soc Interface 79* (2012), 20120810.

[226] TREON, S., AND MERLINI, G. Macroglobulinemia. In *Williams Hematology, 8th ed.*, K. Kaushansky, M. Lichtman, E. Beutler, T. Kipps, U. Seligsohn, and J. Prchal, Eds. New York: Mc Graw Hill, 2010, pp. 1695–1708.

[227] VAN DELFT, F., HORSLEY, S., COLMAN, S., ANDERSON, K., BATEMAN, C., KEMPSKI, H., ZUNA, J., ECKERT, C., SAHA, V., KEARNEY, L., FORD, A., AND GREAVES, M. Clonal origins of relapse in ETV6-RUNX1 acute lymphoblastic leukemia. *Blood 117* (2011), 6247–54.

[228] VASIL'EVA, A., BUTUZOV, V., AND KALACHEV, L. *The Boundary Function Method for Singular Perturbed Problems*. SIAM, Phiadelphia, 1993.

[229] VELLENGA, E., DE WOLF, J., BEENTJES, J., ESSELINK, M., SMIT, J., AND HALIE, M. Divergent effects of interleukin-4 (IL-4) on the granulocyte colony-stimulating factor and IL-3-supported myeloid colony formation from normal and leukemic bone marrow cells. *Blood 75* (1990), 633–37.

[230] VELLENGA, E., YOUNG, D., WAGNER, K., WIPER, D., OSTAPOVICZ, D., AND GRIFFIN, J. The effects of GM-CSF and G-CSF in promoting growth of clonogenic cells in acute myeloblastic leukemia. *Blood 69* (1987), 1771–1776.

[231] WALENDA, T., STIEHL, T., BRAUN, H., FROEBEL, J., HO, A., SCHROEDER, T., GOECKE, T., RATH, B., GERMING, U., MARCINIAK-CZOCHRA, A., AND WAGNER, W. Feedback signals in myelodysplastic syndromes: increased self-renewal of the malignant clone suppresses normal hematopoiesis. *PLoS Comput Biol 10* (2014), e1003599.

[232] WALKLEY, C., OLSEN, G., DWORKIN, S., FABB, S., SWANN, J., MCARTHUR, G., WESTMORELAND, S., CHAMBON, P., SCADDEN, D., AND PURTON, L. A microenvironment-induced myeloproliferative syndrome caused by retinoic acid receptor γ deficiency. *Cell 129* (2007), 1097–1110.

[233] WALKLEY, C., SHEA, J., SIMS, N., PURTON, L., AND ORKIN, S. Rb regulates interactions between hematopoietic stem cells and their bone marrow microenvironment. *Cell 129* (2007), 1081–95.

[234] WALTER, W. *Gewöhnliche Differentialgleichungen, 7th ed.* Springer, Heidelberg, 2000.

[235] WANG, J. C., DOEDENS, M., AND DICK, J. E. Primitive human hematopoietic cells are enriched in cord blood compared with adult bone marrow or mobilized peripheral blood as measured by the quantitative in vivo SCID-repopulating cell assay. *Blood 89* (1997), 3919–3924.

[236] WASOW, W. *Asymptotic expansions for ordinary differential equations*. Interscience Publishers, New York, 1965. Section 39.2.

[237] WEISSER, M., KERN, W., SCHOCH, C., HIDDEMANN, W., HAFERLACH, T., AND SCHNITTGER, S. Risk assessment by monitoring expression levels of partial tandem duplications in the MLL gene in acute myeloid leukemia during therapy. *Haematologica 90* (2005), 881–9.

[238] WELCH, J., LEY, T., LINK, D., MILLER, C., LARSON, D., KOBOLDT, D., WARTMAN, L., LAMPRECHT, T., LIU, F., XIA, J., KANDOTH, C., FULTON, R., MCLELLAN, M., DOOLING, D., WALLIS, J., CHEN, K., HARRIS, C., SCHMIDT, H., KALICKI-VEIZER, J., LU, C., ZHANG, Q., LIN, L., O'LAUGHLIN, M., MCMICHAEL, J., DELEHAUNTY, K., FULTON, L., MAGRINI, V., MCGRATH, S., DEMETER, R., VICKERY, T., HUNDAL, J., COOK, L., SWIFT, G., REED, J., ALLDREDGE, P., WYLIE, T., WALKER, J., WATSON, M., HEATH, S., SHANNON, W., VARGHESE, N., NAGARAJAN, R., PAYTON, J., BATY, J., KULKARNI, S., KLCO, J., TOMASSON, M., WESTERVELT, P., WALTER, M., GRAUBERT, T., DIPERSIO, J., DING, L., MARDIS, E., AND WILSON, R. The origin and evolution of mutations in acute myeloid leukemia. *Cell 150* (2012), 264–78.

[239] WERNER, B., DINGI, D., AND TRAULSEN, A. A deterministic model for the occurrence and dynamics of multiple mutations in hierarchically organized tissues. *J R Soc Interface 10* (2013), 20130349.

[240] WERNER, B., LUTZ, D., BRUEMMENDORF, T., TRAULSEN, A., AND BALABANOV, S. Dynamics of resistance development to imatinib under increasing selection pressure: a combination of mathematical models and in vitro data. *PLoS One 6* (2011), e28955.

[241] WHICHARD, Z. L., SARKAR, C. A., KIMMEL, M., AND COREY, S. J. Hematopoiesis and its disorders: a systems biology approach. *Blood 115* (2010), 2339–2347.

[242] WODARZ, D., GARG, N., KOMAROVA, N., BENJAMINI, O., KEATING, M., WIERDA, W., KANTARJIAN, H., JAMES, D., O'BRIEN, S., AND BURGER, J. Kinetics of cll cells in tissues and blood during therapy with the btk inhibitor ibrutinib. *Blood 123* (2014), 4132–5.

[243] YAMAUCHI, T., NEGORO, E., LEE, S., TAKAI, M., MATSUDA, Y., TAKAGI, K., KISHI, S., TAI, K., HOSONO, N., TASAKI, T., IKEGAYA, S., INAI, K., YOSHIDA, A., URASAKI, Y., IWASAKI, H., AND UEDA, T. A high serum uric acid level is associated with poor prognosis in patients with acute myeloid leukemia. *Anticancer Res 33* (2013), 3947–51.

[244] YANG, B., AND KIDO, A. Pharmacokinetics and pharmacodynamics of pegfilgrastim. *Clin Pharmacokinet 50* (2011), 295–306.

[245] ZAPPERI, S., AND LA PORTA, C. Do cancer cells undergo phenotypic switching? the case for imperfect cancer stem cell markers. *Sci Rep 2* (2012).

[246] ZHANG, J., NIU, C., YE, L., HUANG, H., HE, X., TONG, W., ROSS, J., HAUG, J., JOHNSON, T., FENG, J., HARRIS, S., WIEDEMANN, L., MISHINA, Y., AND LI, L. Identification of the hematopoietic stem cell niche and control of the niche size. *Nature 425* (2003), 836–841.

Appendices

APPENDIX A

ANALYTICAL RESULTS OF THE MODEL OF HEMATOPOIESIS

A.1 Basic results

We cite the following basic results from *Stiehl and Marciniak-Czochra, Characterization of stem cells using mathematical models of multistage cell lineages, 2011*, [215]. For Proofs we refer to reference [215].

Proposition A.1 (Positive Steady States)
System (2.3) has a unique positive steady state $\bar{c}_1, ..., \bar{c}_n$*, if and only if the following conditions are satisfied.*

(1) $(2a_{1,max} - 1)p_1 > d_1$

(2) $2a_{1,max}p_1(d_i + p_i) - 2a_{i,max}p_i(d_1 + p_1) > 0,$ for $i = 2, \ldots, n-1.$

The steady state is given by

$$\bar{c}_l = \bar{c}_n \Pi_{l+1}^n \Theta_i, \text{ for } l = 1, \ldots, n,$$

where

$\bar{c}_n = \frac{1}{k}(\frac{2a_{1,max}p_1}{d_1+p_1} - 1)$,

$\Theta_i := \frac{d_i+p_i-2a_{i,max}p_i\bar{s}}{2(1-a_{i-1,max}\bar{s})p_{i-1}} > 0,$ for $i = 2, \ldots, n-1$,

$\Theta_n := \frac{d_n}{2(1-a_{n-1,max}\bar{s})p_{n-1}} > 0$, *and*

$\bar{s} := \frac{d_1+p_1}{2a_{1,max}p_1}$.

Definition A.2 (Semitrivial Steady State)
Let $(\bar{c}_1, \cdots, \bar{c}_n)$ *be a steady state of system 2.3. This steady state is called semi-trivial, if there exists* $1 \leq i \leq n$ *such that* $\bar{c}_i = 0$ *and* $1 \leq j \leq n$ *such that* $\bar{c}_j \neq 0$.

Lemma A.3
All semi-trivial steady states are of the form $\bar{c}_1 = \cdots = \bar{c}_k = 0$ *and* $\bar{c}_l \neq 0$ for $l = k+1, \ldots, n$, *with* $1 \leq k \leq n$.

Proposition A.4 (Semitrivial Steady States)
Assume that $(2a_{1,max} - 1)p_1 > d_1$, *and let*

$$s_i := \frac{d_1+p_1}{2a_{1,max}p_1} - \frac{d_i+p_i}{2a_{i,max}p_i},$$

$$\mathbb{J} := \{i \mid s_i \leq 0\},$$

$$\mathbb{S} := \{s_i \mid s_i \leq 0\}, \text{ and}$$

$$k := \max\{i \in \mathbb{J} \mid s_i = \min \mathbb{S}\}.$$

If $\bar{c}_k > 0$, *then* $\bar{c}_l = 0$ for $l < k$ *and the steady state values* $\bar{c}_k, \ldots, \bar{c}_n$ *are positive and unique.*

Biological Remark A.5
In biological terms, this means that cells at the top of a hierarchy need less environmental stimulation, i.e., smaller values of s, *to maintain the size of their population than cell types further down the hierarchy, i.e.,* $s = \frac{a_{i,max}p_i}{d_i+p_i}$ *implies* $(2a_i^c s - 1)p_i^c - d_i^c < 0$ *for* $i > 1$. *In this sense, stem cells are more resistant to environmental stress that all other cell types.*

Corollary A.6 (Instability)

(i) If there exists a positive steady state, each semi-trivial steady state is unstable. The trivial steady state is also unstable.

(ii) If there exists a steady state with k *positive components, each steady state with less than* k *positive components is unstable.*

Remark A.7 (Further properties)

- *For* $n = 2$, $a_1 > 0.5$, $c_1(0) > 0$, $c_2(0) \geq 0$ *the positive equilibrium is globally stable, [85].*
- *For* $n = 3$ *there exists a Hopf-Bifurcation for appropriate parameter choice, [123].*

Lemma A.8
Let $(2a_1 - 1)p_1 - d_1 > 0$, $d_n > 0$, $d_i \geq 0$ *for* $i = 1, \cdots, n-1$, $p_i > 0$, *and* $a_i \in (0, 1)$ *for* $i = 1, \cdots, n-1$. *Furthermore,* $c_1(0) > 0$, $c_i(0) \geq 0$ *for* $i = 2, \cdots, n$. *Then, the solutions of system (2.3) are globally bounded with respect to time.*

PROOF

We can assume that $c_i(0) > 0$ for all i. Otherwise there exists $t_0 > 0$ such that $c_i(t_0) > 0$ for all i, since $c_1(0) > 0$. We consider $q_{1/2} := \frac{c_1}{c_2}$ fulfilling the initial value problem

$$\begin{aligned}
\frac{d}{dt}q_{1/2} &= \frac{\left(\frac{d}{dt}c_1\right)c_2 - \left(\frac{d}{dt}c_2\right)c_1}{c_2^2} \\
&= [(2a_1 s - 1)p_1 - d_1]q_{1/2} - \frac{(2(1-a_1 s)p_1 c_1 + (2a_2 s - 1)p_2 c_2 - d_2 c_2)c_1}{c_2^2} \\
&= [(2a_1 s - 1)p_1 - d_1]q_{1/2} - 2(1-a_1 s)p_1 q_{1/2}^2 - (2a_2 s - 1)p_2 q_{1/2} + d_2 q_{1/2} \\
&< [(2a_1 - 1)p_1 - d_1]q_{1/2} - 2(1-a_1)p_1 q_{1/2}^2 + p_2 q_{1/2} + d_2 q_{1/2} \qquad \text{(A.1)}
\end{aligned}$$

We used that $q_{1/2}$ is non-negative. Due to equation (A.1),

$$q_{1/2} > \frac{[(2a_1 - 1)p_1 - d_1] + d_2 + p_2}{2(1-a_1)p_1} =: Q_{1/2} \qquad \text{(A.2)}$$

implies $\frac{d}{dt}q_{1/2} < 0$.

Therefore, we obtain $q_{1/2}(t) \leq \max\{q_{1/2}(0), Q\} =: K_{1/2}$ for all $t > 0$. Consequently, we obtain

$$c_1 \leq K_{1/2} c_2. \qquad \text{(A.3)}$$

If $n > 3$, let iteratively for $k = 2, \cdots, n-2$, $q_{k/k+1} = \frac{c_k}{c_{k+1}}$

$$\begin{aligned}
\frac{d}{dt}q_{k/k+1} =& \frac{\left(\frac{d}{dt}c_k\right)c_{k+1} - \left(\frac{d}{dt}c_{k+1}\right)c_k}{c_{k+1}^2} \\
=& \frac{[(2a_k s - 1)p_k - d_k]c_k + 2(1-a_{k-1}s)p_{k-1}c_{k-1}}{c_{k+1}} \\
& - \frac{(2(1-a_k s)p_k c_k + (2a_{k+1}s - 1)p_{k+1}c_{k+1} - d_{k+1}c_{k+1})c_k}{c_{k+1}^2} \\
<& [(2a_k - 1)p_k - d_k]q_{k/k+1} + \frac{2p_{k-1}c_{k-1}}{c_{k+1}} - 2(1-a_k)p_k q_{k/k+1}^2 \\
& + p_{k+1}q_{k/k+1} + d_{k+1}q_{k/k+1} \\
<& [(2a_k - 1)p_k - d_k]q_{k/k+1} + 2p_{k-1}K_{k-1/k}q_{k/k+1} - 2(1-a_k)p_k q_{k/k+1}^2 \\
& + p_{k+1}q_{k/k+1} + d_{k+1}q_{k/k+1}.
\end{aligned} \qquad \text{(A.4)}$$

Consequently,

$$q_{k/k+1} > \frac{[(2a_k - 1)p_k - d_k] + 2p_{k-1}K_{k-1/k} + p_{k+1} + d_{k+1}}{2(1-a_k)p_k}$$

implies

$$\frac{d}{dt}q_{k/k+1} < 0,$$

therefore,

$$q_{k/k+1} \leq \max\left\{\frac{[(2a_k-1)p_k - d_k] + 2p_{k-1}K_{k-1/k} + p_{k+1} + d_{k+1}}{2(1-a_k)p_k}, q_{k/k+1}(0)\right\} =: K_{k/k+1}$$

and

$$c_k \leq K_{k/k+1}c_{k+1} \text{ for } k = 2, \cdots, n-2. \tag{A.5}$$

Set $q_{n-1/n} = \frac{c_{n-1}}{c_n}$.

$$\begin{aligned}
\frac{d}{dt}q_{n-1/n} =& \frac{\left(\frac{d}{dt}c_{n-1}\right)c_n - \left(\frac{d}{dt}c_n\right)c_{n-1}}{c_n^2} \\
=& \frac{[(2a_{n-1}s-1)p_{n-1} - d_{n-1}]c_{n-1} + 2(1-a_{n-2}s)p_{n-2}c_{n-2}}{c_n} \\
& - \frac{(2(1-a_{n-1}s)p_{n-1}c_{n-1} - d_nc_n)c_{n-1}}{c_n^2} \\
<& [(2a_{n-1}-1)p_{n-1} - d_{n-1}]q_{n-1/n} \\
& + \frac{2p_{n-2}c_{n-2}}{c_n} - 2(1-a_{n-1})p_{n-1}q_{n-1/n}^2 + d_nq_{n-1/n} \\
<& [(2a_{n-1}-1)p_{n-1} - d_{n-1}]q_{n-1/n} + \frac{2p_{n-2}K_{n-2/n-1}c_{n-1}}{c_n} \\
& - 2(1-a_{n-1})p_{n-1}q_{n-1/n}^2 + d_nq_{n-1/n}
\end{aligned} \tag{A.6}$$

Consequently,

$$q_{n-1/n} > \frac{[(2a_{n-1}-1)p_{n-1} - d_{n-1}] + 2p_{n-2}K_{n-2/n-1} + d_n}{2(1-a_{n-1})p_{n-1}}$$

implies

$$\frac{d}{dt}q_{n-1/n} < 0,$$

therefore,

$$q_{n-1/n} \leq \max\left\{\frac{[(2a_{n-1}-1)p_{n-1} - d_{n-1}] + 2p_{n-2}K_{n-2/n-1} + d_n}{2(1-a_{n-1})p_{n-1}}, q_{n-1/n}(0)\right\} =: K_{n-1/n}$$

and

$$c_{n-1} \leq K_{n-1/n} c_n. \tag{A.7}$$

Inductively, we get $c_1 \leq K_{1/2} \dots K_{n-1/n} c_n$. Analogously, we obtain

$$c_i \leq K_i c_n \text{ for } 1 \leq i < n \tag{A.8}$$

for appropriate positive K_i.
This yields

$$\frac{d}{dt} c_1 = \left(\frac{2a_1 p_1}{1 + k c_n} - p_1 - d_1 \right) c_1 =: K c_1 \tag{A.9}$$

$$\leq \left(\frac{2a_1 p_1}{1 + k c_1 / K} - p_1 - d_1 \right) c_1. \tag{A.10}$$

Therefore,

$$c_1 > \frac{[(2a_1 - 1)p_1 - d_1]K}{k(p_1 + d_1)} \text{ implies } \frac{d}{dt} c_1 < 0. \tag{A.11}$$

This implies that

$$c_1(t) \leq \max \left\{ c_1(0), \frac{[(2a_1 - 1)p_1 - d_1]K}{k(p_1 + d_1)} \right\} := L_1. \tag{A.12}$$

Consequently, c_1 is globally bounded in time. For $k = 2, \cdots, n-1$ we obtain iteratively (using estimate A.8)

$$\frac{d}{dt} c_k = 2 \left(1 - \frac{a_{k-1}}{1 + k c_n} \right) p_{k-1} c_{k-1} + \left(\frac{2a_k}{1 + k c_n} - 1 \right) p_k c_k - d_k c_k \tag{A.13}$$

$$< 2 p_{k-1} L_{k-1} + \left(\frac{2a_k}{1 + k c_k / K_k} - 1 \right) p_k c_k - d_k c_k =: \mathcal{P}_k(c_k). \tag{A.14}$$

We see that $\mathcal{P}_k(c_k) \to -\infty$ for $c_k \to \infty$. Therefore, there exists l_k such that $\mathcal{P}_k(x) < 0$ for $x > l_k$, consequently, $c_k < \max\{l_k, c_k(0)\} =: L_k$ uniformly in time.

In analogy (using estimate A.8):

$$\frac{d}{dt} c_n = 2(1 - \frac{a_{n-1}}{1 + k c_n}) p_{n-1} c_{n-1} - d_n c_n \tag{A.15}$$

$$< 2 p_{n-1} L_{n-1} - d_n c_n. \tag{A.16}$$

This is negative, if $c_n > \frac{2 p_{n-1} L_{n-1}}{d_n} =: \hat{L}_n$. Consequently, $c_n \leq \max\{\hat{L}_n, c_n(0)\} =: L_n$ uniformly in time. We obtain that all c_i, $i = 1, \cdots, n$ are globally bounded with respect to time.

■

Remark A.9
This lemma yields existence, uniqueness and boundedness of solutions of system (2.3), using Picard-Lindelöf's Theorem.

APPENDIX B

PROOFS OF RESULTS IN CHAPTERS 3 AND 4

B.1 Proof of Lemma 3.37

Lemma 3.37 is formulated on page 59.

PROOF
We use notations from equation (3.11).
(i) The zero order term of $\tilde{\chi}_M$ is equivalent to $\nu^c\alpha^c \cdot d_2^l + \nu^l\alpha^l \cdot d_2^c$ and, therefore, positive, since $d_2^c > 0$, $d_2^l > 0$, $\nu^c\alpha^c > 0$, and $\nu^l\alpha^l > 0$.
(ii) Exploiting

$$\begin{aligned}
\bar{s} &= \frac{d_1^c + p_1^c}{2a_1^c p_1^c} = \frac{d_1^l + p_1^l}{2a_1^l p_1^l}, \\
\bar{c}_1 &= \frac{\bar{c}_2 d_2^c}{2\left(1 - a_1^c \bar{s}\right) p_1^c}, \\
\bar{l}_1 &= \frac{\bar{l}_2 d_2^l}{2\left(1 - a_1^l \bar{s}\right) p_1^l} \text{ and} \\
k\bar{c}_2 &= \frac{1}{\bar{s}} - 1 - k\bar{l}_2,
\end{aligned}$$

it follows for the second order term:

$$-(\rho^l + \rho^c) = \left(-2\frac{d_2^c a_1^c p_1^c}{p_1^c - d_1^c} + \frac{d_2^c\left(p_1^c + d_1^c\right)}{p_1^c - d_1^c} + \frac{\left(p_1^c + d_1^c\right) d_2^c}{p_1^c - d_1^c} k\bar{l}_2 - \frac{d_2^l\left(d_1^l + p_1^l\right)}{p_1^l - d_1^l} k\bar{l}_2\right)\bar{s} + d_2^c + d_2^l.$$

We define

$$\begin{aligned}
\eta &:= \left(-2\frac{d_2^c a_1^c p_1^c}{p_1^c - d_1^c} + \frac{d_2^c\left(p_1^c + d_1^c\right)}{p_1^c - d_1^c}\right)\bar{s} + d_2^c,\\
\xi &:= -\frac{d_2^l\left(d_1^l + p_1^l\right)}{p_1^l - d_1^l}k\bar{l}_2\bar{s} + d_2^l,\\
\theta &:= \frac{\left(p_1^c + d_1^c\right)d_2^c}{p_1^c - d_1^c}k\bar{l}_2\bar{s} \geq 0,
\end{aligned}$$

with $-(\rho^l + \rho^c) = \eta + \xi + \theta$.
It follows:

$$\begin{aligned}
\eta &= \frac{d_2^c}{2\left(p_1^c - d_1^c\right)a_1^c p_1^c}\left(-4\,p_1^c a_1^c d_1^c + \left(d_1^c\right)^2 + 2\,d_1^c p_1^c + \left(p_1^c\right)^2\right)\\
&> \frac{d_2^c}{2\left(p_1^c - d_1^c\right)a_1^c p_1^c}\left(\left(d_1^c\right)^2 - 2\,d_1^c p_1^c + \left(p_1^c\right)^2\right)\\
&= \frac{d_2^c}{2\left(p_1^c - d_1^c\right)a_1^c p_1^c}\left(d_1^c - p_1^c\right)^2 \geq 0,
\end{aligned}$$

since $a_1^c < 1$ and $p_1^c - d_1^c > (2a_1^c - 1)p_1^c - d_1^c$, which is assumed to be positive, if we are interested in non-negative steady states (Proposition 3.16). Since we assume $\bar{l}_2 \geq 0$ and $\bar{c}_2 \geq 0$, $k\bar{c}_2 + k\bar{l}_2 = \frac{1}{s} - 1$ implies that $k\bar{l}_2 \leq \frac{1}{s} - 1 = \frac{2a_1^l p_1^l - d_1^l - p_1^l}{p_1^l + d_1^l}$. It holds

$$\begin{aligned}
\xi &\geq -\frac{d_2^l\left(d_1^l + p_1^l\right)}{p_1^l - d_1^l}\frac{2a_1^l p_1^l - d_1^l - p_1^l}{p_1^l + d_1^l}\bar{s} + d_2^l\\
&= \frac{d_2^l}{2\left(p_1^l - d_1^l\right)a_1^l p_1^l}\left(-4\,p_1^l a_1^l d_1^l + {d_1^l}^2 + 2\,d_1^l p_1^l + {p_1^l}^2\right)\\
&> \frac{d_2^l}{2\left(p_1^l - d_1^l\right)a_1^l p_1^l}\left(p_1^l - d_1^l\right)^2 \geq 0.
\end{aligned}$$

Consequently, the second order term is positive.
(iii) follows by direct calculation.

■

B.2 Proof of Lemma 3.39

Lemma 3.39 is presented on page 59.
PROOF
i) We write $\tilde{\beta} = \rho^l + \zeta$, with

$$\rho^l := \left(p_1^l (d_2^l)^2 + (d_2^c)^2 d_2^l\right)\bar{s}^2 - \hat{\alpha}\bar{s}(1 - \bar{s}) > 0,$$

$$\zeta := -(p_1^c(d_2^c)^2 + d_2^c(d_2^l)^2)\bar{s}^2 < 0.$$

Exploiting $X = k\bar{l}_2 < 2a_1^c - 1$ and $a_1^c < 1$, it follows

$$\begin{aligned} H_2(X) &= \hat{\alpha}\bar{s}^2X^2 + \rho^l X + \zeta X + \tilde{\gamma} \\ &\geq \hat{\alpha}\bar{s}^2X^2 + \rho^l X + \zeta(2a_1^c - 1) + \tilde{\gamma} \\ &= \hat{\alpha}\bar{s}^2X^2 + \rho^l X + \big(1 - (2a_1^c - 1)s\big)\bar{s}d_2^c(d_2^l)^2 + (d_2^c)^2 d_2^l \bar{s}^2 \\ &> \hat{\alpha}\bar{s}^2X^2 + \rho^l X \\ &\geq \hat{\alpha}\bar{s}^2X^2 - \hat{\alpha}\bar{s}(1-\bar{s})X \\ &= \hat{\alpha}\bar{s}X\big(\bar{s}X - (1-\bar{s})\big), \end{aligned}$$

which is positive in the relevant range $X \in [0, \frac{1}{\bar{s}} - 1 = 2a_1^c - 1]$, since $\hat{\alpha} < 0$.
(ii)We write $\tilde{\beta} = \rho^l + \zeta$, with

$$\rho^l := \big(p_1^l(d_2^l)^2 + (d_2^c)^2 d_2^l\big)\bar{s}^2 > 0$$

$$\zeta := -(p_1^c(d_2^c)^2 + d_2^c(d_2^l)^2)\bar{s}^2 < 0$$

Exploiting $X < 2a_1^c - 1$ and $a_1^c < 1$ it follows

$$\begin{aligned} H_2(X) &= \rho^l X + \zeta X + \tilde{\gamma} \\ &\geq \rho^l X + \zeta(2a_1^c - 1) + \tilde{\gamma} \\ &= \rho^l X + \big(1 - (2a_1^c - 1)\bar{s}\big)\bar{s}d_2^c(d_2^l)^2 + (d_2^c)^2 d_2^l \bar{s}^2 \\ &> \rho^l X \geq 0. \end{aligned}$$

■

B.3 Proof of Proposition 3.42

Proposition 3.42 is presented on page 60. Statement (i) follows from Lemmas 3.37 and 3.39 and from the Routh-Hurwitz-Theorem, [79]. Proof of statements (ii)-(iii) requires further considerations. These are given in the following Lemmas and Corollaries. At the end of this Section we will obtain statements (ii)-(iii).

Remark B.1
In the case $\hat{\alpha} > 0$ it holds: If $\tilde{\beta} \geq 0$, then $H_2(X) > 0$, since $\tilde{\gamma} > 0$.

Corollary B.2
Assume $k^l = k^c$ and $d_1^c = d_1^l = 0$. Then, it is necessary that $\hat{\alpha} > 0$ and $\tilde{\beta} < 0$ to obtain $H_2 < 0$ within the biologically relevant range of parameters.

PROOF
The corollary follows from Proposition 3.39 and from Remark B.1. ■

We now analyze, if there exist relevant parameters that fulfill $H_2 < 0$. Note that $H_2 > 0$ implies linear stability, due to the Hurwitz theorem, since the quadratic and absolute term of $\tilde{\chi}_M(\lambda)$ are positive (Lemma 3.37).

Remark B.3
$\hat{\alpha} > 0$ *implies*

(i) $(p_1^l d_2^l - p_1^c d_2^c) > 0$ and $(d_2^c - d_2^l) > 0$ *or*

(ii) $(p_1^l d_2^l - p_1^c d_2^c) < 0$ and $(d_2^c - d_2^l) < 0$.

Renaming variables ($p_i^c \leftrightarrow p_i^l$, $a_i^c \leftrightarrow a_i^l$, $c_i \leftrightarrow l_i^l$, $d_2^l \leftrightarrow d_2^c$) does not change the ODE system, but transforms case (i) to case (ii). For this reason we can assume without loss of generality that $(p_1^l d_2^l - p_1^c d_2^c) > 0$ and $(d_2^c - d_2^l) > 0$.

Remark B.4
For the remainder of this Section we assume

- $(p_1^l d_2^l - p_1^c d_2^c) > 0$,
- $(d_2^c - d_2^l) > 0$,
- $k^l = k^c$ *and*
- $d_1^c = d_1^l = 0$.

In the following, we set $\tilde{\delta} := [p_1^l (d_2^l)^2 - p_1^c (d_2^c)^2 + d_2^c d_2^l (d_2^c - d_2^l)]$, *then* $\tilde{\beta} = \bar{s}^2 \tilde{\delta} - \hat{\alpha}\bar{s}(1-\bar{s})$.

Lemma B.5
Let $\tilde{\beta} < 0$. *We consider* $H_2(X)$ *as a quadratic polynomial in* $X = k\bar{l}_2$. *The minimal point of the corresponding parabola lies in the relevant range* $0 \leq k\bar{l}_2 \leq (2a_1^c - 1)$, *if and only if*

$$\hat{\alpha}(1-\bar{s}) + \tilde{\delta}\bar{s} \geq 0.$$

PROOF
The minimum of this parabola is at $X_{min} := -\frac{\tilde{\beta}}{2\hat{\alpha}\bar{s}^2}$. Since we assumed $\tilde{\beta} < 0$, it follows that $X_{min} > 0$. It holds

$$\begin{aligned} -\frac{\tilde{\beta}}{2\hat{\alpha}\bar{s}^2} &\leq \frac{1}{\bar{s}} - 1 \quad \Leftrightarrow \\ -\tilde{\beta} &\leq 2(1-\bar{s})\bar{s}\hat{\alpha} \quad \Leftrightarrow \\ -\bar{s}^2\tilde{\delta} + \hat{\alpha}\bar{s}(1-\bar{s}) &\leq 2(1-\bar{s})\bar{s}\hat{\alpha} \quad \Leftrightarrow \\ \hat{\alpha}(1-\bar{s}) + \tilde{\delta}\bar{s} &\geq 0. \end{aligned}$$

■

Lemma B.6

(i) *Let* $\tilde{\beta} < 0$. *Assume* $\hat{\alpha}(1-\bar{s}) + \tilde{\delta}\bar{s} \geq 0$. *There exists* kl_2 *in the relevant range* $[0, (2a_1^c - 1)]$ *such that* $H_2(kl_2) < 0$, *if and only if* $\frac{-\tilde{\beta}^2}{4\hat{\alpha}\bar{s}^2} + \tilde{\gamma} < 0$.

(ii) *If* $\hat{\alpha}(1-\bar{s}) + \tilde{\delta}\bar{s} < 0$, *then* $H_2(X) > 0$.

PROOF
(i) Due to Lemma B.5, the minimum of $H_2(X)$ lies within the relevant range. The minimum value of $H_2(X)$ is $\frac{-\tilde{\beta}^2}{4\hat{\alpha}\bar{s}^2} + \tilde{\gamma}$. " $\Rightarrow$ " If the minimum is negative and lies within the relevant range, then there exist relevant parameters such that $H_2(X) < 0$. " $\Leftarrow$ " If there exist relevant parameters such that $H_2 < 0$, then the minimum of $H_2(X)$ in the relevant range is negative and, therefore, $\frac{-\tilde{\beta}^2}{4\hat{\alpha}\bar{s}^2} + \tilde{\gamma} < 0$.
(ii) Due to Lemma B.5 and since $X_{min} > 0$, X_{min} is greater than the maximal relevant value of $k\bar{l}_2$. Therefore, the minimum of the parabola $H_2(X)$ in the relevant range is at $X = \frac{1}{\bar{s}} - 1$. It holds

$$
\begin{aligned}
& H_2\left(\frac{1}{\bar{s}} - 1\right) \\
= \;& \hat{\alpha}\left(1-\bar{s}\right)^2 + \tilde{\beta}\left(\frac{1}{\bar{s}} - 1\right) + \tilde{\gamma} \\
= \;& \hat{\alpha}(1-\bar{s})^2 + \tilde{\delta}\bar{s}(1-\bar{s}) - \hat{\alpha}(1-\bar{s})^2 + \tilde{\gamma} \\
= \;& [p_1^l (d_2^l)^2 - p_1^c (d_2)^2 + d_2 d_2^l (d_2^c - d_2^l)]\bar{s}(1-\bar{s}) + d_2^c (d_2^l)^2 \bar{s} + (d_2^c)^2 d_2^l \bar{s}^2 \\
& + (d_2^c)^2 p_1^c (2a_1^c - 1)\bar{s}^2 \\
= \;& [p_1^l (d_2^l)^2 - p_1^c (d_2^c)^2 + d_2 d_2^l (d_2^c - d_2^l)]\bar{s}(1-\bar{s}) + d_2^c (d_2^l)^2 \bar{s} + (d_2^c)^2 d_2^l \bar{s}^2 \\
& + (d_2^c)^2 p_1^c (1-\bar{s})\bar{s} \\
= \;& [p_1^l (d_2^l)^2 + d_2^c d_2^l (d_2^c - d_2^l)]\bar{s}(1-\bar{s}) + d_2^c (d_2^l)^2 \bar{s} + (d_2^c)^2 d_2^l \bar{s}^2 > 0.
\end{aligned}
$$

■

Corollary B.7 (Reformulation of Corollary B.2)
Assume $k^l = k^c$ *and* $d_1^c = d_1^l = 0$. *For existence of* $k\bar{l}_2$ *in the biological relevant range with* $H_2(k\bar{l}_2) < 0$ *it is necessary and sufficient that* $\hat{\alpha} > 0$, $\tilde{\beta} < 0$, $\hat{\alpha}(1-\bar{s}) + \tilde{\delta}\bar{s} \geq 0$ *and* $\frac{-\tilde{\beta}^2}{4\hat{\alpha}\bar{s}^2} + \tilde{\gamma} < 0$.

PROOF
The corollary follows from Proposition 3.39, Lemmas B.5, B.6 and and from Remark B.1. ■

We now elaborate on this case and try to give a more explicit formulation.

Lemma B.8
Assume $\hat{\alpha}(1-\bar{s}) + \tilde{\delta}\bar{s} \geq 0$. *Let* $\bar{s} \in (0.5, 1)$.

(i) *It holds* $\tilde{\beta} < 0$, *if and only if* $0 < \bar{s} < \frac{\hat{\alpha}}{\hat{\alpha}+\tilde{\delta}}$.

(ii) *There exists* $\bar{s} \in \left(\frac{1}{2}, 1\right)$ *with* $\tilde{\beta} < 0$, *if and only if* $p_1^c > \frac{p_1^l(2d_2^l - d_2^c) + (d_2^c)^2 - d_2^c d_2^l}{d_2^c}$.

PROOF
(i) Note that $\hat{\alpha}(1-\bar{s}) + \tilde{\delta}\bar{s} \geq 0$, $\hat{\alpha} > 0$, implies $\hat{\alpha} + \tilde{\delta} > 0$. This is the case, since $\hat{\alpha} > 0$, due to assumptions and $\bar{s} > 0.5$. If we had $\hat{\alpha} + \tilde{\delta} \leq 0$, then it would hold $|\tilde{\delta}| \geq \hat{\alpha}$ and then also $\hat{\alpha}(1-\bar{s}) + \tilde{\delta}\bar{s} < 0$, since $\bar{s} > 0.5$. This would be a contradiction. It holds $\tilde{\beta} = \bar{s}\big((\hat{\alpha} + \tilde{\delta})\bar{s} - \hat{\alpha}\big)$, which gives the result.

(ii) Due to (i), $\tilde{\beta} < 0$, if and only if $0 < \bar{s} < \frac{\hat{\alpha}}{\hat{\alpha}+\tilde{\delta}}$. It is, therefore, necessary and sufficient for existence of $\bar{s} > 0.5$ that $\frac{\hat{\alpha}}{\hat{\alpha}+\tilde{\delta}} > \frac{1}{2}$, which is equivalent to $\hat{\alpha} > \tilde{\delta}$, which is equivalent to $p_1^c > \frac{p_1^l(2d_2^l - d_2^c) + (d_2^c)^2 - d_2^c d_2^l}{d_2^c}$:

$$\begin{aligned}
(p_1^l d_2^l - p_1^c d_2^c)(d_2^c - d_2^l) &> p_1^l (d_2^l)^2 - p_1^c (d_2^c)^2 + d_2^c d_2^l (d_2^c - d_2^l) \Leftrightarrow \\
p_1^c d_2^c &> 2p_1^l d_2^l - p_1^l d_2^c + d_2^c (d_2^c - d_2^l) \Leftrightarrow \\
p_1^c &> \frac{p_1^l(2d_2^l - d_2^c) + (d_2^c)^2 - d_2^c d_2^l}{d_2^c}.
\end{aligned}$$

■

With this result we can reformulate Corollary B.7:

Corollary B.9 (Reformulation of Corollary B.7)
Assume $k^l = k^c$ *and* $d_1^c = d_1^l = 0$. *After possible renaming of variables* ($a_i^c \leftrightarrow a_i^l$, $p_i^c \leftrightarrow p_i^l$, $d_2^l \leftrightarrow d_2^c$) *it holds: For existence of* $k\bar{l}_2$ *in the biologically relevant range with* $H_2(k\bar{l}_2) < 0$ *it is necessary and sufficient that* $d_2^c > d_2^l$, $p_1^l d_2^l > p_1^c d_2^c$, $0 < \bar{s} < \frac{\hat{\alpha}}{\hat{\alpha}+\tilde{\delta}}$, $p_1^c > \frac{p_1^l(2d_2^l - d_2^c) + (d_2^c)^2 - d_2^c d_2^l}{d_2^c}$, $\hat{\alpha}(1-\bar{s}) + \tilde{\delta}\bar{s} \geq 0$ *and* $\frac{-\tilde{\beta}^2}{4\hat{\alpha}\bar{s}^2} + \tilde{\gamma} < 0$.

PROOF
The corollary follows from Proposition 3.39, Lemmas B.5, B.6 and B.8 and from Remarks B.1 and B.3. ■

We further elaborate on the condition $\hat{\alpha}(1-\bar{s}) + \tilde{\delta}\bar{s} \geq 0$ and on compatibility of $p_1^c > \frac{p_1^l(2d_2^l - d_2^c) + (d_2^c)^2 - d_2^c d_2^l}{d_2^c}$ and $p_1^l d_2^l > p_1^c d_2^c$.

Lemma B.10
$\hat{\alpha}(1-\bar{s}) + \tilde{\delta}\bar{s} \geq 0$ *is equivalent to*

$$p_1^c \leq \frac{p_1^l d_2^l (d_2^c - d_2^l)(1-\bar{s}) + d_2^c d_2^l (d_2^c - d_2^l)\bar{s} + p_1^l (d_2^l)^2 \bar{s}}{d_2^c (d_2^c - d_2^l)(1-\bar{s}) + (d_2^c)^2 \bar{s}}.$$

PROOF
The proof follows from a direct calculation:

$$\begin{aligned}
\hat{\alpha}(1-\bar{s}) + \tilde{\delta}\bar{s} &\geq 0 \Leftrightarrow \\
(p_1^l d_2^l - p_1^c d_2^c)(d_2^c - d_2^l)(1-\bar{s}) + \bar{s}p_1^l(d_2^l)^2 - \bar{s}p_1^c(d_2^c)^2 + d_2^c d_2^l(d_2^c - d_2^l)\bar{s} &\geq 0 \Leftrightarrow \\
\frac{p_1^l d_2^l(d_2^c - d_2^l)(1-\bar{s}) + d_2^c d_2^l(d_2^c - d_2^l)\bar{s} + p_1^l(d_2^l)^2\bar{s}}{d_2^c(d_2^c - d_2^l)(1-\bar{s}) + (d_2^c)^2\bar{s}} &\geq p_1^c.
\end{aligned}$$

■

Since our choice of notation and $\hat{\alpha} > 0$ requires $p_1^l d_2^l > p_1^c d_2^c$, it is necessary that $p_1^l \frac{d_2^l}{d_2^c} > \frac{p_1^l(2d_2^l - d_2^c) + (d_2^c)^2 - d_2^c d_2^l}{d_2^c}$ to satisfy Lemma B.8 (ii).

Lemma B.11
To fulfill $p_1^l \frac{d_2^l}{d_2^c} > \frac{p_1^l(2d_2^l - d_2^c) + (d_2^c)^2 - d_2^c d_2^l}{d_2^c}$ *it is necessary and sufficient that* $p_1^l > d_2^c$.

PROOF
The proof follows from a direct calculation:

$$\begin{aligned}
p_1^l d_2^l &> p_1^l(2d_2^l - d_2^c) + (d_2^c)^2 - d_2^c d_2^l \Leftrightarrow \\
p_1^l(d_2^c - d_2^l) &> d_2^c(d_2^c - d_2^l).
\end{aligned}$$

■

Lemma B.12
If $p_1^l > d_2^c$*, it holds:*
$p_1^l \frac{d_2^l}{d_2^c} > \frac{p_1^l d_2^l(d_2^c - d_2^l)(1-\bar{s}) + d_2^c d_2^l(d_2^c - d_2^l)\bar{s} + p_1^l(d_2^l)^2\bar{s}}{d_2^c(d_2^c - d_2^l)(1-\bar{s}) + (d_2^c)^2\bar{s}} > \frac{p_1^l(2d_2^l - d_2^c) + (d_2^c)^2 - d_2^c d_2^l}{d_2^c}$.

PROOF
The proof follows from a direct calculation:

$$\begin{aligned}
p_1^l \frac{d_2^l}{d_2^c} &> \frac{p_1^l d_2^l(d_2^c - d_2^l)(1-\bar{s}) + d_2^c d_2^l(d_2^c - d_2^l)\bar{s} + p_1^l(d_2^l)^2\bar{s}}{d_2^c(d_2^c - d_2^l)(1-\bar{s}) + (d_2^c)^2\bar{s}} \Leftrightarrow \\
p_1^l(d_2^c - d_2^l)d_2^l &> d_2^c d_2^l(d_2^c - d_2^l),
\end{aligned}$$

$$\begin{aligned}
\frac{p_1^l d_2^l(d_2^c - d_2^l)(1-\bar{s}) + d_2^c d_2^l(d_2^c - d_2^l)\bar{s} + p_1^l(d_2^l)^2\bar{s}}{d_2^c(d_2^c - d_2^l)(1-\bar{s}) + (d_2^c)^2\bar{s}} &> \\
\frac{p_1^l(2d_2^l - d_2^c) + (d_2^c)^2 - d_2^c d_2^l}{d_2^c} &\Leftrightarrow \\
d_2^c(d_2^c - d_2^l)^2 &< p_1^l(d_2^c - d_2^l)^2.
\end{aligned}$$

■

Remark B.13
Lemma B.12 demonstrates that the conditions from Lemma B.8 and Lemma B.10 are compatible to each other.

Corollary B.14 (Reformulation of Corollary B.9)

(i) *Assume $k^l = k^c$ and $d_1^c = d_1^l = 0$. For existence of $k\bar{l}_2$ in the biologically relevant range fulfilling $H_2(k\bar{l}_2) < 0$, it is necessary and sufficient that $\hat{\alpha} > 0$, $\tilde{\beta} < 0$, $\hat{\alpha}(1-\bar{s}) + \tilde{\delta}\bar{s} \geq 0$ and $\frac{-\tilde{\beta}^2}{4\hat{\alpha}\bar{s}^2} + \tilde{\gamma} < 0$.*

(ii) *After possible renaming of variables, the condition $\hat{\alpha} > 0$ is equivalent to $d_2^c > d_2^l$ and $p_1^l d_2^l > p_1^c d_2^c$. Consequently, the following additional conditions are necessary and sufficient for existence of a biologically relevant $k\bar{l}_2$ with $H_2(k\bar{l}_2) < 0$:*

- $\bar{s} < \frac{\hat{\alpha}}{\hat{\alpha}+\tilde{\delta}}$, $p_1^c > \frac{p_1^l(2d_2^l - d_2^c) + (d_2^c)^2 - d_2^c d_2^l}{d_2^c}$, $p_1^l > d_2^c$
  $\left(\Leftrightarrow \tilde{\beta} < 0 \text{ while } p_1^l d_2^l > p_1^c d_2^c \text{ and } \bar{s} > \frac{1}{2}\right)$,
- $p_1^c \leq \frac{p_1^l d_2^l (d_2^c - d_2^l)(1-\bar{s}) + d_2^c d_2^l (d_2^c - d_2^l)\bar{s} + p_1^l (d_2^l)^2 \bar{s}}{d_2^c (d_2^c - d_2^l)(1-\bar{s}) + (d_2^c)^2 \bar{s}}$ $\left(\Leftrightarrow \hat{\alpha}(1-\bar{s}) + \tilde{\delta}\bar{s} \geq 0)\right)$,
- $\frac{-\tilde{\beta}^2}{4\hat{\alpha}\bar{s}^2} + \tilde{\gamma} < 0$.

PROOF
Statement (i) is Corollary B.7. Then, the Corollary follows from Proposition 3.39, Lemmas B.5, B.6, B.8, B.10 and B.11 and from Remarks B.3 and B.1. ■

We now elaborate on the constraints on $\bar{s}$.

Lemma B.15
Assume $\hat{\alpha}(1-\bar{s}) + \tilde{\delta}\bar{s} \geq 0$, then $\bar{s} < \frac{\hat{\alpha}}{\hat{\alpha}+\tilde{\delta}}$ is equivalent to

$$p_1^c > \frac{d_2^l(p_1^l d_2^c \bar{s} - p_1^l(d_2^c - d_2^l) + (d_2^c)^2\bar{s} - d_2^c d_2^l \bar{s})}{d_2^c(d_2^c(2\bar{s}-1) + d_2^l(1-\bar{s}))}.$$

PROOF

$$\begin{aligned}
\bar{s} &< \frac{\hat{\alpha}}{\hat{\alpha}+\tilde{\delta}} \Leftrightarrow \\
\tilde{\delta}\bar{s} &< (1-\bar{s})\hat{\alpha} \Leftrightarrow \\
p_1^c d_2^c\big(d_2^c(1-2\bar{s}) - d_2^l(1-\bar{s})\big) &< d_2^l\big(p_1^l(d_2^c - d_2^l) - p_1^l d_2^c \bar{s} - (d_2^c)^2\bar{s} + d_2^c d_2^l \bar{s}\big) \Leftrightarrow \\
p_1 &> \frac{d_2^l\big(p_1^l d_2^c \bar{s} - p_1^l(d_2^c - d_2^l) + (d_2^c)^2\bar{s} - d_2^c d_2^l \bar{s}\big)}{d_2^c\big(d_2^c(2\bar{s}-1) + d_2^l(1-\bar{s})\big)},
\end{aligned}$$

since $p_1^c d_2^c(d_2^c(1-2\bar{s}) - d_2^l(1-\bar{s})) < 0$. We used $\bar{s} > 1/2$.

■

Lemma B.16
Denote:

- $P_{max} := \frac{p_1^l d_2^l (d_2^c - d_2^l)(1-\bar{s}) + d_2^c d_2^l (d_2^c - d_2^l)\bar{s} + p_1^l (d_2^l)^2 \bar{s}}{d_2^c (d_2^c - d_2^l)(1-\bar{s}) + (d_2^c)^2 \bar{s}}$,
- $P_{min} := \frac{d_2^l (p_1^l d_2^c \bar{s} + (d_2^c)^2 \bar{s} - d_2^c d_2^l \bar{s} - p_1^l d_2^c + p_1^l d_2^l)}{d_2^c (2 d_2^c \bar{s} - d_2^l \bar{s} - d_2^c + d_2^l)}$,
- $P_0 := \frac{p_1^l (2d_2^l - d_2^c) + (d_2^c)^2 - d_2^c d_2^l}{d_2^c}$.

Assume $p_1^l > d_2$, then

(i) $P_{max} > P_{min}$,

(ii) $P_{min} > P_0$.

PROOF

The expression for P_{min} comes from Lemma B.15. Since both denominators are positive, (i) is equivalent to

$$\begin{aligned} \left(p_1^l d_2^l (d_2^c - d_2^l)(1-\bar{s}) + d_2^c d_2^l (d_2^c - d_2^l)\bar{s} + p_1^l (d_2^l)^2 \bar{s}\right)\left(2 d_2^c \bar{s} - d_2^l \bar{s} - d_2^c + d_2^l\right) &> \\ \left(d_2^l (p_1^l d_2^c \bar{s} + (d_2^c)^2 \bar{s} - d_2^c d_2^l \bar{s} - p_1^l d_2^c + p_1^l d_2^l)\right)\left((d_2^c - d_2^l)(1-\bar{s}) + d_2^c \bar{s}\right) &\Leftrightarrow \\ (d_2^c - d_2^l)^2 (1-\bar{s})(p_1^l - d_2^c) > 0. & \end{aligned}$$

Since both denominators are positive, (ii) is equivalent to

$$\begin{aligned} d_2^l (p_1^l d_2^c \bar{s} + (d_2^c)^2 \bar{s} - d_2^c d_2^l \bar{s} - p_1^l d_2^c + p_1^l d_2^l) &> \\ \left[\left(p_1^l (2d_2^l - d_2^c) + (d_2^c)^2 - d_2^c d_2^l\right)\right]\left[(2 d_2^c \bar{s} - d_2^l \bar{s} - d_2^c + d_2^l)\right] &\Leftrightarrow \\ (d_2^c - d_2^l)^2 (2\bar{s} - 1)(p_1^l - d_2^c) > 0. & \end{aligned}$$

■

Remark B.17
Due to Lemma B.16, we obtain a stronger condition on p_1^c:

$$p_1^c \in (P_{min},\ P_{max}].$$

Proposition 3.42 follows from:

Proposition B.18 (Reformulation of Corollary B.14)

(i) *Assume $k^l = k^c$ and $d_1^c = d_1^l = 0$. Then, it is necessary and sufficient that $\hat{\alpha} > 0$, $\tilde{\beta} < 0$, $\hat{\alpha}(1-\bar{s}) + \tilde{\delta}\bar{s} \geq 0$ and $\frac{-\tilde{\beta}^2}{4\hat{\alpha}\bar{s}^2} + \tilde{\gamma} < 0$ to obtain $H_2 < 0$ within the biologically relevant range of parameters.*

(ii) *After possible renaming of variables, the condition $\hat{\alpha} > 0$ is equivalent to $d_2^c > d_2^l$ and $p_1^l d_2^l > p_1^c d_2^c$. Consequently, the following additional conditions are necessary and sufficient for existence of a biologically relevant $k\bar{l}_2$ with $H_2(k\bar{l}_2) < 0$:*

- $p_1^c > P_{min}$, $p_1^l > d_2^c$ $\left(\Leftrightarrow \tilde{\beta} < 0 \text{ while } p_1^l d_2^l > p_1^c d_2^c \text{ and } \bar{s} > \frac{1}{2}\right)$,
- $p_1^c \leq P_{max}$ $\left(\Leftrightarrow \hat{\alpha}(1-\bar{s}) + \tilde{\delta}\bar{s} \geq 0\right)$,
- $\frac{-\tilde{\beta}^2}{4\hat{\alpha}\bar{s}^2} + \tilde{\gamma} < 0$.

(iii) *$-\tilde{\beta}^2 + 4\hat{\alpha}\tilde{\gamma}\bar{s}^2$ is a polynomial of order two in p_1^c, with a negative maximum order coefficient. Denote by $\tilde{p}_{min}$ and $\tilde{p}_{max}$ the zeros of this polynomial, if they are real. Then, the conditions in (ii) are equivalent to*

- $p_1^l > d_2^c$,
- $p_1^c \in (P_{min},\ P_{max}] \backslash [\tilde{p}_{min}, \tilde{p}_{max}]$.

If the zeros are not real, the only constraint on p_1^c is $p_1^c \in (P_{min},\ P_{max}]$.

(iv) *If the necessary and sufficient conditions are fulfilled, then the biologically relevant range of $k\bar{l}_2$ with $H_2(k\bar{l}_2) < 0$ is given by*

$$\emptyset \neq \left\{ \left[0,\ \frac{1}{\bar{s}} - 1\right] \cap \left(\frac{-\tilde{\beta}}{2\hat{\alpha}\bar{s}^2} - \sqrt{\frac{\tilde{\beta}^2 - 4\hat{\alpha}\bar{s}^2\tilde{\gamma}}{(2\hat{\alpha}\bar{s}^2)^2}},\ \frac{-\tilde{\beta}}{2\hat{\alpha}\bar{s}^2} + \sqrt{\frac{\tilde{\beta}^2 - 4\hat{\alpha}\bar{s}^2\tilde{\gamma}}{(2\hat{\alpha}\bar{s}^2)^2}} \right) \right\} \subset \mathbb{R}.$$

PROOF

Statement (i) comes from Corollary B.7. Statements (i) and (ii) follow from Proposition 3.39, Lemmas B.5, B.6, B.8, B.10, B.11, B.15, B.16 and from Remarks B.3 and B.1.

(iii) The maximum order coefficient is

$$-\left(\bar{s}(1-\bar{s})d_2^c(d_2^c - d_2^l) - \bar{s}^2(d_2^c)^2\right)^2 - 4\,(d_2^c)^3\left(d_2^c - d_2^l\right)\bar{s}^4\left(\frac{1}{\bar{s}} - 1\right) < 0,$$

therefore, the positive part lies between the two zeros, if they are real. If quadratic polynomial with negative highest order term has no real zeros, then it is everywhere negative.

(iv) As in Lemma 3.37 we write $H_2(X) = \hat{\alpha}\bar{s}^2X^2 + \tilde{\beta}X + \tilde{\gamma}$, with $\hat{\alpha} > 0$, $\tilde{\gamma} > 0$. Due to the assumptions, it holds $\frac{-\tilde{\beta}^2}{4\hat{\alpha}\bar{s}^2} + \tilde{\gamma} < 0$, therefore, the square root is real. Due to Lemma B.5, $\frac{-\tilde{\beta}}{2\hat{\alpha}\bar{s}^2} \in \left[0,\ \frac{1}{\bar{s}} - 1\right]$, therefore, the intersection is not empty. ■

Remark B.19
The conditions originating from Proposition B.18 by renaming $p_i^c \leftrightarrow p_i^l$, $a_i^c \leftrightarrow a_i^l$, $c_i \leftrightarrow l_i^l$, $d_2^l \leftrightarrow d_2^c$, are necessary and sufficient conditions for the case $d_2^c < d_2^l$ and $p_1^l d_2^l < p_1^c d_2^c$.

Remark B.20
The set of parameters characterized by Proposition B.18 is not empty, e.g. set $a_1^c = a_1^l = 0.98039$, $p_1^c = 22$, $p_1^l = 4000$, $d_1^c = d_1^l = 0$, $d_2^c = 0.5$, $d_2^l = 0.2$, $k^l = k^c = 12.8 \cdot 10^{-10}$, $\bar{l}_2 = 0.15/k^l$, *which leads to* $H_2 \approx -0.061$.

Remark 3.46 (i) follows from $y := \frac{-\tilde{\beta}}{2\hat{\alpha}\bar{s}^2} - \sqrt{(\frac{-\tilde{\beta}}{2\hat{\alpha}\bar{s}^2})^2 - \frac{\tilde{\gamma}}{\hat{\alpha}\bar{s}^2}} > 0$, i.e., the interval $[0, y)$ is not contained in the interval specified in Proposition B.18 (iv).

B.4 Proof of Lemma 4.8

The Lemma is formulated on page 69.

PROOF
(a) Assumptions (i)-(iii) provide that in the case $d = 0$ there exists a fully positive unique steady state, see Proposition A.1. Denote the steady state value of s as $\bar{s}^0$ and it holds $\bar{s}^0 = \frac{p_1^c + d_1^c}{2a_1^c p_1^c}$. We denote the steady state value of s for $d > 0$ as $\bar{s}^d$. Assumption (iv) guarantees the existence of a steady state for the case $d > 0$ with at least one nonzero component (Lemma 4.4). Due to Lemma 4.4, we know that $\bar{s}^0 = \min\{\frac{d_i^c + p_i^c}{2a_i^c p_i^c} | i = 1, \cdots, n-1\}$ and $\bar{s}^d = \min\{\frac{d_i^c + p_i^c + d}{2a_i^c p_i^c} | i = 1, \cdots, n-1\}$. Since $\frac{d_i^c + p_i^c + d}{2a_i^c p_i^c} > \frac{d_i^c + p_i^c}{2a_i^c p_i^c}$ for all $i = 1, \cdots, n-1$, it holds $\bar{s}^d > \bar{s}^0$. This implies $\bar{c}_n^d < \bar{c}_n^0$, due to $\bar{c}_n = \left(\frac{1}{s} - 1\right)\frac{1}{k}$.

It remains to show that $\bar{c}_{n-1}^d < \bar{c}_{n-1}^0$.

It holds $\bar{s}^0 = \frac{d_1^c + p_1^c}{2a_1^c p_1^c}$, due to Assumption (iii) and $\bar{s}^d = \frac{d_{i_0}^c + p_{i_0}^c + d}{2a_{i_0}^c p_{i_0}^c}$. This implies

$$\begin{aligned}\bar{c}_n^d &= \left(\frac{1}{\bar{s}} - 1\right)\frac{1}{k} = \frac{2a_{i_0}^c p_{i_0}^c - (d_{i_0}^c + p_{i_0}^c + d)}{d_{i_0}^c + p_{i_0}^c + d}\frac{1}{k} \\ &= \frac{(2a_{i_0}^c - 1)p_{i_0}^c - (d_{i_0}^c + d)}{d_{i_0}^c + p_{i_0}^c + d}\frac{1}{k}\end{aligned}$$

and $\bar{c}_n^0 = \frac{(2a_1^c - 1)p_1^c - d_1^c}{d_1^c + p_1^c}\frac{1}{k}$.
It holds

$$\bar{c}_{n-1}^d = \frac{d_n^c}{2\left(1 - a_{n-1}^c \frac{d + d_{i_0}^c + p_{i_0}^c}{2a_{i_0}^c p_{i_0}^c}\right)p_{n-1}^c}\frac{(2a_{i_0}^c - 1)p_{i_0}^c - (d_{i_0}^c + d)}{d_{i_0}^c + p_{i_0}^c + d}\frac{1}{k}$$

and

$$\bar{c}_{n-1}^0 = \frac{d_n^c}{2\left(1 - a_{n-1}^c \frac{d_1^c + p_1^c}{2a_1^c p_1^c}\right)p_{n-1}^c}\frac{(2a_1^c - 1)p_1^c - d_1^c}{d_1^c + p_1^c}\frac{1}{k}.$$

We note that $(2a_1^c - 1)p_1^c - d_1^c > 0$ (Assumption (ii)) implies that $1 > \frac{p_1^c + d_1^c}{2a_1^c p_1^c}$. Assumption (iv) and the definition of i_0 imply $0 < s_{i_0} < 1$. Therefore, $2\left(1 - a_{n-1}^c \frac{d_1^c + p_1^c}{2a_1^c p_1^c}\right) > 0$ and $2\left(1 - a_{n-1}^c \frac{d_{i_0}^c + d + p_{i_0}^c}{2a_{i_0}^c p_{i_0}^c}\right) > 0$. It holds

$$
\begin{aligned}
&\bar{c}_{n-1}^d - \bar{c}_{n-1}^0 < 0 \quad \Leftrightarrow \\
&\frac{d_n^c}{2\left(1 - a_{n-1}^c \frac{d + d_{i_0}^c + p_{i_0}^c}{2a_{i_0}^c p_{i_0}^c}\right) p_{n-1}^c} \frac{(2a_{i_0}^c - 1)p_{i_0}^c - (d_{i_0}^c + d)}{d_{i_0}^c + p_{i_0}^c + d} \\
&< \frac{d_n^c}{2\left(1 - a_{n-1}^c \frac{d_1^c + p_1^c}{2a_1^c p_1^c}\right) p_{n-1}^c} \frac{(2a_1^c - 1)p_1^c - d_1^c}{d_1^c + p_1^c} \quad \Leftrightarrow \\
&(d_1^c + p_1^c)\left(1 - a_{n-1}^c \frac{d_1^c + p_1^c}{2a_1^c p_1^c}\right)\left((2a_{i_0}^c - 1)p_{i_0}^c - d_{i_0}^c - d\right) \\
&< (d_{i_0}^c + p_{i_0}^c + d)\left(1 - a_{n-1}^c \frac{d + d_{i_0}^c + p_{i_0}^c}{2a_{i_0}^c p_{i_0}^c}\right)\left((2a_1^c - 1)p_1^c - d_1^c\right) \quad \Leftrightarrow \\
&\left(d_1^c + p_1^c - a_{n-1}^c \frac{(d_1^c + p_1^c)^2}{2a_1^c p_1^c}\right)\left((2a_{i_0}^c - 1)p_{i_0}^c - d_{i_0}^c - d\right) \\
&< \left((d_{i_0}^c + p_{i_0}^c + d) - a_{n-1}^c \frac{(d + d_{i_0}^c + p_{i_0}^c)^2}{2a_{i_0}^c p_{i_0}^c}\right)\left((2a_1^c - 1)p_1^c - d_1^c\right) \quad \Leftrightarrow \\
&(d_1^c + p_1^c)\left(2a_{i_0}^c p_{i_0}^c - p_{i_0}^c - d_{i_0}^c - d\right) - \left(2a_{i_0}^c p_{i_0}^c - p_{i_0}^c - d_{i_0}^c - d\right)\left(a_{n-1}^c \frac{(d_1^c + p_1^c)^2}{2a_1^c p_1^c}\right) \\
&< (d_{i_0}^c + p_{i_0}^c + d)(2a_1^c p_1^c - p_1^c - d_1^c) \\
&- \left(a_{n-1}^c \frac{(d + d_{i_0}^c + p_{i_0}^c)^2}{2a_{i_0}^c p_{i_0}^c}\right)(2a_1^c p_1^c - p_1^c - d_1^c) \quad \Leftrightarrow \\
&(d_1^c + p_1^c)\left(2a_{i_0}^c p_{i_0}^c - p_{i_0}^c - d_{i_0}^c - d\right) - (d_{i_0}^c + p_{i_0}^c + d)(2a_1^c p_1^c - p_1^c - d_1^c) \\
&+ \left[\left(\frac{(d + d_{i_0}^c + p_{i_0}^c)^2}{2a_{i_0}^c p_{i_0}^c}\right)(2a_1^c p_1^c - p_1^c - d_1^c)\right. \\
&\left. - \left(2a_{i_0}^c p_{i_0}^c - p_{i_0}^c - d_{i_0}^c - d\right)\left(\frac{(d_1^c + p_1^c)^2}{2a_1^c p_1^c}\right)\right] a_{n-1}^c < 0 \qquad \text{(B.1)}
\end{aligned}
$$

We now investigate, when the condition

$$
\begin{aligned}
&\left[\left(\frac{(d + d_{i_0}^c + p_{i_0}^c)^2}{2a_{i_0}^c p_{i_0}^c}\right)(2a_1^c p_1^c - p_1^c - d_1^c)\right. \\
&\left. - \left(2a_{i_0}^c p_{i_0}^c - p_{i_0}^c - d_{i_0}^c - d\right)\left(\frac{(d_1^c + p_1^c)^2}{2a_1^c p_1^c}\right)\right] > 0 \qquad \text{(B.2)}
\end{aligned}
$$

is fulfilled. It holds

$$\left[\left(\frac{(d+d_{i_0}^c+p_{i_0}^c)^2}{2a_{i_0}^c p_{i_0}^c}\right)(2a_1^c p_1^c - p_1^c - d_1^c)\right.$$
$$\left.-\left(2a_{i_0}^c p_{i_0}^c - p_{i_0}^c - d_{i_0}^c - d\right)\left(\frac{(d_1^c+p_1^c)^2}{2a_1^c p_1^c}\right)\right] > 0 \Leftrightarrow$$
$$[(d+d_{i_0}^c+p_{i_0}^c)^2(2a_1^c p_1^c - p_1^c - d_1^c)(a_1^c p_1^c)$$
$$-\left(2a_{i_0}^c p_{i_0}^c - p_{i_0}^c - d_{i_0}^c - d\right)(d_1^c+p_1^c)^2(a_{i_0}^c p_{i_0}^c)] > 0 \tag{B.3}$$

The latter is always true, since

$$\bar{s}^0 < \bar{s}^d \Leftrightarrow \frac{p_1^c+d_1^c}{2a_1^c p_1^c} < \frac{p_{i_0}^c+d_{i_0}^c+d}{2a_{i_0}^c p_{i_0}^c} \Leftrightarrow$$
$$(p_1^c+d_1^c)(a_{i_0}^c p_{i_0}^c) < (a_1^c p_1^c)(p_{i_0}^c+d_{i_0}^c+d) \tag{B.4}$$

and since

$$\bar{s}^0 < \bar{s}^d \Leftrightarrow$$
$$\frac{2a_1^c p_1^c}{d_1^c+p_1^c} > \frac{2a_{i_0}^c p_1^c i_0}{d_{i_0}^c+p_{i_0}^c+d} \Leftrightarrow$$
$$\frac{2a_1^c p_1^c}{d_1^c+p_1^c} - 1 > \frac{2a_{i_0}^c p_1^c i_0}{d_{i_0}^c+p_{i_0}^c+d} - 1 \Leftrightarrow$$
$$\frac{(2a_1^c-1)p_1^c - d_1^c}{d_1^c+p_1^c} > \frac{(2a_{i_0}^c p_1^c i_0 - 1) - d_{i_0}^c - d}{d_{i_0}^c+p_{i_0}^c+d} \Leftrightarrow$$
$$((2a_1^c-1)p_1^c - d_1^c)(d_{i_0}^c+p_{i_0}^c+d) > (d_1^c+p_1^c)((2a_{i_0}^c-1)p_{i_0}^c - d_{i_0}^c - d).$$

Therefore, (B.2) is always true. Condition (B.2) and since $a_{n-1}^c < 1$ imply

$$(d_1^c+p_1^c)\left(2a_{i_0}^c p_{i_0}^c - p_{i_0}^c - d_{i_0}^c - d\right) - (d_{i_0}^c+p_{i_0}^c+d)(2a_1^c p_1^c - p_1^c - d_1^c)$$
$$+\left[\left(\frac{(d+d_{i_0}^c+p_{i_0}^c)^2}{2a_{i_0}^c p_{i_0}^c}\right)(2a_1^c p_1^c - p_1^c - d_1^c)\right.$$
$$\left.-\left(2a_{i_0}^c p_{i_0}^c - p_{i_0}^c - d_{i_0}^c - d\right)\left(\frac{(d_1^c+p_1^c)^2}{2a_1^c p_1^c}\right)\right]a_{n-1}^c$$
$$< (d_1^c+p_1^c)\left(2a_{i_0}^c p_{i_0}^c - p_{i_0}^c - d_{i_0}^c - d\right) - (d_{i_0}^c+p_{i_0}^c+d)(2a_1^c p_1^c - p_1^c - d_1^c)$$
$$+\left[\left(\frac{(d+d_{i_0}^c+p_{i_0}^c)^2}{2a_{i_0}^c p_{i_0}^c}\right)(2a_1^c p_1^c - p_1^c - d_1^c)\right.$$
$$\left.-\left(2a_{i_0}^c p_{i_0}^c - p_{i_0}^c - d_{i_0}^c - d\right)\left(\frac{(d_1^c+p_1^c)^2}{2a_1^c p_1^c}\right)\right]. \tag{B.5}$$

Using estimates (B.1) and (B.5), we get the following sufficient condition

$$\begin{aligned}
&(d_1^c + p_1^c)\left(2a_{i_0}^c p_{i_0}^c - p_{i_0}^c - d_{i_0}^c - d\right) - (d_{i_0}^c + p_{i_0}^c + d)\left(2a_1^c p_1^c - p_1^c - d_1^c\right) \\
&\quad + \Bigg[\left(\frac{(d + d_{i_0}^c + p_{i_0}^c)^2}{2a_{i_0}^c p_{i_0}^c} \right) \left(2a_1^c p_1^c - p_1^c - d_1^c\right) \\
&\quad - \left(2a_{i_0}^c p_{i_0}^c - p_{i_0}^c - d_{i_0}^c - d\right) \left(\frac{(d_1^c + p_1^c)^2}{2a_1^c p_1^c} \right) \Bigg] < 0 \\
&\quad \Rightarrow \bar{c}_{n-1}^d - \bar{c}_{n-1}^0 < 0
\end{aligned} \tag{B.6}$$

We check, when condition (B.6) is fulfilled:

$$\begin{aligned}
&(d_1^c + p_1^c)\left(2a_{i_0}^c p_{i_0}^c - p_{i_0}^c - d_{i_0}^c - d\right) - (d_{i_0}^c + p_{i_0}^c + d)\left(2a_1^c p_1^c - p_1^c - d_1^c\right) \\
&\quad + \Bigg[\left(\frac{(d + d_{i_0}^c + p_{i_0}^c)^2}{2a_{i_0}^c p_{i_0}^c} \right) \left(2a_1^c p_1^c - p_1^c - d_1^c\right) \\
&\quad - \left(2a_{i_0}^c p_{i_0}^c - p_{i_0}^c - d_{i_0}^c - d\right) \left(\frac{(d_1^c + p_1^c)^2}{2a_1^c p_1^c} \right) \Bigg] < 0 \quad \Leftrightarrow \\
&2(a_{i_0}^c p_{i_0}^c)(a_1^c p_1^c)(d_1^c + p_1^c)\left(2a_{i_0}^c p_{i_0}^c - p_{i_0}^c - d_{i_0}^c - d\right) \\
&-2(a_{i_0}^c p_{i_0}^c)(a_1^c p_1^c)(d_{i_0}^c + p_{i_0}^c + d)\left(2a_1^c p_1^c - p_1^c - d_1^c\right) \\
&\quad + \Bigg[(a_1^c p_1^c)(d + d_{i_0}^c + p_{i_0}^c)^2 \left(2a_1^c p_1^c - p_1^c - d_1^c\right) \\
&\quad - (a_{i_0}^c p_{i_0}^c)\left(2a_{i_0}^c p_{i_0}^c - p_{i_0}^c - d_{i_0}^c - d\right)(d_1^c + p_1^c)^2 \Bigg] < 0 \quad \Leftrightarrow \\
&2(a_{i_0}^c p_{i_0}^c)(a_1^c p_1^c)(d_1^c + p_1^c)\left(2a_{i_0}^c p_{i_0}^c - p_{i_0}^c - d_{i_0}^c - d\right) \\
&-(a_{i_0}^c p_{i_0}^c)\left(2a_{i_0}^c p_{i_0}^c - p_{i_0}^c - d_{i_0}^c - d\right)(d_1^c + p_1^c)^2 \\
&+(a_1^c p_1^c)(d + d_{i_0}^c + p_{i_0}^c)^2 \left(2a_1^c p_1^c - p_1^c - d_1^c\right) \\
&-2(a_{i_0}^c p_{i_0}^c)(a_1^c p_1^c)(d_{i_0}^c + p_{i_0}^c + d)\left(2a_1^c p_1^c - p_1^c - d_1^c\right) < 0 \Leftrightarrow \\
&(a_{i_0}^c p_{i_0}^c)(2a_1^c p_1^c - p_1^c - d_1^c)(d_1^c + p_1^c)\left(2a_{i_0}^c p_{i_0}^c - p_{i_0}^c - d_{i_0}^c - d\right) \\
&-(2a_{i_0}^c p_{i_0}^c - p_{i_0}^c - d_{i_0}^c - d)(a_1^c p_1^c)(d_{i_0}^c + p_{i_0}^c + d)\left(2a_1^c p_1^c - p_1^c - d_1^c\right) < 0 \quad \Leftrightarrow \\
&(2a_1^c p_1^c - p_1^c - d_1^c)\left(2a_{i_0}^c p_{i_0}^c - p_{i_0}^c - d_{i_0}^c - d\right) \\
&\cdot[(a_{i_0}^c p_{i_0}^c)(d_1^c + p_1^c) - (a_1^c p_1^c)(d_{i_0}^c + p_{i_0}^c + d)] < 0.
\end{aligned} \tag{B.7}$$

The latter is true, since $(2a_1^c p_1^c - p_1^c - d_1^c) > 0$, $\left(2a_{i_0}^c p_{i_0}^c - p_{i_0}^c - d_{i_0}^c - d\right) > 0$ and $(p_1^c + d_1^c)(a_{i_0}^c p_{i_0}^c) < (a_1^c p_1^c)(p_{i_0}^c + d_{i_0}^c + d)$, as stated in equation (B.4). This implies condition (B.6) and, therefore, $\bar{c}_{n-1}^d - \bar{c}_{n-1}^0 < 0$.

(b) For simplicity, we assume $i_0 = 1$. For $i \in \{i_0 + 1, \ldots, n-1\}$ it holds

$\bar{c}_{i-1}^d = \frac{-\left(2a_i^c \frac{p_1^c+d_1^c+d}{2a_1^c p_1^c}-1\right)p_i^c+d_i^c+d}{2\left(1-a_{i-1}^c \frac{p_1^c+d_1^c+d}{2a_1^c p_1^c}\right)p_{i-1}^c}\bar{c}_i^d := \alpha_i^d \bar{c}_i^d$. We calculate

$$\begin{aligned}
&\frac{d}{dd}\left[\frac{-\left(2a_i^c \frac{p_1^c+d_1^c+d}{2a_1^c p_1^c}-1\right)p_i^c+d_i^c+d}{2\left(1-a_{i-1}^c \frac{p_1^c+d_1^c+d}{2a_1^c p_1^c}\right)p_{i-1}^c}\right] \\
&= \frac{\left(2\left(1-a_{i-1}^c \frac{p_1^c+d_1^c+d}{2a_1^c p_1^c}\right)p_{i-1}^c\right)\left(-\frac{a_i^c p_i^c}{a_1^c p_1^c}+1\right)}{\left(2\left(1-a_{i-1}^c \frac{p_1^c+d_1^c+d}{2a_1^c p_1^c}\right)p_{i-1}^c\right)^2} \\
&\quad + \frac{\left(\frac{a_{i-1}^c p_{i-1}^c}{a_1^c p_1^c}\right)\left(-\left(2a_i^c \frac{p_1^c+d_1^c+d}{2a_1^c p_1^c}-1\right)p_i^c+d_i^c+d\right)}{\left(2\left(1-a_{i-1}^c \frac{p_1^c+d_1^c+d}{2a_1^c p_1^c}\right)p_{i-1}^c\right)^2}
\end{aligned}$$

We want to check, if there exist parameters, where this derivative has negative sign at $d=0$. We consider parameter sets fulfilling $d_1^c = ... = d_{n-1}^c = 0$. We obtain for the nominator at $d=0$:

$$\begin{aligned}
g &:= \left(\left(2-\frac{a_{i-1}^c}{a_1^c}\right)p_{i-1}^c\right)\left(-\frac{a_i^c p_i^c}{a_1^c p_1^c}+1\right)+\left(\frac{a_{i-1}^c p_{i-1}^c}{a_1^c p_1^c}\right)\left(-\left(\frac{a_i^c}{a_1^c}-1\right)p_i^c\right) \\
&= \left[2\left(1-\frac{a_{i-1}^c}{2a_1^c}\right)-2\left(1-\frac{a_{i-1}^c}{2a_1^c}\right)\frac{a_i^c p_i^c}{a_1^c p_1^c}+\frac{a_{i-1}^c p_i^c}{a_1^c p_1^c}\left(1-\frac{a_i^c}{a_1^c}\right)\right]p_{i-1}^c
\end{aligned}$$

For $i=2$ we obtain

$$\begin{aligned}
g &= p_1^c\left(1-\frac{a_2^c p_2^c}{a_1^c p_1^c}\right)+\left(1-\frac{a_2^c}{a_1^c}\right)p_2^c = \left(p_1^c-\frac{a_2^c p_2^c}{a_1^c}\right)+\left(1-\frac{a_2^c}{a_1^c}\right)p_2^c \\
&= p_1^c+p_2^c-2\frac{a_2^c p_2^c}{a_1^c}
\end{aligned}$$

This is negative, if $a_1^c < 2a_2^c$ and p_2^c large enough.

Let $3 \le i < n$. We assume for simplicity $a_2^c = ... = a_{n-1}^c$. This yields

$$\begin{aligned}
g &= \left[2\left(1-\frac{a_i^c}{2a_1^c}\right)-2\left(1-\frac{a_i^c}{2a_1^c}\right)\frac{a_i^c p_i^c}{a_1^c p_1^c}+\frac{a_i^c p_i^c}{a_1^c p_1^c}\left(1-\frac{a_i^c}{a_1^c}\right)\right]p_{i-1}^c \\
&= \left[2\left(1-\frac{a_i^c}{2a_1^c}\right)-\frac{a_i^c p_i^c}{a_1^c p_1^c}\right]p_{i-1}^c,
\end{aligned}$$

which is negative for p_i^c large enough. Therefore, there exist parameters such that $\alpha_i^d < \alpha_i^0$ for $i \in \{i_0+1, \ldots, n-1\}$. In (a) we have shown that $\bar{c}_n^d < \bar{c}_n^0$ and $\bar{c}_{n-1}^d < \bar{c}_{n-1}^0$. We, therefore, obtain $\bar{c}_i^d < \bar{c}_i^0$ for all $i \in \{i_0+1, \ldots, n-1\}$ for the considered parameter choice.

(c) For simplicity, we assume $i_0 = 1$. As above for $i \in \{i_0 + 1, \ldots, n-1\}$ it holds $\bar{c}_{i-1}^d = \frac{-\left(2a_i^c \frac{p_1^c + d_1^c + d}{2a_1^c p_1^c} - 1\right) p_i^c + d_i^c + d}{2\left(1 - a_{i-1}^c \frac{p_1^c + d_1^c + d}{2a_1^c p_1^c}\right) p_{i-1}^c} \bar{c}_i^d := \alpha_i^d \bar{c}_i^d$. Let $i \geq 3$.

It holds

$$\frac{d}{dd}\left[\frac{-\left(2a_i^c \frac{p_1^c + d_1^c + d}{2a_1^c p_1^c} - 1\right) p_i^c + d_i^c + d}{2\left(1 - a_{i-1}^c \frac{p_1^c + d_1^c + d}{2a_1^c p_1^c}\right) p_{i-1}^c}\right]\Bigg|_{d=0} > 0 \Leftrightarrow$$

$$2\left(1 - a_{i-1}^c \frac{p_1^c + d_1^c + d}{2a_1^c p_1^c}\right) p_{i-1}^c \left(1 - \frac{2a_i^c p_i^c}{2a_1 p_1}\right)\Bigg|_{d=0}$$

$$+ \frac{2a_{i-1}^c p_{i-1}^c}{2a_i^c p_i^c}\left(-\left(2a_i^c \frac{p_1^c + d_1^c + d}{2a_1^c p_1^c} - 1\right) p_i^c + d_i^c + d\right)\Bigg|_{d=0} > 0 \Leftrightarrow$$

$$2\left(1 - a_{i-1}^c \frac{p_1^c + d_1^c}{2a_1^c p_1^c}\right) p_{i-1}^c \left(1 - \frac{2a_i^c p_i^c}{2a_1 p_1}\right)$$

$$+ \frac{2a_{i-1}^c p_{i-1}^c}{2a_i^c p_i^c}\left(-\left(2a_i^c \frac{p_1^c + d_1^c}{2a_1^c p_1^c} - 1\right) p_i^c + d_i^c\right) > 0$$

It follows

$$\frac{d}{dd}\left[\frac{-\left(2a_i^c \frac{p_1^c + d_1^c + d}{2a_1^c p_1^c} - 1\right) p_i^c + d_i^c + d}{2\left(1 - a_{i-1}^c \frac{p_1^c + d_1^c + d}{2a_1^c p_1^c}\right) p_{i-1}^c}\right]\Bigg|_{d=0, a_i^c = a_{i-1}^c = 0} = 2p_{i-1}^c > 0. \tag{B.8}$$

This implies that for small a_i, a_{i-1} the value of α_i increases, if d increases from zero to a small positive value. Furthermore, it follows with $\bar{s} = \frac{p_1^c + d_1^c}{2a_1^c p_1^c}$ and $p_i^c = p_{i-1}^c$ and $a_i^c = a_{i-1}^c$

$$\frac{-\left(2a_i^c s - 1\right) p_i^c + d_i^c + d}{2\left(1 - a_{i-1}^c s\right) p_{i-1}^c} > 1$$

$$\Leftrightarrow -\left(2a_i^c s - 1\right) p_i^c + d_i^c + d > 2\left(1 - a_{i-1}^c s\right) p_{i-1}^c$$

$$\Leftrightarrow d_i^c + d - p_i^c > 0. \tag{B.9}$$

We now construct a solution with the desired properties. This solution will fulfill $a_2 = \cdots = a_{n-1}$, $d_2 = \cdots = d_{n-1}$ and $p_2 = \cdots = p_{n-1}$. We choose d and a_i small enough such that $\alpha_i^d > \alpha_i^0$, see relation (B.8). We choose p_i and d_i satisfying condition (B.9). It holds $\bar{c}_{i-1}^d > \bar{c}_i^d$, due condition (B.9). Therefore, $\bar{c}_2^d \to \infty$ for $n \to \infty$. Furthermore, due to relation (B.8), it holds $\alpha_i^d > \alpha_i^0$. Moreover, $\alpha_i^d > 1$, due to relation (B.9). Therefore, $\frac{c_2^d}{c_2^0} \to \infty$ for $n \to \infty$. We now choose a_1, p_1 such that $\frac{d + p_i + d_i}{2a_i p_i} > \frac{d + p_1}{2a_1 p_1}$ and $\frac{p_i + d_i}{2a_i p_i} > \frac{p_1}{2a_1 p_1}$. Based on this, we calculate α_2^0 and α_2^d. We then choose n such that $\alpha_2^d \bar{c}_2^d > \alpha_2^0 \bar{c}_2^0$. This implies $\bar{c}_1^d > \bar{c}_1^0$. For n large it also holds $\sum_{i=1}^n \bar{c}_i^0 < \sum_{i=1}^n \bar{c}_i^d$.

■

APPENDIX C

CALIBRATION OF THE HEMATOPOIETIC BRANCH FOR n=3

In the following, we present the calibration used for the numerical studies in Chapter 6. In the steady state, the model of the hematopoietic system has the following form, where bars indicate steady state values.

$$
\begin{aligned}
0 &= (2a_1\bar{s}-1)p_1\bar{c}_1 && \text{(C.1)}\\
0 &= 2(1-a_1\bar{s})p_1\bar{c}_1 + (2a_2\bar{s}-1)p_2\bar{c}_2 && \text{(C.2)}\\
0 &= 2(1-a_2\bar{s})p_2\bar{c}_2 - d_3\bar{c}_3 && \text{(C.3)}\\
\bar{s} &= \frac{1}{1+k\bar{c}_3} && \text{(C.4)}
\end{aligned}
$$

Using

$$\bar{s} = \frac{1}{2a_1} = \frac{1}{1+k\bar{c}_3}, \tag{C.5}$$

we can express k as a function of a_1 and the steady state population size of mature cells $\bar{c}_3$:

$$k = \frac{2a_1-1}{\bar{c}_3}.$$

We obtain further from (C.2) and (C.5):

$$\frac{\bar{c}_1}{\bar{c}_2} = \left(1-\frac{a_2}{a_1}\right)\frac{p_2}{p_1} \Leftrightarrow p_2 = \frac{\bar{c}_1}{\bar{c}_2}\frac{p_1}{\left(1-\frac{a_2}{a_1}\right)}. \tag{C.6}$$

We obtain further from (C.3) and (C.5):

$$\frac{\bar{c}_3}{\bar{c}_2} = \left(2-\frac{a_2}{a_1}\right)\frac{p_2}{d_3}. \tag{C.7}$$

Inserting p_2 from equation (C.6) we obtain:

$$\frac{\bar{c}_3 d_3}{\bar{c}_1 p_1}\left(1-\frac{a_2}{a_1}\right) = \left(2-\frac{a_2}{a_1}\right) \Leftrightarrow \tag{C.8}$$

$$\frac{\bar{c}_3 d_3}{\bar{c}_1 p_1} - 2 = \left(\frac{\bar{c}_3 d_3}{\bar{c}_1 p_1 a_1} - \frac{1}{a_1}\right) a_2 \Leftrightarrow \tag{C.9}$$

$$a_2 = \frac{\frac{\bar{c}_3 d_3}{\bar{c}_1 p_1} - 2}{\left(\frac{\bar{c}_3 d_3}{\bar{c}_1 p_1 a_1} - \frac{1}{a_1}\right)}. \tag{C.10}$$

We restrict ourselves to a calibration based on the neutrophil lineage, which constitutes the majority of mature white blood cells ($50\% - 70\%$). Lymphocytopoiesis is a complicated process involving lymphatic organs and not only the bone marrow, [52]. For the steady state count of neutrophils it holds (see reference [168]),

$$\bar{c}_3 \in (3 - 5.8) \cdot 10^9/l.$$

Assuming an average blood volume of 6 liters and an average body weight of 70 kg, we calculate a mature neutrophil count of

$$\bar{c}_3 \approx 4 \cdot 10^8/kg.$$

By $\bar{c}_2$ we denote the total amount of dividing neutrophil precursors. Based on the data from [143] we assume that about 20% of marrow cells are dividing precursors of neutrophils (the inter-individual variation is considerable). The total marrow cellularity is about 10^{10} cells per kg of body weight, [96].

We, therefore, assume that

$$\bar{c}_2 \approx 2 \cdot 10^9/kg.$$

As $\bar{c}_1$ we interpret the total amount of primitive progenitors (namely HSC, LT-CIC, CFUs) in bone marrow. Neutrophils' half life in blood stream, $T_{1/2}$, is about 7 (4-10) hours, [40]. From this we calculate

$$d_3 = \frac{\ln(2)}{T_{1/2}} \approx 2.3/day.$$

Counts of primitive cells can only be roughly estimated. Concerning HSC counts, estimates vary between hundreds and several thousands per kg of body weight, see e.g., [1, 235]. LTC-IC are estimated to be of order 10^6 per kg and CFU-GM of the order of 10^7, [38]. We, therefore, assume

$$\bar{c}_1 \in (10^7,\ 10^8).$$

Estimations suggest that HSC divide about once per year, [1, 203], less primitive not committed progenitors divide more often. We assume for all primitive cells

an average division frequency of once per week, which lies between estimates for HSC and committed progenitors [51, 71, 203, 214]. This leads to $p_1 \approx 0.1$.

We estimate a_2 as a function of a_1 using equation (C.10) and then p_2 using equation (C.6). We know from bone marrow transplantation data, [120], that patients need about 15 days to engraft to $5 \cdot 10^8$ neutrophils per liter of blood ($4 \cdot 10^7$ per kg) after infusion of $5 \cdot 10^6$ immature cells per kg of body weight.
For

$$a_1 \approx 0.85$$

this condition is satisfied.

We then obtain the following parameters: $a_2 \approx 0.841$, $p_2 \approx 0.4$, leading to $\bar{c}_1 \approx 8 \cdot 10^7$, $\bar{c}_2 \approx 2 \cdot 10^9$ cells per kg, $\bar{c}_3 \approx 5.5 \cdot 10^9$ cells liter of blood and $k = 1.75 \cdot 10^{-9}$.

APPENDIX D

SIMULATION OF EARLY RELAPSES

Ten of the 41 patients considered in Chapter 6 show fast expansion of leukemic cell mass that is not compatible with a small number of surviving LSC under complete reconstitution of hematopoiesis upon induction treatment. Modifications of Model 1 can be applied to investigate, which scenarios may be responsible for acceleration of leukemic cell expansion. For each of the 10 rapidly relapsing patients at least one of the following scenarios 1-3 is compatible with clinical observations.

1. Impairment of healthy hematopoiesis might lead to fast expansion of leukemic cells, for example, due to availability of resources such as space, niches, environmental factors. Toxic effects of the therapy to the hematopoietic micro-environment could underlie this scenario, [211]. This scenario is simulated by choosing initial conditions smaller than steady state hematopoietic cell counts, such as 10%, 50% or 90% of the steady state values of c_1, c_2, c_3.

2. Insufficient induction chemotherapy or resistance might lead to reduced clearance of leukemic cells, which results in a large number of surviving LSC and hence a rapid relapse, [33, 188]. This scenario is simulated choosing initial conditions for the post-treatment period including large numbers of LSC (e.g., 100, 1000 or 10000 LSCs per kg of body weight).

3. Autonomous or partially autonomous expansion (i.e., expansion independently of environmental growth signals) of leukemic cells may lead to perturbed sensitivity to regulatory mechanisms responsible for homeostasis, [54, 193]. Emergence of cells with more genetic aberrations can explain very fast, nearly exponential expansion of leukemic blast counts. This is simulated by changing the form of s in the leukemic compartments.

Independence of environmental cues can be obtained by replacing s by $s + k(1 - s)$ with $k \in [0,\ 1]$, where $k = 1$ means total independence of environmental signals and $k = 0$ means that LSCs' dependence of environmental signals is comparable to that of HSC. In reality, spatial constraints prevent unbounded growth. For this reasons the described modifications are only valid for short time intervals.

Due to complex interaction of cells and their environment, these simulations only provide qualitative insights into the dynamics. In some of the patients, bone marrow histology showed reduced numbers of hematopoietic cells during complete remission, such that it seems probable that impaired hematopoiesis may be the reason for the observed fast relapses.

In summary, the model allows distinguishing between two types of relapses:

- Type 1: A small number of LSC (less than 100 per kg of body weight) survived therapy. The hematopoietic system recovered after chemotherapy and leukemic cells expanded in a functional hematopoietic environment.
- Type 2: Relapses occurred faster than it is compatible with Type 1. This suggests impairment of hematopoiesis, inefficiency of therapy or autonomous cell growth; see Scenarios 1-3 above.

APPENDIX E

CALIBRATION AND PARAMETERS FOR MODELS IN CHAPTER 7

E.1 Calibration of the hematopoietic cell lineage for n=2

For simplcity, we write a^c instead of a^c_{max}. In absence of leukemic clones, both considered models reduce to the same model of the hematopoietic system. In steady state this model has the following form

$$0 = (2a^c\bar{s} - 1)p^c\bar{c}_1 \tag{E.1}$$

$$0 = 2(1 - a^c\bar{s})p^c\bar{c}_1 - d^c_2\bar{c}_2 \tag{E.2}$$

$$\bar{s} = \frac{1}{1 + k\bar{c}_2} \tag{E.3}$$

Assume we know $\bar{c}_1$ and $\bar{c}_2$. It holds

$$\frac{\bar{c}_2}{\bar{c}_1} = \frac{p^c}{d^c_2} \tag{E.4}$$

$$\bar{c}_2 = \frac{2a^c - 1}{k^c} \tag{E.5}$$

Knowing a^c, we can calculate $k^c = (2a^c - 1)/\bar{c}_2$, such that the steady state population size c_2 is satisfied. We calibrate the model to the data on production of neutrophil granulocytes, which constitute the majority of mature white blood cells ($50\% - 70\%$). Lymphocytopoiesis is a complicated process involving lymphatic organs and not only the bone marrow, [52]. Therefore, we restrict ourselves to the myeloid line. It holds for the steady state count of neutrophils, [168],

$\bar{c}_2 \in (3 - 5.8) \cdot 10^9/l$. We interpret $\bar{c}_1$ as the total amount of mitotic neutrophil precursors in bone marrow. Based on the data from [143], we assume that about 20% of bone marrow cells are mitotic precursors of neutrophils (the interindividual variations are considerable). The total bone marrow cellularity is about 10^{10} cells per kg of body weight, [96]. Therefore, we take

$$\bar{c}_1 \approx 2 \cdot 10^9/kg. \tag{E.6}$$

Assuming an average blood volume of 6 liters and an average body weight of 70 kg, we calculate a mature neutrophil count of

$$\bar{c}_2 \approx 4 \cdot 10^8/kg. \tag{E.7}$$

Neutrophils have half-life in blood stream, $T_{1/2}$, of about 7 hours, [40]. From this we calculate

$$d_2^c = \frac{\ln(2)}{T_{1/2}} \approx 2.3/days. \tag{E.8}$$

We obtain

$$p^c = \frac{\bar{c}_2}{\bar{c}_1} d_2^c \approx 0.45/day, \tag{E.9}$$

i.e., about once per 1.5 days. We know from bone marrow transplantation, [120], that patients need about 15 days to reconstitute to $5 \cdot 10^8$ neutrophils per liter of blood ($4 \cdot 10^7$ per kg) after infusion of $5 \cdot 10^6$ immature cells per kg of body weight. For

$$a^c \approx 0.87 \tag{E.10}$$

this constraint is met. The calibration provided in this Appendix served as point of departure for the calibration used in [85].

E.2 Model parameters

For the hematopoietic branch we chose parameters obtained from the calibration in the Section above. For simplicity, we assume $k^c = k^l$ for the feedback mechanism in Model 1. We set the clearance rate of blasts (in absence of effects of overcrowding) to $d_2^{l^i} = 0.1$. This is based on the apoptotic indices (fraction of dying cells) reported in literature, which are $\approx 0.19 \pm 0.16$ $(19\% \pm 16\%)$, [152,195]. Choosing blast clearance between 0.1 and 0.5, changes the speed of leukemic cell accumulation but, as revealed by additional simulations, not the cell properties that are selected.

We chose $d(x) = d_{const} \cdot \max\{0, x - x_{max}\}$. In histological images of healthy adult bone marrow a large part of the bone marrow cavity consists of fat and connective tissue and is free of hematopoietic cells. To reflect this fact, we set $x_{max} \approx 2\bar{c}_1$, where $\bar{c}_1$ is the steady state count of mitotic healthy cells. In the

simulations, d_{const} was set to 10^{-10}. This choice implies that if bone marrow cell counts are three times higher than in the steady state, the additional death rate due to overcrowding is of the order of magnitude of mature cell clearance. The results remain unchanged qualitatively, even if values of d_{const} vary within different orders of magnitude.

We apply chemotherapy on seven following days for 2 hours. Different treatment intervals lead to comparable results. In the depicted simulations k_{chemo} has been set to values between 20 and 30 for less efficient therapy and to values between 40 and 60 for efficient chemotherapy. For different choices similar results are obtained. The higher k_{chemo}, the stronger the selection for high self-renewal and slow proliferation and the lower the probability of relapse. The lower k_{chemo}, the higher the probability that clones contributing to primary presentation are among clones contributing to relapse. For k_{chemo} between 40 and 45, the obtained results are similar to the results obtained in experiments, [56]. The parameters of the leukemic clones are chosen randomly from uniform distributions, assuming that cells divide at most twice per day and that self-renewal is between zero and one.

E.3 Calibration to patient examples

Both patients were treated within clinical trials at the University Hospital of Heidelberg after obtaining their written consent. Details on the patients' characteristics and therapeutic regimens can be found in Supplemental Table E.1. Model parameters can be found in Supplemental Tables E.2 and E.3. For both patients the presence of specific key mutations was assessed in clinical routine. We chose cases, where mutations got lost due to treatment and new mutation are detected at relapse. We interpret this as the result of clonal evolution. Since the two patients harbor different mutations, their leukemic cells can have different properties. Chemotherapy is modeled by increasing death rates for mitotic cell types during the duration of each cycle. For simplicity, we did not model kinetics of single chemotherapeutic agents. Instead, the therapy-induced death rates are assumed to remain constant from the first to the last day of each treatment cycle. In pharmacology, the exposition to a drug is measured using the *'area under the curve' (AUC)*. This is the integral of concentration (or drug effect) over time, [36]. The AUC in our case is $k_{chemo} \cdot \Delta t$, where Δt is the period of drug action. The AUC over one day of therapy is similar for the single patient examples and the simulations in Figure 7.5. Only myeloablative treatment before transplantation has a higher AUC. The presented results are based on Model 2. Model 1 is not compatible with remissions lasting less than 150 days. For simplicity, we count all leukemic cell types as blasts.

	Patient 1	**Patient 2**
Gender	Male	Male
Age at diagnosis	63	60
Diagnosis	AML	AML FAB M2
Therapy	Days 30-37 (Induction): - Mitoxantron(10 mg/m^2) (d 1-3) - AraC (2000 mg/m^2) (d 1,3,5,7) Days 70-74 (Consolidation): - Mitoxantron(10 mg/m^2) (d 1,2) - AraC (1000 mg/m^2) (d 1,3,5)	Days 1-7 (Induction I) -AraC(100 mg/m^2)(d1-7) -DA(60mg/m^2)(d3-5) Days 23-29 (Induction II) -AraC(100 mg/m^2)(d1-7) -DA(60mg/m^2)(d3-5) Days 60-64 (Consolidation I) -AraC(6000 mg/m^2)(d1,3,5) Days 109-113 (Consolidation II) -AraC(6000 mg/m^2)(d1,3,5) Days 145-146 (Conditioning) -Allogeneic, HLA-identical HSCT (after Treosulfan/Fludarabin/ATG)

Table E.1: Demographic and treatment data of the 2 patients considered. Day 0 is defined as the day of diagnosis. ATG=Anti-Thymocyte Globulin, HSCT=Hematopoietic Stem Cell Transplantation.

Cell Property	**Clone 1**	**Clone 2**	**Clone 3**
Leukemic cell proliferation rate (1/days)	0.25	0.25	1.2
Leukemic cell self-renewal	0.755	0.76	0.6
Blast death rate (1/days)	0.5	0.5	0.5
k_{chemo} (Induction)	3	3	3
k_{chemo} (Consolidation)	3	3	3

Table E.2: Parameters used for Patient 1: Simulations are based on Model 2. The function $d(x)$, describing cell death due to space competition has been set to $\max(0, x - 3c)$, where c is steady state bone marrow cell count in absence of leukemic cells.

Cell Property	**Clone 1**	**Clone 2**
Leukemic cell proliferation rate (1/days)	0.45	1.2
Leukemic cell self-renewal	0.75	0.6
Blast death rate (1/days)	0.5	0.5
k_{chemo} (Induction I, II)	3	3
k_{chemo} (Consolidation I, II)	5	5
k_{chemo} (Conditioning)	16	16

Table E.3: Parameters used for Patient 2: Simulations are based on Model 2. The function $d(x)$, describing cell death due to space competition has been set to $\max(0, x - 3c)$, where c is steady state bone marrow cell count in absence of leukemic cells.

APPENDIX F

PROOFS OF PROPOSITIONS 7.16 AND 7.19

F.1 Proof of Proposition 7.16

The following reasoning is the discrete version of [91]. We neglect death rates of mitotic cells. For simplicity, we rewrite the model using a different notation:

$$\begin{aligned}
\frac{d}{dt}c_1^1(t) &= \big(2a^1 s(t) - 1\big)p^1 c_1^1(t) \\
\frac{d}{dt}c_2^1(t) &= 2\big(1 - a^1 s(t)\big)p^1 c_1^1(t) - d_2^1 c_2^1(t) \\
&\vdots \quad \vdots \quad \vdots \\
\frac{d}{dt}c_1^n(t) &= \big(2a^n s(t) - 1\big)p^n c_1^n(t) \\
\frac{d}{dt}c_2^n(t) &= 2\big(1 - a^n s(t)\big)p^n c_1^n(t) - d_2^n c_2^n(t) \\
s(t) &= \frac{1}{1 + k\sum_{i=1}^n c_2^i(t)}.
\end{aligned} \tag{F.1}$$

We assume $1 > a^i > 0.5$, $p^i > 0$, $d_2^i > 0$ for $1 \leq i \leq n$, $k > 0$.

Definition F.1
We define $\rho_1(t) := \sum_{i=1}^N c_1^i(t)$, $\rho_2 := \sum_{i=1}^N c_2^i(t)$.

Lemma F.2
Assume $c_1^i(0) > 0$ *for all* $i \in \{1, \cdots, N\}$. *The quantities* ρ_1 *and* ρ_2 *are globally bounded with respect to time.*

PROOF
Since $c_1^i(0) > 0$ for all $i \in \{1, \cdots, N\}$, it holds after an infinitesimal time t also $c_2^i(t) > 0$ for all $i \in \{1, \cdots, N\}$. Therefore, we can assume that $c_1^i(0) > 0$ for all $i \in \{1, \cdots, N\}$ and $c_2^i(0) > 0$ for all $i \in \{1, \cdots, N\}$. Let $1 \leq i \leq N$. We consider

$$\begin{aligned}\frac{d}{dt}\frac{c_1^i}{c_2^i} &= \frac{\frac{d}{dt}c_1^i}{c_2^i} - \frac{c_1^i \frac{d}{dt}c_2^i}{(c_2^i)^2} \\ &= \frac{(2a^i s - 1)p^i c_1^i}{c_2^i} + d_2^i \frac{c_1^i}{c_2^i} - \frac{2(1 - a^i s)p^i (c_1^i)^2}{(c_2^i)^2} \\ &< \frac{(2a^i - 1)p^i c_1^i}{c_2^i} + d_2^i \frac{c_1^i}{c_2^i} - \frac{2(1 - a^i)p^i (c_1^i)^2}{(c_2^i)^2}\end{aligned}$$

This is a Bernoulli equation $y' = ay - by^2$, which is solved by $y(x) = \frac{ae^{ax}}{be^{ax} + const}$. For non-negative y it holds $y' < 0 \Leftrightarrow y > \frac{a}{b}$. This implies for non-negative $y(0)$ that $y(t) \leq \max\left\{y(0), \frac{a}{b}\right\}$.

Therefore, it holds

$$\frac{c_1^i}{c_2^i} \leq \max\left\{\max_{i=1,, \cdots, N}\left\{\frac{c_1^i(0)}{c_2^i(0)}\right\}, \max_{i=1,, \cdots, N}\left\{\frac{(2a^i - 1)p^i + d_2^i}{2(1 - a^i)p^i}\right\}\right\} =: M_1.$$

We, therefore, have $c_1^i < M_1 c_2^i$. This implies $\rho_1 \leq M_1 \rho_2$.
Furthermore, we have

$$\begin{aligned}\frac{d}{dt}c_1^i &= \left(\frac{2a_1^i}{1 + k\rho_2} - 1\right) p^i c_1^i \\ &\leq \left(\frac{2a_1^i}{1 + k\rho_1/M_1} - 1\right) p^i c_1^i\end{aligned}$$

We sum over i to obtain

$$\frac{d}{dt}\rho_1 \leq \left(\frac{2\max_{1 \leq i \leq N}\{a_1^i\}}{1 + k\rho_1/M_1} - 1\right) \sum_{i=1}^{N} p^i c_1^i \tag{F.2}$$

Consequently, $\frac{d}{dt}\rho_1 > 0 \Leftrightarrow 0 < \rho_1 < \frac{(2\max_{1 \leq i \leq N}\{a_1^i\} - 1)M_1}{k}$. Therefore, $\rho_1(t) \leq \max\left\{\rho_1(0), \frac{(2\max_{1 \leq i \leq N}\{a_1^i\} - 1)M_1}{k}\right\} =: M_2$.
We, furthermore, have

$$\begin{aligned}\frac{d}{dt}c_2^i &= 2\left(1 - \frac{a_1^i}{1 + k\rho_2}\right) p^i c_1^i - d_2^i c_2^i \\ &\leq 2\max\{p^i\}_{1 \leq i \leq N} c_1^i - \min\{d_2^i\}_{1 \leq i \leq N} c_2^i\end{aligned}$$

We sum over i to obtain

$$\begin{aligned}\frac{d}{dt}\rho_2 &\leq 2\max_{1\leq i\leq N}\{p^i\}\rho_1 - \min_{1\leq i\leq N}\{d_2^i\}\rho_2\\ &\leq 2\max_{1\leq i\leq N}\{p^i\}M_2 - \min_{1\leq i\leq N}\{d_2^i\}\rho_2 \end{aligned} \tag{F.3}$$

Consequently, $\frac{d}{dt}\rho_2 > 0 \Leftrightarrow \rho_2 < \frac{2\max_{1\leq i\leq N}\{p^i\}M_2}{\min_{1\leq i\leq N}\{d_2^i\}}$
Therefore, $\rho_2(t) \leq \max\left\{\rho_2(0), \frac{2\max_{1\leq i\leq N}\{p^i\}M_2}{\min_{1\leq i\leq N}\{d_2^i\}}\right\} =: M_3$

■

Lemma F.3
Let $\min_{1\leq i\leq N}\{a^i\} > 0.5$. *For positive initial conditions* ρ_1 *and* ρ_2 *are strictly positive.*

PROOF

Let $0 < \gamma < 1$ such that $\max_{1\leq i\leq N}\{p^i\}\gamma - \min_{1\leq i\leq N}\{d_2^i\} < 0$.

$$\begin{aligned}\frac{d}{dt}\frac{\rho_2(t)}{\rho_1(t)^\gamma} &= \frac{\frac{d}{dt}\rho_2(t)}{\rho_1(t)^\gamma} - \frac{\rho_2(t)\frac{d}{dt}\rho_1(t)^\gamma}{\rho_1(t)^{2\gamma}}\\ &\leq \frac{2\max_{1\leq i\leq N}\{p^i\}}{\rho_1(t)^{\gamma-1}} - \frac{\min_{1\leq i\leq N}\{d_2^i\}\rho_2(t)}{\rho_1(t)^\gamma}\\ &+ \frac{\rho_2(t)\max_{1\leq i\leq N}\{p^i\}\rho_1(t)\gamma\rho_1(t)^{\gamma-1}}{\rho_1(t)^{2\gamma}}\\ &= \frac{2\max_{1\leq i\leq N}\{p^i\}}{\rho_1(t)^{\gamma-1}} + \frac{\rho_2(t)}{\rho_1(t)^\gamma}\left(\max_{1\leq i\leq N}\{p^i\}\gamma - \min_{1\leq i\leq N}\{d_2^i\}\right)\\ &\leq \frac{2\max_{1\leq i\leq N}\{p^i\}}{M_2^{\gamma-1}} + \frac{\rho_2(t)}{\rho_1(t)^\gamma}\left(\max_{1\leq i\leq N}\{p^i\}\gamma - \min_{1\leq i\leq N}\{d_2^i\}\right)\end{aligned} \tag{F.4}$$

The last inequality holds, since $\gamma - 1 < 0$. We used estimates (F.2) and (F.3).
Therefore,

$$\frac{\rho_2(t)}{\rho_1(t)^\gamma} \leq \max\left(\frac{\rho_2(0)}{\rho_1(0)^\gamma}, \frac{-2\max_{1\leq i\leq N}\{p^i\}}{M_2^{\gamma-1}\left(\max_{1\leq i\leq N}\{p^i\}\gamma - \min_{1\leq i\leq N}\{d_2^i\}\right)}\right) =: M_4 \tag{F.5}$$

using that $\left(\max_{1\leq i\leq N}\{p^i\}\gamma - \min_{1\leq i\leq N}\{d_2^i\}\right) < 0$ and $\rho_1 \leq M_2$.
We then have $\rho_2(t) \leq M_4\rho_1(t)^\gamma$. We get for ρ_1

$$\begin{aligned}\frac{d}{dt}\rho_1(t) &\geq \left(2\frac{\min_{1\leq i\leq N}\{a^i\}}{1+k\rho_2(t)} - 1\right)\sum_{i=1}^N p^i c_1^i\\ &\geq \left(2\frac{\min_{1\leq i\leq N}\{a^i\}}{1+kM_4\rho_1(t)^\gamma} - 1\right)\sum_{i=1}^N p^i c_1^i,\end{aligned} \tag{F.6}$$

Which implies

$$\rho_1(t) \geq \min\left(\rho_1(0), \left(\frac{2\min_{1\leq i\leq N}\{a^i\}-1}{kM_4}\right)^{1/\gamma}\right) =: M_5 > 0, \tag{F.7}$$

since we have assumed, that $a^i > 0.5$.

Since we have from above $\rho_2(t) \geq \rho_1(t)/M_1 > 0$, we get

$$\rho_2(t) \geq M_5/M_1. \tag{F.8}$$

■

We now consider two special cases:

Lemma F.4
Let $p^1 = \cdots = p^N =: p$. Let all $c_1^k(0) > 0$. It holds

(i) If $a^k < \max_{1\leq i\leq N}\{a^i\}$, then $\lim_{t\to\infty} c_1^k = 0$.

(ii) If $a^k = a^j$ for $j \neq k$, then $\frac{c_1^k}{c_1^j}$ is constant in time.

PROOF
(i) Let $a^k < a^m$. Then, it holds with $s(t) \equiv \frac{1}{1+k\rho_2(t)}$

$$\begin{aligned}\frac{d}{dt}\frac{c_1^k}{c_1^m} &= \frac{\frac{d}{dt}c_1^k}{c_1^m} - \frac{c_1^k\frac{d}{dt}c_1^m}{(c_1^m)^2}\\ &= (2a^k s(t)-1)p\frac{c_1^k}{c_1^m} - (2a^m s(t)-1)p\frac{c_1^k}{c_1^m}\\ &= \frac{2(a^k-a^m)}{1+k\rho_2}p\frac{c_1^k}{c_1^m} < -\alpha\end{aligned}$$

for an $\alpha > 0$, since ρ_2 is globally bounded from above.
This implies $\frac{c_1^k}{c_1^m} \leq \frac{c_1^k(0)}{c_1^m(0)}e^{-\alpha t}$ and, therefore, $c_1^k \leq c_1^m\frac{c_1^k(0)}{c_1^m(0)}e^{-\alpha t} \leq M_2\frac{c_1^k(0)}{c_1^m(0)}e^{-\alpha t}$. Consequently, all c_1^i with $a^i < \max_{1\leq i\leq N}\{a_1^i\}$ tend to zero for t tending to infinity.
(ii) If $a^k - a^m = 0$, we obtain $\frac{d}{dt}\frac{c_1^k}{c_1^m} = 0$. ■

Remark F.5
Since ρ_1 and ρ_2 are strictly positive, it follows that if $a^k = \max_{1\leq i\leq N}\{a^i\}$, then c_1^k does not tend to zero for long times.

Lemma F.6
Let $a^1 = \cdots = a^N =: a$. Let all $c_1^k(0) > 0$. It holds $\frac{c_1^k}{c_1^m} \in [\alpha, \beta]$ for all t, where $\alpha, \beta > 0$.

PROOF
We obtain

$$\begin{aligned}\frac{d}{dt}\frac{c_1^k}{c_1^m} &= \frac{\frac{d}{dt}c_1^k}{c_1^m} - \frac{c_1^k \frac{d}{dt}c_1^m}{(c_1^m)^2} \\ &= (2as(t)-1)p^k \frac{c_1^k}{c_1^m} - (2as(t)-1)p^m \frac{c_1^k}{c_1^m}.\end{aligned}$$

This implies $\frac{c_1^k}{c_1^m} = \frac{c_1^k(0)}{c_1^m(0)} e^{\int_0^t \left(2\frac{a}{1+k\rho_2(\tau)}-1\right)d\tau(p^k-p^m)}$
Using Lemmas F.2 and F.3, we have

$$\begin{aligned}\infty > M_2 \geq \rho_1(t) &= \rho_1(0) + \int_0^t \partial_\tau \rho_1(\tau) d\tau \\ &= \rho_1(0) + \int_0^t \sum_{i=1}^N \left(2\frac{a}{1+k\rho_2(\tau)} - 1\right) p^i c_1^i(\tau) d\tau \\ &\geq \rho_1(0) + \min_{1\leq i\leq N} p^i \int_0^t \left(2\frac{a}{1+k\rho_2(\tau)} - 1\right) \rho_1(\tau) d\tau \\ &\geq \rho_1(0) + \min_{1\leq i\leq N} p^i M_5 \int_0^t \left(2\frac{a}{1+k\rho_2(\tau)} - 1\right) d\tau.\end{aligned}$$

This implies

$$\int_0^t \left(2\frac{a}{1+k\rho_2(\tau)} - 1\right) d\tau \leq \frac{M_2 - \rho_1(0)}{M_5 \cdot \min_{1\leq i\leq N} p^i}.$$

We note that $M_6 := \frac{M_2-\rho_1(0)}{M_5 \cdot \min_{1\leq i\leq N} p^i} \geq 0$. Furthermore,

$$\begin{aligned}0 < M_5 \leq \rho_1(t) &= \rho_1(0) + \int_0^t \partial_\tau \rho_1(\tau) d\tau \\ &= \rho_1(0) + \int_0^t \sum_{i=1}^N \left(2\frac{a}{1+k\rho_2(\tau)} - 1\right) p^i c_1^i(\tau) d\tau \\ &\leq \rho_1(0) + \max_{1\leq i\leq N} p^i \int_0^t \left(2\frac{a}{1+k\rho_2(\tau)} - 1\right) \rho_1(\tau) d\tau \\ &\leq \rho_1(0) + \max_{1\leq i\leq N} p^i M_2 \int_0^t \left(2\frac{a}{1+k\rho_2(\tau)} - 1\right) d\tau.\end{aligned}$$

This implies

$$\int_0^t \left(2\frac{a}{1+k\rho_2(\tau)} - 1\right) d\tau \geq \frac{M_5 - \rho_1(0)}{M_2 \max_{1\leq i\leq N} p^i}. \tag{F.9}$$

We note that $M_7 := \frac{M_5 - \rho_1(0)}{M_2 \max_{1\le i\le N} p^i} \le 0$.
Therefore,

$$\begin{aligned}\frac{c_1^k}{c_1^m} &= \frac{c_1^k(0)}{c_1^m(0)} e^{\int_0^t \left(2\frac{a}{1+k\rho_2(\tau)}-1\right)d\tau(p^k-p^m)} \\ &\in \left[\frac{c_1^k(0)}{c_1^m(0)} e^{\min\{M_6(p^k-p^m),M_7(p^k-p^m)\}}, \frac{c_1^k(0)}{c_1^m(0)} e^{\max\{M_6(p^k-p^m),M_7(p^k-p^m)\}}\right]\end{aligned}$$

is bounded away from zero and infinity.

■

Remark F.7
Under the assumptions of Lemma F.6 it is not possible that c_1^i is bounded away from zero and that at the same time c_1^k converges to zero. Either all c_1^i are bounded away from zero or all of them converge to zero.

Proposition 7.16 is a summary of the above results.

F.2 Proof of Proposition 7.19

We now adapt the reasoning from the previous Section to Model 2. For simplicity, we assume that post-mitotic leukemic cells do not stay in bone marrow. We then obtain the system.

$$\begin{aligned}\frac{d}{dt}c_1(t) &= \left(2a^c_{max}s(t)-1\right)p^c c_1(t) - d(\rho(t))c_1(t) \\ \frac{d}{dt}c_2(t) &= 2\left(1-a^c_{max}s(t)\right)p^c c_1(t) - d^c_2 c_2(t) \\ s(t) &= \frac{1}{1+k^c c_2(t)} \\ \frac{d}{dt}\tilde{l}^1_1(t) &= \left(2a^{\tilde{l}^1}-1\right)p^{\tilde{l}^1}\tilde{l}^1_1(t) - d(\rho(t))\tilde{l}^1_1(t) \\ \frac{d}{dt}\tilde{l}^1_2(t) &= 2\left(1-a^{\tilde{l}^1}\right)p^{\tilde{l}^1}\tilde{l}^1_1(t) - d^{\tilde{l}^1}_2\tilde{l}^1_2(t) - d(\rho(t))\tilde{l}^1_2(t) \\ &\vdots \quad \vdots \quad \vdots \\ \frac{d}{dt}\tilde{l}^n_1(t) &= \left(2a^{\tilde{l}^n}-1\right)p^{\tilde{l}^n}\tilde{l}^n_1(t) - d(\rho(t))\tilde{l}^n_1(t) \\ \frac{d}{dt}\tilde{l}^n_2(t) &= 2\left(1-a^{\tilde{l}^n}\right)p^{\tilde{l}^n}\tilde{l}^n_1(t) - d^{\tilde{l}^n}_2\tilde{l}^n_2(t) - d(\rho(t))\tilde{l}^n_2(t) \\ \rho(t) &= c_1(t) + \sum_{i=1}^n \tilde{l}^i_1(t).\end{aligned} \tag{F.10}$$

We assume $1 > a^c_{max} > 0.5$, $p^c > 0$, $d^c_2 > 0$, $a^{l^i} \in (0,1)$, $p^{l^i} > 0$, $d^{l^i}_2 > 0$ for $1 \leq i \leq n$, $k^c > 0$, $k^l > 0$.

Definition F.8
We set $\tilde{\rho} := \sum_{i=1}^{n} \tilde{l}^i_1(t)$.

Lemma F.9
It holds for non-negative initial conditions that $0 \leq c_1 \leq K_1$ *for all* $t > 0$ *and a constant* K_1.

PROOF
Non-negativity is straightforward. It holds

$$\begin{aligned}\frac{d}{dt}c_1(t) &= \big(2a^c_{max}s(t) - 1\big)p^c c_1(t) - d(\rho(t))c_1(t)\\ &\leq \big(2a^c_{max}s(t) - 1\big)p^c c_1(t)\end{aligned}$$

Solutions of the system

$$\begin{aligned}\frac{d}{dt}c_1(t) &= \big(2a^c_{max}s(t) - 1\big)p^c c_1(t)\\ \frac{d}{dt}c_2(t) &= 2\big(1 - a^c_{max}s(t)\big)p^c c_1(t) - d^c_2 c_2(t)\\ s(t) &= \frac{1}{1 + k^c c_2(t)}\end{aligned}$$

are globally bounded as shown in Lemma A.8. This implies the result.

■

Lemma F.10
Assume $\min_{1\leq i\leq N}\{(2a^{\tilde{l}^i} - 1)p^{\tilde{l}^i}\} > d(K_1)$. *Let* $\tilde{\rho}(0) > 0$, *then there exists a positive constant* K_2 *such that* $\tilde{\rho} > K_2$.

PROOF

$$\begin{aligned}\frac{d}{dt}\tilde{\rho} &= \sum_{i=1}^{N}(2a^{\tilde{l}^i} - 1)p^{\tilde{l}^i}\tilde{l}^i_1 - d(\tilde{\rho} + c_1)\sum_{i=1}^{N}\tilde{l}^i_1\\ &\geq \min_{1\leq i\leq N}\{(2a^{\tilde{l}^i} - 1)p^{\tilde{l}^i}\}\tilde{\rho} - d(\tilde{\rho} + c_1)\tilde{\rho}\end{aligned}$$

Due to the assumptions, there exists $\hat{\tilde{\rho}} > 0$ such that $\min_{1\leq i\leq N}\{(2a^{\tilde{l}^i} - 1)p^{\tilde{l}^n}\} > d(K_1 + c)$ for $0 \leq c \leq \hat{\tilde{\rho}}$. Consequently, $\tilde{\rho} < \hat{\tilde{\rho}}$ implies $\frac{d}{dt}\tilde{\rho} > 0$. Therefore, $\tilde{\rho} \geq \min\{\tilde{\rho}(0), \hat{\tilde{\rho}}\} := K_2$. ■

Lemma F.11
For a positive constant K_3 *it holds* $\tilde{\rho} \leq K_3$.

PROOF
It holds

$$\begin{aligned}\frac{d}{dt}\tilde{\rho} &\leq \max_{1\leq i\leq N}\{(2a^{\tilde{l}^i}-1)p^{\tilde{l}^i}\}\tilde{\rho} - d(\tilde{\rho}+c_1)\tilde{\rho}\\ &\leq \max_{1\leq i\leq N}\{(2a^{\tilde{l}^i}-1)p^{\tilde{l}^i}\}\tilde{\rho} - d(\tilde{\rho})\tilde{\rho}\end{aligned}$$

It holds $\frac{d}{dt}\tilde{\rho} < 0 \Leftrightarrow d(\tilde{\rho}) > \max_{1\leq i\leq N}\{(2a^{\tilde{l}^i}-1)p^{\tilde{l}^i}\}$. Due to strict monotony of d, it follows that there exists a constant $\tilde{K}_3$ such that $\frac{d}{dt}\tilde{\rho} < 0 \Leftrightarrow \tilde{\rho} > \tilde{K}_3$. The constant $K_3 := \max\{\tilde{K}_3, \tilde{\rho}(0)\}$ has the desired properties.

■

Lemma F.12
Set $\zeta^i := (2a^{\tilde{l}^i}-1)p^{\tilde{l}^i}$. It holds

(i) If $\zeta^i < \max_{1\leq i\leq N}\{\zeta^i\}$, then $\lim_{t\to\infty}\tilde{l}_1^i = 0$.

(ii) If $\zeta^k = \zeta^j$ for $j \neq k$, then $\frac{\tilde{l}_1^k}{\tilde{l}_1^j}$ is constant over time.

PROOF
(i)

$$\begin{aligned}\frac{d}{dt}\left(\frac{\tilde{l}_1^j}{\tilde{l}_1^k}\right) &= \frac{\frac{d}{dt}\tilde{l}_1^j}{\tilde{l}_1^k} - \frac{\tilde{l}_1^j\frac{d}{dt}\tilde{l}_1^k}{\left(\tilde{l}_1^k\right)^2}\\ &= \left(\frac{\tilde{l}_1^j}{\tilde{l}_1^k}\right)\zeta^j - \left(\frac{\tilde{l}_1^j}{\tilde{l}_1^k}\right)d(\rho) - \left(\frac{\tilde{l}_1^j}{\tilde{l}_1^k}\right)\zeta^k + \left(\frac{\tilde{l}_1^j}{\tilde{l}_1^k}\right)d(\rho)\\ &= \left(\frac{\tilde{l}_1^j}{\tilde{l}_1^k}\right)(\zeta^j - \zeta^k)\end{aligned}$$

Therefore, $\frac{\tilde{l}_1^j}{\tilde{l}_1^k} = \frac{\tilde{l}_1^j(0)}{\tilde{l}_1^k(0)}e^{(\zeta^j-\zeta^k)t}$.
Let $\zeta^k = \max_{1\leq i\leq N}\{\zeta^i\}$ and $\zeta^k > \zeta^j$. Then, it holds

$$\tilde{l}_1^j = \frac{\tilde{l}_1^j(0)}{\tilde{l}_1^k(0)}e^{(\zeta^j-\zeta^k)t}\tilde{l}_1^k \leq \frac{\tilde{l}_1^j(0)}{\tilde{l}_1^k(0)}e^{(\zeta^j-\zeta^k)t}K_3,$$

which tends to zero for t tending to infinity.

(ii) For $\zeta^j = \zeta^k$ we have $\frac{d}{dt}\left(\frac{\tilde{l}_1^j}{\tilde{l}_1^k}\right) = 0$ for all t. ■

Remark F.13
Since $\tilde{\rho}$ is bounded away from zero, it follows from Lemma F.12 that all $\tilde{l}_1^j$ with $\zeta^k = \max_{1\leq i\leq N}\{\zeta^i\}$ are bounded away from zero.

Lemma F.14
Set $\zeta^i := (2a^{\tilde{l}^i} - 1)p^{\tilde{l}^i}$ *and* $\zeta := \max_{1\leq i\leq N} \zeta^i$. *Assume that there exits* $0 < \hat{s} < 1$ *such that* $(2a^c_{max}\hat{s} - 1)p^c - \zeta > 0$. *Let* $c_1(0) > 0$. *Then,* c_1 *is bounded away from zero.*

PROOF
We set $R := \sum_{\{j|\zeta^j=\zeta\}} \tilde{l}^j_1$ and $\hat{R} := \sum_{\{j|\zeta^j<\zeta\}} \tilde{l}^j_1$.
It holds $\frac{d}{dt}R = \zeta R - d(R + \hat{R} + c_1)R \leq \zeta R - d(R)R$. We set $K_4 := d^{-1}(\zeta)$, where d^{-1} denotes the inverse of d. Due to strict monotony, $d^{-1}(\zeta)$ is well defined. Then, $R > K_4$ implies $\frac{d}{dt}R < 0$. If $R > K_4 + \delta$ for a $\delta > 0$, then $\frac{d}{dt}R < -\alpha$ for a positive constant α.

Choose $\varepsilon_1, \varepsilon_2 > 0$ such that $(2a^c_{max}\hat{s} - 1)p^c - d(K_4 + \varepsilon_1 + \varepsilon_2) > 0$. This is possible, due to the assumptions.

We know from Lemma F.12 that all $\tilde{l}^i_1$ with $\zeta^i < \zeta$ tend to zero for t tending to infinity. Therefore, there exists $t_0 > 0$ such that $\hat{R} < \varepsilon_1$ for $t > t_0$. Furthermore, there exists $t_1 > t_0$ such that $R \leq K_4 + \varepsilon_2$ for $t > t_1$,
We now consider for $0 < \gamma < 1$ and for $t > t_1$

$$\begin{aligned}
\frac{d}{dt}\frac{c_2}{c_1^\gamma} &= \frac{\frac{d}{dt}c_2(t)}{c_1(t)^\gamma} - \gamma\frac{c_2(t)\frac{d}{dt}c_1(t)}{c_1(t)^{\gamma+1}} \\
&= \frac{2(1 - a^c_{max}s)p^c}{c_1^{\gamma-1}} - \frac{d^c_2 c_2}{c_1^\gamma} - \gamma\frac{c_2(t)}{c_1(t)^\gamma}((2a^c_{max}s - 1)p^c - d(R + \hat{R} + c_1)) \\
&= \frac{2(1 - a^c_{max}s)p^c}{c_1^{\gamma-1}} + \frac{c_2}{c_1^\gamma}[-d^c_2 - 2a^c_{max}sp^c\gamma + p^c\gamma + d(R + \hat{R} + c_1)\gamma] \\
&\leq \frac{2p^c}{K_1^{\gamma-1}} + \frac{c_2}{c_1^\gamma}[-d^c_2 + p^c\gamma + d(R + \varepsilon_1 + \varepsilon_2 + K_1)\gamma].
\end{aligned}$$

We used Lemma F.9 and $\gamma - 1 < 0$. We now choose γ such that $-d^c_2 + p^c\gamma + d(R + \varepsilon_1 + \varepsilon_2 + K_1)\gamma < 0$. Then, it follows that there exists $\tilde{K}_6 > 0$ such that $\frac{c_2}{c_1^\gamma} > \tilde{K}_6$ implies $\frac{d}{dt}\frac{c_2}{c_1^\gamma} < 0$. Consequently, $\frac{c_2}{c_1^\gamma} \leq \min\left\{\tilde{K}_6, \frac{c_2(0)}{c_1(0)^\gamma}\right\} =: K_6$.

This implies $c_2 < K_6 c_1^\gamma$. Insertion into the ODE for c_1 yields

$$\begin{aligned}
\frac{d}{dt}c_1 &= \left(\frac{2a^c_{max}}{1 + kc_2} - 1\right)p^c c_1 - d(R + \hat{R} + c_1)c_1 \\
&\geq \underbrace{\left[\left(\frac{2a^c_{max}}{1 + kM_6c_1^\gamma} - 1\right)p^c - d(R + \varepsilon_1 + \varepsilon_2 + c_1)\right]}_{=:f(c_1)} c_1.
\end{aligned}$$

Due to choice of ε_1 and ε_2, it holds $f(0) > 0$. Consequently, there exists $\alpha > 0$ such that $f(x) > 0$ for $0 \leq x \leq \alpha$. Therefore, $c_1 \geq \min\{\alpha, c_1(t_1)\}$ for $t > t_1$. Let $\mu := \min_{0 \leq t \leq t_1} c_1(t)$. This is positive for positive $c_1(0)$, since c_1 decays at most exponentially. Therefore, $c_1 \geq \min\{\alpha, \mu\} > 0$. ■

Proposition 7.19 is a summary of the obtained results.

APPENDIX G

ADDITIONAL PATIENT EXAMPLES TO CHAPTERS 6 AND 7

Figure G.1 ***(facing page)*****: Estimated LSC properties in first and second relapse.** (a, c, e, g) Marrow blast dynamics of 4 patients experiencing two relapses. Horizontal arrows at the bottom of the graph denote treatment duration (in case of chemotherapy from the beginning of the first until the end of last cycle, in case of targeted therapy from the beginning until the end of drug administration). (b, d, f, h) Estimated properties of the LSC responsible for first and second relapse. Figure (b) corresponds to the patient data in (a), Figure (d) to that in (c), etc. The results demonstrate that LSC properties change between the relapses. Higher self-renewal and / or proliferation in second relapse correspond to selection of more aggressive, faster expanding, LSC than in the first relapse. In all cases except one (a, b) proliferation/self-renewal is higher at relapse in comparison to primary manifestation.

Patient 3

(a)

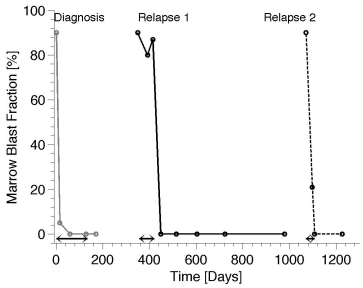

(b)

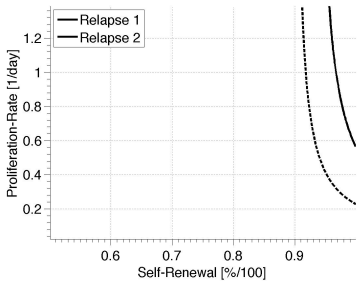

Patient 4

(c)

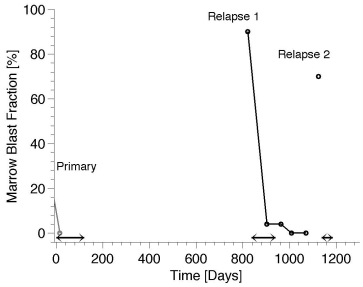

(d)

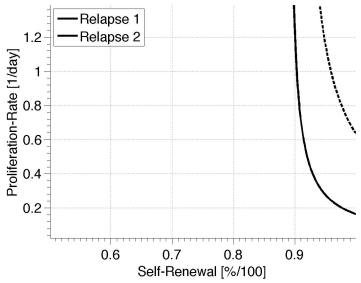

Patient 5

(e)

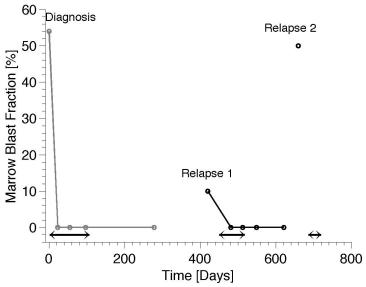

(f)

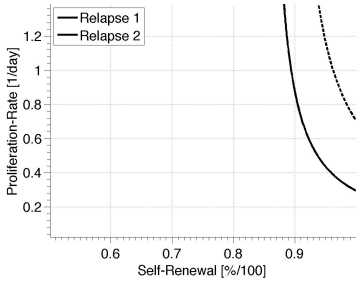

Patient 6

(g)

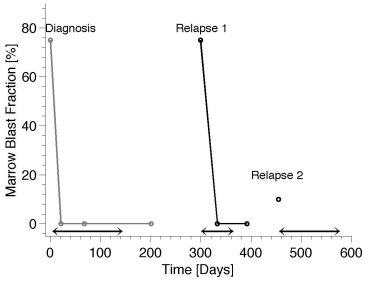

(h)

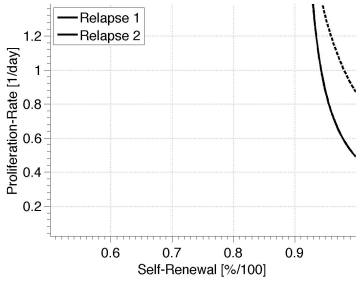

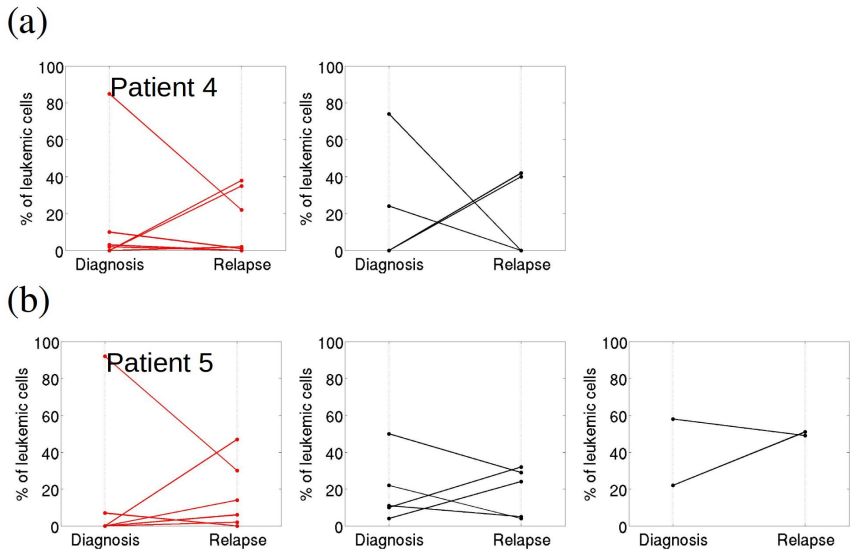

Figure G.2: Patterns of clonal evolution - Comparison of model and data. Clonal size is measured in % of total leukemic cell mass, 100% means that all leukemic cells originate from one clone. Sensitivity of methods is around 1%. Size 0% means that the corresponding clone could not be detected at the respective time-point. The diagrams depict clonal size for each clone detected at primary diagnosis and/or relapse, i.e., for each clone there exist two measurements. The two measurements referring to the same clone are connected by a line to visualize changes in clonal contribution. Panels (a), (b): Comparison of experimental measurements to model simulations. Red curves correspond to measurements (patient data), black curves in the same row to model simulations with similar behavior. The data were taken from [9].

APPENDIX H

PROOFS OF CHAPTER 9

H.1 Proof of Lemma 9.7

Lemma 9.7 is formulated on page 169.

PROOF
The proof follows the lines of Theorem 21.2 from [6] and Lemma 2.1/Theorem 2.1 from [140]. Let $Y(t)$ be a fundamental solution of (9.9). The variation of constants formula, [234], then implies for problem (9.10)

$$\mathbf{x}(t) = Y(t)Y^{-1}(\nu)\mathbf{x}_\nu + \int_\nu^t Y(t)Y^{-1}(\tau)B(\tau)\mathbf{x}(\tau)\,d\tau \tag{H.1}$$

Let $t > t_1 \geq \nu$. Let $||\cdot||$ denote e.g., the euclidean and the matrix norm induced by it. We estimate

$$\begin{aligned} ||\mathbf{x}(t)|| &\leq ||Y(t)Y^{-1}(\nu)||\,||\mathbf{x}_\nu|| + \int_\nu^t ||Y(t)Y^{-1}(\tau)||\,||B(\tau)||\,||\mathbf{x}(\tau)||\,d\tau \\ &\leq Ke^{-\alpha(t-\nu)}||\mathbf{x}_\nu|| + C\int_0^{t_1} Ke^{-\alpha(t-\tau)}||\mathbf{x}(\tau)||\,d\tau + c\int_{t_1}^t Ke^{-\alpha(t-\tau)}||\mathbf{x}(\tau)||\,d\tau \end{aligned} \tag{H.2}$$

This is equivalent to

$$||\mathbf{x}(t)||e^{\alpha(t-\nu)} \leq K||\mathbf{x}_\nu|| + C\int_0^{t_1} Ke^{\alpha(\tau-\nu)}\,||\mathbf{x}(\tau)||\,d\tau + c\int_{t_1}^t Ke^{\alpha(\tau-\nu)}||\mathbf{x}(\tau)||\,d\tau \tag{H.3}$$

Equation (H.1) also implies

$$\begin{aligned}||\mathbf{x}(t)|| &\leq ||Y(t)Y^{-1}(\nu)||\,||\mathbf{x}_\nu|| + \int_0^t ||Y(t)Y^{-1}(\tau)||\,||B(\tau)||\,||\mathbf{x}(\tau)||\,d\tau \\ &\leq Ke^{-\alpha(t-\nu)}||\mathbf{x}_\nu|| + \int_0^t Ke^{-\alpha(t-\tau)}\,||B(\tau)||\,||\mathbf{x}(\tau)||\,d\tau \\ &\leq K||\mathbf{x}_\nu|| + K\max\{c,C\}\int_0^t ||\mathbf{x}(\tau)||\,d\tau \end{aligned} \tag{H.4}$$

Gronwall's lemma yields

$$||\mathbf{x}(t)|| \leq K||\mathbf{x}_\nu||e^{K\max\{c,C\}t} \tag{H.5}$$

Insertion of equation (H.5) into equation (H.3) results in

$$\begin{aligned}&||\mathbf{x}(t)||e^{\alpha(t-\nu)} \\ &\leq K||\mathbf{x}_\nu|| + CK^2||\mathbf{x}_\nu||\int_0^{t_1} e^{K\max\{c,C\}\tau+\alpha(\tau-\nu)}\,d\tau + c\int_{t_1}^t Ke^{\alpha(\tau-\nu)}||\mathbf{x}(\tau)||\,d\tau \\ &\leq K||\mathbf{x}_\nu|| + CK^2||\mathbf{x}_\nu||\int_0^{t_1} e^{K\max\{c,C\}\tau+\alpha\tau}\,d\tau + c\int_{t_1}^t Ke^{\alpha(\tau-\nu)}||\mathbf{x}(\tau)||\,d\tau \\ &=: \tilde{K}||\mathbf{x}_\nu|| + c\int_{t_1}^t Ke^{\alpha(\tau-\nu)}||\mathbf{x}(\tau)||\,d\tau \end{aligned} \tag{H.6}$$

with $\tilde{K} := K + \frac{CK^2}{K\max\{c,C\}+\alpha}\left(e^{K\max\{c,C\}t_1+\alpha t_1} - 1\right) < \infty$.

Gronwall's lemma, [21, 97], yields

$$||\mathbf{x}(t)||e^{\alpha(t-\nu)} \leq \tilde{K}||\mathbf{x}_\nu||e^{cK(t-t_1)}$$

This is equivalent to

$$||\mathbf{x}(t)|| \leq \tilde{K}||\mathbf{x}_\nu||e^{(-\alpha+cK)t+\alpha\nu}e^{-cKt_1}$$

Since we consider the case $\nu \leq t_1$, it holds $cK\nu \leq cKt_1$ and $\alpha\nu - cK\nu \geq \alpha\nu - cKt_1$. Therefore,

$$\begin{aligned}||\mathbf{x}(t)|| &\leq \tilde{K}||\mathbf{x}_\nu||e^{(-\alpha+cK)t+\alpha\nu}e^{-cKt_1} \\ &\leq \tilde{K}||\mathbf{x}_\nu||e^{(-\alpha+cK)t+\alpha\nu}e^{-cK\nu} \leq \tilde{K}||\mathbf{x}_\nu||e^{-\hat{\alpha}(t-\nu)} \end{aligned} \tag{H.7}$$

with $\hat{\alpha} := \alpha - cK > 0$, since $cK < \alpha$.

Let $t \geq \nu \geq t_1$. Then, we obtain

$$||\mathbf{x}(t)|| \leq ||Y(t)Y^{-1}(\nu)||\,||\mathbf{x}_\nu|| + \int_\nu^t ||Y(t)Y^{-1}(\tau)||\,||B(\tau)||\,||\mathbf{x}(\tau)||\,d\tau$$
$$\leq Ke^{-\alpha(t-\nu)}||\mathbf{x}_\nu|| + c\int_\nu^t Ke^{-\alpha(t-\tau)}||\mathbf{x}(\tau)||\,d\tau \tag{H.8}$$

This is equivalent to

$$||\mathbf{x}(t)||e^{\alpha(t-\nu)} \leq K||\mathbf{x}_\nu|| + c\int_{t_1}^t Ke^{\alpha(\tau-\nu)}||\mathbf{x}(\tau)||\,d\tau \tag{H.9}$$

Gronwall implies

$$||\mathbf{x}(t)||e^{\alpha(t-\nu)} \leq K||\mathbf{x}_\nu||e^{cK(t-\nu)}, \tag{H.10}$$

therefore,

$$||\mathbf{x}(t)|| \leq K||\mathbf{x}_\nu||e^{(-\alpha+cK)(t-\nu)} =: K||\mathbf{x}_\nu||e^{-\hat{\alpha}(t-\nu)} \tag{H.11}$$

with $-\hat{\alpha} = (-\alpha + cK) < 0$, due to the Assumptions.

We, therefore, obtain in case $t \geq t_1$ that $||\mathbf{x}(t)|| \leq K'||\mathbf{x}_\nu||e^{-\hat{\alpha}(t-\nu)}$ for $t \geq \nu$ with $K' = \max\{K, \tilde{K}\}$. The constants $K', \hat{\alpha}$ are independent of ν, $\mathbf{x}_\nu$.

In the case $\nu \leq t \leq t_1$ we get

$$||\mathbf{x}(t)|| \leq ||Y(t)Y^{-1}(\nu)||\,||\mathbf{x}_\nu|| + \int_\nu^t ||Y(t)Y^{-1}(\tau)||\,||B(\tau)||\,||\mathbf{x}(\tau)||\,d\tau$$
$$\leq Ke^{-\alpha(t-\nu)}||\mathbf{x}_\nu|| + C\int_\nu^t Ke^{-\alpha(t-\tau)}||\mathbf{x}(\tau)||\,d\tau, \tag{H.12}$$

which yields using Gronwall

$$||\mathbf{x}(t)|| \leq K||\mathbf{x}_\nu||e^{(-\alpha+CK)(t-\nu)} \leq K||\mathbf{x}_\nu||e^{(-\alpha+CK)t_1} =: L||\mathbf{x}_\nu||. \tag{H.13}$$

This implies that $||\mathbf{x}(t)|| \leq ||\mathbf{x}_\nu||\hat{L}e^{-\hat{\alpha}(t-\nu)}$, where $\hat{L} = Le^{\hat{\alpha}t_1}$ and $\hat{\alpha}$ as above.

We used that $e^{\hat{\alpha}t_1 - \hat{\alpha}(t-\nu)} > 1$. Therefore, we get for all $t \geq \nu$ that $||\mathbf{x}(t)|| \leq ||\mathbf{x}_\nu||\hat{K}e^{-\hat{\alpha}(t-\nu)}$, where $\hat{K} = \max\{\hat{L}, K'\}$.

Using the fundamental solution of system (9.10) it holds for all $t \geq \nu$

$$||\tilde{Y}(t)\tilde{Y}^{-1}(\nu)\mathbf{x}(\nu)|| = ||\mathbf{x}(t)|| \leq ||\mathbf{x}_\nu||\hat{K}e^{-\hat{\alpha}(t-\nu)}$$

This implies (for $||\mathbf{x}_\nu|| > 0$) $\frac{||Y(t)Y^{-1}(\nu)x(\nu)||}{||\mathbf{x}(\nu)||} \leq \hat{K}e^{-\hat{\alpha}(t-\nu)}$. Therefore, due to definition of the matrix norm, $||Y(t)Y^{-1}(\nu)|| \leq Ke^{-\hat{\alpha}(t-\nu)}$ for all $t \geq \nu$.

■

H.2 Proof of Corollary 9.8 and Remark 9.10

Corollary 9.8 and Remark 9.10 are formulated on page 170.

PROOF
Step 1: Let k and C be the constants from Assumption 9.4. Due to Assumption 9.2, the set $U_A := \{(\mathbf{A}(t), \varphi(\mathbf{A}(t))|t \in \mathbb{R}_0^+\}$ is bounded. Therefore, its closure $\bar{U}_A$ is compact. Denote by $\bar{U}$ a compact set including a neighborhood of $\bar{U}_A$. Due to Assumption 9.1, the function $(\mathbf{x}, y) \mapsto \left(\nabla_u \mathbf{f}(\mathbf{x}, y) + \partial_v \mathbf{f}(\mathbf{x}, y) \otimes \nabla\varphi(\mathbf{x})\right)$ is continuous. On the compactum $\bar{U}$ it is, thus, uniformly continuous, i.e., there exist positive constants $\tilde{\tilde{b}}$, $\tilde{\lambda}$ such that for $(\mathbf{x}, y)$, $(\mathbf{x}_0, y_0) \in \bar{U}$ the conditions $||\mathbf{x} - \mathbf{x}_0|| \leq \tilde{\tilde{b}}$ and $|y - y_0| \leq \tilde{\lambda}$ imply

$$\left\| \left(\nabla_u \mathbf{f}(\mathbf{x}, y) + \partial_v \mathbf{f}(\mathbf{x}, y) \otimes \nabla\varphi(\mathbf{x})\right) - \left(\nabla_u \mathbf{f}(\mathbf{x_0}, y_0) + \partial_v \mathbf{f}(\mathbf{x_0}, y_0) \otimes \nabla\varphi(\mathbf{x_0})\right) \right\| \leq \frac{k}{2C} \tag{H.14}$$

for all $(\mathbf{x}, y), (\mathbf{x}_0, y_0) \in \bar{U}$. We can choose $\tilde{b}$ such that $|x^i - x_0^i| \leq \tilde{b}$ for $i = 1, \cdots, n$ implies $||\mathbf{x} - \mathbf{x}_0|| \leq \tilde{\tilde{b}}$, where x^i, x_0^i are the components of $\mathbf{x}$, $\mathbf{x}_0$.

Step 2: Due to Assumption 9.3 (i), we have $\alpha - \partial_y \Phi(\mathbf{x}, y)|_{(\mathbf{x}=\mathbf{A}, y=\varphi(\mathbf{A}))} \geq M_0 > 0$ for all $t \geq 0$. The function $(\mathbf{u}, v) \mapsto \alpha - \partial_y \Phi(\mathbf{x}, y)|_{(\mathbf{x}=\mathbf{u}, y=v)}$ is continuous and, therefore, uniformly continuous on $\bar{U}$. Therefore, there exist positive constants $\hat{\tilde{b}}$, $\hat{\lambda}_0$ such that $(\mathbf{u}, v)$, $(\tilde{\mathbf{u}}, \tilde{v}) \in \bar{U}$, $||\mathbf{u} - \tilde{\mathbf{u}}|| \leq \hat{\tilde{b}}$ and $|v - \tilde{v}| \leq \hat{\lambda}_0$ imply $||(\alpha - \partial_y \Phi(\mathbf{x}, y)|_{(\mathbf{x}=\mathbf{u}, y=v)}) - (\alpha - \partial_y \Phi(\mathbf{x}, y)|_{(\mathbf{x}=\tilde{\mathbf{u}}, y=\tilde{v})})|| \leq \frac{M_0}{2}$. Therefore, for all continuous functions $(\mu, \nu) : \mathbb{R}_0^+ \to \mathbb{R}^n \times \mathbb{R}$ fulfilling $||\mu(t) - \mathbf{A}(t)|| \leq \hat{\tilde{b}}$ for all t and $|\nu(t) - \varphi(\mathbf{A}(t))| \leq \hat{\lambda}_0$ it holds $\alpha - \partial_y \Phi(\mathbf{x}, y)|_{(\mathbf{x}=\mu(t), y=\nu(t))} \geq \frac{M_0}{2}$ for all $t \geq 0$. We can choose $\hat{b}$ such that $|u^i - u_0^i| \leq \hat{b}$ for $i = 1, \cdots, n$ implies $||\mathbf{u} - \mathbf{u}_0|| \leq \hat{\tilde{b}}$, where u^i, u_0^i are the components of $\mathbf{u}$, $\mathbf{u}_0$. We can always choose $\hat{\tilde{b}}$, $\hat{\lambda}_0$ such that $||\mu(t) - \mathbf{A}(t)|| \leq \hat{\tilde{b}}$ and $|\nu(t) - \varphi(\mathbf{A}(t))| \leq \hat{\lambda}_0$ for all t implies $\{(\mu(t), \nu(t))|t \in \mathbb{R}_0^+\} \subset \bar{U}$.

In summary for continuous functions $(\mu, \nu) : \mathbb{R}_0^+ \to \mathbb{R}^n \times \mathbb{R}$ it holds

$$\begin{aligned} &|\nu(t) - \varphi(\mathbf{A}(t))| \leq \hat{\lambda}_0,\ |\mu^i(t) - A^i(t)| \leq \hat{b} \\ &\Rightarrow \alpha - \partial_y \Phi(\mathbf{x}, y)|_{(\mathbf{x}=\mu(t), y=\nu(t))} \geq \frac{M_0}{2} \qquad (\star) \end{aligned}$$

In case that $|v^0 - \varphi(\mathbf{u}^0)| \leq \min\{\tilde{\lambda}_0, \hat{\lambda}_0\}$ we can finish here and set $\lambda^a = \min\{\tilde{\lambda}_0, \hat{\lambda}_0\} + \varphi(\mathbf{A}(t))$ and $\lambda^b = \min\{\tilde{\lambda}_0, \hat{\lambda}_0\} - \varphi(\mathbf{A}(t))$. This domain is depicted in Figure H.1

(a). Step 3 extends the domain to the case general case. The construction is illustrated by Figure H.1 (b).
Step 3a: Due to Assumption 9.3(iii), it holds $\alpha - \partial_y \Phi(\mathbf{x}, y)|_{(\mathbf{x}=\mathbf{u}^0, y\in\mathcal{I})} \geq \frac{M_0}{2} > 0$ for $\mathcal{I} = [\min\{\varphi(\mathbf{u}^0), v^0\}, \max\{\varphi(\mathbf{u}^0), v^0\}]$. Let $\bar{V} \subset \mathbb{R}^n \times \mathbb{R}$ be a compactum containing a neighborhood of the set $\{\mathbf{u}^0, \mathcal{I}\} \subset \mathbb{R}^n \times \mathbb{R}$. The function $(\mathbf{u}, v) \mapsto \alpha - \partial_y \Phi(\mathbf{x}, y)|_{(\mathbf{x}=\mathbf{u}, y=v)}$ is continuous and, thus, uniformly continuous on $\bar{V}$. Therefore, there exist positive constants β, γ such that

$$
\begin{aligned}
&(\mathbf{u}, v),\ (\tilde{\mathbf{u}}, \tilde{v}) \in \bar{V},\ |\mathbf{u} - \tilde{\mathbf{u}}| \leq \beta,\ |v - \tilde{v}| \leq \gamma \\
&\Rightarrow\ |(\alpha - \partial_y \Phi(\mathbf{x}, y)|_{(\mathbf{x}=\mathbf{u}, y=v)}) - (\alpha - \partial_y \Phi(\mathbf{x}, y)|_{(\mathbf{x}=\tilde{\mathbf{u}}, y=\tilde{v})})| \leq \frac{M_0}{4} \qquad (*)
\end{aligned}
$$

Step 3b: We can choose β, γ such that $|\mathbf{u}^0 - \mathbf{u}| \leq \beta$, $\operatorname{dist}(v, \mathcal{I}) \leq \gamma$ imply $(\mathbf{u}, v) \in \bar{V}$. Let $|\mathbf{u} - \mathbf{u}^0| \leq \beta$ and $\operatorname{dist}(v, \mathcal{I}) \leq \frac{\gamma}{2}$. Then, there exists $\hat{v} \in \mathcal{I}$ such that $|v - \hat{v}| \leq \gamma$.
Therefore, by Step 3a $(*)$

$$
\begin{aligned}
&|\mathbf{u} - \mathbf{u}^0| \leq \beta,\ \operatorname{dist}(v, \mathcal{I}) \leq \frac{\gamma}{2} \\
&\Rightarrow\ \exists \hat{v} \in \mathcal{I} : |(\alpha - \partial_y \Phi(\mathbf{x}, y)|_{\mathbf{x}=\mathbf{u}^0, y=\hat{v}}) - (\alpha - \partial_y \Phi(\mathbf{x}, y)|_{\mathbf{x}=\mathbf{u}, y=v})| \leq \frac{M_0}{4} \qquad (**)
\end{aligned}
$$

We obtain

$$
\begin{aligned}
\frac{M_0}{4} &\geq |(\alpha - \partial_y \Phi(\mathbf{x}, y)|_{\mathbf{x}=\mathbf{u}, y=v}) - (\alpha - \partial_y \Phi(\mathbf{x}, y)|_{\mathbf{x}=\mathbf{u}^0, y=\hat{v}})| \\
&\geq -|(\alpha - \partial_y \Phi(\mathbf{x}, y)|_{\mathbf{x}=\mathbf{u}, y=v})| + |(\alpha - \partial_y \Phi(\mathbf{x}, y)|_{\mathbf{x}=\mathbf{u}^0, y=\hat{v}})|
\end{aligned}
$$

$$
\begin{aligned}
\Leftrightarrow -|(\alpha - \partial_y \Phi(\mathbf{x}, y)|_{\mathbf{x}=\mathbf{u}, y=v})| &\leq \frac{M_0}{4} - |(\alpha - \partial_y \Phi(\mathbf{x}, y)|_{\mathbf{x}=\mathbf{u}^0, y=\hat{v}})| \\
&\leq -\frac{M_0}{4}
\end{aligned}
$$

The latter, since $\alpha - \partial_y \Phi(\mathbf{x}, y)|_{\mathbf{x}=\mathbf{u}^0, y=\hat{v}} \geq \frac{M_0}{2}$, due to Assumption 9.3. Therefore, we obtain

$$
|(\alpha - \partial_y \Phi(\mathbf{x}, y)|_{\mathbf{x}=\mathbf{u}, y=v})| \geq \frac{M_0}{4}. \qquad (***)
$$

Since it holds $\alpha - \partial_y \Phi(\mathbf{x}, y)|_{\mathbf{x}=\mathbf{u}^0, y=\hat{v}} \geq \frac{M_0}{2}$, due to Assumption 9.3 (iii) and $\hat{v} \in \mathcal{I}$, the estimates $(**)$ and $(***)$ imply $(\alpha - \partial_y \Phi(\mathbf{x}, y)|_{\mathbf{x}=\mathbf{u}, y=v}) > 0$ and, thus, $\alpha - \partial_y \Phi(\mathbf{x}, y)|_{\mathbf{x}=\mathbf{u}, y=v} \geq \frac{M_0}{4}$. In summary

$$|\mathbf{u}-\mathbf{u}^0|\leq\beta,\ \mathrm{dist}(v,\mathcal{I})\leq\frac{\gamma}{2}\Rightarrow\alpha-\partial_y\Phi(\mathbf{x},y)|_{\mathbf{x}=\mathbf{u},y=v}\geq\frac{M_0}{4}\qquad(***)$$

Step 3c: Since $\mathbf{A}$ and $\varphi(\mathbf{A})$ are continuous and $\mathbf{A}(0)=\mathbf{u}^0$ and $\mathrm{dist}(\varphi(\mathbf{u}^0),\mathcal{I})=0$, we can choose $t_0>0$ such that

$$|\mathbf{A}(t)-\mathbf{u}^0|\leq\frac{\beta}{2}\text{ and }\mathrm{dist}(\varphi(\mathbf{A}(t)),\mathcal{I})<\frac{\gamma}{4}\text{ for }0\leq t\leq t_0.\qquad(\#)$$

Let $|\mathbf{u}-\mathbf{A}(t)|\leq\frac{\beta}{2}$, for a $t\in[0,t_0]$, then it holds $|\mathbf{u}-\mathbf{u}^0|\leq|\mathbf{u}-\mathbf{A}(t)|+|\mathbf{A}(t)-\mathbf{u}^0|\leq\beta$. Therefore,

$$\begin{aligned}&|\mathbf{u}-\mathbf{A}(t)|\leq\frac{\beta}{2},\text{ for a }t\in[0,t_0],\mathrm{dist}(v,\mathcal{I})\leq\frac{\gamma}{2}\\&\Rightarrow\alpha-\partial_y\Phi(\mathbf{x},y)|_{\mathbf{x}=\mathbf{u},y=v}\geq\frac{M_0}{2}\qquad(\#\#)\end{aligned}$$

by Step 3b $(***)$.

Step 3d: For the moment we assume that $v^0>\varphi(\mathbf{u}^0)$, in the opposite case the construction works analogously. The construction is illustrated in Figure H.1 (b).

We now choose smooth functions $\lambda^a,\lambda^b:\mathbb{R}_0^+\to\mathbb{R}$ such that $\lambda^a(t)>\varphi(\mathbf{A}(t))$, $\lambda^b(t)<\varphi(\mathbf{A}(t))$, $\lambda^a(0)\in(v^0,v^0+\frac{\gamma}{2})$, $\lambda^b(0)\in(\varphi(\mathbf{u}^0)-\frac{\gamma}{2},\varphi(\mathbf{u}^0))$, $(\lambda^a(t),\ \lambda^b(t))\in(\varphi(\mathbf{u}^0))-\frac{\gamma}{2},v^0+\frac{\gamma}{2})$ for $0\leq t\leq t_0$. This is possible, since

$$\mathrm{dist}(\varphi(\mathbf{A}(t)),\mathcal{I})=\mathrm{dist}(\varphi(\mathbf{A}(t)),(\varphi(\mathbf{u}^0),v^0))<\frac{\gamma}{4}\text{ for }0\leq t\leq t_0,\qquad(\star\star)$$

due to Step 3c $(\#)$.

We set $\lambda_0<\min\{\hat{\lambda}_0,\ \tilde{\lambda}_0,\ \varphi(\mathbf{A}(t_0))-\varphi(\mathbf{u}^0)+\frac{\gamma}{2},\ v^0+\frac{\gamma}{2}-\varphi(\mathbf{A}(t_0))\}>0$. Positivity follows from $(\star\star)$. We, furthermore, set

$$\begin{aligned}&\lambda^a(t)=\varphi(\mathbf{A}(t))+\lambda_0,\text{ for }t\geq t_0\\&\lambda^b(t)=\varphi(\mathbf{A}(t))-\lambda_0,\text{ for }t\geq t_0.\qquad(\#\#\#)\end{aligned}$$

This is possible, since for this choice $\lambda^a(t_0)>\varphi(\mathbf{A}(t_0))$, $\lambda^b(t_0)<\varphi(\mathbf{A}(t_0))$ and $(\lambda^a(t_0),\ \lambda^b(t_0))\in(\varphi(\mathbf{u}^0))-\frac{\gamma}{2},v^0+\frac{\gamma}{2})$, see Figure H.1 (b).

We set $b:=\min\{\tilde{b},\hat{b},\frac{\beta}{2}\}$. Let $\mathbf{u}:\mathbb{R}_0^+\to\mathbb{R}^n$ $v:\mathbb{R}_0^+\to\mathbb{R}$ be functions fulfilling $|\mathbf{u}(t)-\mathbf{A}(t)|\leq b$, $v(t)\in(\lambda^b(t),\lambda^a(t))$.

Let $t > t_0$, then it holds $\alpha - \partial_y \Phi(\mathbf{x}, y)|_{\mathbf{x}=\mathbf{u}, y=v} \geq \frac{M_0}{4}$ by Step 2 $(\star)$, since $v(t) - \varphi(A(t)) \leq \lambda_0$.

Let $0 \leq t \leq t_0$, then it holds $v(t) \in [\varphi(\mathbf{u}^0) - \frac{\gamma}{2}, v^0 + \frac{\gamma}{2}]$, since $\lambda^a(t),\ \lambda^b(t) \in [\varphi(\mathbf{u}^0)) - \frac{\gamma}{2}, v^0 + \frac{\gamma}{2}]$, due to construction, see Step 3d. Therefore, by Step 3c $(\#\#)$

$$\alpha - \partial_y \Phi(\mathbf{x}, y)|_{\mathbf{x}=\mathbf{u}, y=v} \geq \frac{M_0}{4}.$$

Therefore, $\alpha - \partial_y \Phi(\mathbf{x}, y)|_{\mathbf{x}=\mathbf{u}, y=v} \geq \frac{M_0}{4}$ for all $(\mathbf{u}, v) \in \mathcal{T}_{b,\lambda}$.
In case $v^0 = \varphi(\mathbf{A}(0))$ we set $\lambda^a(t) := \varphi(\mathbf{A}(t)) + \min\{\tilde{\lambda}_0,\ \hat{\lambda}_0\}$ and $\lambda^b(t) := \varphi(\mathbf{A}(t)) - \min\{\tilde{\lambda}_0,\ \hat{\lambda}_0\}$

Step 4: We now apply Lemma 9.7 with $\alpha = k$, $K = C$ (C from Assumption 9.4), $c = \frac{k}{2C}$, $t_1 = t_0$ and we set C from Lemma 9.7 to $C = \max\Big\{ \Big\| \Big(D_u \mathbf{f}(\mathbf{x}, y) + \partial_v \mathbf{f}(\mathbf{x}, y) \otimes \nabla\varphi(\mathbf{x}) \Big) - \Big(D_u \mathbf{f}(\mathbf{x_0}, y_0) + \partial_v \mathbf{f}(\mathbf{x_0}, y_0) \otimes \nabla\varphi(\mathbf{x_0}) \Big) \Big\| \ \Big| (\mathbf{x}, y) \in \bar{U}_A,\ \mathrm{dist}(y_0, \mathcal{I}) \leq \gamma, \mathrm{dist}(\mathbf{x_0}, \bar{U}_n) \leq b \Big\}$, where $U_n := \{\mathbf{A}(t) | t \geq 0\}$. Due to continuity and compactness of the set from which $\mathbf{x},\ \mathbf{x_0},\ y,\ y_0$ are taken, C is finite. Due to Step 1 (H.14), the Lemma yields the result concerning exponential dichotomy.

Proof of Remark 9.10: Due to construction, $\min_{t \in \mathbb{R}_0^+} \{\lambda^a(t) - \varphi(\mathbf{A}(t))\} = c_1 > 0$ and $\min_{t \in \mathbb{R}_0^+} \{\varphi(\mathbf{A}(t)) - \lambda^b(t)\} = c_2 > 0$. We know that φ is uniformly continuous on the compactum $\bar{U}_n$. Therefore, there exists b^* such that $|u_i - A_i(t)| \leq b^*$ $(i = 1, \cdots, n)$ implies $|\varphi(\mathbf{u}) - \varphi(\mathbf{A}(t))| \leq \min\{c_1, c_2\}$, which implies $\varphi(\mathbf{u}) \in (\lambda^b(t), \lambda^a(t))$. If we replace b from above by $\min\{b, b^*\}$, we obtain the result. ■

H.3 Proof of Lemma 9.13

The Lemma is formulated on page 172.

PROOF
It holds $\tilde{\Phi}(\mathbf{x}, y, t) = \Phi(\tilde{x}_1(x_1, t), \cdots, \tilde{x}_n(x_n, t), \tilde{y}(y, t))$. Due to Definition, 9.11 it holds $|\tilde{x}_i(x_i, t) - A(t)| \leq b$. Therefore, due to Remark 9.10,

$$\varphi(\tilde{x}_1(x_1, t), \cdots, \tilde{x}_n(x_n, t)) \in (\lambda^b(t), \lambda^a(t)).$$

This implies

$$\tilde{y}(\varphi(\tilde{x}_1(x_1, t), \cdots, \tilde{x}_n(x_n, t)), t) = \varphi(\tilde{x}_1(x_1, t), \cdots, \tilde{x}_n(x_n, t)).$$

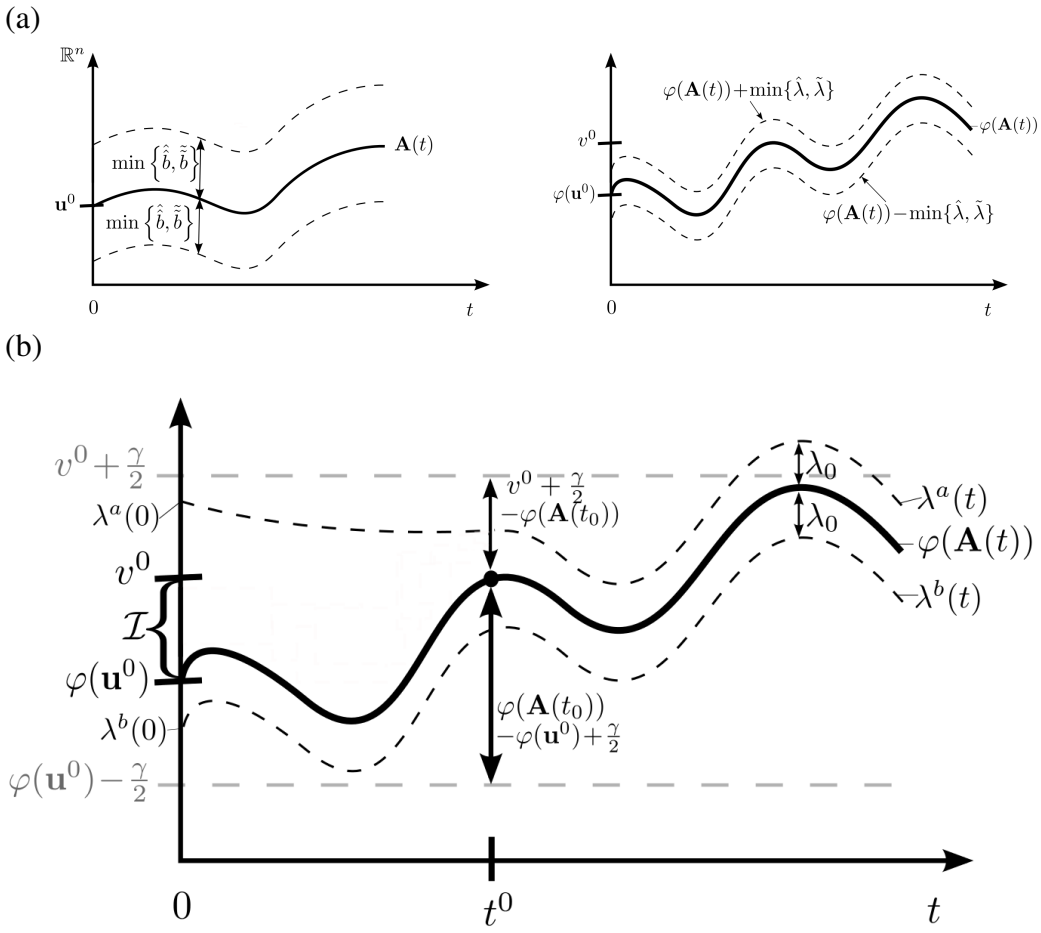

Figure H.1: Construction of tubular domain: Illustration of the proof of Corollary 9.8. (a) Domain constructed in Steps 1 and 2. (b) Domain constructed in Step 3. Notations are explained in the text of the proof.

Due to definition of φ, it holds

$$\begin{aligned}
0 =& -\alpha\varphi(\tilde{x}_1(x_1,t),\ \cdots,\ \tilde{x}_n(x_n,t)) \\
&+ \Phi(\tilde{x}_1(x_1,t),\ \cdots,\ \tilde{x}_n(x_n,t), \varphi(\tilde{x}_1(x_1,t),\ \cdots,\ \tilde{x}_n(x_n,t))) \\
=& -\alpha\varphi(\tilde{x}_1(x_1,t),\ \cdots,\ \tilde{x}_n(x_n,t)) \\
&+ \Phi(\tilde{x}_1(x_1,t),\ \cdots,\ \tilde{x}_n(x_n,t), \tilde{y}(\varphi(\tilde{x}_1(x_1,t),\ \cdots,\ \tilde{x}_n(x_n,t)),t)) \\
=& -\alpha\varphi(\tilde{x}_1(x_1,t),\ \cdots,\ \tilde{x}_n(x_n,t)) \\
&+ \tilde{\Phi}(x_1,,\ \cdots,\ x_n, \varphi(\tilde{x}_1(x_1,t),\ \cdots,\ \tilde{x}_n(x_n,t)))
\end{aligned}$$

This implies $\tilde{\varphi}(x_1,\ \cdots,\ x_n,t) = \varphi(\tilde{x}_1(x_1,t),\ \cdots,\ \tilde{x}_n(x_n,t))$, since then we obtain $0 = -\alpha\tilde{\varphi}(x_1,\ \cdots,\ x_n,t) + \tilde{\Phi}(x_1,\ \cdots,\ x_n, \tilde{\varphi}(x_1,\ \cdots,\ x_n,t),t)$.
We know that φ is differentiable. The functions $\tilde{x}_i$ are differentiable but the derivatives are discontinuous at the boundary of $\mathcal{T}_{b,\lambda}$.

■

H.4 Proof of Lemma 9.17

Lemma 9.17 is formulated on page 173.

PROOF
We can always choose M_0 in Assumption 9.3 such that $M_0 \leq \alpha$. We obtain by Tailor expansion and Lagrange's estimates for the error, [75]:

$$\begin{aligned}
\frac{d\zeta_0}{dt} &= -\alpha\zeta_0 + \Phi(\mathbf{u}^0, \varphi(\mathbf{u}^0) + \zeta_0) - \Phi(\mathbf{u}^0, \varphi(\mathbf{u}^0)) \\
&= -\alpha\zeta_0 + \partial_v\Phi(\mathbf{u}^0, v^*)\zeta_0,
\end{aligned}$$

where v^* depends on t and lies between $\varphi(\mathbf{u}^0)$ and $\varphi(\mathbf{u}^0)+\zeta_0$. Due to Assumption 9.3 (iii), we know that there exists $\gamma > 0$ such that $\alpha - \partial_y\Phi(\mathbf{x},y)|_{(\mathbf{x}=\mathbf{u}^0, y\in\mathcal{J})} \geq \frac{M_0}{4} > 0$ for $\mathcal{J} = [\min\{\varphi(\mathbf{u}^0), v^0\} - \gamma, \max\{\varphi(\mathbf{u}^0), v^0\} + \gamma]$. At $t = 0$ it holds $v^* \in \mathcal{J}$.
As long as $v^* \in \mathcal{J}$ it holds $|\zeta_0(t)| \leq |\zeta_0(0)|e^{-\frac{M_0}{4}t}$. Therefore, $\varphi(\mathbf{u}^0) + \zeta_0(t)$ will remain in $\mathcal{J}$ for all $t > 0$, since $\varphi(v^0) + \kappa(v_0 - \varphi(v^0)) \in \mathcal{J}$ for all $0 \leq \kappa \leq 1$. We obtain $|\zeta_0| \leq Ce^{-\frac{M_0}{4}t}$. Local Lipschitz continuity and boundedness lead to existence and uniqueness of ζ_0 for all t, [97, 106].

In the case of $\tilde{\zeta}_0$ existence and uniqueness follow from global Lipschitz continuity. Since outside of $\mathcal{T}_{b,\lambda}$ $\partial_v\tilde{\Phi} \equiv 0$ and inside $\mathcal{T}_{b,\lambda}$ and at the boundary it holds $\alpha - \partial_y\Phi(\mathbf{x},y)|_{(\mathbf{x}=\mathbf{u}^0, y\in\mathcal{J})} \geq \frac{M_0}{4} > 0$, we obtain $\alpha - \partial_y\Phi(\mathbf{x},y)|_{(\mathbf{x}=\mathbf{u}^0, y\in\mathcal{J})} \geq \min\{\frac{M_0}{4}, \alpha\} > 0$. Taylor expansion yields the analogous estimate as for ζ_0.

■

H.5 Existence of exponential dichotomies (Lemma 9.23)

In the following, we proof Corollaries stating the existence of negative dichotomies in the context that is needed in Chapter 9. The Corollaries are based on Lemma 9.7. The following corollary is a reformulation of Theorem 21.1 from [6].

Corollary H.1
Let all eigenvalues of $M \in \mathbb{R}^{n,n}$ have negative real parts. Let $B : \mathbb{R}^+ \to \mathbb{R}^{n,n}$, $t \mapsto B(t)$ be continuous with $||B(t)|| < \infty$ for all $t \geq 0$ and $\lim_{t\to\infty} ||B(t)|| = 0$. Then, a fundamental system of solutions S of the initial value problem

$$\begin{aligned} \frac{d}{dt}\mathbf{x} &= (M + B(t))\mathbf{x} \\ \mathbf{x}(0) &= \mathbf{x}_0 \end{aligned} \tag{H.15}$$

fulfills $||S(t)S^{-1}(\tau)|| \leq Ce^{-c(t-\tau)}$ for $c > 0$, $C > 0$, $t \geq \tau$.

PROOF

We note that M is a constant matrix. Due to Theorem 9.3 in [92], there exists $k > 0$, $K > 0$ s.t. each solution of

$$\begin{aligned} \frac{d}{dt}\mathbf{y} &= M\mathbf{y}, \\ \mathbf{y}(0) &= \mathbf{y}_0 \end{aligned} \tag{H.16}$$

satisfies $||\mathbf{y}(t)|| \leq K||\mathbf{y}_0||e^{-kt}$ for all $t \geq 0$. Let $\tilde{S}$ be a fundamental system of solutions. Then, it holds $||\tilde{S}(t)|| \leq Ke^{-kt}$, due to the semi-group property, it holds $||\tilde{S}(t)\tilde{S}^{-1}(\tau)|| = ||\tilde{S}(t-\tau)|| \leq Ke^{-k(t-\tau)}$ for all $t > \tau$. Since $\lim_{t\to\infty} ||B(t)|| = 0$, we can choose finite positive values t_1 and c such that $||B(t)|| \leq c < \frac{\alpha}{K}$ for $t \geq t_1$. We then set $C := \sup\{||B(t)|||t \geq 0\} < \infty$ and apply Lemma 9.7. ■

Corollary H.2
Let $\mathbf{f} : \mathbb{R}^+ \to \mathbb{R}^m$, $t \mapsto \mathbf{f}(t)$ and $D : \mathbb{R}^m \to \mathbb{R}^{n,n}$, $\mathbf{y} \mapsto D(\mathbf{y}(t))$ be continuous functions, $||D(\mathbf{y})|| < \infty$ for all $t \in \mathbb{R}^+$. Let $\lim_{t\to\infty} \mathbf{f}(t) = \bar{\mathbf{f}}$. Let all eigenvalues of $D(\bar{\mathbf{f}})$ have negative real part. Then there exist positive constants c, C such that a fundamental solution S of the initial value problem

$$\begin{aligned} \frac{d}{dt}\mathbf{x} &= D(t)\mathbf{x} \\ \mathbf{x}(0) &= \mathbf{x}_0 \end{aligned} \tag{H.17}$$

fulfills $||S(t)S^{-1}(\tau)|| \leq Ce^{-c(t-\tau)}$ for all $t \geq \tau$.

PROOF

We set $M := D(\bar{\mathbf{f}})$ and $B(t) := D(t) - M$. Then all eigenvalues of M have negative real part and $\lim_{t\to\infty} ||B(t)|| = 0$. We then apply the above Corollary H.1. ■

We can now prove Lemma 9.23.

PROOF

We use the above Corollary H.2. It holds $\lim_{t\to\infty} \mathbf{A}(t) = \bar{\mathbf{A}}$ and $\lim_{t\to\infty} \varphi(\mathbf{A}(t)) = \varphi(\bar{\mathbf{A}})$ (continuity of φ). Then, the above corollary can be applied to $D(t) := \Big(\nabla_u \mathbf{f}(\mathbf{x}, y) + \partial_v \mathbf{f}(\mathbf{x}, y) \otimes \nabla\varphi(\mathbf{x})|_{\mathbf{x}=\mathbf{A}(\mathbf{t}), y=\varphi(\mathbf{A}(\mathbf{t}))}\Big)$. ■

H.6 Details to Remark 9.31

The following proposition leads to Remark 9.31.

Proposition H.3
The linearization around the trivial equilibrium ($\bar{c}_1 = ... = \bar{c}_n = 0$) of the reduced system has only eigenvalues with negative real part, if and only if the linearization around the corresponding semi-trivial equilibrium ($\bar{c}_{1,\varepsilon} = ... = \bar{c}_{n,\varepsilon} = 0$, $\bar{s}_\varepsilon = 1$) of the full system has only eigenvalues with negative real part.

PROOF
The linearization $\mathcal{L}$ of the right hand-side of the reduced system has the form:

$$\mathcal{L} := \begin{pmatrix} \mathcal{B}_1 & 0 & 0 & \dots & 0 & -\mathcal{C}_1 \\ \mathcal{A}_1 & \mathcal{B}_2 & 0 & \dots & 0 & \mathcal{C}_1 - \mathcal{C}_2 \\ 0 & \mathcal{A}_2 & \mathcal{B}_3 & & 0 & \mathcal{C}_2 - \mathcal{C}_3 \\ \vdots & \ddots & \ddots & \ddots & & \vdots \\ 0 & \dots & \dots & \mathcal{A}_{n-2} & \mathcal{B}_{n-1} & \mathcal{C}_{n-2} - \mathcal{C}_{n-1} \\ 0 & 0 & 0 & 0 & \mathcal{A}_{n-1} & -d_n + \mathcal{C}_{n-1} \end{pmatrix},$$

where we set $s^* = s(c_2) = \frac{1}{1+kc_2}$ and $\mathcal{A}_i = (2a_i s^* - 1)p_i$, $\mathcal{B}_i = 2(1 - a_i s^*)p_i$, $\mathcal{C}_i = 2k(s^*)^2 a_i p_i c_i$.

If we set $c_1 = ... = c_n = 0$, it follows $s^* = 1$. We then obtain

$$\mathcal{L}^0 := \begin{pmatrix} \mathcal{B}_1^0 & 0 & 0 & \dots & 0 & 0 \\ \mathcal{A}_1^0 & \mathcal{B}_2^0 & 0 & \dots & 0 & 0 \\ 0 & \mathcal{A}_2^0 & \mathcal{B}_3^0 & & 0 & 0 \\ \vdots & \ddots & \ddots & \ddots & & \vdots \\ 0 & \dots & \dots & \mathcal{A}_{n-2}^0 & \mathcal{B}_{n-1}^0 & 0 \\ 0 & 0 & 0 & 0 & \mathcal{A}_{n-1}^0 & -d_n \end{pmatrix}$$

with $\mathcal{A}_i^0 = (2a_i - 1)p_i$, $\mathcal{B}_i^0 = 2(1 - a_i)p_i$. The eigenvalues of $\mathcal{L}^0$ are $\mathcal{B}_1^0, \cdots, \mathcal{B}_{n-1}^0, -d_n$.

The linearization $\tilde{\mathcal{L}}$ of the right hand-side of the full system has the form

$$\tilde{\mathcal{L}} := \begin{pmatrix} \tilde{\mathcal{B}}_1 & 0 & 0 & \dots & 0 & 0 & -\mathcal{D}_1 \\ \tilde{\mathcal{A}}_1 & \tilde{\mathcal{B}}_2 & 0 & \dots & 0 & 0 & \mathcal{D}_1 - \mathcal{D}_2 \\ 0 & \tilde{\mathcal{A}}_2 & \tilde{\mathcal{B}}_3 & & 0 & 0 & \mathcal{D}_2 - \mathcal{D}_3 \\ \vdots & \ddots & \ddots & 0 & 0 & \vdots & \\ 0 & \dots & \dots & \tilde{\mathcal{A}}_{n-2} & \tilde{\mathcal{B}}_{n-1} & 0 & \mathcal{D}_{n-2} - \mathcal{D}_{n-1} \\ 0 & \dots & \dots & 0 & \tilde{\mathcal{A}}_{n-1} & -d_n & \mathcal{D}_{n-1} \\ 0 & \dots & \dots & 0 & 0 & -ks_\varepsilon & -1 - kc_n \end{pmatrix},$$

where we set $\tilde{\mathcal{A}}_i = (2a_i s_\varepsilon - 1)p_i$, $\tilde{\mathcal{B}}_i = 2(1 - a_i s_\varepsilon)p_i$, $\mathcal{D}_i = -2a_i p_i c_{i,\varepsilon}$. For $c_{1,\varepsilon} = ... = c_{n,\varepsilon} = 0$, $s_\varepsilon = 1$, we obtain

$$\tilde{\mathcal{L}}^0 := \begin{pmatrix} \tilde{\mathcal{B}}_1^0 & 0 & 0 & \dots & 0 & 0 & 0 \\ \tilde{\mathcal{A}}_1^0 & \tilde{\mathcal{B}}_2^0 & 0 & \dots & 0 & 0 & 0 \\ 0 & \tilde{\mathcal{A}}_2^0 & \tilde{\mathcal{B}}_3^0 & & 0 & 0 & 0 \\ \vdots & \ddots & \ddots & 0 & 0 & \vdots & \\ 0 & \dots & \dots & \tilde{\mathcal{A}}_{n-2}^0 & \tilde{\mathcal{B}}_{n-1}^0 & 0 & 0 \\ 0 & \dots & \dots & 0 & \tilde{\mathcal{A}}_{n-1}^0 & -d_n & 0 \\ 0 & \dots & \dots & 0 & 0 & -k & -1 \end{pmatrix}$$

with $\tilde{\mathcal{A}}_i^0 = \mathcal{A}_i^0$, $\tilde{\mathcal{B}}_i = \mathcal{B}_i^0$.

The eigenvalues of $\tilde{\mathcal{L}}^0$ are $\mathcal{B}_1^0, \cdots, \mathcal{B}_{n-1}^0, -d_n, -1$. For this reason the linearization around the trivial equilibrium of the reduced system has only eigenvalues with negative real part, if and only if the linearization around the corresponding semi-trivial equilibrium of the full system has only eigenvalues with negative real part. The number of zero eigenvalues is the same for both linearizations. ■

H.7 Further technical details

Lemma H.4
Let $k, l > 0$. Then, $|\int_0^t e^{-k(t-\tau)}e^{-l\tau}d\tau| \leq Ce^{-mt}$ for a $m > 0$ and a $C > 0$.

PROOF
Let $k \neq l$, then

$$\begin{aligned}\int_0^t e^{-k(t-\tau)}e^{-l\tau}d\tau &= e^{-kt}\int_0^t e^{(k-l)\tau}dt \\ &= \frac{e^{-kt}}{k-l}\left(e^{(k-l)t}-1\right) \\ &= \frac{e^{-lt}-e^{-kt}}{k-l} \\ &\leq \frac{e^{-\min\{l,k\}t}}{|k-l|}\end{aligned}$$

Let $k = l$, then

$$\begin{aligned}\int_0^t e^{-k(t-\tau)}e^{-l\tau}d\tau &= e^{-kt}\int_0^t e^{(k-l)\tau}dt \\ &= e^{-kt}t \\ &\leq Ce^{-mt}\end{aligned}$$

for

$$0 < m < k, \quad \log C > \log(\frac{1}{k-m}) - 1, \tag{H.18}$$

since

$$\begin{aligned}te^{-kt} \leq Ce^{-mt} \quad &\Leftrightarrow \\ \log(t) - kt \leq \log(C) - mt \quad &\Leftrightarrow \\ \log(t) + (m-k)t \leq \log(C)\end{aligned}$$

The left hand-side is maximal for $t = \frac{1}{k-m} > 0$. The maximum is $\log(\frac{1}{k-m}) - 1$. Therefore, constraint (H.18) is sufficient to obtain $te^{-kt} \leq Ce^{-mt}$.

■